POLARIZED TARGETS AND ION SOURCES

POLARIZED TARGETS
and
ION SOURCES

Proceedings of the
International Conference on
Polarized Targets and Ion Sources

Saclay, France
December 5-9, 1966

Edited by La Direction de la Physique
Centre d'Etudes Nucléaires de Saclay
Boite postale N° 2
91 - Gif-sur-Yvette, France

PREFACE

During the last four or five years a new tool has emerged in nuclear and high energy physics : dynamically polarized nuclear targets. Quite a few have already been constructed throughout the world and more are being built. Some very significant scattering experiments have been performed ; others are in progress or being planned for the future.

It had appeared to several of the users and of the constructors of these devices that it would be useful to have an international meeting dealing with the subject.

The aim of the meeting was to bring together, the potential constructors of polarized targets, resonance and low temperature physicists, and the potential users, nuclear and high energy physicists, including theoreticians. After taking stock of what had been achieved so far, trends for the future were the main concern : what kind of improvements on existing designs appeared desirable to the users in connection with the new experiments they wished to attempt, and what kind of improvements appeared to the builders of targets as feasible in the foreseeable future.

Although there is little doubt that some day polarized targets will become a standard part of high energy instrumentation and pass into the hands of engineers, the general feeling was that we are still far removed from this situation and that there is still considerable room for basic research in that field.

As had been stressed by many and very clearly expressed by Dr Steiner who unfortunately was unable to attend the meeting : "one of the essential features of this conference is that it should bridge the gap between the "Two cultures" i.e. between the elementary particle (or

nuclear) physicist who uses these targets but is rather inexpert when it comes to many of the technical questions involved in their theory and even their operation, and the solid state or cryogenics expert who may not be familiar with the current fields of interest in high energy physics. Great emphasis should be placed on trying to establish effective communication between practitioners of these two fields of study. In particular sufficient time should be allotted so that the current problems in both of these fields can be presented in an understandable way to all of the participants". By and large so it was.

This volume contains all the invited talks and some short communications delivered at the conference held at Saclay December 5-9 1966. There is a large amount of new and hitherto unpublished material distributed evenly between the "two cultures".

We hope that it will be of use to potential builders and users of polarized targets.

A. ABRAGAM

LIST OF PARTICIPANTS

BELGIUM

BÖCKOFF, K.H. ..... Euratom, Geel.
LIBERT, J. ..... Faculté Polytechnique, Mons.
THEOBALD, G. ..... Euratom, Geel.
VAN GERVEN, L. ..... Institut voor Lage Temperaturen en Technische Fysica, Leuven.

CANADA

DANIELS, J.M. ..... University of Toronto, Toronto.
PRENTICE, J.D. ..... Id.

FRANCE

ABRAGAM, A. ..... Centre d'Etudes Nucléaires, Saclay.
ARVIEUX, J. ..... Id.
BARJON, R. ..... Faculté des Sciences, Grenoble.

LIST OF PARTICIPANTS

BELLICARD, J.B. ..... Centre d'Etudes Nucléaires, Saclay.
BENOIT, H. ..... Faculté des Sciences, Orsay.
BERTHET, G. ..... Faculté des Sciences, Clermont-Ferrand.
BEURTEY, R. ..... Centre d'Etudes Nucléaires, Saclay.
BLAIR, A. ..... Id.
BLOCH, C. ..... Id.
BOUCHEZ, R. ..... Faculté des Sciences, Grenoble.
BOUNIN, P. ..... Centre d'Etudes Nucléaires, Saclay.
CAHILL, T. ..... Id.
CATILLON, P. ..... Id.
CHAPELLIER, M. ..... Id.
COIGNET, G. ..... Institut de Physique Nucléaire, Orsay.
COMBRISSON, J. ..... Centre d'Etudes Nucléaires, Saclay.
CONZETT, H.E. ..... Faculté des Sciences, Grenoble.
COTTON, J.P. ..... Centre d'Etudes Nucléaires, Saclay.
COZZIKA, G. ..... Id.
DE GENNES, P.G. ..... Faculté des Sciences, Orsay.
DELAUNAY, B. ..... Centre d'Etudes Nucléaires, Saclay.
DEREGEL, J. ..... Faculté des Sciences, Caen.
DESPORTES, H. ..... Centre d'Etudes Nucléaires, Saclay.
DE SWINIARSKI, R. ..... Id.
DUCROS, Y. ..... Id.
DUTHIL, R. ..... Id.
EZRATTY, J. ..... Id.
FALK-VAIRANT, P. ..... Id.
GARRETA, D. ..... Id.
GASTEBOIS, J. ..... Id.
GLASHAUSSER, C. ..... Id.
GLATTLI, H. ..... Id.
GOLDMAN, M. ..... Id.
ISABELLE, D.B. ..... Faculté des Sciences, Clermont-Ferrand.
JACOB, M. ..... Centre d'Etudes Nucléaires, Saclay.
JUNGERMAN, J. ..... Id.
KASTLER, A. ..... Ecole Normale Supérieure, Paris.
KURODA, K. ..... Institut de Physique Nucléaire, Orsay.

LANDESMAN, A. ..... Centre d'Etudes Nucléaires, Saclay.
LEGRAND, A. ..... Faculté des Sciences, Paris.
MASSUE, J.P. ..... Centre de Recherches Nucléaires, Strasbourg-Cronenbourg.
MERLO, J.P. ..... Centre d'Etudes Nucléaires, Saclay.
MEYER, J. ..... Id.
MICHALOWICZ, A. ..... Institut de Physique Nucléaire, Orsay.
MILLER, J. ..... Centre d'Etudes Nucléaires, Saclay.
MOVCHET, J. ..... Id.
ODEHNAL, M. ..... Id.
ORRY, R. ..... Brevatome, Paris.
PAPINEAU, A. ..... Centre d'Etudes Nucléaires, Saclay.
PAPINEAU, L. ..... Id.
PHAM-DINH-LIEN, ... Faculté des Sciences, Grenoble.
PRUGNE, P. ..... Centre d'Etudes Nucléaires, Saclay.
RAYNAL, J. ..... Id.
REVEL, D. ..... Id.
RIEUBLAND, M. ..... Id.
RIPOUTEAU, F. ..... Faculté des Sciences, Grenoble.
ROUBEAU, P. ..... Centre d'Etudes Nucléaires, Saclay.
ROYET, J. ..... Faculté des Sciences, Orsay.
RYTER, C. ..... Centre d'Etudes Nucléaires, Saclay.
SALTMARSH,..... Faculté des Sciences, Grenoble.
SCHERER, M. ..... Faculté des Sciences, Caen.
SOLOMON, I. ..... Ecole Polytechnique, Paris.
SONDEREGGER, P. ..... Centre d'Etudes Nucléaires, Saclay.
TESTONI, J. ..... Id.
THIRION, J. ..... Id.
TSAI, B. ..... Id.
TZARA, C. ..... Id.
VALLADAS, G. ..... Id.
VAN ROSSUM, L. ..... Id.
WINTER, J.M. ..... Id.
ZYLBERAJCH, S. ..... Id.

GERMANY

CRIEGEE, L. ..... Deutsches Elektronen Synchrotron DESY, Hamburg.

EBINGHAUS, H. ..... Physikalisches Staatsinstitut, Hamburg.

FICK, D. ..... Physikalisches Institut der Universität, Erlangen-Nürnberg, Erlangen.

KAJIKAWA, R. ..... Deutsches Elektronen Synchrotron DESY, Hamburg.

KLINGER, W. ..... Physikalisches Institut der Universität, Erlangen-Nürnberg, Erlangen.

KÖRNER, H.J. ..... Physik Department der Technischen Hochschule, München.

KUIPER, H. ..... Physikalisches Institut der Universität, Erlangen-Nürnberg, Erlangen.

KUTSCHERA, K.H. ..... Id.

LADAGE, A. ..... Deutsches Elektronen-Synchrotron DESY, Hamburg.

OTTEN, W. ..... Physikalisches Institut der Universität, Heidelberg.

PENSELIN, S. ..... Institüt für angewandte Physik der Universität, Bonn.

PÜHLER, A. ..... Physikalisches Institut der Universität, Erlangen-Nürnberg, Erlangen.

GREAT-BRITAIN

ATKINSON, H.H. ..... Rutherford High Energy Laboratory, Chilton.

BEROVIC, N. ..... University of Birmingham, Birmingham.

COATES, M.S. ..... A.E.R.E., Harwell.

DALITZ, R.H. ..... Clarendon Laboratory, Oxford.

FARAGO, P.S. ..... University of Edinburgh, Edinburgh.

GRIFFITH, J.A.R. ..... University of Birmingham, Birmingham.

HAYMAN, P.J. ..... University of Liverpool, Liverpool.

HILL, R.E. ..... Rutherford High Energy Laboratory, Chilton.

KURTI, N. ..... Clarendon Laboratory, Oxford.
McCLAUSLAND, M.A.H. ..... The University, Manchester.
NICHOLAS, O.J. ..... Rutherford High Energy Laboratory, Chilton.
PATTENDEN, N.J. ..... A.E.R.E., Harwell.
PHILLIPS, R.J.N. ..... Id.
READ, S.F.J. ..... Rutherford High Energy Laboratory, Chilton.
SCANLON, J.P. ..... A.E.R.E., Harwell.
SIEGMANN, H. ..... University of Edinburgh, Edinburgh.
WIGAN, R. ..... A.E.R.E., Harwell.
ZUCKER, A. ..... Rutherford High Energy Laboratory, Chilton.

INDIA

CHANDRA, G. ..... Tata Institute of Fundamental Research, Bombay.

ITALY

FASOLI, U. ..... Istituto di Fisica "G. Galilei", Padova.
MANNELLI, I. ..... Istituto di Fisica Nucleare, Pisa.
PAPPALARDO, G. ..... Istituto di Fisica-Università, Catania.
POIANI, G. ..... Istituto di Fisica-Università, Trieste.
POTENZA, R. ..... Istituto di Fisica-Università, Catania.
SAMBO, P. ..... Istituto di Fisica "G. Galilei", Padova.
STOPPINI, G. ..... Istituto di Fisica Nucleare, Pisa.

NETHERLANDS

BRUIL, W.A. ..... Technological University, Eindhoven.
GORTER, C.J. ..... Kamerlingh Onnes Laboratory, Leiden.
LUBBERS, J. ..... Id.
MESS, K.W. ..... Id.
NIESEN, L. ..... Id.
POPPEMA, O.J. ..... Technische Hogeschool, Eindhoven.
POSTMA, H. ..... Kamerlingh Onnes Laboratory, Leiden.
SWANENBURG, T.J.B. ..... Id.
VAN DER HEIDE, J.A. ..... Technische Hogeschool, Eindhoven.
VAN DER WOUDE, A. ..... Natuurkundig Laboratory, Groningen.
VERHAAR, B.J. ..... Technische Hogeschool, Eindhoven.

SWITZERLAND

BORGHINI, M. ..... C.E.R.N., Geneva.
DAUM, C. ..... Id.
DICK, L. ..... Id.
DI LELLA, L. ..... Id.
ERDMAN, K. ..... Eidg. Technische Hochschule, Zurich.
GREGOIRE, G. ..... C.E.R.N., Geneva.
GREGORY, B. ..... Id.
GRÜEBLER, W. ..... Eidg. Technische Hochschule, Zurich.
MAGLIC, B. ..... C.E.R.N., Geneva.
MANGO, S. ..... Id.
OLIVIER, J.C. ..... Id.
PRENTKI, J. ..... Id.
RUNOLFSSON, Ö. ..... Id.
VERMEULEN, J. ..... Id.

TCHECOSLOVAQUIA

BURGET, J. ..... Nuclear Research Institute, Rez.

UNITED STATES

ALFORD, W.P. ..... University of Rochester, Rochester.
BOOTH, N.E. ..... Enrico Fermi Institute for Nuclear Studies, Chicago.
CARVER, T.R. ..... Palmer Physical Laboratory, Princeton.
CHAMBERLAIN, O. ..... University of California, Berkeley.
DABBS, J.W.T. ..... Oak Ridge National Laboratory, Oak Ridge
JACKSON, J.D. ..... University of Illinois, Urbana.
JEFFRIES, C.D. ..... University of California, Berkeley.
MULADY, J.R. ..... Id.
NOYES, H.P. ..... Stanford University, Stanford.
PHILLIPS, G.C. ..... Rice University, Houston.
REBKA, G.A. ..... Yale University, New Haven.
SANDERSON, J.T. ..... Harvard University, Cambridge.
SCHERMER, R.I. ..... Brookhaven National Laboratory, Upton.
SCHULTZ, C.H. ..... Columbia University, New York.
SHAPIRO, G. ..... University of California, Berkeley.
SIMMONS, J.E. ..... Scientific Laboratory, University of California, Los Alamos.
STAPLETON, H.J. ..... University of Illinois, Urbana.
STEFFEN, R.M. ..... Purdue University, Lafayette.
TOM, J.L. ..... The Cyclotron Corporation, Berkeley.
VERNON, H. ..... Yale University, New Haven.
WALTERS, G.K. ..... Rice University, Houston.
WOLLAN, D.S. ..... Virginia Polytechnic Institute, Blacksburg.
YOKOSAWA, A. ..... Argonne National Laboratory, Argonne.

U.S.S.R.

JANOUT, Z. ..... Joint Institute for Nuclear Research, Doubna.

LEHAR, F. ..... Id.

LOUTCHIKOV, ... Id.

WINTERNITZ, P. ..... Id.

TABLE OF CONTENTS

PAPERS PRESENTED AT THE CONFERENCE

POLARIZED TARGETS : WHY?

J.D. JACKSON
University of Illinois, Urbana

I INTRODUCTION

This conference on polarized targets and ion sources brings together two rather disparate groups, nuclear and high energy physicists on the one hand and those knowledgeable in handling aggregates of atoms and molecules on the other. The purpose of such a confrontation is to make each group more aware of the needs and problems of the other, with the quite reasonable hope that advances will result in the technology of polarized targets and ion sources and their use in nuclear and particle physics.

I stand before you unknown as either a maker or a user of polarized targets. You may well reconstruct the title of my talk to read "J.D. Jackson : Why ?". The answer is this : Physics has grown so specialized that many members of the two cultures present today look on the activities of the other as bordering on the occult. The terminology illustrates the problem : forbidden transitions, doped crystals of LMN and YES (perhaps even LSD ?), space-charge-neutralized ionizers, electrons relaxing in an helium bath, all of these terms smack of the bizarre and are only vaguely understood by the average nuclear or high energy phycicist. And terms like octet dominance, quarks, current commutators (Gell-Mann's, not Faraday's), Regge poles and PCAC or, as is now favoured, PPDAC conjure up probably erroneous images in minds usually occupied elsewhere. Another pertinent aspect is the inevitable feeling by the aggregates crowd that they are here as technologists and servants required to stir their witches' brews and produce better targets and ion sources for the benefit of the nuclear and high energy experimenters.

My aim, then, is two fold : a) to bridge the gap in notation, terminology and background so that all of the audience will be

better equipped to listen to the talks on the present and proposed uses of polarized targets and ion sources, and b) to convince the disbeliever or agnostic that exciting developments in nuclear and particle physics can be hastened immeasurably by the use of polarized targets ; indeed, some things seem to be impossible without them.

In the time available to me it is impossible to discuss more than a few examples of the uses of polarized targets and ion sources. The existence of the Proceedings of the Karlsruhe Conference, September 6-10, 1965 (Huber and Schopper, 1966), with its many papers on polarization phenomena in nuclear physics and in nucleon-nucleon scattering, allows me to follow my natural inclination to concentrate on applications in high energy physics. If further excuse is needed, I point to five speakers on the program (G.C. Phillips, P. Catillon, H.P. Noyes, F.L. Shapiro, R.I. Schermer) who will discuss nuclear and nucleon-nucleon interactions. Needless to say, the basic terminology is common to all fields, even if the details are different.

It will be assumed that polarized beams or targets of nucleons exist. How, in exactly what form, and what problems arise in the real world will undoubtedly be discussed in great detail before this conference is out. For completeness, I mention the more or less standard references on the state of the art as of two years ago : Abragam and Borghini (1964), Dickson (1965), Jeffries (1963, 1964), Shapiro (1965), as well as the Karlsruhe Conference (Huber and Schopper, 1966).

II WOLFENSTEIN PARAMETERS

For the scattering of spin 1/2 particles on an unpolarized target the changes in direction and magnitude of the spin caused by the scattering act are customarily described in terms of the so-called Wolfenstein parameters, P, D, A, R, A' and R'. The polarization $\vec{P}_f$ of the scattered particle bears at most a linear relation to the initial polarization $\vec{P}_i$, as first discussed by Wolfenstein and Ashkin (1952), Dalitz (1952), Wolfenstein (1954) and Oehme (1955). This relation can be displayed by expressing the final polarization in terms of components along various directions. The relevant coordinates are shown in figure 1. The final polarization $\vec{P}_f$ is :

$$I\,\vec{P}_f = I_o\Big\{(P + D\,\vec{P}_i\cdot\hat{n})\hat{n} + (A\,\vec{P}_i\cdot\hat{k}_i + R\,\vec{P}_i\cdot\hat{s}_i)\hat{s}_f + (A'\,\vec{P}_i\cdot\hat{k}_i + R'\,\vec{P}_i\cdot\hat{s}_i)\hat{k}_f\Big\} \qquad (1)$$

where $I = I_o(1 + P\,\vec{P}_i\cdot\hat{n})$ and I_o is the cross-section for scattering of an unpolarized beam by an unpolarized target. Equation (1) serves to define the parameters P, D, A, R, A', R' in an operational manner. We note that the final polarization $\vec{P}_f$ of an initially unpolarized beam is along the normal to the scattering plane $\hat{n}$ and has a sign and magnitude given by the parameter P. The parameter P is also equal to the left-right asymmetry of the scattering of a beam that is completely polarized normal to the incident direction. This is a consequence of time-reversal invariance. It means that, if one accepts time-reversal invariance, P can be measured in two ways, or if one wishes to test time-reversal invariance, the results of the measurements in the two ways can be compared. Experiments to determine the other parameters (D, A, R, A', R') are described pictorially in the first chapter of the book by Moravcsik (1963).

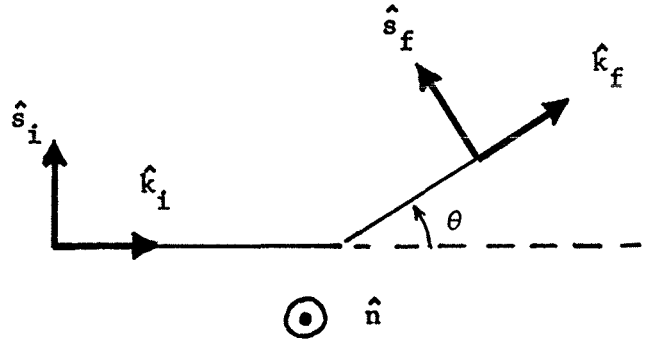

Fig. 1 Coordinate vectors used to define the Wolfenstein parameters in equation (1). $\hat{k}_i$ and $\hat{k}_f$ are unit vectors in the direction of the initial and final momentum, respectively, of the spin 1/2 particle in the center of mass system ; $\hat{n}$ is the unit normal to the scattering plane ($\hat{n} = \hat{k}_i \times \hat{k}_f / |\hat{k}_i \times \hat{k}_f|$) ; $\hat{s}_i$ and $\hat{s}_f$ are unit vectors in the scattering plane and perpendicular to $\hat{k}_i$ and $\hat{k}_f$, as shown.

Needless to say, the various Wolfenstein parameters depend in different ways on the amplitudes involved. Consequently, their observation yields information on different aspects of the scattering process and can remove ambiguities present if only the cross-section for unpolarized beam and target is observed. We will see this in detail immediately for a special, but common, choice for the spins of the projectile and target.

III SPIN ZERO-SPIN 1/2 SCATTERING AND REACTIONS : INTRINSIC PARITY DETERMINATION

The example of spin zero projectiles incident on a spin 1/2 target is a common one in particle physics and is also the simplest interesting case. Pion-nucleon scattering ($\pi N \to \pi N$), K-meson-nucleon scattering ($KN \to KN$ or $\bar{K}N \to \bar{K}N$), associated production ($\pi N \to K\Sigma$ or $K\Lambda$) are all examples. Soon after the discovery of strange particles it was pointed out by Bilenky (1958) that a study of polarization phenomena in the initial and final states could be used to determine the intrinsic parities of the strange particles. The relevant fact is whether the product of the intrinsic parities in the initial state is the same as that in the final state. Thus we distinguish two cases, "same" and "opposite", corresponding to the initial and final intrinsic parity products being equal in sign or opposite, respectively.

For the <u>same</u> intrinsic parities arguments of Lorentz covariance, parity conservation, and conservation of 4-momentum restrict the form of the invariant matrix element to :

$$\mathcal{M} = \bar{u}(p') \left[- A + iB\sigma . \frac{q + q'}{2} \right] u(p) \qquad (2)$$

where the initial 4-momenta of the spin 0 and spin 1/2 particles are q and p, respectively, and the final 4-momenta are q' and p'. The Dirac spinors are normalized according to $\bar{u}u$ = constant (often 2m). The invariant amplitudes A and B are functions of the scalar kinematic variables, e.g., center of mass total energy W and scattering angle θ. Equation (2) is not the most suitable for examining the spin aspects of the process. The explicit two-component form of the Dirac spinors can be used to express the amplitude $\mathcal{M}$ in terms of Pauli spinors for the spin 1/2 particles :

$$\mathcal{M} \to \langle \chi' | \mathcal{F}_S | \chi \rangle \qquad (3)$$

where the scattering operator $\mathcal{F}_S$ is :

$$\mathcal{F}_S = f_1 + f_2 \, \vec{\sigma}.\hat{p}' \, \vec{\sigma}.\hat{p} \qquad (4)$$

In equation (4), $\hat{p}$ and $\hat{p}'$ are unit vectors along the momenta of the initial and final spin 1/2 particles, respectively, in the center of mass system. The scalar amplitudes f_1 and f_2 are linear combinations of A and B in equation (2). The subscript S in (3) and (4) stands for scalar (under space inversion) or "same".

If the intrinsic parities are <u>opposite</u>, the invariant amplitude is of the form :

$$\mathcal{M} = \bar{u}(p')\gamma_5 \left[\quad \right] u(p) \qquad (5)$$

where the empty bracket denotes the operator structure appearing in equation (2). The Dirac matrix γ_5 gives a pseudoscalar character to $\mathcal{M}$, as required by the parity change in going from initial to final state. The Pauli reduction gives :

$$\mathcal{M} \rightarrow \langle \chi' | \mathcal{F}_P | \chi \rangle \tag{6}$$

where

$$\mathcal{F}_P = \vec{\sigma}.\hat{p}' \, \mathcal{F}_S \quad . \tag{7}$$

Here the operator $\mathcal{F}_S$ is of the same form as (4) and the pseudoscalar operator $\vec{\sigma}.\hat{p}'$ gives the necessary parity properties. The subscript P is for pseudoscalar or "opposite".

The two amplitudes (4) and (7) are particularly convenient for studying the observable aspects of the process and their dependence or lack of dependence on the spin states of the spin 1/2 particles. The differential cross-section for an unpolarized target and with no observation of polarization of the final particle is :

$$\frac{d\sigma}{d\Omega} = \frac{1}{2} \frac{q'}{q} \sum_{\lambda\lambda'} |\langle \lambda' | \mathcal{F} | \lambda \rangle|^2 \quad . \tag{8}$$

We note that in (4) and (7) the Pauli operators are just the helicity operators and so chose the spin states in the helicity representation for convenience, with λ and λ' denoting initial and final helicities, respectively.

Consider now the question of distinguishing between the "same" and "opposite" intrinsic parities. The only difference in structure between (4) and (7) is an additional $\vec{\sigma}.\hat{p}'$ on the left in $\mathcal{F}_P$. But $\vec{\sigma}.\hat{p}'$ is an eigenoperator in the helicity representation :

$$\vec{\sigma}.\hat{p}' |\lambda'\rangle = (-1)^{\lambda' - 1/2} |\lambda'\rangle \tag{9}$$

with eigenvalues of modulus unity. Thus in the sum of absolute squares in (8) the distinction between $\mathcal{F}_S$ and $\mathcal{F}_P$ is lost. The two cases cannot be distinguished if we sum over spins.

It is a different story if polarization is studied. Conventionally "up" and "down" refer to polarization in the positive and negative senses along the normal $\hat{n}$ to the reaction plane. The operator $\vec{\sigma}.\hat{p}'$ is <u>not</u> an eigenoperator for spin quantized along the normal. In fact, we find :

$$\begin{aligned} \vec{\sigma}.\hat{p}' \, |\text{SPIN UP}\rangle &= |\text{SPIN DOWN}\rangle \\ \vec{\sigma}.\hat{p}' \, |\text{SPIN DOWN}\rangle &= |\text{SPIN UP}\rangle \end{aligned} \tag{10}$$

This means that the presence or absence of an additional factor $\vec{\sigma}.\hat{p}'$ can be detected by comparison of results for polarization

in the initial and final states. We saw in section II that for elastic scattering the final polarization along the normal in scattering from an unpolarized target was the same in magnitude and sign as the left-right asymmetry from a polarized target. This result also holds for a reaction, provided the intrinsic parities are the same*. We now see from equation (10) that for "opposite" intrinsic parities the signs of the final polarization and the left-right asymmetry will be opposite. This difference is Bilenky's method for determination of intrinsic parities.

The explicit formulas are of some interest. Suppose the spin 1/2 target has polarization $\vec{P}_i$. The cross-section obtained from (4) for observation of the final spin 1/2 particle with its spin in an arbitrary direction $\hat{s}_f$ is, if the intrinsic parities are the same :

$$\frac{d\sigma}{d\Omega} = \frac{1}{2}\left[|f_1|^2 + |f_2|^2 + 2\mathrm{Re}(f_1^* f_2)\cos\theta\right](1 + \hat{s}_f\cdot\vec{P}_i)$$
$$+ \mathrm{Im}(f_1^* f_2)\sin\theta\ \hat{n}\cdot(\vec{P}_i + \hat{s}_f)$$
$$+ \left[\mathrm{Re}(f_1^* f_2) + |f_2|^2\cos\theta\right]\sin\theta\ \hat{s}_f\cdot(\hat{n}\times\vec{P}_i)$$
$$+ |f_2|^2\sin^2\theta\ \hat{s}_f\cdot(\hat{n}\times(\hat{n}\times\vec{P}_i)) \qquad (11)$$

Equation (11) describes the complete experiment, with both initial and final polarizations. If the final particle is detected independently of its polarization, one multiplies (11) by two and omits all terms proportional to $\hat{s}_f$. For an unpolarized target, one sets $\vec{P}_i = 0$. The statement concerning equality in magnitude and sign of the left-right asymmetry and the final polarization is contained in the second line of (11) where the factor $\hat{n}\cdot(\vec{P}_i + \hat{s}_f)$ appears.

For opposite intrinsic parities a straightforward calculation using (7) shows that (11) is altered by the replacement of the unit vector $\hat{s}_f$ according to :

$$\hat{s}_f \to -\hat{s}_f + 2(\hat{s}_f\cdot\hat{p}')\hat{p}' \quad . \qquad (12)$$

Among the other modifications, the second line in (11) is transformed as :

$$\hat{n}\cdot(\vec{P}_i + \hat{s}_f) \to \hat{n}\cdot(\vec{P}_i - \hat{s}_f) \ , \qquad (13)$$

showing the equal magnitude but opposite sign for the left-right asymmetry and final polarizations associated with opposite initial and final intrinsic parities. More generally, equation (12) shows that the longitudinal polarization remains the same as in the previous case while the transverse components change sign.

Two Bilenky experiments to determine the intrinsic parities of strange particles have been performed, one at Berkeley on the reac-

tion $\pi N \rightarrow K\Sigma$ and one at CERN on $\bar{K}N \rightarrow K\Xi$. The results have not been published so far. But the Berkeley experiment is described by Professor Chamberlain in his report at this Conference. The $K\Sigma$ intrinsic parity is reasonably well established to be the same as that of πN on the basis of indirect arguments. But a direct determination is of value. For the $K\Xi$ system there is no experimental evidence one way or the other. Obviously there are strong theoretical arguments in favour of the same intrinsic parity for $K\Xi$ as for πN, but this makes the direct observation all the more important. Think of the apple carts that would be overturned by an experimental result contrary to theoretical expectations !

IV SPINS AND PARITIES OF RESONANT STATES

Another class of experiments in which polarization studies play an important rôle is pion-nucleon elastic and charge exchange scattering in the resonance region. The use of polarization data allows the determination of the parities of resonant states, as well as their angular momentum, in a manner closely analogous to the intrinsic parity determination of the previous section. This is not a new idea. For many years studies have been made of the polarization of the recoil proton by secondary scattering. One of the most recent such experiments was performed by a Saclay-Caen collaboration with positive pions of 410 and 492 MeV kinetic energy (Bareyre, 1965). But greatly improved statistical accuracy and detail has resulted from the use of polarized targets. Pion-nucleon scattering experiments with a polarized LMN target were first performed by a Berkeley group in 1963 (Chamberlain et al, 1963). Since that time work has continued at Berkeley, and has begun at Argonne and the Rutherford Laboratory. Particularly noteworthy are the beautiful experiments with positive and negative pions of momenta from 875 to 1579 MeV/c at the Rutherford Laboratory (Duke et al, 1965 ; Atkinson et al, 1965), those at Argonne by a Chicago-Argonne collaboration with negative pions of momenta from 1.7 to 2.5 GeV/c (Suwa et al, 1965 ; Yokosawa et al, 1966), and the very recent results from Berkeley with positive and negative pions of momenta from 670 to 3750 MeV/c (Chamberlain et al, 1966). All of these data show impressive statistical accuracy and allow relatively accurate Legendre polynomial expansions of both cross-sections and polarizations. Professor Chamberlain discusses these experiments in detail in his report. In any event space does not permit me to give more than an outline of the theory and how polarization information can help untangle a complicated situation.

For πN scattering the basic amplitude is given by equation (4), where f_1 and f_2 are functions of center of mass total energy W and

scattering angle θ. Conservation of angular momentum and parity allows a description in terms of partial waves of definite j and parity, traditionally designated as $s_{1/2}$, $p_{1/2}$; $p_{3/2}$, $d_{3/2}$; $d_{5/2}$, $f_{5/2}$ ... . Very early in the analysis of πN scattering it was recognized that there was a basic ambiguity, pointed out first by Minami, in that the cross-section was unchanged if all the parities of the contributing states were reversed, i.e. : $s_{1/2} \leftrightarrow p_{1/2}$; $p_{3/2} \leftrightarrow d_{3/2}$; $d_{5/2} \leftrightarrow f_{5/2}$; ... .

The resolution of this Minami ambiguity was originally made on the basis of reasonableness of the energy dependence of amplitudes, but later confirmed by recoil polarization measurements. Nowadays the data taken at higher energies with polarized targets eliminates the Minami ambiguity completely and allows determination of parities and spins of resonant states**.

A proof of the Minami ambiguity and its resolution with polarization data can be made with notions of atomic physics. Consider a single electron with spin moving in a central field of force. The spin-angular functions can be chosen as simultaneous eigenfunctions of L^2, S^2, J^2 and J_z. For our purposes we note that the parity of the state is related to the orbital angular momentum ℓ. The eigenfunctions are $\psi^{(\pm)}_{j,\ell,m}$, where the superscript $\pm$ means $j = \ell \pm 1/2$. The operator $\vec{\sigma}.\hat{r}$, where $\hat{r}$ is a unit vector in the radial direction, is a pseudoscalar operator that will change the parity when acting on a state. It is easy to establish that its action on the eigenfunctions above is :

$$\vec{\sigma}.\hat{r}\, \psi^{(\pm)}_{j,\ell,m} = \psi^{(\mp)}_{j,\ell',m} \quad . \tag{14}$$

Thus $\vec{\sigma}.\hat{r}$ reverses the parity of the state, but keeps J^2 and J_z the same. In a scattering problem the momentum representation, rather than the coordinate representation, is appropriate and $\vec{\sigma}.\hat{p}'$ replaces $\vec{\sigma}.\hat{r}$. From the arguments of section III, concerning equations (7)-(10), we see that the Minami substitution :

- does not alter the spin-averaged cross-section ;
- reverses the sign of the polarization.

Unless the experimental situation is terribly complex, observation of the polarization along with the differential cross-section thus allows parity, as well as spin, assignments to be made unambiguously.

Without presenting details we cite the following recent examples of spin and parity determinations using polarized targets :

N*(1674)	$T = \frac{1}{2}$,	$J^P = \frac{5}{2}^-$	(Duke et al, 1965)
N*(1688)	$T = \frac{1}{2}$,	$J^P = \frac{5}{2}^+$	(Duke et al, 1965)
N*(1920)	$T = \frac{3}{2}$,	$J^P = \frac{7}{2}^+$	(Duke et al, 1965)

$\underline{N^*(2190)}$ $\quad T = \frac{1}{2} \quad , \quad J^P = \frac{7}{2}^-$ (Yokosawa et al, 1966)

As evidence of the power of experiments with polarized targets we note that the presence of the N*(1674) resonance underneath the N*(1688) was not even suspected until the detailed Rutherford Laboratory experiment on the $\pi^- p$ polarization.

Before leaving the resonant region I want to point out that the pion-nucleon system is not the only place where resonances occur. We also know of baryonic resonant states with hypercharge Y = 0, -1, -2, and possibly Y = 2. One of the main tasks of experiments in strong interactions is the discovery and identification of these resonant states, in particular their spins and parities and their classification within SU(3), and perhaps higher symmetry, multiplets. Figure 2 indicates the current status of these baryonic resonant states. Obviously much is already known, but much needs to be done.

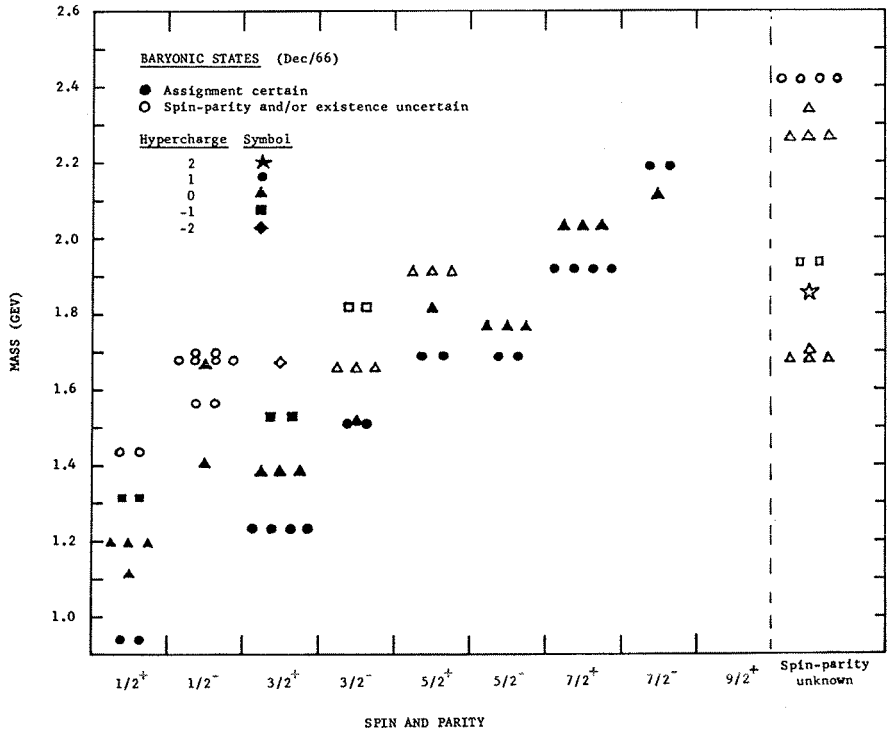

Fig. 2 Baryonic resonant states arranged according to spin and parity. Different values of hypercharge are denoted by different symbols, as indicated on the figure. The number of symbols in each entry is the isospin multiplicity, or number of charge states. By virtue of the mass splittings the arrays of states correspond to their SU(3) weight diagrams. Solid symbols represent certain, or almost certain, assignments of spin and parity. Open symbols indicate existence and/or spin and parity uncertain. The column at the right contains some of the bumps that have been observed but not identified.

There are completed and incipient octets and decimets visible in figure 2, along with other states satisfying no obvious pattern.

When we know how helpful polarized targets have been in elucidating the pion-nucleon states we can expect similar exciting progress for the systems of different hypercharge. The $\bar{K}N$ ($Y = 0$) interaction is rich in complications with its strongly coupled reaction channels. This makes the use of polarized targets less immediate on two scores : a) the small elasticities of many of the resonances make their study in K^-p elastic scattering very difficult, and b) the information obtained from several different reaction channels aids appreciably in the assignment of quantum numbers. Nevertheless, the $Y = 0$ states are sufficiently complex that polarization information will be a necessity. And the possibility of a <u>complete</u> experiment on a reaction like $K^-p \to \pi\Lambda$, with a polarized target and with the Λ polarization observed from its decay, should be kept in mind. Experiments on K^-p elastic scattering are, in fact, in progress at CERN and at the Rutherford Laboratory.

V POLARIZATION IN PION-NUCLEON ELASTIC SCATTERING AND CHARGE EXCHANGE AT HIGH ENERGIES

Another example of polarized targets : why ? is found in the scattering of pions on protons at high energies. Since Dr R.J.N. Phillips treats the subject of the spin dependence of high energy scattering in his report to the Conference, I will restrict my discussion to the rather entertaining story of the charge exchange and the Regge amplitude for ρ-exchange.

The charge exchange process $\pi^-p \to \pi^0n$ is observed to have a total cross-section that decreases somewhat faster than P_{LAB}^{-1} at high energies and shows a typical diffraction pattern. Its peripheral nature implies a simple t-channel exchange. The allowed quantum numbers are $T = 1$, $G = +1$, integer J, and $P = (-1)^J$. The only well established state with these quantum numbers is the ρ-meson. It is therefore natural to attempt to explain charge exchange at high energies with a Regge pole model involving only the ρ-meson trajectory. The detailed differential cross-section measurements from 3 to 18 GeV/c by the Saclay-Orsay group (Sonderegger et al, 1966) are shown in figure 3. These data are quite consistent with the single trajectory hypothesis and allow an accurate determination of the Regge trajectory and residue functions for the ρ-meson

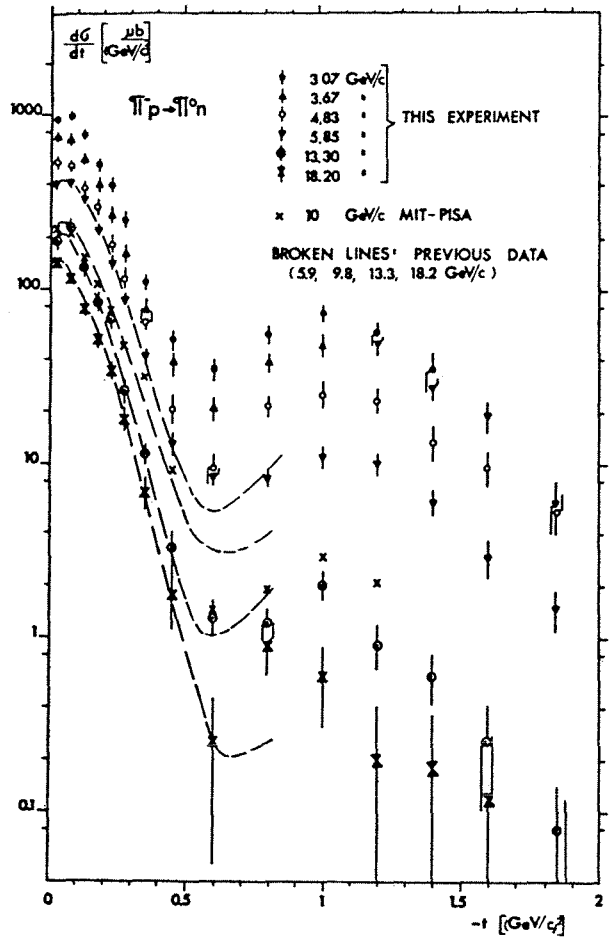

Fig. 3 Differential cross-sections for $\pi^- p \to \pi^0 n$ at various incident momenta from 3 to 18 GeV/c in $\mu b/(GeV/c)^2$ versus momentum transfer, $-t$, in $(GeV/c)^2$. From Sonderegger et al (1966).

(Höhler et al, 1966). The basic Regge pole formula for the differential cross-section in this case is :

$$\frac{d\sigma}{dt} = \left(\frac{\omega}{M}\right)^{2\alpha(t)-2} \left(1 + \frac{t}{4M\omega}\right)^{2\alpha(t)} \frac{1}{2M^4} \left(1 - \frac{t}{4M^2}\right)^{-1} \cdot$$

$$\cdot \left[\frac{2^\alpha \Gamma(\alpha + \frac{3}{2})}{\Gamma(\alpha + 1) \cos\frac{\pi\alpha}{2}}\right]^2 \cdot V(t) \qquad (15)$$

where

$$V(t) = b_+^2(t) - \frac{t\,\alpha^2(t)}{4M^2}\, b_-^2(t) \qquad (16)$$

and ω is the total energy of the incident pion in the laboratory, M is the nucleon mass, $-t$ is the square of the 4-momentum transfer and $\alpha(t)$ is the trajectory of the ρ-meson. The function $V(t)$, equation (16), consists of two terms involving the residue functions $b_\pm(t)$, the first corresponding to the non-helicity-flip amplitude $f_{++} = (f_1 + f_2)\cos\theta/2$ and the second to the helicity-flip amplitude $f_{+-} = (f_1 - f_2)\sin\theta/2$.

The data shown in figure 3 have two especially noteworthy characteristics, the first being the small rise in cross-section from $t = 0$ to $-t \simeq 0.1$ $(\mathrm{GeV}/c)^2$ and the second the minimum at $-t \simeq 0.6$ $(\mathrm{GeV}/c)^2$ followed by a small secondary maximum. The first feature implies a relatively large spin-flip amplitude, while the second can be associated with the vanishing of $\alpha(t)$ at $t \simeq -0.6$. Höhler et al (1966) show that the simplest model, namely constant residues ($b_-/b_+ \simeq 13$) and a linear trajectory ($\alpha(t) = 0.57 + 0.91t$), gives a plausible fit to all the data for $-t < 0.8$ $(\mathrm{GeV}/c)^2$. Other possibilities, involving t-dependences for $b_\pm(t)$, are allowed (see the second reference under Höhler et al, 1966). Despite some arbitrariness and flexibility the overall impression gained is one of success for the Regge pole model.

The story of the ρ-trajectory and residues can be followed further. Elastic pion-nucleon scattering has a Regge pole description customarily in terms of three trajectories P, P' and ρ. The P and P' trajectories describe the universal diffraction scattering process and correspond to the exchange of the unit representations of the symmetry groups such as isospin (often called the quantum numbers of the vacuum). Since the ρ-trajectory carries unit isospin its contribution will appear with opposite signs relative to P and P' in π^+p and π^-p elastic scattering. This is the interpretation of the somewhat different magnitudes and energy dependences of the π^+p and π^-p total cross-section as they approach "asymptopia". But our interest is on another aspect. The phases of Regge amplitudes are related to their trajectories through the so-called signature factor :

$$\frac{\mp 1 - e^{-i\pi\alpha}}{\sin\pi\alpha} = \begin{cases} i - \cot\dfrac{\pi\alpha}{2} & \text{(even)} \\ i + \tan\dfrac{\pi\alpha}{2} & \text{(odd)} \end{cases} \qquad (17)$$

Amplitudes having different trajectories and signatures have different (and t-dependent) phases ; interference terms will give rise to polarization.

For π^+p and π^-p polarization the consequences of the ρ-trajectory and residues discussed above can be understood qualitatively by the following oversimplified argument. We neglect the P' trajectory and assume that the P trajectory is close to unity for all t values of interest. Then (17) shows that the P amplitudes (even signature) are almost purely imaginary. On the other hand, the ρ amplitude (odd signature) at $t = 0$ has roughly equal real and imaginary parts since $\alpha_\rho(0) \simeq 0.57$. Furthermore, the helicity flip amplitude for the ρ-trajectory is an order of magnitude larger than the non-flip amplitude. This means that the polarization :

$$P \frac{d\sigma}{d\Omega} = 2\mathrm{Im}(f_{++} f^*_{+-}) \quad , \tag{18}$$

is given mainly by the imaginary part of the product of the non-flip P amplitude and the complex conjugate of the helicity-flip amplitude. At small t the cross-section is dominated by the non-flip P amplitude. Hence, in rough approximation :

$$P \simeq \frac{2\mathrm{Re}(f_{+-}(\rho))}{\mathrm{Im}(f_{++}(P))} \tag{19}$$

and the denominator in (19) can be obtained as the square root of the elastic differential cross-section. Because of the sign change already mentioned we expect roughly equal and opposite polarizations for π^+p and π^-p elastic scattering. Figure 4 shows a comparison made by Höhler et al (1966) between (19) and experimental data on π^-p polarization at 6 GeV/c observed using a polarized target (Borghini et al, 1966). Similar good agreement is found at

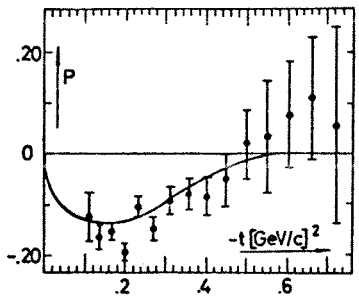

Fig. 4 Comparison of theory and experiment for polarization in π^-p elastic scattering at 6 GeV/c. From Höhler et al (1966). The data are those of Borghini et al (1966).

other momenta and with more elaborate calculations (Chiu et al, 1967). Recent and so far unpublished results on π^+p polarization by the same CERN group show the expected reversal of the sign of the polarization from π^-p and a similar magnitude. Thus the Regge pole description gains credence and the properties of the ρ-trajectory in charge exchange are indirectly confirmed.

The final and most interesting chapter concerns the polarization in charge exchange scattering at high energies. The theoretical expectations are easy to discuss. Since the differential cross-section over a wide range of incident momenta can be understood well in terms of a single Regge exchange both the helicity-flip and non-flip amplitudes have the same phase, namely that of the second line in (17). As a consequence, the polarization (18) vanishes. The theoretical expectation is then that polarization in charge exchange should be very small, certainly smaller than the typical values of 0.15-0.20 found for $\pi^{\pm}p$ elastic scattering.

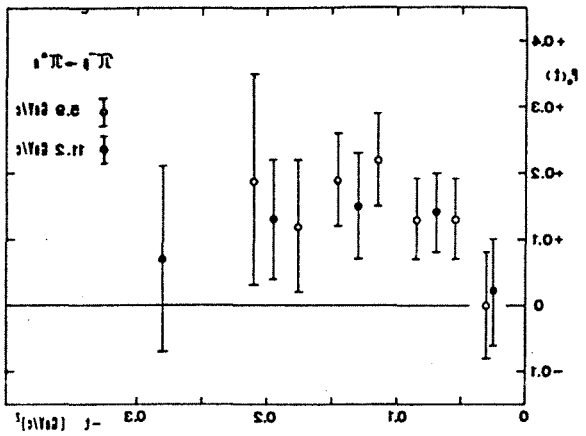

Fig. 5 Polarization in $\pi^-p \to \pi^0n$ at 5.9 and 11.2 GeV/c as a function of momentum transfer $-t$ $(GeV/c)^2$. From Bonamy et al (1966).

The experiment has been performed recently at CERN with a polarized LMN target at incident momenta of 5.9 and 11.2 GeV/c by a Saclay-Orsay-Pisa collaboration (Bonamy et al, 1966). The experiment is described in detail elsewhere in this Conference. Only the results are shown in figure 5. The errors are rather large but it appears that, contrary to theoretical expectations, the polarization is of the same order of magnitude and shape as for elastic scattering and only slowly varying with incident momentum.

This development is, to my mind, a delightful example of physics research, an experiment on the forefront of technology using a polarized target to obtain a result confounding, at least initial-

ly, to the theorists. Explanations in terms of a Regge amplitude interfering with s-channel resonant amplitudes (Phillips, 1966 ; Logan and Sertorio, 1966) suffer from difficulties in producing the experimental dependences on t and s, the predicted polarization generally rising too slowly as a function of angle and decreasing rapidly with increasing incident momentum. Another rabbit up the sleeves of the followers of Regge is the possibility of a ρ' trajectory in addition to the ρ. But the close connection between the phase (17) of a Regge amplitude and its energy dependence $s^{\alpha(t)}$ makes it questionable whether the lack of energy variation of the polarization and its magnitude can be fitted simultaneously. Another possible theoretical model invokes Regge poles with absorptive corrections (equivalent to a certain type of Regge cut in the complex angular momentum plane) (Cohen-Tannoudji et al, 1967 ; Arnold, 1967), but it is too early to tell whether this is the right approach. Out of the confusion of us theorists will undoubtedly come better understanding of high energy scattering. But for the moment the experimenters have the upper hand. Obviously polarization data at 18 GeV/c would be most interesting, but that probably must await hydrocarbon or other targets with a much higher proportion of polarized protons.

VI POLARIZATION IN NUCLEON-NUCLEON SCATTERING

Studies of polarization phenomena in nucleon-nucleon scattering have been made for more than ten years with data at higher and higher energies as time goes on. The theoretical and experimental literature is extensive. We only list some of the basic papers and some of the latest work in order to give an idea of present trends and interests. The theoretical literature goes back to Wolfenstein and Ashkin (1952), Dalitz (1952), Wolfenstein (1954), Oehme (1955), Puzikov et al (1957). Stapp (1956) discussed the relativistic theory carefully and showed the relativistic interpretation of the Pauli spin formulation, such as equation (20) below. Raynal (1961) gave a formulation in terms of helicity amplitudes. The theoretical and experimental situation as of 1960 is treated by MacGregor, Moravcsik and Stapp (1960), and developments up to 1965 are covered in the Proceedings of the Karlsruhe Conference (Huber and Schopper, 1966).

The scattering amplitude for nucleon-nucleon scattering can be written in several different forms. Let $\vec{K}$, $\vec{P}$, $\vec{N}$ be a set of orthogonal unit vectors in the directions $\vec{k}' - \vec{k}$, $\vec{k} + \vec{k}'$ and $\vec{k} \times \vec{k}'$, respectively where $\vec{k}$ and $\vec{k}'$ are the initial and final momenta of

one of the nucleons in the center of mass. Then the most general scattering operator in the combined Pauli spin space of the two nucleons, consistent with parity conservation, time reversal invariance and the Pauli principle (or charge independence), is of the form :

$$\mathcal{F}(\vec{k}',\vec{k}) = a + b(\vec{\sigma}_1 + \vec{\sigma}_2).\vec{N} + d\ \vec{\sigma}_1.N\ \vec{\sigma}_2.\vec{N} + g(\vec{\sigma}_1.\vec{P}\ \vec{\sigma}_2.\vec{P} + \vec{\sigma}_1.\vec{K}\ \vec{\sigma}_2.\vec{K}) + h(\vec{\sigma}_1.\vec{P}\ \vec{\sigma}_2.\vec{P} - \vec{\sigma}_1.\vec{K}\ \vec{\sigma}_2.\vec{K}) \qquad (20)$$

where the scalar amplitudes a, b, d, g, h are functions of W and θ.

Because both projectile and target have spin more complicated spin correlations can occur. Besides the standard Wolfenstein parameters P, D, A, R, A', R' of equation (1) which can be observed with only one of the two nucleons polarized, there are double correlation parameters denoted by C_{NN}, C_{KP}, etc (corresponding to $\langle\vec{\sigma}_1\rangle.\vec{N}\ \langle\vec{\sigma}_2\rangle.\vec{N}$ terms in the cross-section, etc), and even triple correlations that have been observed. The first observation of C_{NN} was made at Saclay in 1962 by Abragam et al (1962), using a 20 MeV proton beam, almost completely polarized by scattering, incident on a polarized target ($\pm$ 20 % polarization). The scattering at 90° was observed for the target polarization parallel and antiparallel to the incident beam's polarization, both being perpendicular to the scattering plane. The result was $C_{NN} = -0.91 \pm 0.05$. The Saclay experiment illustrates one way to determine C_{NN}, with both projectile and target polarized initially. But by having only one polarized initially and detecting the other nucleon's polarization after the scattering, the same spin correlation parameters can be studied. This is the basis of the recent Dubna experiment (Golovin et al, 1966) on p-p scattering at 605 MeV in which C_{NN}, C_{KP} and C_{QKN} (the first triple correlation) were measured at 90°.

Recent measurements of P for p-p scattering using a polarized target have been made at Berkeley in the 300 to 750 MeV region (Betz et al, 1966) and also from 1.7 to 6.15 GeV (Grannis et al, 1966). Representative experiments without polarized targets, using the double scattering technique, are those of McManigal et al (1965, 1966) at 725 MeV.

At low and medium energies observations of the Wolfenstein and spin correlation parameters limit the allowable sets of phase shifts and help to discriminate between different models of the nucleon-nucleon interaction (for a comprehensive analysis of data up to 330 MeV, see Arndt and MacGregor, 1966). At high energies the comparison between theory and experiment is phrased in terms of Regge poles. If two Regge poles are dominant in the description of the scattering, quantities such as the polarization should show power law behaviour in $s = W^2$ ($P \sim s^{\alpha_1(t) - \alpha_2(t)}$) at fixed momentum transfer. Grannis et al (1966) finds $P \sim s^n$ with $n \simeq 0.7 \pm 0.3$ for all $-t < 0.4$ (GeV/c)^2.

This is consistent with the idea that the polarization is produced by interference between amplitudes associated with the P, P' and ω trajectories, the latter two having intercepts at $t = 0$ of $\alpha(0) \simeq 0.5$.

Of even more interest at high energies are observations that test the basic assumptions of the Regge pole theory. Leader and Slansky (1966) show, among other things, that as a consequence of the hypothesis of factorization of residues the spin correlation parameter C_{NN} should fall off roughly as $E_{Lab}^{-1/2}$ (actually as $s^{\alpha_2 - \alpha_1}$, where α_1 is the P trajectory and α_2 is the next highest trajectory to contribute). If factorization does not hold, C_{NN} is expected to approach a constant value in "asymptopia". Detailed measurements on C_{NN} and P for p-p scattering as a function of angle and energy from 0.5 to 1.2 GeV have been performed at Saclay (Cozzika et al, 1966). When combined with other data the behaviour of C_{NN} as a function of energy begins to emerge***. But the observations must be extended to much higher energies before questions such as the power law behaviour can be answered. The experimenter should address himself to the problem of creating a polarized beam or detecting the polarization of a scattered beam at 10 to 30 GeV/c. Polarized targets are waiting.

VII VECTOR MESON PRODUCTION FROM A POLARIZED TARGET

Our discussion so far has been about experiments that have actually been performed. We now give an example of the use of a polarized target that has not as yet been done, and probably is much too difficult to do with existing targets, but which potentially contains useful information on production mechanisms and Regge poles. It is the study of the production and decay of vector mesons (or higher spin boson resonances) from a polarized target. The general theory has been discussed by Byers and Yang (1964), but I will give a somewhat different treatment.

For definiteness consider the reaction, $KN \rightarrow K^*N'$, in which the $K^*(892)$ decays subsequently into $K\pi$. The process is shown schematically in figure 6. In the rest frame of the K^* the angular distribution of decay is :

$$W_o(\alpha,\beta) = \frac{3}{4\pi}\left\{\rho_{00}\cos^2\alpha + \rho_{11}\sin^2\alpha - \rho_{1,-1}\sin^2\alpha\cos 2\beta - \sqrt{2}\,\mathrm{Re}\,\rho_{10}\sin 2\alpha\cos\beta\right\} \quad (21)$$

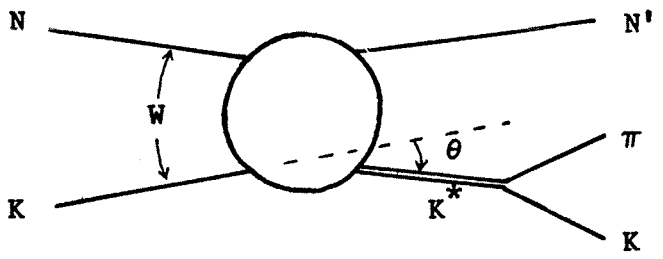

Fig. 6 Schematic diagram of vector meson production and subsequent decay from a polarized target.

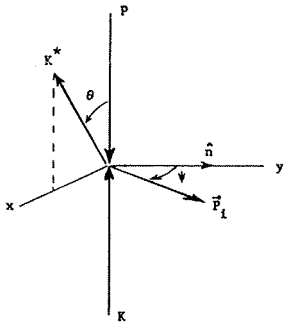

Fig. 7 Definition of angles for production plane and target polarization direction.

where (α,β) are the polar and azimuthal angles of decay relative to a z-axis in the production plane, and $\rho_{mm'}$ are the elements of the spin density matrix of the K* produced from an unpolarized target (Gottfried and Jackson, 1964). For higher spin resonances the decay angular distribution has a more complicated angular dependence, but a similar structure involving the density matrix elements of the resonant state.

Production from a polarized target involves an azimuthal angle ψ between the target polarization $\vec{P}_i$ (chosen perpendicular to the incident beam for simplicity) and the normal to the production plane, as shown in figure 7. $\psi = 0$ and $\psi = \pi$ correspond to the left and right scatterings in an asymmetry experiment. For an unpolarized target the density matrix elements of the vector (or higher spin) meson are functions of center of mass energy and angle :

$$\rho_{mm'} = A_{mm'}(W,\theta) \quad . \tag{22}$$

With a polarized target each element behaves similarly to the π-N cross-section, equation (11), for a polarized target with no recoil polarization being observed namely :

$$\rho_{mm'} = A_{mm'}(W,\theta) + P_i\left[\cos\psi\, B_{mm'}(W,\theta) + \sin\psi\, C_{mm'}(W,\theta)\right] \tag{23}$$

Thus the decay correlations described by equation (21) will, in general, show a left-right asymmetry, that is, the decay angular distribution will be different for a K* meson produced on the right from that of one produced on the left.

The coefficients $A_{mm'}$ in (22) are elements of the usual density matrix, given in unnormalized form in the helicity representation by :

$$\langle \lambda_V | \rho_o | \lambda'_V \rangle = \frac{1}{2} \sum_{\lambda_N \lambda_{N'}} \langle \lambda_V \lambda_N, |T| \lambda_N \rangle \langle \lambda'_V\ \lambda_N, |T| \lambda_N \rangle^* \quad . \tag{24}$$

The polarization coefficients $B_{mm'}$ are related to the nonhermitean density matrix ρ_1 :

$$\langle \lambda_V |\rho_1| \lambda_V' \rangle = \frac{1}{2} \sum_{\lambda_N'} \langle \lambda_V \lambda_N', |T| \tfrac{1}{2} \rangle \langle \lambda_V' \lambda_N', |T| -\tfrac{1}{2} \rangle^* \quad . \quad (25)$$

The decay distribution (21) is augmented by terms proportional to P_i :

$$\begin{aligned} W(\alpha,\beta) = W_o(\alpha,\beta) + \frac{3}{4\pi} P_i \cos\psi \Big\{ & 2\mathrm{Im}(\rho_1)_{00} \cos^2\alpha \\ & + 2\mathrm{Im}(\rho_1)_{11} \sin^2\alpha - \mathrm{Im}[(\rho_1)_{1,-1} + (\rho_1)_{-1,1}] \sin^2\alpha \cos 2\beta \\ & - \sqrt{2}\, \mathrm{Im}[(\rho_1)_{10} + (\rho_1)_{01}] \sin 2\alpha \cos\beta \Big\} \\ - \frac{3}{4\pi} P_i \sin\psi \Big\{ & \mathrm{Im}[(\rho_1)_{1,-1} - (\rho_1)_{-1,1}] \sin^2\alpha \sin 2\beta \\ & + \sqrt{2}\, \mathrm{Im}[(\rho_1)_{10} - (\rho_1)_{01}] \sin 2\alpha \sin\beta \Big\} \quad . \end{aligned} \quad (26)$$

Here $W_o(\alpha,\beta)$ is given by (21) with elements of the density matrix (24).

Reactions in which production from a polarized target might prove interesting are (a) $\pi N \to \rho N$ and (b) $\pi N \to \omega N$. In ρ-production up to the highest momenta pion exchange seems to dominate, although ω and A_2 exchange should be present and be increasingly more important as the energy is increased. Perhaps the presence of these higher spin exchanges can be established through interference effects in the polarization, although the fact that pion-exchange contributes mainly to A_{00}, while ω exchange produces nonvanishing A_{11} and $A_{1,-1}$, probably means that the polarization effects are small. The production of ω's is probably more interesting, although technically more difficult. The only simple peripheral mechanism is ρ exchange. The Born amplitude leads to $\rho_{00} = \rho_{10} = 0$ in (21) if the z-axis is the momentum transfer direction, and consequently a characteristic $\sin^2\alpha(a + b\cos 2\beta)$ decay correlation. Instead, at incident momenta of 2-3 GeV/c the decay angular distribution is found to be roughly $(1 + \cos^2\alpha)$, corresponding to $\rho_{00} \simeq 0.5$. One

fairly satisfactory explanation of this discrepancy is in terms of absorptive corrections to the low partial waves (Jackson et al, 1965). But other explanations are possible. One invokes the exchange of the B-meson, with conjectured spin-parity 1^+, in addition to the 1^- ρ-meson. With Regge amplitudes whose phases are given by equation (17) sizeable interference effects can occur provided the B and ρ trajectories are sufficiently different. This means that if polarization effects are studied a choice between explanations should be possible, as well as a further elucidation of Regge trajectories. Calculations on some of these problems are in progress.

VIII TIME-REVERSAL AND ELECTROMAGNETIC INTERACTIONS

The final example of uses of polarized targets is a test of time-reversal invariance for electromagnetic interactions proposed by Christ and Lee (1966). As is well known, the violation of PC invariance in the decay of the long-lived neutral K meson led T.D. Lee to propose that electromagnetic interactions did not have particle-antiparticle conjugation (C_{st}) invariance, or time-reversal (T_{st}) invariance in the sense of the strong interactions. The seemingly instant objections to this proposal were shown not to exist. Most of the aspects of electromagnetic interactions that we attribute to charge conjugation invariance follow from hermiticity and/or current conservation alone.

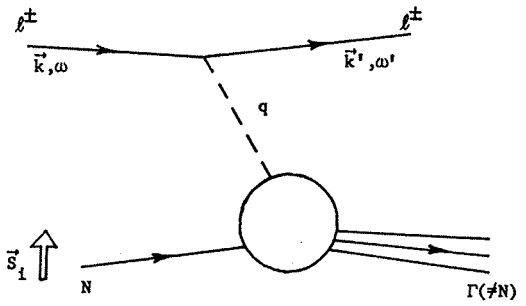

Fig. 8 Schematic diagram of inelastic lepton scattering from a polarized target as a test of the time-reversal invariance of electromagnetic interactions.

The Christ-Lee experiment using a polarized target is inelastic charged lepton scattering, as indicated in figure 8. The reaction leading to a final state Γ distinct from the initial state N (to avoid a null effect as a consequence of current conservation) has a cross-section, to lowest order in e^2 :

$$d\sigma = \frac{4\pi\alpha^2 k'}{m_\Gamma k (q^2)^2} \left\{ \quad \right\} d\omega' d(\cos\theta) \qquad (27)$$

where $(\vec{k},\omega)$ and $(\vec{k}',\omega')$ are the laboratory momentum and energy of the incident and outgoing lepton, respectively, q^2 is the square of the 4-momentum transfer, θ is the angle between the $\vec{k}$ and $\vec{k}'$, and the curly bracket is :

$$\left\{ \quad \right\} = \Big\{ 2(\omega\omega' - kk' \cos\theta - 2m_\ell^2) W_1(q^2, m_\Gamma) + (\omega\omega' + kk' \cos\theta + m_\ell^2) W_2(q^2, m_\Gamma) + \vec{S}_i \cdot (\vec{k} \times \vec{k}') \left(\frac{\omega^2 - \omega'^2}{m_N^2} \right) W_3(q^2, m_\Gamma) \Big\} \quad . \qquad (28)$$

$\vec{S}_i$ is the polarization of the target (taken as spin 1/2 for simplicity). The functions W_i are quadratic in the three form factors F_j that describe the $\gamma N\Gamma$ vertex. W_1 and W_2 involve absolute squares or real parts of products of form factors. But W_3 is proportional to the imaginary part of $F_i^* F_j$. If the electromagnetic interaction violates T_{st} the F_j are not necessarily relatively real ; W_3 does not have to vanish.

Observation of a left-right asymmetry would thus establish lack of time-reversal invariance in electromagnetic interactions, provided single photon exchange dominates. An effect specific to failure of time-reversal invariance can be distinguished from that caused by two-photon exchange by means of positively and negatively charged leptons. The contribution from two-photon exchange will change sign with the sign of the charge of the lepton ; the other will not.

This experiment presents a real challenge to the makers of polarized targets : the small electromagnetic cross-sections necessitate intense electron beams which present serious problems of heat dissipation and radiation damage. But that is the province of others at this Conference.

IX SUMMARY

Study of polarization phenomena is a good thing. Observation of the transformation of a spin in a scattering act (described by the so-called Wolfenstein parameters, Section II) yields additional information about the scattering amplitudes beyond what stems from the cross-section alone. Some of the examples are :

1. Intrinsic parity determination (Section III) - Comparison of the polarization of an outgoing fermion with the left-right asymmetry from a polarized target determines intrinsic parity of the final state relative to the initial.

2. Spins and parities of resonant states (Section IV) - Polarization measurements remove the Minami ambiguity and, when combined with differential cross-section data, allow assignments of spins and parities of resonances.

3. Polarization at high energies (Section V) - Regge pole and other models of high energy scattering are subjected to stringent tests by polarization data. Pion-nucleon charge exchange is an excellent object lesson.

4. Polarization in nucleon-nucleon scattering (Section VI) - At low and medium energies measurements of Wolfenstein and spin correlation parameters limit choices of phase shifts and potential models of the N-N interactions. At high energies such data can yield information on Regge trajectories and test the basic assumptions of the model.

5. Vector meson production from a polarized target (Section VII) - The exchange mechanisms in peripheral production processes can be elucidated with data from polarized targets.

6. Test of time-reversal invariance in electromagnetic interactions (Section VIII) - Observation of a left-right asymmetry in the inelastic scattering of charged leptons from a polarized target can establish T.D. Lee's idea that there is T (and C) violation in the electromagnetic Hamiltonian.

Notes and References

* For the present circumstances of spin 0-spin 1/2 interactions the result does not depend on time reversal invariance.

** There is another ambiguity, $\delta_i \rightarrow -\delta_i$, or equivalently complex conjugation of all amplitudes, and it combined with the Minami transformation. But the requirement that a resonant amplitude move in a counter-clockwise manner with increasing energy removes these further ambiguities.

*** The value of C_{NN} at 90° is small between 50 and 100 MeV, rises rapidly above 100 MeV to positive values of the order of 0.4 to 0.9 between 150 and 500 MeV, reaches a peak of 0.8 in the neighbourhood of 700-750 MeV, and then falls rapidly to 0.15 ± 0.20 at 1.2 GeV.

Abragam A., Borghini M., Catillon P., Coustham J., Roubeau P. and Thirion J., Phys. Letters, 1962, 2, 310.
Abragam A. and Borghini M., Progress in Low Temperature Physics, 4 (C.J. Gorter, ed., North-Holland, Amsterdam, and Interscience, N.Y., 1964).
Arndt R.A. and MacGregor M.H., Phys. Rev., 1966, 141, 873.
Arnold R.C., Phys. Rev., (to be published, 1967).
Atkinson H.H., Cox C.R., Duke P.J., Heard K.S., Jones D.P., Kemp M.A.R., Murphy P.G., Prentice J.D. and Thresher J.J., Proc. Roy. Soc., 1965, A289, 449.
Bareyre P., Proc. Roy. Soc., 1965, A289, 463.
Betz F., Arens J., Chamberlain O., Dost H., Grannis P., Hansroul M., Holloway L., Schultz C. and Shapiro G., Phys. Rev., 1966, 148, 1289.
Bilenky S.M., Nuovo Cimento, 1958, 10, 1049.
Bonamy P., Borgeaud P., Bruneton C., Falk-Vairant P., Guisan O., Sonderegger P., Caverzasio C., Guillaud J.P., Schneider J., Yvert M., Mannelli I., Sergiampietri F. and Vincelli L., Phys. Letters, 1966, 23, 501.
Borghini M., Coignet G., Dick L., DiLella L., Michalowicz A., Macq P.C. and Olivier J.C., Phys. Letters, 1966, 21, 114.
Byers N. and Yang C.N., Phys. Rev., 1964, 135, B796.
Chamberlain O., Jeffries C.D., Schultz C.H., Shapiro G. and Van Rossum L., Phys. Letters, 1963, 7, 293.
Chamberlain O., Hansroul M.J., Johnson C.H., Grannis P.D., Holloway L.E., Valentin L., Robrish P.R. and Steiner H.M., Phys. Rev. Letters, 1966, 17, 975.
Chiu C.B., Phillips R.J.N. and Rarita W., Phys. Rev., (to be published, 1967).
Christ N. and Lee T.D., Phys. Rev., 1966, 143, 1310.
Cohen-Tannoudji G., Morel A. and Navelet H., Saclay preprint, (to be published, 1967).
Cozzika G., Ducros Y., De Lesquen A., Movchet J., Raoul J.C., Van Rossum L., Deregel J. and Fontaine J.M., Paper submitted to Session 8-C, Berkeley Conference, 1966.
Dalitz R.H., Proc. Phys. Soc., 1952, A65, 175.
Dickson J.M., Progress in Nuclear Techniques and Instrumentation, 1 (F.J.M. Farley, ed., North-Holland, Amsterdam, 1965).
Duke P.J., Jones D.P., Kemp M.A.R., Murphy P.G., Prentice J.D., Thresher J.J., Atkinson H.H., Cox C.R. and Heard K.S., Phys. Rev. Letters, 1965, 15, 468.

Golovin B.M., Zulkarneyev R.Ya., Kiselev V.S., Medved S.V., Nikanorov V.I., Pisarev A.F. and Semashko G.L., Paper submitted to Session 8-C, Berkeley Conference, 1966.
Gottfried K. and J.D. Jackson, Nuovo Cimento, 1964, 33, 309.
Grannis P., Arens J., Betz F., Chamberlain O., Dieterle B., Schultz C., Shapiro G., Steiner H., Van Rossum L. and Weldon D., Phys. Rev., 1966, 148, 1297.
Höhler G., Baacke J., Schlaile H. and Sonderegger P., Phys. Letters, 1966, 20, 79.
Höhler G., Baacke J. and Eisenbeiss G., Phys. Letters, 1966, 22, 203.
Huber P. and Schopper H., ed., Proceedings of the 2nd International Symposium on Polarization Phenomena of Nucleons, Karlsruhe, Sept. 6-10, 1965 (Birkhaüser Verlag, Basel and Stuttgart, 1966).
Jackson J.D., Donohue J.T., Gottfried K., Keyser R. and Svensson B.E.Y., Phys. Rev., 1965, 139, B428.
Jeffries C.D., Dynamical Nuclear Orientation, (John Wiley, New York, 1963).
Jeffries C.D., Ann. Rev. Nucl. Sci., 14 (E. Segré, ed., Annual Reviews, Palo Alto, 1964).
Leader E. and Slansky R.C., Phys. Rev., 1966, 148, 1491.
Logan R.K. and Sertorio L., Phys. Rev. Letters, 1966, 17, 834.
MacGregor M.H., Moravcsik M.J. and Stapp H.P., Ann. Rev. Nucl. Sci., 10 (E. Segré, ed., Annual Reviews, Palo Alto, 1960).
McManigal P.G., Eandi R.D., Kaplan S.N. and Moyer B.J., Phys. Rev., 1965, 137, B620.
McManigal P.G., Eandi R.D., Kaplan S.N. and Moyer B.J., Phys. Rev., 1966, 148, 1280.
Moravcsik M.J., Two-Nucleon Interaction (Oxford University Press, 1963).
Oehme R., Phys. Rev., 1955, 98, 147, 216.
Phillips R.J.N., Nuovo Cimento, 1966, 45A, 245.
Puzikov L., Ryndin R. and Smorodinsky J., Nucl. Phys., 1957, 3, 436.
Raynal J., Nucl. Phys., 1961, 28, 220.
Shapiro G., Progress in Nuclear Techniques and Instrumentation, 1 (F.J.M. Farley, ed., North-Holland, Amsterdam, 1965).
Sonderegger P., Kirz J., Guisan O., Falk-Vairant P., Bruneton C., Borgeaud P., Stirling A.V., Caverzasio C., Guillaud J.P., Yvert M. and Amblard B., Phys. Letters, 1966, 20, 75.
Stapp H.P., Phys. Rev., 1956, 103, 425.
Suwa S., Yokosawa A., Booth N.E., Esterling R.J. and Hill R.E., Phys. Rev. Letters, 1965, 15, 560.
Wolfenstein L. and Ashkin J., Phys. Rev., 1952, 85, 947.
Wolfenstein L., Phys. Rev., 1954, 96, 1654.
Yokosawa A., Suwa S., Hill R.E., Esterling R.J. and Booth N.E., Phys. Rev. Letters, 1966, 16, 714.

This work was supported by the U.S. Office of Naval Research under Contract Task A-05-T.

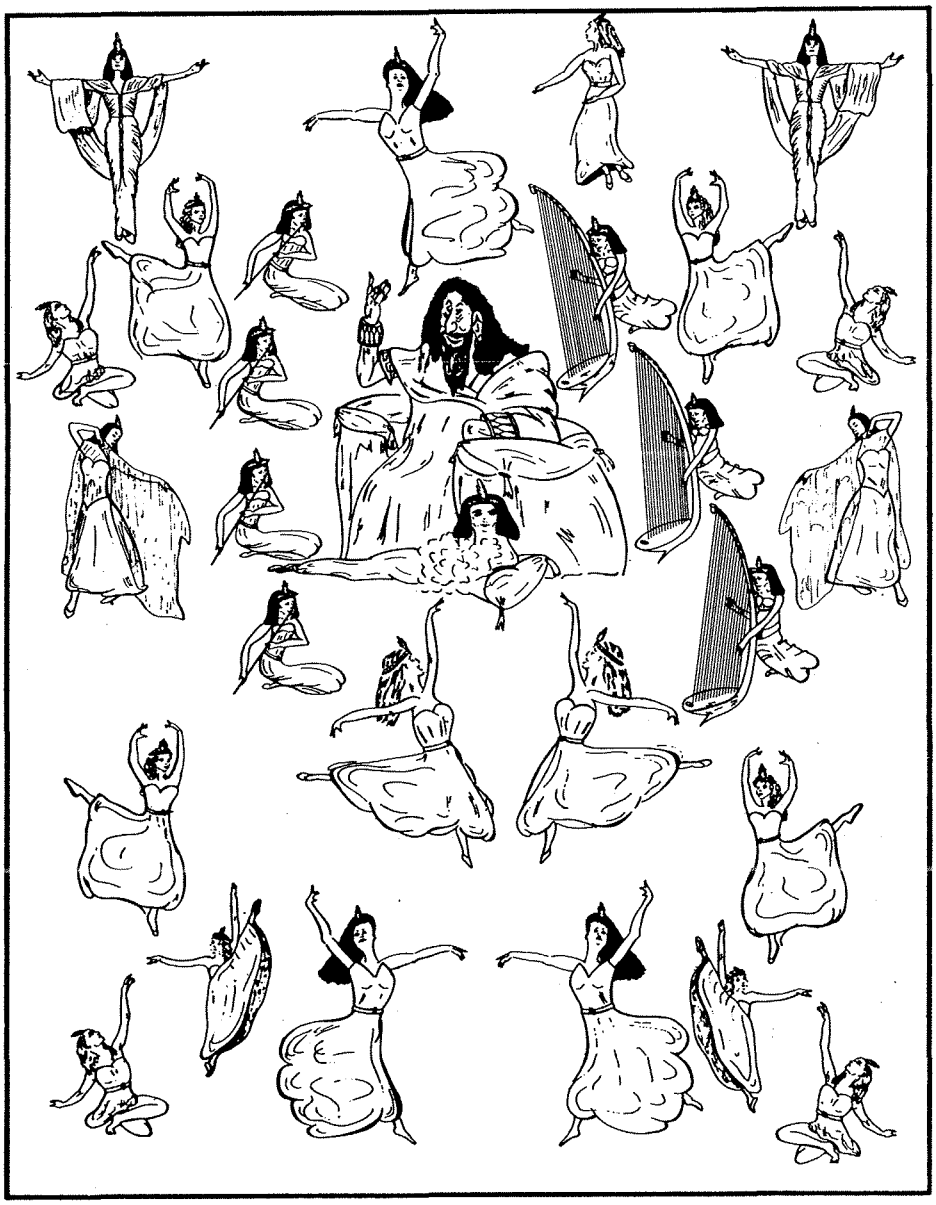

« Le Roi Salomon eut donc sept cents femmes princesses... »

(I Rois XI)

$(N_t/N_s) = 700$ *(see page 33)*

POLARIZED TARGETS : HOW?

A. ABRAGAM

Direction de la Physique, Saclay

INTRODUCTION

It is well known that an assembly of magnetic moments μ embedded in a sample of bulk matter in thermal equilibrium at a temperature T will, when placed in a magnetic field H, orient themselves preferentially in the direction of the field. This orientation is not perfect : there is competition between the magnetic energy μH which tends to orient the moments parallel to the field and the thermal energy kT, which destroys the orientation. If N is the number of moments per unit volume, the magnetization M along the field will reach the value $M = N\mu P$ where P, a number smaller than unity, is called the polarization. For weak polarizations, P is simply the ratio $\mu H/kT$ of these two energies ; this is the celebrated Curie law. For nuclear spins I the magnetic moment is an operator $\underset{\sim}{\mu}_n = \gamma_n \hbar \underset{\sim}{I}$ where γ_n is a constant, characteristic of the nuclear species. The nuclear polarization P_n is the ensemble average $\langle I_z \rangle / I$, taken over all the spins of the sample, Oz being the direction of the field.

For a spin $I = 1/2$, P_n is given by :

$$P_n = \tanh \left(\frac{\gamma_n \hbar H}{2kT} \right) \qquad (1)$$

which reduces to $\mu H/kT$ when P_n is small.

For fields and temperatures easily obtainable in the laboratories the nuclear polarizations are exceedingly small (0.1 % for protons with H = 10 kilogauss, T = 1° K).

Recent progress in the production of very high magnetic fields by means of superconducting coils and of very low temperatures by

means of the new ^3He-^4He refrigerators may open in the future new prospects for the so-called "brute force" method which aims at producing sizeable nuclear polarization through the sheer increase of the (H/T) ratio.

In the meantime we shall concern ourselves with polarizations obtainable by dynamical methods in "conventional" fields and temperatures ($H \sim 20$ kilogauss, $T \sim 1°$ K).

All methods of dynamic nuclear polarization in bulk matter stem from the remark that for "conventional" values of field and temperature the equilibrium polarization P_e^o of electronic spins localized on paramagnetic atoms or ions (given by (1), where γ_n is replaced by the electronic gyromagnetic ratio γ_e, three orders of magnitude greater than γ_n) is large and may approach 100 %.

Dynamic methods use the magnetic couplings that exist between electronic and nuclear spins to transfer to the latter a polarization comparable in magnitude to the electronic polarization P_e and of the same sign or of opposite sign.

The first of these methods is due to Overhauser [1] who predicted that in metals the saturation of the spin resonance of conduction electrons could lead to a nuclear polarization comparable to the electronic polarization but of opposite sign. (More accurately, to the polarization that the conduction electrons would exhibit if they obeyed Boltzmann rather than Fermi statistics).

Shortly afterwards, this prediction received an experimental confirmation [2]. A detailed theoretical analysis [3] showed that although this method could under certain conditions be extended to non-metallic substances and in particular to liquids containing in solution paramagnetic impurities, it did not apply to diamagnetic solids containing localized paramagnetic impurities, which is by far the most interesting case for the construction of polarized targets.

There exists however a different method, sometimes called the "solid effect" which is applicable to non-metallic solids at low temperatures.

The solid effect and the Overhauser effect are "orthogonal" in the sense that in substances where one of these two methods is operative the other is not, in general (metals, liquids, paramagnetic substances with strong exchange forces between the electronic spins, for the Overhauser effect ; fixed paramagnetic impurities for the solid effect).

Although proposed at a later date the solid effect is conceptually simpler than the Overhauser effect. It is also the only method that has been used successfully so far for dynamically polarized solid targets. In the following we shall concern ourselves with the solid effect only.

A FEW FACTS ABOUT MAGNETIC RESONANCE [4)]

Larmor frequency

The behaviour of nuclear magnetic moments in magnetic fields (d-c or r-f) can be described either classically or quantum-mechanically whichever is more convenient. We shall consider spins 1/2 only, a simplifying but by no means essential restriction. Quantum-mechanically, the Larmor frequency of a nuclear spin in a d-c field H_0, $\omega_n = \gamma_n H_0$ is the energy difference between the two orientations of this spin in the field H_0 expressed in frequency units :

$$\omega_n = \frac{\Delta E}{\hbar} = \frac{2\mu_n H_0}{\hbar} \quad .$$

Classically it is the angular frequency of the free precession of the nuclear magnetization $\underset{\sim}{M}$ around the field $\underset{\sim}{H}_0$. At thermal equilibrium the magnetization is aligned along $\underset{\sim}{H}_0$ and the precession cannot be observed. On the other hand it will become observable if by means such as say a sudden change in the orientation of $\underset{\sim}{H}_0$, or by other means to be described shortly, $\underset{\sim}{M}$ is brought to make a finite angle with $\underset{\sim}{H}_0$.

Magnetic resonance

A sample of bulk matter in thermal equilibrium in a d-c field $\underset{\sim}{H}_0$ will have an equilibrium nuclear magnetization $\underset{\sim}{M}_0 = \chi \underset{\sim}{H}_0$. If a rotating r-f field of amplitude H_1 and frequency ω in the neighbourhood of the nuclear Larmor frequency ω_0 is applied to the sample at right angle to H_0, the nuclear magnetization of the sample will change appreciably even if H_1 is several orders of magnitude smaller than H_0.

This is easily understood in a simple-minded quantum-mechanical language : the r-f field induces transitions (emission and absorption of photons of frequency ω) between the two energy levels $I_z = \pm 1/2$ of the nuclear spin, separated by $\hbar\omega_0$. The resonance condition $\omega \approx \omega_0$ is simply the conservation of energy. In thermal equilibrium the lower level is more populated than the higher, there will be more upward than downward transitions, whence a net absorption of r-f energy by the system of nuclear spins and a decrease of the total nuclear magnetization.

This approach disregards an important feature of the r-f field, namely its coherence, preserved in the classical description. It is convenient to analyze the phenomenon in a frame of reference rotating at the frequency ω of the r-f field. In that frame the r-f field appears as a small d-c field of amplitude $H_x = H_1$ whereas the rotation of the frame is taken into account by adding to H_0

a fictitious field of magnitude $H_f = -\omega/\gamma$. The nuclear spins in the rotating frame "see" a so-called d-c effective field $\underset{\sim}{H}_{eff}$ with components :

$$H^z_{eff} = H_o - \frac{\omega}{\gamma} = \frac{\omega_o - \omega}{\gamma} \quad \text{and} \quad H^x_{eff} = H_1 \ .$$

Far from resonance $\underset{\sim}{H}_{eff}$ is practically parallel to H_o and the nuclear magnetization $\underset{\sim}{M}_o$, aligned along $\underset{\sim}{H}_o$, has no reason to change. Near resonance $\underset{\sim}{H}_{eff}$ can make a large angle with $\underset{\sim}{H}_o$ and the nuclear magnetization will tend to precess around $\underset{\sim}{H}_{eff}$ rather than $\underset{\sim}{H}_o$. Going back to the laboratory frame we see that the nuclear magnetization acquires a transverse component precessing at the frequency ω, a feature which did not appear in the quantum-mechanical treatment above. Needless to say, a more sophisticated quantum-mechanical treatment where the statistical behaviour of the nuclear spins is described by a statistical operator with off-diagonal matrix elements restores the proper picture.

Spin-lattice relaxation

The establishment of thermal equilibrium which leads to the value (1) for the nuclear polarization is not instantaneous. The time constant associated with this process which provides some measure of the strength of the coupling between the spins and the other degrees of freedom of the sample is represented in the literature by the symbol T_1 and called the spin-lattice relaxation time [4]. Depending on the nature of the sample, its physical state, its temperature, its purity, etc.., the nuclear relaxation time varies between very large limits. The shortest times observed are of the order of microseconds or even less, the largest, of the order of hours, days or more, are often limited only by the impurities content of the sample. Whatever the relaxation mechanism and there are many, its effect is to establish an inequality among the populations of the nuclear spin energy levels. When a resonant r-f field is applied to the sample, resonance and relaxation are competing processes, the former striving to equalize the populations between which the r-f transition takes place, the latter attempting to maintain between them the Boltzmann ratio $\exp -(\hbar\omega_o/kT)$.

If the r-f field is so strong that the transition probability W is much larger than the relaxation rate $1/T_1$, the populations of the two levels between which the transition takes place become equal and the resonance is said to be saturated.

Line width, local field, spin diffusion

The interaction between two nuclear moments at a distance r from each other is given by the dipole-dipole Hamiltonian :

$$\mathcal{H}_d = \frac{\sigma\sigma'\hbar^2}{r^3}\left\{\underset{\sim}{I}\cdot\underset{\sim}{I}' - \frac{3(\underset{\sim}{I}\cdot\underset{\sim}{r})(\underset{\sim}{I}'\cdot\underset{\sim}{r})}{r^2}\right\} \qquad (2)$$

Its effect is to broaden the energy levels of a system of many nuclear spins and thus also the resonance line. It is convenient, if not quite accurate, to introduce the concept of local field which is the field produced at the site of a nuclear spin by its neighbours. The local field is in general of the order of a few gauss and thus usually much smaller than the applied d-c field H_o. The local field varies from site to site in a random way, whence the broadening of the resonance.

If the nuclear polarization is very weak, for every spin that "sees" a local field, say parallel to the applied field, there will be another spin whose local field is equal but opposite and the resonance line will be symmetrical with respect to the central frequency. On the other hand for high polarizations the spins will "see" more local fields of one sign than of the other and the line will become asymmetrical.

Another effect of the interaction (2) is the spin-diffusion. This interaction contains operators such as $I_+I'_-$ whereby neighbouring spins can exchange their orientations by "flip-flops" that conserve energy if $\sigma = \sigma'$. A local inhomogeneity in the nuclear polarization will diffuse through the sample by means of these "flip-flops". The probability W per unit time of a "flip-flop" between, say, two neighbouring protons, is in general of the order of 10^{-4} s-1. For dimensional reasons it is clear that the diffusion coefficient D will be of the order of Wa^2, where a is the distance between neighbouring spins, that is of the order of 10^{-12}, 10^{-13}.

Electronic spins

Most of what has been said above applies to electronic spins and to electron spin resonance. The main changes are :

a. much larger Larmor frequencies which in "conventional" fields fall into the microwave range ,

b. much shorter relaxation times.

At very low temperatures, the relaxation mechanism is due to the direct process, absorption or emission of a single phonon of energy $\hbar\omega_o$. For this process the lifetimes τ_+ and τ_- of the ground and excited electron spin state are proportional respectively to $\bar{n} + 1$ and $\bar{n}$ where according to Planck's law :

$$\bar{n} = \left[\exp\left(\frac{\hbar\omega_o}{kT}\right) - 1\right]^{-1} . \qquad (3)$$

From (1) we get :

$$\left.\begin{aligned} \frac{1}{\tau_+} \propto (\bar{n}+1) = \frac{1+P_0}{2P_0} \qquad \frac{1}{\tau_-} \propto \bar{n} = \frac{1-P_0}{2P_0} \\ \frac{1}{T_e} = \frac{1}{\tau_+} + \frac{1}{\tau_-} \propto \frac{1}{P_0} \end{aligned}\right\} \qquad (4)$$

For very low temperatures $P_0 \to 1$, and the electron relaxation time tends toward a finite limit which is simply the lifetime of the upper state.

c. for many paramagnetic ions, large anisotropy of the Larmor frequency.

Elementary theory of the solid-effect

Consider an assembly of nuclear spins $I = 1/2$ embedded in a diamagnetic solid that contains a few paramagnetic impurities with spins $S = 1/2$.

Assume for simplicity (but quite realistically) values of H and T such that to a good approximation the electronic spins S are completely polarized, say all "up" and the nuclear spins I completely unpolarized, as many "up" as "down". The dipolar interaction (2) (where I' is replaced by S) permits simultaneous reversals of S and I in opposite directions, or flip-flops and also reversals in the same direction which we shall call flip-flips. However in such reversals the total energy of the spin system changes by an amount $h(\omega_S \pm \omega_I)$ and the process will not occur unless the missing energy is supplied by the crystalline lattice, usually in the form of one or several phonons. It is precisely those simultaneous reversals that are responsible for the classical mechanism of nuclear relaxation by paramagnetic impurities. The rate of these processes can be very small at low temperatures ($1/T_n \sim 10^{-3}$ s^{-1} is a typical value for polarized targets materials). On the other hand the reversal of an electronic spin <u>alone</u>, caused by its coupling to the lattice occurs at a much higher rate: $1/T_e$ ($1/T_e \sim 10^3$ s^{-1} is a typical value). Suppose now that an external source of microwave energy at a frequency $\Omega = \omega_S \pm \omega_I$ is capable of inducing either flip-flops ($\Omega = \omega_S - \omega_I$) or flip-flips ($\Omega = \omega_S + \omega_I$). Assume also that the electronic line-width $\Delta\omega_S$ is much smaller than the nuclear frequency ω_I so that when the flip-flops occur ($\Omega = \omega_S - \omega_I$), flip-flips are impossible because they are off-resonance with the driving frequency Ω, and vice-versa. In principle the simplest way of inducing such flip-flops (flip-flips) which has not been tried so far, is to use a hypersonic generator at the microwave frequency Ω and to modulate at that frequency the dipolar interaction (2) [5].

In practice a microwave magnetic field is used. A flip-flop is then a forbidden transition in first approximation but, as for the nuclear relaxation process, it becomes allowed through the dipolar interaction which scrambles the electronic and nuclear states. Assume then that we drive, say, forced flip-flops and that the strength of the source is such that the rate at which they occur is much greater than the nuclear relaxation rate $1/T_n$. We shall show that it is possible in that way to force "up" all the spins I.

Consider first a spin I that is up. The spins S being all up, the spin I could only do a flip-flip which is forbidden as being off-resonance. On the other hand a spin I that is down may do a flip-flop with a spin S that is up, ending in a situation where I is up and S is down. This spin S, which has come down, is a danger for all the I spins that are up, since it could bring one of them down through a forced flip-flop. Fortunately, before any harm is done, its powerful relaxation mechanism will have brought this spin S to its "up" position of thermal equilibrium and the cycle can start again until all the I spins are up.

It is easy to see that if the source frequency $\Omega = \omega_S + \omega_I$ drives flip-flips rather than flip-flops, the I spins will all go "down" with a polarization opposite to that of the S spins.

It is also easy to see that for an incomplete electronic polarization $|P_e| < 1$, these processes lead to a nuclear polarization $P_n = \pm P_e$.

This very simple model of the solid effect spells out some of the requirements for a polarized target material. It should be possible to dope it with paramagnetic impurities. The electronic line width should be sufficiently narrow to forbid the simultaneous occurrence of forced flip-flips and flip-flops which would cancel each other. This precludes large concentrations of electronic spins S which would lead to a broadening of the electronic resonance through dipolar S-S coupling. On the other hand for small electronic concentrations, each electronic spin S must "service" a large number N_I/N_S of nuclear spins.

In order to be effective it must be able after each forced flip-flop (flip-flip) to flip back into its thermal equilibrium position before <u>any</u> of the N_I/N_S nuclear spins of its sphere of influence has flipped through a nuclear relaxation mechanism. The condition for this is clearly :

$$f = \left(\frac{N_I}{T_n}\right) \Big/ \left(\frac{N_S}{T_e}\right) \ll 1 \quad . \qquad (5)$$

It can be shown that this condition is always verified in reasonably high fields if the nuclear relaxation of the spins I has no other origin than their couplings with the spins S [6]. If however

other nuclear relaxation mechanisms, sometimes called leakage relaxation, are present, caused either by couplings with another species of electronic spins S' with a Larmor frequency $\omega_S' \neq \omega_S$, or by a purely nuclear mechanism, the condition (5) may be violated and the nuclear polarization P_n could be much smaller than P_e.

The two conditions, narrow electron resonance and short electronic relaxation time, are well met by impurities of rare earth ions. These ions have a largely unquenched orbital moment which ensures a strong coupling between the orientation of the electronic magnetic moments and the lattice. On the other hand a large orbital magnetism implies a strong magnetic anisotropy which makes it imperative to use single crystals. It is not suprising that the polarized targets materials successfully used so far are single crystals of rare earth ions.

By far the best results have been obtained so far from double nitrates $(La)_2(Mg)_3(NO_3)_{12}\ 24H_2O$ where a small fraction of lanthanum has been replaced by neodymium (cerium and dysprosium have also been tried) and where the protons to be polarized are those of the water molecules.

Very low temperatures (below 1° K)

Assuming for simplicity that there is no leakage relaxation we see that dynamic polarization is essentially a competition between a "forced" nuclear flip caused by forced electron nuclear flip-flops (or flip-flips) driven by the microwave source and a "natural" nuclear flip caused by "natural" flip-flops and flip-flips resulting from the coupling of the electron nuclear spin system with the lattice vibrations. Increasing the rate of the first type of process by raising the microwave power or decreasing the second by lowering the temperature should increase the nuclear polarization. It would seem however that at least at the microwave driving frequencies currently used (4 mm wavelength), there is little to be gained by going to temperatures below 1° K since both the equilibrium electron polarization which is practically unity and the electron relaxation rate which is practically the lifetime of the upper electronic level change very little.

Not so however the nuclear relaxation rate which is the rate of "natural" flips. In order to flip "naturally" a nuclear spin must find an electron willing to flip-flop or flip-flip with it, with the help of a phonon or more generally of the lattice. The probability of this process is proportional to $(N_+/\tau_+ + N_-/\tau_-)$ where N_+ and N_- are the populations of the electron levels and τ_+ and τ_- their lifetimes given by (4) (for the direct process). When the temperature goes to zero the population N_+ of the excited state and the inverse lifetime $1/\tau_-$ of the ground state go to zero and so does :

$$\frac{1}{T_n} \propto \left(\frac{N_+}{\tau_+} + \frac{N_-}{\tau_-} \right) .$$

Using (1) and (4) it is easily found :

$$\frac{1}{T_n} \propto \frac{1 - P_o P_e}{P_o}$$

where for the sake of generality it was assumed that the electronic polarization $P_e = N_- - N_+$ was not necessarily the equilibrium polarization P_o given by (1).

If $P_e = P_o$:

$$\frac{1}{T_n} \propto \frac{(1 - P_o^2)}{P_o} \qquad (6)$$

$1 - P_o^2$ decreases very rapidly with T, a fact which opens up interesting possibilities for the use of the new refrigerators in dynamic polarization also.

At such low temperatures as provided by these refrigerators the coupling with paramagnetic impurities may be the only nuclear relaxation mechanism for non metallic diamagnetic solids. In fields large enough for the nuclear equilibrium polarization to be sizeable, the electronic polarization P_o would be so near unity as to make the nuclear relaxation time and the establishment of the nuclear equilibrium polarization forbiddingly long. On the other hand the time for the establishment of a dynamic polarization, or polarization time, independent of P_o, could conceivably be kept within reasonable limits.

Dynamic polarization and spin diffusion

The probabilities of a flip-flop (flip-flip) "forced" or natural, decrease very rapidly with the distance r_{IS} (we call Γ/r^6 and C/r^6 their values at a distance $r = r_{IS}$). One would thus expect a broad distribution of the relaxation and polarization times for the various spins I, depending on their distance to the nearest spin S. These variations are smoothed out to a large extent by the nuclear spin diffusion. The "information" of polarization or relaxation collected by spins I in the immediate vicinity of the spins S is carried by diffusion to all the other spins I. A spin diffusion coefficient D as small as 10^{-13} will still carry this information over 100 Å in a time of the order of ten seconds which is very much faster than the rate of direct flip-flops, "forced" or "natural", between an electron and a nuclear spin separated by 100 Å. The role of spin diffusion in relaxation and polarization processes is thus essential.

Actually, the nuclear spins that are nearest to the impurities "see" a sizeable electronic field h_e produced by the impurity

and their Larmor frequency may be appreciably different from that of a neighbouring spin I farther removed from S. The nuclear flip-flop between these two spins does not conserve energy and the spin diffusion is quenched.

We use a crude model where D is zero inside a sphere of radius b_o, called the diffusion barrier, and is constant outside. The radius b_o is defined approximately by the condition $h_e(b_o) = \Delta H$ where ΔH is the nuclear line width.

If $(C + \Gamma)$ is not too large (moderate electronic relaxation rates and moderate driving powers) it is reasonable to assume that outside the diffusion barrier the flipping information reaches every nuclear spin through spin diffusion faster than through a direct electron-nuclear flip. The nuclear polarization is then uniform outside the small sphere of radius b_o and we can assume a single relaxation time T_n and a single polarization time τ_p which are averages of C/r^6 and $(\Gamma + C)/r^6$ outside the diffusion barrier.

An elementary calculation [7] gives :

$$\frac{1}{T_n} = \frac{4\pi N_S C}{b_o^3} \qquad \frac{1}{\tau_p} = \frac{4\pi N_S (\Gamma + C)}{b_o^3} \,. \tag{7}$$

The maximum nuclear polarization P_n will be given by :

$$P_n = \pm P_e \frac{\Gamma}{C + \Gamma} = P_e \frac{T_n}{\tau_p + T_n} \,. \tag{8}$$

If on the other hand $C + \Gamma$ is large (large driving power for instance), there may still be large nuclear inhomogeneities in the nuclear polarizations outside the diffusion barrier and up to a radius b such that :

$$\frac{C + \Gamma}{b^6} = \frac{D}{b^2} \,. \tag{9}$$

Beyond b, spin diffusion maintains a uniform polarization and the formulae (7) and (8) are still valid but with b_o replaced by b. We call this case the diffusion limited relaxation (and polarization) rate. Because of the non linear dependence of $1/T_n$ and $1/\tau_p$ on C and Γ, the average probabilities for "forced" and "natural" nuclear flips are no more additive and T_n has no other simple physical interpretation than that given by the last formula (8).

As for the constant $1/\tau_p$ which is the observed rate of growth of the dynamical polarization it has in the diffusion limited range a dependence on Γ and therefore on the driving power $\mathcal{P}$, much slower than linear since according to (9) it goes like $(C + \Gamma)^{1/4}$.

It should be borne in mind that these theories are crude approximations and that the qualitative agreement with experiment, actually observed in most cases, is quite gratifying.

Dynamic polarization viewed as a cooling of nuclear spins

We have so far kept to the assumption that $\omega_n \gg \Delta\omega_S$ which implied that when driving, say, flip-flops, no flip-flips were induced and furthermore that the electron resonance and the electronic polarization were unaffected. When this condition is not fulfilled a complicated situation arises which I am happy to let my friend Borghini deal with to morrow and I shall be content to introduce the concept of spin-temperature in the rotating frame [8] and more generally the concept of dynamic polarization as a "cooling" of nuclear spins [8-12].

Still with the assumption $\omega_n \gg \Delta\omega_S$ consider the behaviour of the electronic spins S in the frame rotating at the frequency $\Omega = \omega_S - \omega_I$. In that frame, as explained earlier, the main part of the effective Hamiltonian of the spins S is static and given by :

$$\left.\begin{aligned}\mathcal{H}_{eff} &= -\gamma_S \hbar \underset{\sim}{S} \cdot \underset{\sim}{H}_{eff} = \hbar(\Omega - \omega_S)S_z - \hbar\gamma_S H_1 S_x \\ &= -\hbar\omega_I S_z - \hbar\gamma_S H_1 S_x\end{aligned}\right\} \qquad (10)$$

If the microwave field H_1 is not too large so that $|\omega_I| \gg |\gamma_S H_1|$ we can say in first approximation that in the rotating frame the S spins "think" that they have a Larmor frequency ω_I. Since however their polarization along Oz is still given by $\tanh(\hbar\omega_S/2kT)$ rather than $\tanh(\hbar\omega_I/2kT)$ the spins S must also "think" that in the rotating frame they have a temperature $T_S = T\,\omega_I/\omega_S$, lower by three orders of magnitude than that of the sample.

Since no r-f field is applied anywhere near the nuclear frequency ω_I the nuclei should be viewed in the laboratory frame. The combined effect of the part $-\hbar\gamma_S H_1 S_x$ of the Hamiltonian (10) and of the I-S dipolar couplings is to establish a thermal contact between the electrons viewed in the rotating frame and the nuclei still in the laboratory frame. The reason this contact is effective is that now electrons and nuclei have the same Larmor frequency ω_I and are thus on "speaking terms".

If this constact is much stronger than the thermal contact between the lattice and the nuclei the latter will reach in the laboratory frame the same low temperature than that of the electrons in the rotating frame namely $T_S = T\,\omega_I/\omega_S$ positive or negative depending on the sign of ω_I/ω_S. (There is nothing inconsistent in the concept of a negative temperature for a system of spins whose energy spectrum has an upper bound).

If we choose $\Omega = \omega_S + \omega_I$ we reverse the sign of the electronic temperature in the rotating frame, therefore also the sign of the nuclear temperature in the laboratory frame and the sign of the nuclear polarization.

It should be realized that the language just used which at first sight may smack of science-fiction actually does nothing but para-

phrase mathematical equations.

So far the new language of spin temperature although quite consistent has not brought anything new. Its usefulness stems from the fact that when line broadening mechanisms such as spin-spin couplings are important, and the condition $|\omega_I| \gg \Delta\omega_S$ no more fulfilled, by introducing the concept of a local field that accounts for the spin-spin interaction, this language can be generalized so as to handle this more complex situation in a satisfactory way, as will be discussed to-morrow by Dr Borghini.

The only point I wish to emphasize is the double role of the driving microwave field viewed in the rotating frame : by giving to the electronic spins in the rotating frame an effective Larmor frequency ω_I it cools them by a factor of the order of ω_S/ω_I and it puts them on speaking terms with the nuclear spins. This suggests some new methods of dynamic polarization, listed in the literature, which I shall not describe here [10,13].

Dr Jeffries will describe in great detail the only one successful so far [11].

CONCLUSION

I have attempted at some length to explain to non-specialists the physics behind the dynamic polarization method known as the solid effect. I shall not discuss any of the theoretical and practical problems connected with the making and the use of polarized targets since a large part of the Conference will be devoted to these problems.

Let me simply mention one rather farfetched idea. As I have explained earlier an r-f field of frequency ω near the nuclear Larmor frequency ω_I would give to the nuclear polarization a sizeable transverse component precessing at the frequency ω. This makes it possible to modulate the amplitude of a reaction involving strong interactions at the same frequency.

Thus, to mention a crazy gedankene experiment, the coherent forward amplitude for the scattering of neutral K mesons which can be considered as an off-diagonal matrix element between K_L and K_S could be modulated at a frequency of the order of :

$$\omega_K = \frac{m(K_L) - m(K_S)}{\hbar c^2}$$

and thus drive a resonant transition between the two states K_L and K_S. (A target with a nuclear spin $I > 1/2$ would be necessary). In view of the great line-width of K_S, comparable to ω_K, a resonance experiment of that type does not make much sense anyway but it is an amusing speculation.

Perhaps more realistic uses of such possibilities will appear in the future.

References

1) A.W. Overhauser, Phys. Rev., 1953, 92, 411.
2) T.R. Carver and C.P. Slichter, Phys. Rev., 1956, 102, 975.
3) A. Abragam, Phys. Rev., 1955, 98, 1729.
4) A. Abragam, The Principles of Nuclear Magnetism, (Oxford Press, 1961).
5) A. Abragam and W.G. Proctor, Compt. Rend., 1958, 246, 2253.
6) M. Borghini, Phys. Rev. Letters, 1966, 16, 318.
7) W.E. Blumberg, Phys. Rev., 1960, 119, 79.
8) A.G. Redfield, Phys. Rev., 1955, 98, 1787.
9) I. Solomon, Int. Conf. Magn. Electr. Res. Relax., Eindhoven, 1962, p. 25.
10) A. Abragam and M. Borghini, Progress in Low Temperature Physics, 1964, IV, 384.
11) C.D. Jeffries, Cryogenics, 1963, 3, 41.
12) A. Abragam, Cryogenics, 1963, 3, 41.
13) A. Abragam, Proc. Ljubljana Conf., sept. 1966, (to be published).

TECHNOLOGY OF PRESENT HIGH ENERGY TARGETS

H.H. ATKINSON

Rutherford Laboratory, Chilton

1 INTRODUCTION

The first nuclear physics experiment using a polarized proton target was reported from Saclay in 1962 - a measurement of C_{nn} at 20 MeV [1]. The protons concerned were the hydrogen nuclei ("free" protons) in the water of hydration of a small single crystal (volume 1.6 mm^3) of lanthanum magnesium nitrate* $La_2Mg_3(NO_3)_{12}.24H_2O$ doped with cerium. A polarization of these protons of 20 % was achieved using the solid effect [2,3] by placing the crystal in a single mode cavity and irradiating it with microwaves at 35 GHz at a temperature of 1.6° K. The target crystal was very thin, 0.12 mm, to allow the low energy recoil protons to escape, and was cooled indirectly by conduction to liquid helium.

For high energy experiments, however, the penetrating power of the particles involved is much greater. Thus much thicker targets can be used so that workable counting rates can be obtained even with low intensity beams of secondary particles. Similarly, at high energies the scattered and recoil particles usually have little difficulty in emerging from the target material and then through a small thickness of liquid helium ; it is therefore much easier effectively to cool the target by direct contact with liquid helium.

The first high energy target [3,4,5,6] was built at Berkeley in a collaboration between Chamberlain's group (including Schultz and Shapiro) and Jeffries, also using the solid effect (fig. 1). A relatively enormous volume of target material was used -roughly a cube of side 25 mm - comprising four single crystals of LMN doped with Nd. There were many problems in building this big target, including that of providing a sufficiently high microwave field

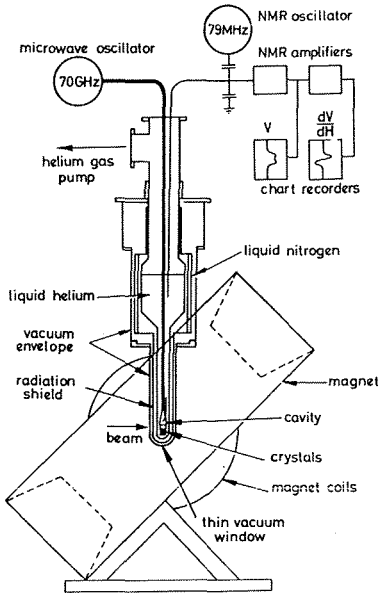

Fig. 1 General arrangement of the first high energy target, that was built at Berkeley.

throughout the large volume of the target crystals : this was solved by using a multimode cavity. At first, a 34 GHz klystron was used and an average polarization of 20-25 % achieved. However, the frequency was soon increased to 70 GHz using a carcinotron oscillator, then polarizations in excess of 60 % were obtained [7]. The problem of measuring such high polarizations using the NMR method, for which the proton line shape becomes distorted, was considered in detail by Schultz [6]. The low energy Saclay target and the high energy Berkeley targets are compared in Table I.

Target	LMN with	Vol. (cc)	H_o (kG)	Freq. (GHz)	Cavity Power (W)	He/ day	P(%)	Physics Application
Saclay	0.3%Ce	.0016	13.3	35	.003	12ℓ	20	Low Energy
LRL-1	1.0%Nd	16	9.1	34			20-25	High Energy
LRL-2	1.0%Nd	16	18.8	71	~1	150ℓ	40-65	

Table I The first polarized targets.

In 1963, three other groups - CERN/Saclay, Argonne and Rutherford - were building targets for high energy experiments. These targets

were working in 1964 and significant high energy experiments have since been completed by all of them. Table II lists some important parameters for these targets, for a target built at Saclay for Saturne, for a high energy target at Dubna, and for the first high energy target to operate with a superconducting magnet, that at Harvard. Also included are two other targets at Dubna which are used to produce beams of polarized neutrons : their size makes them look very much like high energy targets.

Target	Length (nm)	Vol. (cc)	No. Xtls	P(%) (approx)	H_o	Notes	Target Refs.	H.E.P. Refs.
LRL 1	25	16	4	20-25	→		4,5,6	5
2	25	16	4	40-65	→		3,6,8,9	9,10,11
Argonne	38	20	5-6	40-65	→		12,13	14,15
CERN 1	10	1.5	2	45-52	↑	CF cryo.	16,17,18	16
3	53	8	13	50-55	↑	"	18	
4	20	3	2	70-75	↑	"	18	19
5	45	7	2	70-74	↑	"	18	20
6	45	7	2	72-75	↑	"	18	
Dubna 1	42	28	2	37	→	H_o=9.9kG	21	
2	53?	34		71		neutrons	22	
3	30?	12		55		H.E.P.	22	
Harvard	25	16	4	65-70	↑	Supercon.H_o	23	
RHEL 1	25	16	4	50-60	→		24	25,26
2	74	40	11	50	↑	CF cryo.	27	
Saclay 1 (Saturne)	33	16		65	↑		28	28

Notes:
P is the measured polarization of the free protons
H_o, the magnetic field either horizontal (→) or vertical (↑)
CF cryo. means continuous-flow cryostat
CERN: These targets a Saclay/CERN collaboration

Table II High energy targets, past and present.

It is interesting to note how basically similar are present high energy targets (see Table III). All use LMN doped with Nd in which the free protons are polarized by the solid effect, for this is the only method and material which so far has produced high proton polarizations under practical conditions ; all have volumes ~ 10 cm^3 (between about 6 cm^3 and 40 cm^3), and are cooled to about 1° K.

LMN: Nd/La = 0.4-1.5% (soln.)
Length: 25-74 mm
Volume: 1.5-40 cc
H_o = 17-20 kG
T = 0.95-1.3°K
Microwave freq: 64-75 GHz
Helium: <50-150 ℓ/day
Polarization: 40-75%

Table III Present high energy targets. A summary of common denominators.

Most operate with a magnetic field of ~ 19 kG from an iron-cored magnet, and use about 1 watt of microwave power at ~ 70 GHz from

a carcinotron oscillator. The main individualities are : the continuous flow-cryostats and fast sweep NMR systems used at CERN/Saclay and later at the Rutherford ; the CERN magnet which gives good access for high energy physics ; the superconducting magnet at Harvard ; and the long targets used at CERN and the Rutherford. It will become more clear later why it is "natural" for all the targets to be so similar.

The targets are quite well suited to the experiments for which they have been made. However, these experiments have been carefully chosen to be compatible with present target technology, which has the following limitations as far as high energy experiments are concerned.

a. Target material : LMN, the target material universally used so far, has only 3 % free protons. Hence, the experiments must usually be such that it is possible to distinguish between scattering from free protons and bound nucleons.

b. Length and width of target : these are limited, because if scattering from free and bound protons is to be distinguished as required above, the transverse momentum transferred to a beam particle by multiple Coulomb scattering as it passes near the target nuclei must be substantially less than the momentum of nucleons bound in heavy nuclei ($\sim$ 200 MeV/c for LMN). (See reference [29]), which is also a good general review of polarized targets).

c. Access to beam detection equipment : this is limited by the cryostat and by the magnet in which the target must be placed.

d. Radiation damage causes the polarization to decrease at relatively low total dose levels (see section 2.6).

e. Beam heating of the target crystals must be small.

Thus, all the experiments for which targets have so far been used concern strong interactions (in which weak beams can be used causing little radiation damage or heating), using only those channels (e.g. elastic scattering) for which scattering from free protons and bound nucleons can be distinguished kinematically. No experiments have yet been carried out in electromagnetic interactions using electrons, for which radiation damage may make LMN targets impractical. Target materials less susceptible to such damage will probably be required in experiments of this type at present being planned.

There is a long way to go before targets are available which are suitable for all experiments which could make good use of them. However, there are many new ideas which could result in a steady improvement towards this ideal. These include : thin superconducting magnets ; helium-3 cooling to obtain very long relaxation ti-

mes ; materials with a higher proportion of free protons ; brute force polarization with new refrigerators and high magnetic fields produced by superconducting magnets ; the spin refrigerator.

This paper is not concerned with such developments ; nor is it concerned with the theory of the solid effect, or even why in detail LMN is so good. These subjects, and the high energy physics for which the targets are designed, are discussed elsewhere.

2 TARGET MATERIAL - LMN

2.1 Introduction

All present high energy targets are composed of a number of single crystals of LMN doped with Nd, in which the protons in the water of hydration are polarized by the solid effect**. The success of these targets is due to the remarkably high free-proton polarization achievable in LMN, and in the use of methods for discriminating between scattering from free protons and from nucleons bound in heavier nuclei.

A very brief summary will now be given of some important aspects of the solid effect and the influence they have on determining the operating conditions of the targets. This will be followed by a discussion of some properties of LMN crystals.

2.2 The solid effect : operating conditions

Using the solid effect, protons in the LMN are polarized in positive and negative directions (the proton spins parallel and antiparallel with the magnetic field) by irradiation with microwaves at the frequencies $(\nu_e - \nu_p)$ and $(\nu_e + \nu_p)$ respectively of "forbidden" transitions which flip both "electron" (Nd^{3+}) and proton spins simultaneously. ν_e and ν_p are the magnetic resonant frequencies for the allowed electron transitions and for the protons, respectively. For Nd^{3+} in LMN, $\nu_e = 3.78 \times 10^6 H_o$ and $\nu_p = 4.26 \times 10^3 H_o$, where H_o is the magnetic field in gauss.

It can easily be shown that in the solid effect the maximum proton polarization (P_{max}) is equal to the thermal equilibrium polarization of the electrons (P_e) at the operating temperature T(°K) and magnetic field H_o(G) of the target, that is :

$$P_{max} = P_e = \tanh x \qquad (2.1)$$

where $x = h\nu_e/2kT = 2.4 \times 10^{-11}\ \nu_e/T$. This function is plotted in figure 2 from which it can be seen that high polarizations of $\gtrsim 90$ % require values of $x \gtrsim 1.5$, in other words a ratio $H_o/T \gtrsim 16{,}500$ G/°K.

In practice, this theoretical maximum polarization can only be approached if many factors are satisfied including :

a. The forbidden line is on resonance throughout the target. This requires that the magnetic field is uniform in space, and that both this and the microwave frequency are stable in time.

b. Good separation of the allowed and forbidden lines ; this means working at relatively high magnetic fields.

c. Sufficient Nd^{3+} to satisfy the condition :

$$N_p T_{1p}^{-1} \ll N_e T_{1e}^{-1}$$

where N_e and N_p are the densities of "electrons" and protons, and T_{1e} and T_{1p} are their spin-lattice relaxation times. This inequality is satisfied for LMN with "1 %" Nd under normal target conditions (19 kG and 1° K) for reasonably pure crystals (see section 2.3). The values of T_{1e} and T_{1p} are functions of magnetic field and temperature. In particular, it should be noted that below $\sim 1°$ K ($H_o \approx 19$ kG), the relaxation rate of the protons, being roughly proportional to $\mathrm{sech}^2 x = (1 - P_e^2)$, decreases rapidly with temperature as the electron polarization P_e approaches unity [32].

d. Sufficient microwave field (and therefore power) to obtain maximum polarization of the target (see section 5.6).

The operating conditions of the first Berkeley target, 1.2° K and 35 GHz, give $x = 0.7$, and therefore a theoretical maximum polarization of 60 % (fig. 2). Doubling the frequency to 70 GHz (19.0 kG) in the second Berkeley target doubled the value of x, increasing the value of P_{max} by about 50 %. However, the proton polarization obtained in practice rose by more than a factor of two, probably due to better separation of the allowed and forbidden transitions. For essentially these values of field (18.5 kG) and temperature (1.1° K) Borghini et al [16] obtained a polarization of (84 ± 8)% in a small (0.8 cm^3) specially selected crystal of LMN, very near the maximum theoretical value of 91 %. This suggests that it is not necessary to provide magnetic fields above ~ 20 kG for LMN targets.

The operating conditions of the second Berkeley target are all near certain "natural" limits of present technology :

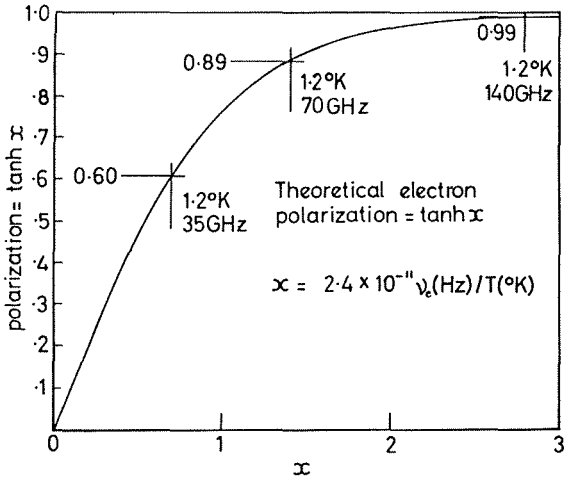

Fig. 2 Theoretical electron polarization.

a. Temperatures of ~ 1° K are the lowest which can be reached by pumping on liquid helium-4 with pumps of reasonable size, and with a power input to the helium of ~ 1 watt (due to microwave power, beam heating and heat leak into the cryostat). Temperatures a factor two lower can only be achieved using liquid helium-3, which is substantially more difficult technically (fig. 3).

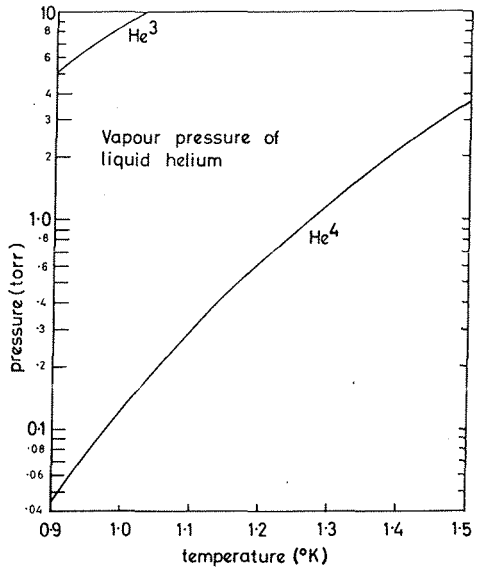

Fig. 3 Vapour pressure of liquid helium-4 (and helium-3).

b. A field of 20 kG is near the maximum obtainable easily with an iron-cored magnet with a reasonable gap. The corresponding microwave frequency to excite electron resonance in Nd^{3+} is ~ 70 GHz. There is only one type of microwave tube available which will provide sufficient power (~ 10 watts at the flange of the tube) for present LMN targets at this frequency, the backward wave oscillator or carcinotron (e.g. as manufactured by C.S.F., Paris).

The next step, say doubling the value of x by doubling the frequency or halving the temperature, would be very expensive, and would only increase the theoretical maximum polarization from 90 to 99 %. (However, there may be other advantages in doing this, both for LMN and for other materials).

2.3 Lanthanum Magnesium Nitrate

The LMN crystals are grown from an aqueous solution of the correct proportions of lanthanum and magnesium nitrates in which a certain fraction (usually 1 %) of the lanthanum ions have been replaced by neodymium ions. The resulting crystals take the form of thin hexagonal plates containing only about 1/5 or 1/6 the Nd/La ratio of the solution, as determined by x-ray fluorescence analysis [27] or by arc spectroscopy [18].

The paramagnetic Nd^{3+} ions have a very anisotropic g-value :

$$g = (g_{\perp}^2 \sin^2 \theta + g_{\parallel}^2 \cos^2 \theta)^{1/2} \qquad (2.2)$$

where θ is the angle between the crystal's z-axis (the direction perpendicular to its wide face) and the magnetic field H_o ; and $g_{\perp} = 2.70$ and $g_{\parallel} = 0.36$ [32]. The crystals have a density of about 2.07 g /cm^3 [2] and free hydrogen density of 0.065 g /cm^3 (close to that of liquid hydrogen, 0.070 g /cm^3).

In targets, the crystals are always orientated with $\theta = 90°$, so that g = 2.70. Hence, for a given frequency, electron spin resonance (ESR) occurs at a lower magnetic field than for a simple electron spin (g = 2), which is convenient. For neodymium isotopes with zero nuclear spin, the allowed ESR spectrum of Nd^{3+} is a single line of width about 6 G at 18 kG. For the odd isotopes ^{143}Nd and ^{145}Nd, the nuclear spins give rise to a hyperfine structure extending over ~ 1500 G ; this, although not interfering with the forbidden transitions for $H_o \approx 19$ kG, would provide extra channels for proton relaxation [32]. Hence it would seem desirable to avoid this effect by using only even isotopes. Natural Nd contains 79.5 % even isotopes. By electromagnetic mass separation the even isotopes ^{142}Nd or ^{144}Nd can be obtained in regular production (e.g. from Oak Ridge, National Laboratory, U.S.A.) with impurities of less than 3 % odd isotopes. Such "enriched" Nd is used in most present tar-

gets although it is much more expensive than the natural element. Schmugge and Jeffries [32] have carried out experiments in which no difference could be observed (within the experimental error, $\gtrsim 10$ %) in the maximum polarization of crystals grown from natural and enriched Nd. Argonne have, in fact, used the natural material (A. Yokosawa, private communication).

Some experiments have been carried out to determine the optimum Nd concentration [32]. These suggest that the best results are obtained for solution containing a Nd/La ratio of about 1 %. However, the Dubna targets achieve good polarizations with crystals grown from 0.4 % solution [21,22,36]. Concentrations of Nd used in present targets are given in Table IV.

Target	Vol. (cc)	H_o (kG)	ΔH_o (G)	T (°K)	Cav. (W)	%Nd	T_{1p} (min)	<P>	P_{max}
LRL 2	16(4)	19	1	1.2	~1	1.0	15-20	40-60	65
Argonne	20(6)	18½		1.2	~0.6	1.5*	20-50	40-60	
CKRN 2	.8(1)	18½		1.1		1.0	52		84
3	8(13)	18½	7+	1.1	~0.4	1.0	92	50	55
6	7(2)	18½	4+	1.1	~0.4	1.0	107	72	75
Dubna 2	34	17	5	0.95	0.15	0.4	127**	71	
3	12	20	2	1.08	0.50	0.4	>120	55	
Harvard	16(4)	18½	2	1.2	>1	1.0	-	65	70
RHEL 1	16(4)	18	2	1.2	~0.7	1.0	30	50-60	
2	40(11)	19	2	1.3	~2	1.0	20	50	
Saclay	16(4)	18			~0.7			65	

Notes:

Vol. number of LMN crystals in brackets
ΔH_o variation in field over target volume
Cav.(W) microwave power dissipated in cavity (watts)
%Nd ratio Nd/La ions in solution used to grow crystals
* unenriched neodymium
T_{1p}(min) proton relaxation time in minutes
** measured at 1.07°K
<P> mean polarization in routine operation
P_{max} best polarization for short time

Table IV High energy targets. Performance.

The LMN crystals should be as free as possible from paramagnetic impurities (other than Nd) which provide an additional relaxation path for the protons, thus increasing the power required to saturate the microwave transitions, and decreasing the polarization obtainable. In particular, small proportions of Fe^{2+} and Pr^{3+} are likely to be present in LMN crystals [32], and the former particularly can increase considerably the proton relaxation rate. Analyses of materials used to grow LMN crystals are given in references 18 and 32.

The observed proton relaxation time gives a guide to the content of paramagnetic impurity, both Nd and other, in the target crystals, especially if it can be measured as a function of field and temperature [32]. Some relaxation times for present targets are given in Table IV. Care must be taken in interpreting these figures, since the relaxation time (T_{1p}) is a rapidly varying function

of temperature (section 2.2 (c)), and the temperature at which the measurements were made may well have been substantially lower than the temperatures quoted for normal target operation. However, it is not possible to explain the range of T_{1p} values of 20 to 130 minutes for "1 %" crystals simply on the basis of temperature ; clearly, there must be substantial differences in the purity of the crystals, or perhaps in the true Nd content. The Dubna targets have long relaxation times ($\sim$ 120 minutes), but have nominally a smaller ("0.4 %") Nd content.

The LMN should be in the form of good single crystals. These should be free from physical imperfections, which have the following undesirable effects. Firstly, such imperfections may result in relative misorientations of different parts of the crystal lattice, which will cause these parts to have slightly different ESR frequencies due to the anisotropy of the g-value of Nd^{3+}. For example, a misorientation of 1/2° (i.e. θ = 89.5° rather than 90°) results (eq. (2.2)) in a change in resonant frequency of about 1 in 20,000 (equivalent to a field change of $\sim$ 1 G in 20 kG). This is about the maximum permissible misorientation, considering the electron line is only $\sim$ 6 G wide.

Also, physical defects will result in the crystal having a lower thermal conductivity, which is most undesirable, as it is then more difficult to keep the crystals cool. Apart from congenital imperfections, physical defects introduced by stresses resulting from thermal shock can lower the thermal conductivity of crystals by orders of magnitude [37]. Thus, over-rapid cooling (or heating) of the target should be avoided, especially in the range 300° K to 100° K in which there is appreciable thermal contraction.

2.4 Preparing and mounting the target crystals

To obtain good single crystals, each LMN crystal is grown from a seed over a period of weeks or months, either by slowly lowering the temperature of a saturated solution of double nitrate [38], or by allowing the solution to evaporate slowly at a constant temperature [39].

Since Nd is less readily deposited in the crystal than La, the concentration of Nd in the solution gradually increases. Care must therefore be taken not to grow crystals from too small a volume of solution, for this will give rise to an appreciable increase in Nd concentration towards the outside of the crystal ; similarly, too many crystals must not be grown from the same solution.

The crystals are usually removed from the solution when they have reached a thickness of about 7 mm. The wide (top and bottom) faces of each crystal as grown are approximately parallel. The edges can

be cut to the required size using a device in which a wet thread drawn across the crystal gradually dissolves its way through [40]. Final trimming can be done using fine carborundum paper. The surfaces of the crystals tend to become dehydrated when exposed in a dry atmosphere or when evacuated. Hence, for protection, the crystals are sometimes covered with a thin coating of Kel-F grease [41].

After cutting to shape, the crystals are stacked together to make a target of the required total thickness, and are held in place either with Teflon string, or in the case of the second Rutherford target by a spring clamp (fig. 4). The maximum misalignment of each individual crystal from $\theta = 90°$ should not exceed about $1/2°$ (see previous section). The crystals should be mounted with thin spacers of Teflon so as to allow the liquid helium used for cooling to penetrate between them, since their thermal conductivity is quite low, and the heat released inside them due to electron relaxations is appreciable. The importance of such cooling channels was discovered in the first target at Berkeley in which it was found that the polarization was substantially lower at the centre of the target when the four crystals comprising it were stuck together with Kel-F grease to form a solid 25 mm cube (see section 8.4).

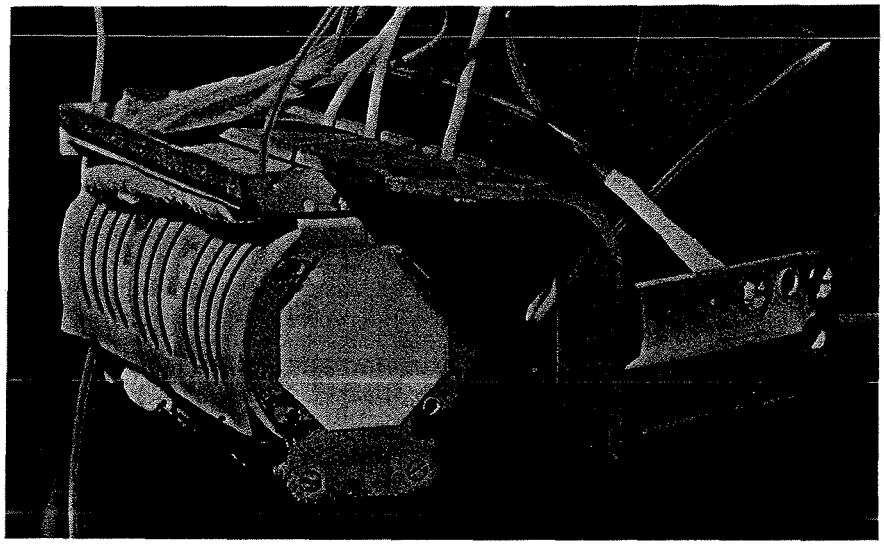

Fig. 4 The latest Rutherford target (RHEL 2) with the lower section of the cavity removed, showing the end of the stack of LMN crystals, their mounting arrangement, the three NMR coils and the bracket which fixes the cavity to the body of the cryostat. A carbon resistor (wrapped in copper coil and then Teflon) used to measure the liquid level can be seen to the top right of the coils ; a wire-wound heater can be seen to the bottom right.

2.5 Size of target

The cross-sectional area of the target is determined by the size of the particle beam, which is usually focussed on the target. For example, for beams used so far at RHEL, a target area of 6 cm^2 is required ; at CERN, target areas of about 1.5 cm^2 are used. The length of the target is determined in practice by several factors : the number of scattering events needed, the extent of the uniform region of the magnetic field, the geometrical resolution required for the scattered particles, and the effects of multiple Coulomb scattering of the beam particles by nuclei in the target (see introduction).

The crystals are usually mounted so that their z-axes are parallel with the high energy beam, but perpendicular to the magnetic field. The targets are built up in this way to the required thickness. The arrangement of crystals in a number of targets are shown in figure 5. The original Berkeley target had four hexagonal crystals as shown in the figure. The CERN 3 target had 12-13 crystals built to a length of 50 mm and diameter 12 mm. The latest Rutherford target, of length 74 mm and octagonal cross-section (minimum dimension 25 mm), is built from 11 crystals. The polarizations achieved both at CERN and at the Rutherford on these long targets with many crystals are not particularly high ($\sim$ 50 %).

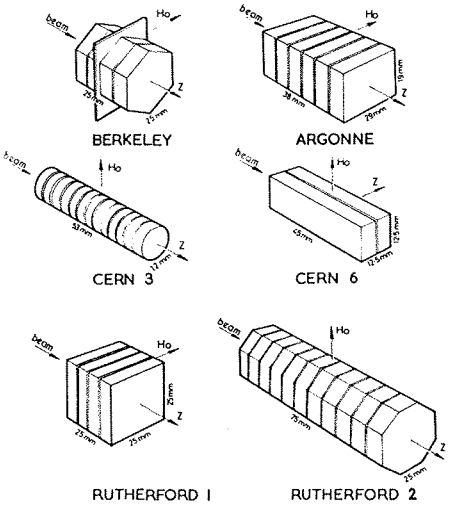

Fig. 5 The arrangement of LMN crystals in targets at Berkeley, Argonne, CERN and RHEL.

However, CERN now use two crystals mounted so that the beam is perpendicular to the z-axis (see fig. 5). Very high polarizations $\sim$ 75 % have been achieved with this arrangement [18]. Note that

CERN finds considerable variation in the maximum polarization from one crystal to another [16].

2.6 Radiation damage

There do not appear to be any published experimental results on the quantitative effect of radiation damage in high energy targets. However, information available from low energy experiments with LMN targets can be extrapolated to higher energies. For example, at A.E.R.E. Harwell [42,43] it was found that the polarization of their low energy LMN target fell to about half its normal value after 2.5 x 10^{12} protons per cm^2, of energy 140 MeV, had passed through it. (The radiation damage only partially annealed out when the crystal was raised to room temperature). At an energy loss of 10 MeV per proton per cm path length, this dose results in a deposition of energy of about 2.5 x 10^{13} MeV/cm^3. At higher energies we may assume that the beam particles are in the minimum ionizing region, and therefore that a total dose of about 10^{13} per cm^2 of the cross-section of the target will reduce its polarization by the same factor of two.

Secondary high energy beams, for example as used so far with the Rutherford target, are of such low intensity ($\sim 10^6/cm^2/s$) that radiation damage is not expected to be appreciable in many months of running.

2.7 Heating by beam

The heating of the target crystals by beams which are weak enough not to cause radiation damage is insignificant in these targets. E.g. in the latest Rutherford experiment the total beam heating is less than 1 milliwatt.

2.8 Dummy target

In many experiments a dummy target, of composition like that of the real target but without the free hydrogen, is required for accurate background determinations.

At the Rutherford Laboratory a convenient material for constructing such a dummy target is made by mixing $BaCO_3$ (26.2 %) and MgO (7.8 %) with Teflon powder (66 %). After thorough mixing, the powder is heated under pressure to form thin discs which have sufficient mechanical strength so that they can be machined to the thickness and size required for the target. The density

of this material is greater than that of LMN, so the dummy is made by stacking together a large number of thin plates (perpendicular to beam direction) leaving gaps between the plates so that the average density is the same as that of LMN.

3 MAGNETIC FIELD

3.1 Introduction

In present LMN targets the magnetic field is always between 18 and 20 kG (Table IV). In principle, the field should be sufficiently uniform over the volume of the target crystals so that every part of the crystal is in resonance : remembering that the electron line width is $\sim$ 6 G, the resonance condition should be reasonably satisfied if the field is uniform to $\lesssim$ 1 G. This conclusion is confirmed by observations (e.g. at the Rutherford Laboratory, fig. 6) which show that a field change of 1 G has a small but appreciable effect on the polarization. In any case, the local internal magnetic field due to the aligned protons can be $\sim$ 1 gauss, depending on the shape of the target (and hence the demagnetising fields), so it is pointless to provide a magnet of uniformity $\ll$ 1 G. Although a uniformity of 1 G is clearly desirable, satisfactory operation has been achieved with a uniformity of only 7 G [18].

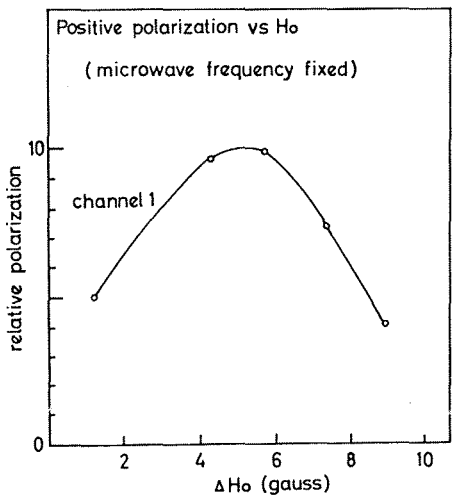

Fig. 6 Polarization as function of magnetic field (fixed microwave frequency) for RHEL 2.

The field must also be stable in time, both to keep the electron line on resonance, and also to avoid variations in the proton line which is used to measure the polarization. Short term stabilities better than 0.2 G can be obtained with conventional power supplies in which the current through the magnet is stabilized using a bank of series transistors. It is better to stabilize the magnet with reference to the field rather than the current. Hall probes are used as a control element at Argonne, Rutherford and CERN. Medium term field stabilities of order 0.3 G are obtained at the first two laboratories. On the other hand, at CERN, the stability (including ripple) is relatively poor, 1 to 2 G ; however, this does not prevent excellent polarizations being obtained.

It is very convenient to be able to measure the field by an absolute method independently of the proton line of the target itself. This is done at the Rutherford using a separate NMR probe mounted just outside the cryostat near the target.

3.2 Iron-cored magnets

Iron-cored magnets are used in all but one of the targets. Field uniformity is most easily obtained using a large ratio of pole-face diameter to gap width, for example, 46 cm to 10 cm at RHEL. For such a magnet design, the edges of the poles (or the coils) subtend a small angle at the target (16° at Berkeley and 10° at RHEL). However, this is no particular disadvantage in experiments where scintillation counters can be put in the gap, with light guides leading to photomultipliers mounted outside the magnetic field (e.g. RHEL 1, see fig. 7). Sometimes this large area of field can be an advantage, for it can be used to provide some rough momentum analysis of the scattered particles.

On the other hand, in experiments using spark chambers a wide solid angle is most desirable. This has been achieved on the CERN target magnets (fig. 8), with some sacrifice in field uniformity. The increased accessibility also allows the crycstat to be designed more compactly.

3.3 Superconducting magnets

An elegant approach is to use a superconducting magnet. The first working target using this system was made at Harvard (fig. 9). A field uniformity of 2 G was achieved, and a persistent-current switch removed all problems of short-term field stability. A total angle of 12° is subtended by the outside edges of the cryosfor the coils. It appears difficult to provide substantially greater access than this with a Helmholtz arrangement of coils.

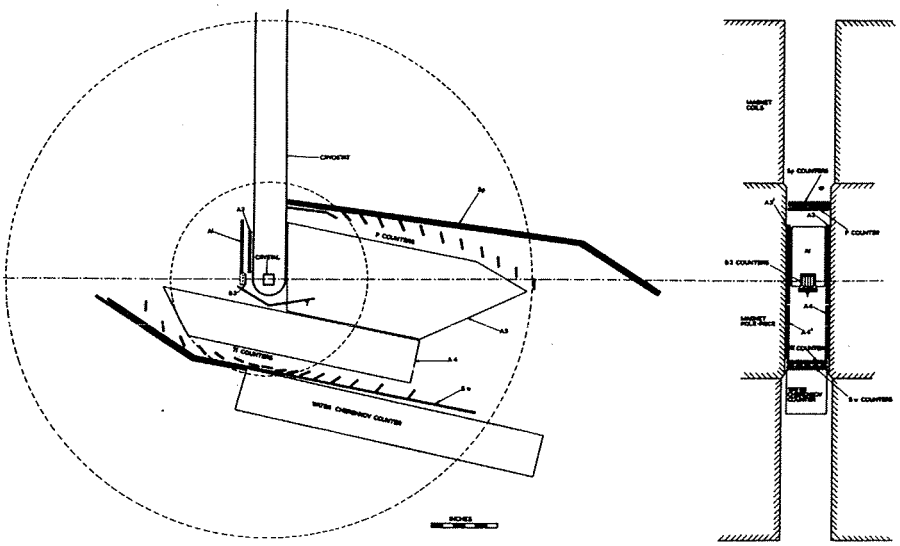

Fig. 7 Counter arrangement in magnet gap of π-p experiment at RHEL [25].

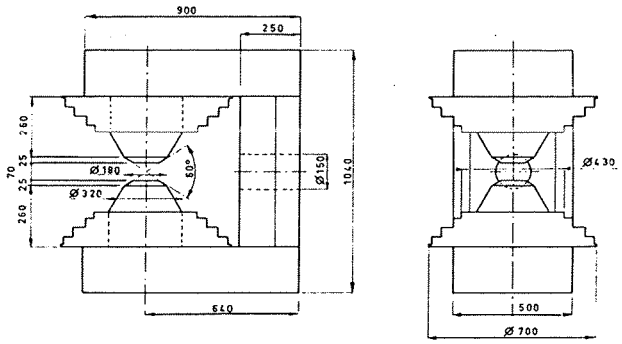

Fig. 8 Wide access magnet at CERN [18].

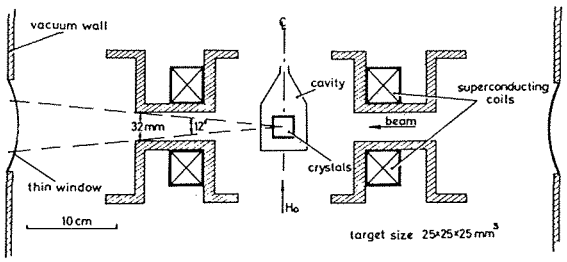

Fig. 9 Superconducting magnet on the Harvard target.

However, excellent accessibility can be obtained for a beam directed along the magnetic field, as can be seen in figure 10 which shows a new target being built at Saclay [44].

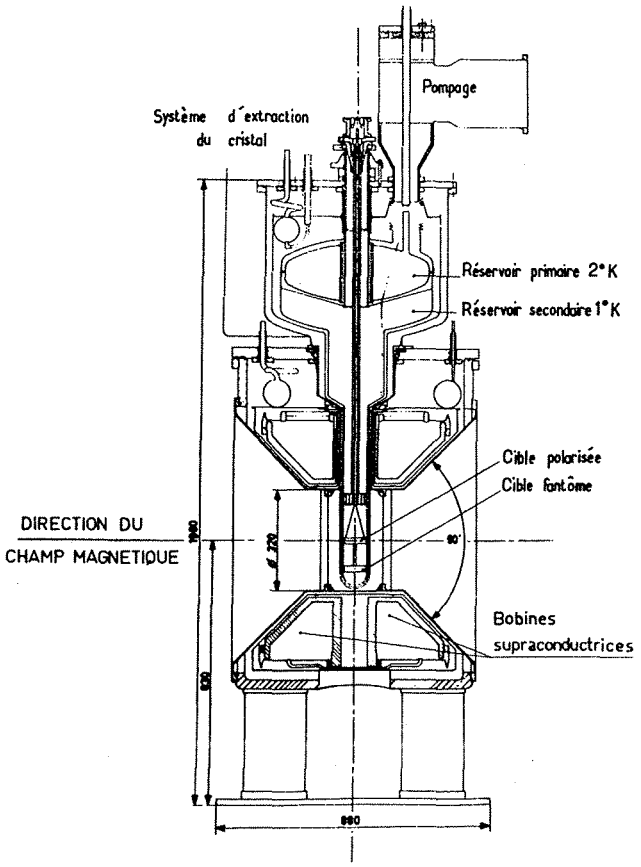

Fig. 10 Superconducting magnet built at Saclay for experiment requiring beam and polarization directions to be parallel.

Superconducting magnets become more attractive for magnetic fields of 25 kG (for g = 2 materials), although iron-cored magnets may still provide better access in many cases at this field. If even higher fields are required, superconducting magnets rapidly become essential.

4 CRYOGENIC SYSTEM

4.1 Introduction

The cryogenic system includes the cryostat in which the target is mounted and cooled, the means for supplying liquid helium to the cryostat, the pumping system to reduce the temperature of the helium in the cryostat, the equipment concerned with temperature, gas-flow and pressure measurement, and finally, perhaps, a helium gas recovery system.

4.2 Conventional cryostats

The design of the cryostat itself depends on a number of factors including the following which are (or should be) dictated by the high energy physics involved : the size of the target, the direction of polarization (e.g. horizontal or vertical), the direction of beam, the importance of continuous operation, and in particular, the disposition of particle detecting equipment round the target.

Most of the earlier targets used the conventional electron paramagnetic resonance arrangement of vertical cryostat and horizontal magnetic field (e.g. see fig. 11). Typically, the cryostat is filled with about 20 litres of liquid helium at 4.2° K, pumped down to 1.2° K, when the volume remaining is about 12 litres, and then polarized. The experiment can then begin, and is limited to 6 to 12 hours of operation ($\sim$ 1 watt of microwave heating) before the cryostat must be warmed to 4.2° K, refilled, pumped down and repolarized ; this whole operation takes 30-45 minutes. Such cryostats are inefficient in the use of helium, since the cooling power of the gas removed during pump-down is largely wasted. Figure 12 shows the helium consumption as a function of power input for a conventional cryostat (RHEL 1).

In many experiments, scattering is measured in a plane perpendicular to the direction of polarization. It is usually most convenient

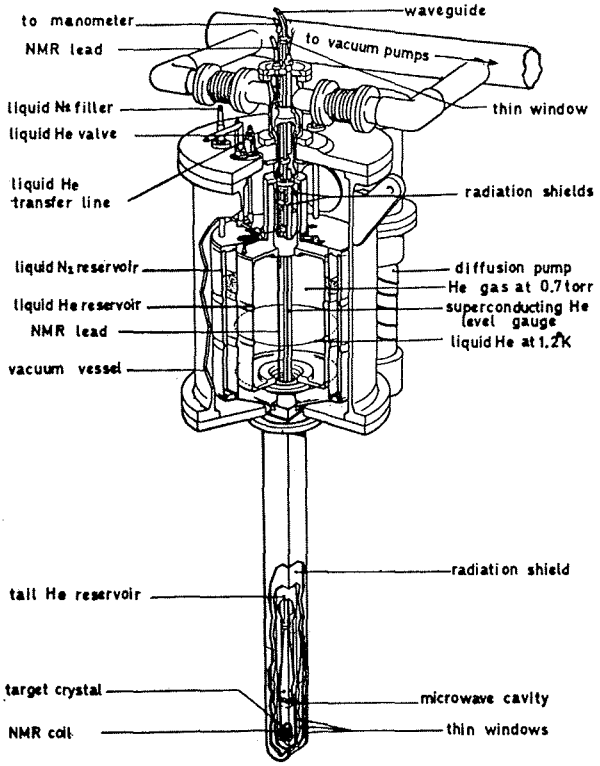

Fig. 11 Typical conventional cryostat (RHEL 1).

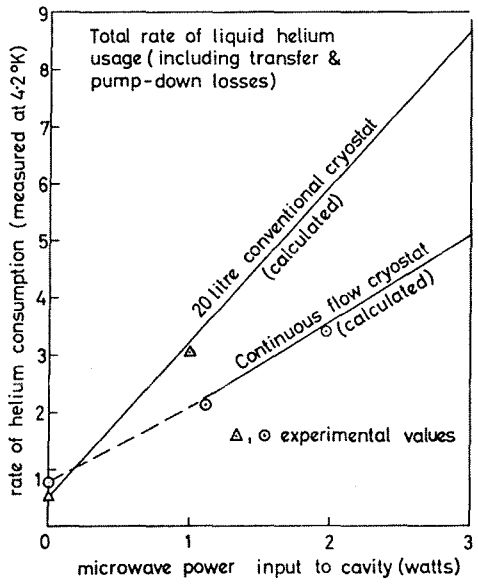

Fig. 12 Total rate of liquid helium consumption as a function of microwave power to cavity (from B. Colyer).

if this plane is also horizontal, that is, the polarization is vertical. This orientation has been obtained with a "conventional" cryostat by using a horizontal leg [28] as shown in figure 13. However, the horizontal, continuous-flow cryostat invented by Roubeau offers an attractive alternative solution to the problem, and at the same time has other advantages.

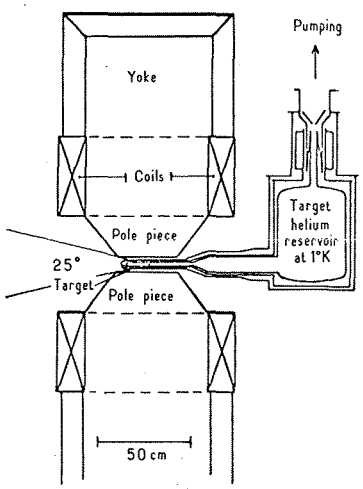

Fig. 13 Cryostat with horizontal tail used on first Saclay (Saturne) target.

4.3 Continuous-flow cryostats

This type of cryostat, which was used on the first Saclay low energy target and on the CERN targets (fig. 14), has been well described in the literature [18, 45, 46] ; only a summary of its important features will be given here, taking as an example the latest Rutherford cryostat (designed by B. Colyer) which is based on Roubeau's principles.

Boiling helium from a 100 litre dewar at ~ 4.2° K, flows continuously through a short transfer line into the cryostat (fig. 15). The helium then passes through a filter into a small inner vessel in which the gaseous and liquid helium are separated. The gas leaves the separator through a helical tube heat exchanger which helps to reduce the conduction of heat to the inside of the cryostat. The liquid leaves the bottom of the separator and flows through a heat exchanger where it is cooled to below 2° K by the counter-flowing cold helium gas from the cavity. The liquid, now

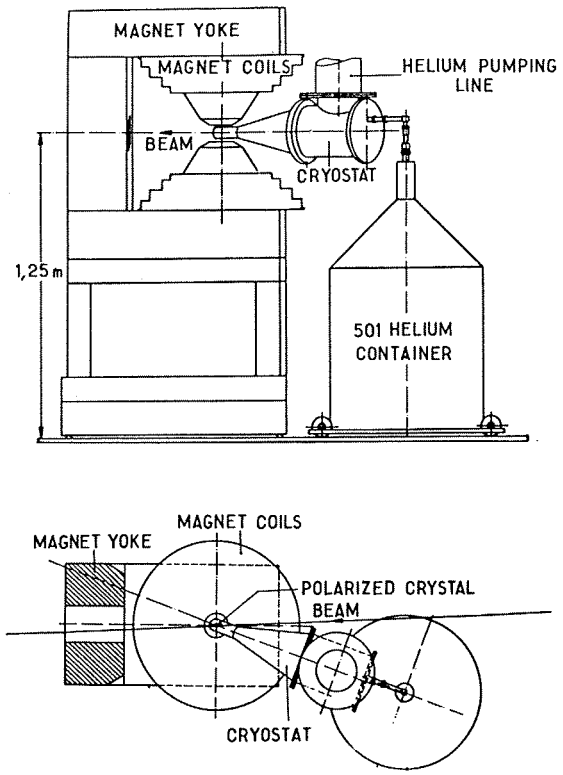

Fig. 14 CERN polarized target [16].

superfluid, flows through a fine needle valve into the microwave cavity which contains the crystals. The helium leaves through many small holes at the top of the cavity at a pressure of ~ 1 torr and passes back along the heat exchanger to a Roots pump of speed 600 ℓ/s. A radiation shield surrounding the helium vessel is cooled by conduction to the cold helium gas. Although during normal operation liquid nitrogen is not required, a liquid nitrogen container connected to the helium vessel by a "thermal check valve" is fitted to the Rutherford target. It is thus possible economically to maintain the target crystals at about 100° K during long "standby" periods.

This type of cryostat not only has a substantially higher helium efficiency than the conventional design (see fig. 12) but also can run continuously for 24 hours, after which the dewar can be changed and polarization regained in less than 15 minutes. Other advantages of the continuous-flow cryostat are that :

a. the cryostat is compact, allowing short NMR and microwave leads ;
b. the inside can be made rigid, allowing accurate alignment of the target crystals ;

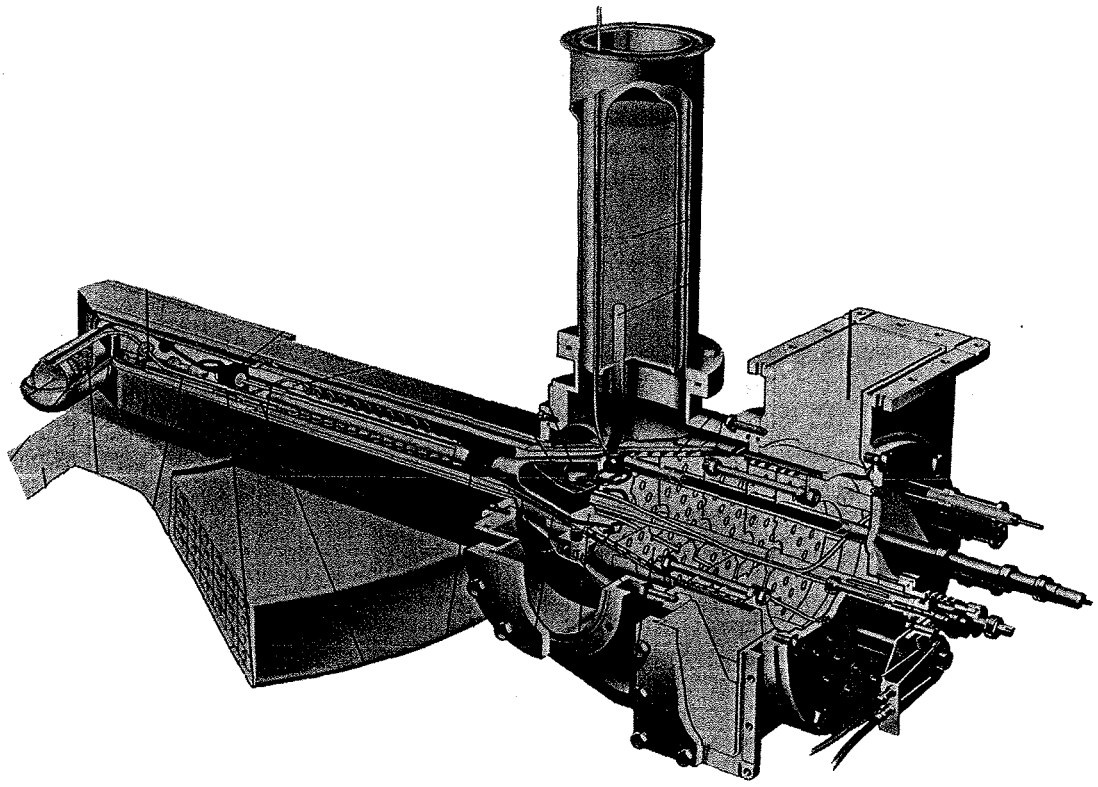

Fig. 15 Continuous-flow cryostat of latest Rutherford target (RHEL 2).

c. the face-plate of the cryostat comes at a more convenient (and safe) height, rather than well above the top of the magnet.

With this type of cryostat it is practicable more easily to "tailor" the target to fit the experiment. For example, in an experiment at present in progress at the Rutherford Laboratory for which the above cryostat is being used, a long target ($\sim$ 75 mm) was required, and counters had to be placed close to the target and almost all round it (fig. 16). This problem would have been more difficult to solve using a conventional cryostat.

4.4 Helium gas pumps

The temperature of the target material is determined by the total heat load to the liquid helium, and the speed of the pumps which remove the helium vapour from above the liquid. The maximum theoretical polarizations P_{max} (section 2.2) for temperatures calcu-

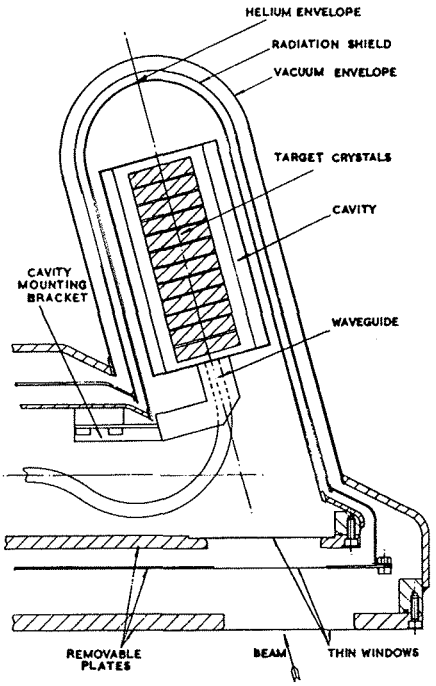

Fig. 16 Tail of RHEL 2 cryostat.

lated for various pumping speeds and microwave power inputs in the case of the second Rutherford cryostat are shown in figure 17.

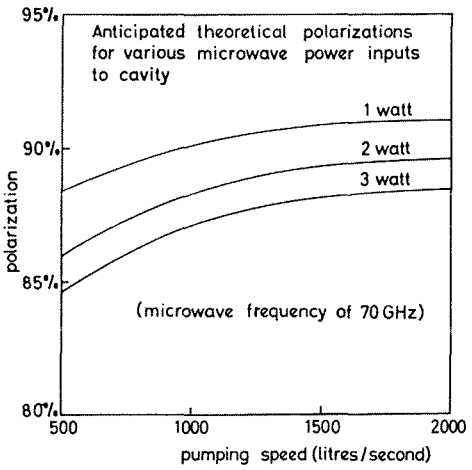

Fig. 17 Anticipated theoretical polarizations for various microwave power inputs to cavity as a function of speed of helium gas pumps (from B. Colyer).

On this simplified picture there is little apparent advantage in using pumps of speed greater than 500 ℓ/s (at ~ 1 torr). Thus, doubling the pumping speed from 500-1000 ℓ/s (with a load of 1 watt) results in a polarization increase of only 2 %. Bigger pumps give increasingly less gain in polarization, due to the shape of the vapour pressure curve of liquid helium-4 (fig. 3), and also because the gas pumping speeds of the inside of the cryostat and of the external pumping lines decrease rapidly as molecular flow becomes important below ~ 0.1 torr.

However, the above calculations of maximum polarization in no way take account of important factors such as the microwave power required to achieve saturation of the forbidden transitions, and the dependence of this on temperature through the proton relaxation rate. Even slightly lower temperatures seem to result in substantially higher polarizations than the corresponding values of P_{max} would suggest (section 8.2).

Unfortunately, the operating pressure for the target is above that at which vapour booster pumps can be used ; hence mechanical pumps - a Roots pump backed by a piston pump - are normally used. The speeds of the pumps used in present targets, and the normal operating temperatures, are given in Table V.

Helium recovery systems will not be described here.

Target	Speed (ℓ/sec)	Cavity Power(W)	Temperature (°K)	He consumed (ℓ/day)
LRL 2	~1400?	~1	~1.2	150
Argonne	570	0.5-0.8	1.15-1.25	150-200
CERN 6	1000	0.3-0.5	1.1	50
Dubna 2	1000	0.15	0.95	20?
3	1500	0.5	1.08	20?
Harvard	750	>1.0	1.25	
RHEL 1	500	0.7-1.0	1.21	60-70
2	600	1.5-2.5	1.25-1.30	90
Saclay 1 (Saturne)		0.5-1.0		50-75

Table V He pumping speeds, microwave powers, temperatures and liquid He consumptions.

4.5 Ancillary equipment

There is much ancillary measuring equipment associated with a conventional cryostat, and even more connected with a continuous-flow cryostat. Thus, a cryostat of the latter type requires : thermo-

couples and carbon resistors to measure temperatures, carbon resistors to measure the liquid helium level inside the microwave cavity (see fig. 4) ; a McLeod gauge to measure He vapour pressure and hence temperature ; a wirewound heater in the cavity (fig. 4 and section 5.4) to calibrate the system regarding power ; and heaters to warm various parts of the inside of the cryostat, if required. This equipment will not be described in detail in the present paper : some of it is described in references 45 and 46.

4.6 Liquid helium consumption

Liquid helium consumption for present targets ranges between < 50 to 150 ℓ/day (see Table V). Thus, targets are expensive to operate, even when using efficient continuous-flow cryostats. The use of lower temperatures (< 1° K), with a consequent substantial reduction in proton relaxation rates and therefore microwave power inputs, should decrease the running costs considerably.

5 THE MICROWAVE SYSTEM

5.1 Introduction

In the solid effect method, the target must be immersed in a microwave field at the frequency of the required transitions. Although relatively little power is absorbed in these transitions, high microwave fields are needed to saturate them. Such fields are obtained by mounting the crystals in a high Q cavity (e.g. fig. 18). However, the cavity walls have a finite resistance (which is not greatly decreased by the low temperature at these high frequencies), and more power is dissipated in them than in the target material (section 5.6). Some new ideas are needed here. Cavities are discussed further in section 5.5.

The remainder of the microwave system can be quite simple, as can be seen from figure 19, which shows the Berkeley arrangement. The oscillator, a carcinotron (see below), is joined to the cavity by a long waveguide. An isolator in this line protects the tube from reflected power. The line is provided with an attenuator to adjust the power and a switch to deflect the power from the cavity. The power can also be controlled by varying the carcinotron anode voltage, although this also changes the frequency. Directional couplers take off a small proportion of the radiation

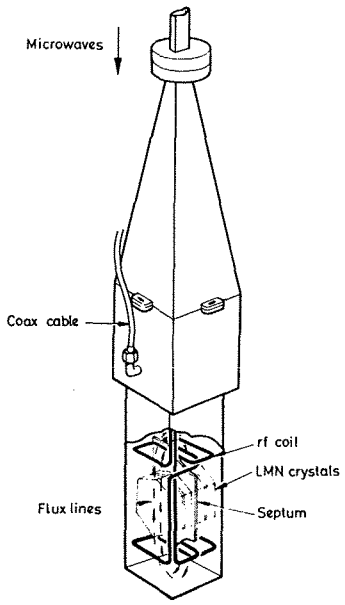

Fig. 18 Drawing of Berkeley microwave cavity showing crystals and NMR coil.

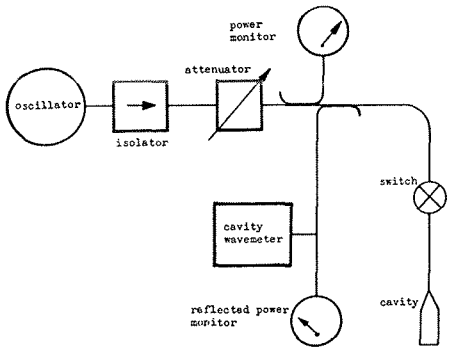

Fig. 19 Berkeley microwave system.

to monitor transmitted and reflected power, and frequency (see sections 5.3 and 5.4).

5.2 Microwave oscillator

For targets operating at ~ 70 GHz, a carcinotron is always used, since it is the only type of source at present available which will give sufficient power (5-20 watts) at its output flange so that it can easily supply the presently required 0.5 to 2 watts into the cavity, despite substantial losses in the long waveguide and other components connecting it to the cavity. Carcinotrons give good power outputs over a wide range of frequencies (4 %) and are tuned electrically.

The frequency of a carcinotron remains reasonably constant if its electrode voltages are kept constant and its cooling water supply temperature is controlled to about 1° C. However, as the frequency depends on the load conditions, it is most desirable to be able to measure it directly rather than to rely on measurements of the electrode voltages of the tube (section 5.3).

Owing to the high attenuation of standard 4 mm waveguide (2.8 db/m for WG 25 and 3.6 db/m for WG 26), the carcinotron, together with its associated measuring equipment, is often placed as near as possible to the cryostat, consistent with the limitation that the tube must not operate in a transverse magnetic field exceeding 10 G. However, it is frequently much more convenient to mount the oscillator and all its ancillary equipment in the control room, and transmit the microwave radiation to the cryostat through oversize wave guide, which is found to have a very low attenuation. This arrangement was used in both the Rutherford targets using 3 cm guide (attenuation for 4 mm waves, 0.30 db/m), and at CERN. Following Berkeley, 8 mm guide (0.89 db/m for 4 mm waves) is used to carry the microwaves inside the cryostat in most present targets. This part of the guide has a section of thin stainless steel or brass to reduce heat conduction into the liquid helium. Tapered transitions enable the 4 mm waves to be launched into and extracted from the larger guide with little loss.

5.3 Frequency measurement

In operating the target and understanding its properties, it is most useful to be able to measure the microwave frequency. Provided that the magnetic field is constant, the frequency is essentially determined when the polarization is at a steady maximum value ; but this is a poor tool, as maximizing the polarization is very time consuming. In principle, it should be possible to determine the frequency by observing an electron transition directly. However, this does not seem to be practicable with the multimode cavities used in high energy targets.

Simple cavity wavemeters can be used to measure the frequency, but at the high frequencies involved ($\sim$ 70 kHz) the Q-values of such meters are low, and the resulting measurement is considerably less accurate than the few parts in 10^5 desired. A cavity has, however, been used at the Argonne to stabilize the frequency of their carcinotron 13).

At the Rutherford Laboratory the carcinotron frequency is measured by comparing it with the harmonic of a lower frequency which can be measured accurately with greater ease. In this system (see fig. 20), which has proved most useful and has an accuracy of better than 1 in 10^5, radiation from a klystron ($\sim$ 10 GHz) is passed into a mixer in which harmonics of the klystron frequency are generated and mixed with a small fraction of the radiation from the carcinotron. The klystron is adjusted so that its frequency is exactly 1/7th that of the carcinotron, when "zero" beats are observed on an oscilloscope. The carcinotron frequency is then simply 7 times the klystron frequency as measured accurately ($\sim$ 1 in 10^6) with a standard microwave converter and counter-type frequency meter. The klystron can be accurately stabilized at any desired frequency by comparison with the harmonic of a crystal oscillator, an arrangement which is particularly useful when continuously monitoring the frequency during routine operation of the target. The system has proved very useful in measuring frequency modulation of the carcinotron, including that deliberately applied. (This system was designed and built by M. Tyrrell).

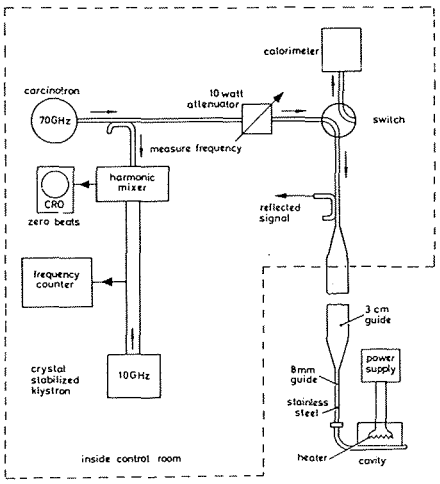

Fig. 20 Schematic diagram of RHEL 2 microwave system.

5.4 Power measurement

The microwave power travelling towards the cavity can easily be monitored by using a crystal detector and attenuator mounted on a directional coupler (fig. 19). A similar arrangement enables the power reflected from the cavity to be monitored.

However, it is very desirable to be able to make an absolute measurement of the power leaving the carcinotron, and also of the power actually dissipated in the crystals and cavity (and that part of the waveguide immersed in the liquid helium). The former can be accomplished using a calorimeter. A continuous water-flow calorimeter was built at the Rutherford for this purpose.

The latter can be measured by using the cryostat itself as a calorimeter. This is straightforward with a conventional cryostat, the helium boil-off rate indicating the power. However, this measurement is rather more difficult with a continuous flow cryostat. On the second Rutherford target the continuous flow cryostat is used as a calorimeter either by measuring the rate of fall of the helium level in the microwave cavity after closing the running valve, or by observing the minimum flow rate of liquid helium just to maintain the cavity full. Either of these methods is calibrated in absolute terms by dissipating a known amount of power in a wirewound resistor mounted inside the cavity. In the former method it must be assumed (probably incorrectly) that the coupling of the cavity to the system is unchanged as the helium level falls.

5.5 Cavities

The cavity (fig. 18) in the original Berkeley target was a square-section box of thin copper. This was coupled by a long horn to the 8 mm waveguide through which the microwave radiation entered the cryostat. A similar arrangement was used in the Argonne target (fig. 21) and on the first Rutherford target. For increased rigidity (see section 7.3), the latest Berkeley target uses a cylindrical cavity of brass, silver-plated internally, with a conical horn.

The CERN cavity (fig. 22) takes the form of a horizontal cylinder, coaxial with the target crystals and with the particle beam. The microwaves are fed into the cavity through a slit in the waveguide, which is joined to the lower surface of the cavity. The top of the cavity is pierced with many small holes to allow the helium, but not the microwaves, to escape [18,46]. The second Rutherford target uses a similar arrangement, though the cavity is larger (length 7.5 cm and diameter 5 cm) to contain the larger

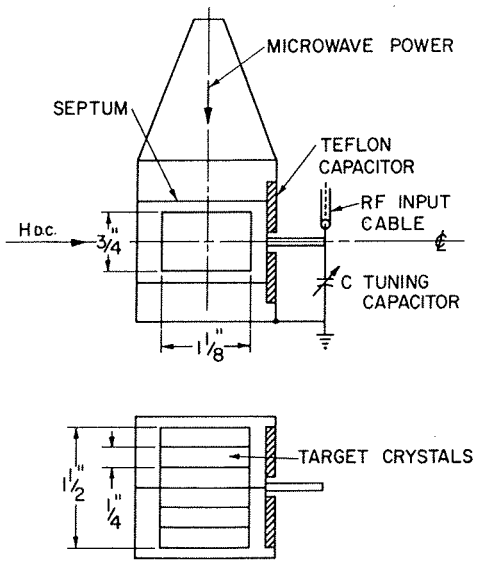

Fig. 21 Argonne microwave cavity showing NMR arrangement [13].

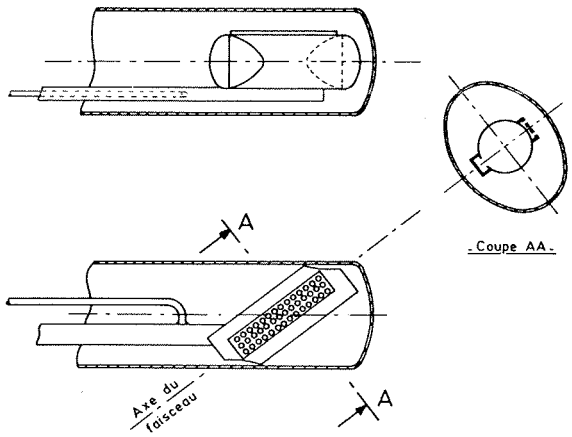

Fig. 22 Tail of CERN cryostat showing microwave cavity [18].

volume of crystals used. Figure 4 shows the top plate of this cavity, with most of its cylindrical shell removed. The end of the stack of LMN crystals can be seen, together with the clamp and bracket which attach them firmly to the body of the cryostat. This arrangement allows the target accurately to be surveyed into the beam line.

All these large cavities can support a great many microwave modes. The frequency separation $\Delta\nu$ between one mode and the next is given approximately by $\Delta\nu/\nu \approx \lambda^3/4\pi V$, where λ is the wavelength of the radiation, and V the volume of the cavity. Neglecting the effect of the LMN, which is considerable due to its high dielectric constant, $\Delta\nu$ equals 3 MHz for a large 150 cm^3 cavity (e.g. RHEL 2) and is 25 MHz for a small CERN cavity. It is not expected that the modes will be clearly distinguishable for these cavities, since in each case the Q-value is unlikely to exceed the ratio of the wall area of the cavity to the area of the waveguide feeding it plus the effective area of any holes in the cavity walls ; this gives a maximum Q of about 3000 for the Rutherford cavity and 200 for that at CERN [18].

Although each mode should give on the average a uniform distribution of microwave field in the cavity, the field will be low near each of the many nodes in the field pattern unless the overlapping modes mentioned above smear out the distribution. As the microwave transitions will not be saturated in these regions, it is desirable to sweep over a number of modes, thereby moving substantially the nodes and anti-nodes so that every individual point in the target receives an equal share of microwave field. This "mode mixing" is most easily carried out by modulating the frequency of the microwave oscillator. Mode-mixing can also be achieved by allowing the liquid helium level to rise and fall periodically inside the cavity ; this changes the distribution of the dielectric material in the cavity sufficiently to change modes. On the RHEL 2 target, substantial spacial variations in the microwave field strength have been observed using three small carbon resistors placed in different parts of the cavity.

Apart from mode-mixing, frequency modulation of the carcinotron is also desirable in that it compensates for small differences in the resonant frequencies at different parts of the crystals (section 8.1). On RHEL 2, modulation to a depth of 10-20 MHz is found to increase the polarization by about 20 %. Such modulation, which was also used on the first Rutherford target and at CERN, is effective due to the long relaxation time of the protons.

Without an isolator, or substantial attenuation in the waveguide, the cavity is found to react back strongly on the carcinotron. The carcinotron can be "pulled" so much that certain frequencies are unobtainable. These effects have been observed at the Ruther-

ford using the zero-beat frequency measuring system. This pulling probably occurs when the whole microwave system including cavity, coupling and complete waveguide is at a point of marginal stability between one system mode and another. As the carcinotron frequency is slowly changed the "reflected power" from the cryostat (indicated on the crystal detector, fig. 20) fluctuates rapidly as also does the resistance of a ("shielded") carbon resistor in the cavity.

5.6 Microwave power

The power absorbed by the forbidden transitions in order to maintain the polarization of the protons in the face of their natural relaxation rate is equal to $N_p T_{1p}^{-1} h\nu_e$ per unit volume. For a "1 %" crystal for which $T_{1p} \approx 1000$ seconds, this work out at about 2 mW/cm^3, or about 80 mW for the large Rutherford target. However, more microwave power than this is required to set up a sufficiently high radiation field in the microwave cavity to ensure maximum polarization of the protons, the balance being dissipated in the cavity walls.

For a given target with a specified helium pumping speed, there is an optimum power for maximum polarization ; at this point the increase in the enhancement resulting from an increase in microwave field is matched by the fall in the absolute polarization due to the rising temperature. For most high energy targets, the optimum power (or at least the published operating power) is $\sim$ 1 watt (see Table IV) : more precisely, the small (7 cm^3) CERN targets require 300-500 mW, the Berkeley target about 1 watt and the latest Rutherford target about 2 watts. One of the Dubna targets, however, uses a power of only 150 mW.

Microwave operating conditions are summarized in section 8.1.

6 MEASUREMENT OF POLARIZATION

The polarization of the protons can be measured by a number of methods :

a. By measuring the net energy of the protons in the magnetic field. This is the basis of the NMR method in which a small proportion of the protons are induced by an r.f. field to reverse their directions with respect to the main magnetic field : the

net absorption (or emission) of energy in this process is a measure of the polarization, and its sign. This standard "Q-meter" method is described in detail in section 7.

b. By measuring the static magnetic field resulting from the polarized protons. The total static magnetic field both inside and outside the target material can be changed by ~ 1 G due to the polarized protons. The internal field has been measured in small crystals (of suitable shape) by observing the resulting shift in the paramagnetic resonance frequency of the neodymium ions themselves [1]. Measurement of the change in external field as a method of determining the polarization was suggested by Abragam [47] and demonstrated by Abragam and Chapellier [48] using two NMR (fluorine in Teflon) probes placed in the cryostat close to the target. Lushchikov and Taran [21] have applied the same method to a large target using water NMR probes placed outside the cryostat. Good agreement was found between the polarization measured by this method and that measured at the same time using the Q-meter technique : the experimental error quoted for each method was ± 10 %. Note that in this method, an error could arise due to fields from other nuclei in the target which may inadvertently have become polarized by the solid effect (e.g. nitrogen in LMN).

c. By measuring the asymmetry resulting from the interaction of a beam of particles and the spins of the protons in the target. For example, targets [24] have been calibrated by observing the asymmetry in the scattering of a beam of high energy protons from the target, under conditions in which the polarization parameter had been measured independently, say by double scattering (see section 8.5). Another example of this method is the calibration of the target by passing through it an unpolarized beam of low energy neutrons. The proton polarization can then be determined by measuring the polarization of the emerging neutron beam using an iron plate. This method has been used at Dubna [36].

7 THE NMR METHOD

7.1 Introduction

All present high energy targets use the "Q-meter" nuclear magnetic resonance technique to measure (or at least monitor) the proton polarization. In this method a small fraction of the protons in the target are caused to flip by an electromagnetic field from a coil near the target. The radiation is at the proton magnetic resonance frequency, and the coil is tuned by a parallel condenser

C to the same frequency (e.g. $\sim$ 80 MHz at 19 kG). The polarization is deduced from measurements of the effect of these protons transitions on the electrical characteristics of the tuned circuit - there is a net absorption of energy from the tuned circuit when the protons are positively polarized, and a net transfer of energy to the circuit for negative polarization.

The magnetic effect of the protons in the target is described by a complex susceptibility $\chi = \chi' - i\chi''$. This modifies the inductance L of the coil to the complex expression $L(1 + 4\pi\eta\chi)$ where η, the "filling factor", expresses the degree of coupling between target and coil, and χ is a function of frequency ω. The proton polarization P is given by :

$$P = \text{const.} \int_0^\infty \chi'' \, d\omega \quad . \tag{7.1}$$

As the proton line shape (i.e. $\chi''(\omega)$) depends on the degree of polarization (as well as on the orientation of the crystals in the case of LMN), especially at high polarizations, this integral must be evaluated in full.

The value of $\chi''(\omega)$ is usually deduced from the impedance Z of the resonant LC circuit measured by passing through it a constant current from a high impedance r.f. oscillator. This system is called the "constant current Q-meter". An alternative method, the "constant voltage Q-meter", in which the admittance of the circuit is measured, has certain advantages and is described in section 7.5. Including the effect χ of the target, $\underline{Z}$ is given by :

$$\frac{1}{\underline{Z}} = \frac{1}{R + i\omega L(1 + 4\pi\eta\chi)} + i\omega C \tag{7.2}$$

where R is the series resistance of the electrical circuit.

The main effect of the target material is to add a real term $4\pi\omega L\eta\chi''$ to the resistance R. Thus, assuming that the term in χ' can be neglected, and also assuming that the circuit is on resonance and that $Q = \omega L/R \gg 1$, then the magnitude of the impedance ($|\underline{Z}| \equiv Z$) is given by :

$$\begin{aligned} Z &= (\omega L)^2/(R + 4\pi\omega L\eta\chi'') \\ &= Q^2R/(1 + 4\pi Q\eta\chi'') \quad . \end{aligned} \tag{7.3}$$

This equation may be written :

$$\chi'' = \frac{1}{4\pi Q\eta} \left(\frac{Z_o - Z}{Z}\right) \tag{7.4}$$

where Z_o is the value of Z in the absence of the proton resonance, i.e. for $\chi'' = \chi' = 0$.

From (7.1) and (7.4) the polarization :

$$P = \text{const.} \int \frac{Z_o - Z}{Z} \, d\omega \quad . \qquad (7.5)$$

For small polarizations, $Z \approx Z_o$, and P is approximately proportional to $\int (Z_o - Z) d\omega$, that is to the observed resonance line. However, for large polarizations, the Q-meter is said to become "non-linear", and equation (7.5) must be used in calculating the polarization from a measurement of Z as a function of frequency.

Note that if the product ηQ is too high, then for high negative polarizations the magnitude of the term $4\pi\eta Q\chi"$ may at some point be greater than 1, and the system will become unstable, exhibiting a type of maser action in which the polarization can be partially destroyed. (This effect has been observed at, for example, the Rutherford [24]). Such instability can be avoided if $Q\eta$ is sufficiently low that $|4\pi Q\eta\chi"|_{max} < 1$ (where "max" indicates the value of the term at the peak of the proton line). However, as discussed in the next section, it is desirable that $|4\pi Q\eta\chi"|_{max} < 0.3$ if errors (or at least difficult corrections) due to the reactive component are to be avoided.

To obtain the absolute value of polarization from (7.5), the value of the constant must be determined. As it is not practicable to calculate this absolutely it is usually obtained either by the particle scattering method (section 6(c)), or by observing with the NMR system the polarization of the protons when they are in thermal equilibrium (TE) with the helium bath a temperature T and field H_o.

The polarization is then given by :

$$P_{TE} = \tanh(g_n \beta H_o / 2kT) \approx g_n \beta H_o / 2kT \qquad (7.6)$$

where g_n is the proton g-value. As this polarization is very small (e.g. 0.17 % at 1.1° K and 18.5 kG), it is not easy to observe the TE proton line above the noise level in the equipment.

The two main practical problems in measuring the polarization can now be stated :

a. The evaluation of the integral in equation (7.5).

b. The measurement of the TE signal to calibrate the NMR system.

These problems are solved in somewhat different ways in the two types of NMR system at present in use. The first is the "slow sweep" system in which the NMR oscillator frequency is swept through the proton line in a few minutes. The results of the sweep are presented on a chart recorder, and also punched on paper tape for subsequent integration in a digital computer. The

TE signal is observed using a phase sensitive detector (PSD). This "traditional" system is described in section 7.3.

The second is the "fast sweep" system (section 7.4) in which the frequency is swept rapidly through the proton line in a time much less than one second. An analogue computer can then be used to calculate the polarization using equation (7.5) ; an immediate result is thus obtained. The TE signal can now be observed directly, without using a PSD. A higher voltage across the NMR circuit can be used during the fast sweep, provided the average power level is not sufficiently high to depolarize the protons. In the simplest application of this method the integral $\int(Z_o - Z)d\omega$ is calculated [18]. This introduces an error which can be obviated by using a more complicated analogue computer to calculate $\int[(Z_o - Z)/Z]\, d\omega$ (section 7.4) or by using the constant voltage Q-meter (section 7.5).

7.2 Theory of constant current Q-meter

More complete expressions than (7.3) for the impedance of the tuned circuit containing the target have been published (e.g. references 6 and 18). These and similar calculations are summarized in this section, giving the errors which arise in calculating the polarization from the simple expression (7.5).

The magnitude of the impedance Z can be found from (7.2), giving :

$$\frac{Z}{Z_o} = \frac{1}{(1 + \varphi'')}\left[1 - \frac{1}{2}\frac{\varphi'^2}{(1 + \varphi'')^2} + \frac{\varphi'}{Q}\right] \qquad (7.7)$$

where $\varphi' = 4\pi\eta Q\chi'$ and $\varphi'' = 4\pi\eta Q\chi''$: in deriving this equation it has been assumed that $Q^2 \gg 1$, that higher order terms in φ' and φ'' may be neglected, and that terms resulting from the frequency sweep are also negligible, as shown by Borghini et al [18].

For comparison with the simplified expression (7.4), (7.7) may be rearranged, again neglecting higher order terms in φ' and φ'', to give :

$$\frac{Z_o - Z}{Z} = \varphi'' + \frac{1}{2}\frac{\varphi'^2}{(1 + \varphi'')^2} - \frac{\varphi'}{Q} \quad . \qquad (7.8)$$

Since $\varphi'' = 4\pi\eta Q\chi''$, it is seen that (7.8) is identical to (7.4), with the exception of the two terms in φ'. Hence, the fractional error in calculating the polarization from (7.1) using (7.4), rather than the full expression (7.8), is equal to the ratio of the integral of the last two terms in (7.8) to the integral of φ'' (all with respect to $d\omega$).

Schultz [6] has shown that these integrals can be evaluated approximately by assuming that the proton line $\chi''(\omega)$ has a Lorentz shape (or is at least the sum of such shapes) : the dispersive component $\chi'(\omega)$ can then be calculated from this, using the Kramers' relation. Note that $\chi'(\omega)$ is of course an odd function, having maximum values $|\chi'|_{max} = 1/2\ |\chi''|_{max}$, and that φ' and φ'' are simply proportional to χ' and χ''.

On this basis, Schultz calculated that for $|\varphi''|_{max} \approx 0.33$, the error due to the second term on the right hand side of (7.8) is ~ 6 %. Borghini et al [18] have carried out similar calculations, quoting approximate errors of 5 % for $|\varphi''|_{max} = 0.3$, 3 % for $|\varphi''|_{max} = 0.2$ and 1.5 % for $|\varphi''|_{max} = 0.1$. Note that this term of (7.8) is always positive ; it acts to make the magnitude of positive polarizations appear larger than they really are, and negative polarizations to appear smaller.

The third term in (7.8) can be neglected, for as φ' is an odd function, its integral should be zero ; if this is not quite the case, the use of a reasonably high value for Q (e.g. $Q \approx 20$) will certainly make it negligible [18].

7.3 Slow sweep system

The Berkeley target [6,9], and those at Argonne and Harvard, all use the slow sweep system, a traditional method for looking at small NMR signals. A block diagram of the Argonne system, which is similar to that used at Berkeley, is shown in figure 23. The magnetic field is modulated by about one gauss at a frequency of a few hundred cycles per second, and the centre frequency of the NMR oscillator is periodically swept through the proton resonance, covering about 150 kHz in a few minutes. The voltage V across the coil (which has a value of the order of millivolts so that the r.f. field does not appreciably depolarize the protons) is amplified and then rectified in a detector.

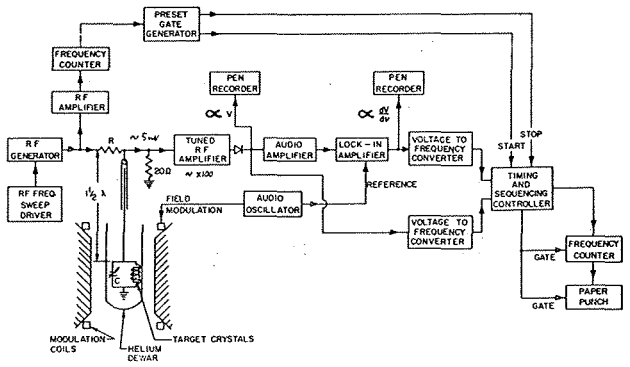

Fig. 23 Schematic diagram of Argonne slow sweep NMR system [13].

The output of this detector (which should be linear) is fed in two directions : firstly, to a chart recorder which presents a trace proportional to V, and hence proportional to Z since a high impedance oscillator is being used ; and secondly, to an audio amplifier and phase sensitive detector which is locked to the oscillator which drives the field modulating coils. The output of the PSD is fed through an integrator, in which the noise tends to cancel out but in which the signal adds coherently, to a second chart recorder which displays dV/dH as a function of time (i.e. frequency). Figure 24 shows typical signals.

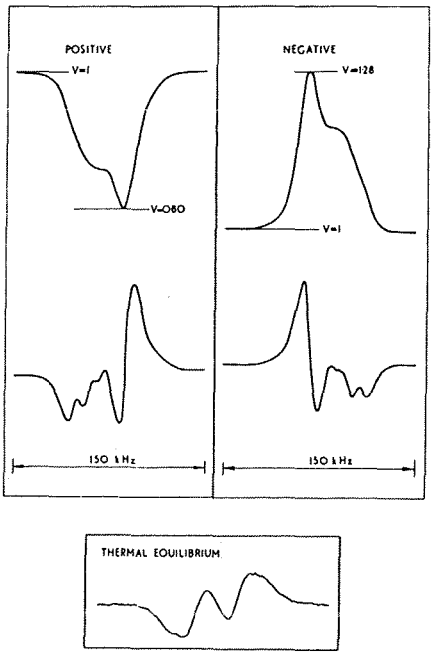

Fig. 24 Typical proton signals (V) and their derivatives (dV/dω) for positive and negative polarizations of about 50 %, observed at RHEL. A thermal equilibrium line (using field sweep) is also shown.

For the enhanced lines the polarization can be calculated from these values of V by means of equation (7.5), since V is proportional to Z. However, as the TE signal can only be observed as a change in dV/dH (proportional to dZ/dH), it is necessary to calculate the polarization from this in order to calibrate the system. This can be done as follows :

By differentiating equation (7.3) and rearranging, we have :

$$\frac{d\chi''}{dH} = - \frac{QR}{4\pi\eta} \left(\frac{1}{Z^2} \frac{dZ}{dH} \right) \quad . \qquad (7.9)$$

Since $(d\chi''/d\omega)$ varies as $-(d\chi''/dH)$, the following expression for the polarization can be obtained from (7.1) and (7.9) :

$$P = \text{const.} \iint \frac{1}{Z(\omega)^2} \frac{dZ(\omega)}{dH} \, d\omega \, d\omega \quad . \qquad (7.10)$$

The constant in (7.10) can be determined using observed values of Z ($\approx Z_0$) and dZ/dH for TE conditions : the equation can then be used in an absolute calculation of any other polarization.

In principle, the dV/dH signal should result entirely from the presence of the protons. However, in practice, a spurious signal can arise due to mechanical vibrations of the cavity walls caused by the field modulation. These vibrations change slightly the capacity between the coil and ground, thus inducing a signal in the NMR system which is coherent with the field modulation and is therefore not suppressed by the PSD. This effect has been largely removed in the new cylindrical cavity at Berkeley (section 5.5).

In the first Rutherford target, NMR frequency modulation was used to obtain the differential signal, rather than field modulation. This has the advantage that no modulating coils need be fitted to the magnet, and the walls of cryostat and cavity can be made without regard to the penetration of an alternating field. The modulation is easily applied direct through the NMR oscillator. The differential recorder now measures $dV/d\omega$, and thus "sees" the electrical characteristics of the circuit. This can be an advantage as it makes it easy to tune the NMR circuit (when $dV/d\omega = 0$). A disadvantage of FM is that the TE line appears on a very sloping base line. (The slope is negligible in the case of enhanced signals).

The TE signal can, however, be observed on a flat base line using FM by sweeping the field rather than the frequency. This method is used on RHEL 2. (Field sweep would be difficult to use for the enhanced line as the microwave frequency would then have to be swept in synchronism with the field - however, this might have its advantages in mode mixing).

For the enhanced lines the present Rutherford target has facilities (designed by R. Downton) both for the slow sweep system, as described here, and for the fast sweep method which is described in section 7.4.

The Argonne workers [12] have pointed out that if the line is swept too quickly there will be a lack of synchronism between V and dV/dH (or $dV/d\omega$) due to the time constant of the PSD circuit. This will result in an error in calculating the polarization, although the effect should not be very important if the integrating time constant is (say) 1 second and the sweep time several minutes.

However, to overcome this difficulty they suggested a different way of looking at the calibration procedure. Instead of carrying out a double integration for every enhanced line, they normally calculate the polarization from $\int[(V_0 - V)/V]\,d\omega$, only using the dV/dH signal and the TE signal to calibrate the scale of the V signal.

In most targets using the slow sweep system, the values of V and dV/dH (or dV/dω) are punched on paper tape, and later fed into a digital computer for calculation of the required integrals.

7.4 Fast sweep system

The fast sweep method has the advantage of continuously displaying the proton line on an oscilloscope screen, and of providing a signal from which the polarization can be easily calculated "on line" using an analogue computer.

The CERN/Saclay group [16,18] were the first to use this method. Their system is shown in figure 25 in which all the timing pulse arrangements have been omitted. The basic operation is as follows.

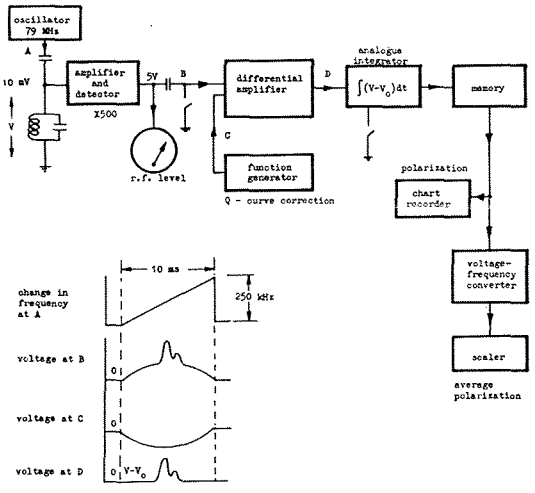

Fig. 25 Simplified diagram of CERN fast-sweep NMR system.

Periodically, the frequency of the NMR oscillator is swept linearly through the proton resonance, increasing by 250 kHz in 10 ms, before being returned to its initial value (A, in the figure). The signal V across the coil is amplified, detected and applied through

a condenser to one input (B) of a differential amplifier : the other input (C) of this amplifier is supplied with a signal synthesised to have the reverse shape to that of the top of the "Q curve". Thus the output (D) of the amplifier shows the signal on a flat base line (see fig. 26). The signal is then fed to an analogue integrator, the output of which is proportional to $\int(V - V_o)dt$. This integral is monotonically related to the polarization. The error in taking this to be proportional to the polarization over a small range is discussed in detail in reference 18.

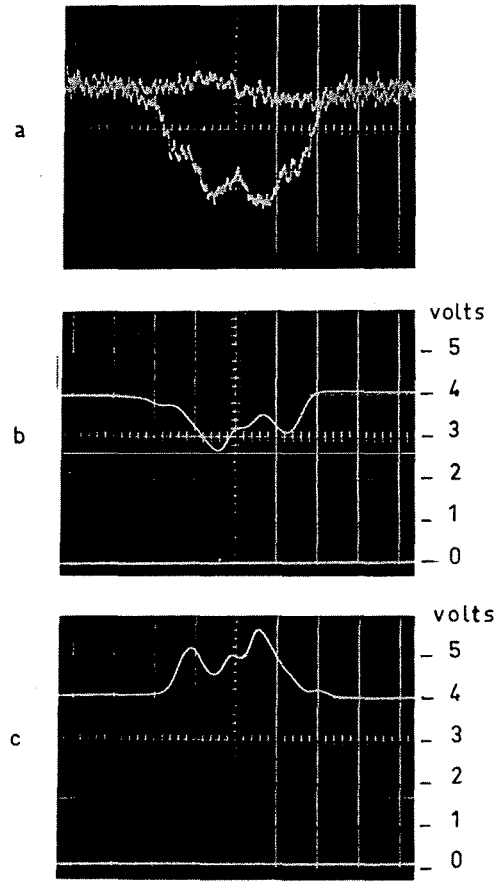

Fig. 26 Proton signals from CERN fast-sweep NMR system for (a) thermal equilibrium at 1.05° K, (b) 72 % positive polarization and (c) 72 % negative polarization 18).

The output of the integrator is fed to an analogue memory, and then through a voltage-frequency converter to a scaler, which accumulates a quantity proportional to the "polarization".

The TE signal (fig. 26) is also measured using this method. The correction for the shape of the Q curve is particularly important in this case. Although the signal-to-noise ratio was about 10 for an individual sweep, for 100 sweeps a 1 % measurement of the TE line could be made by accumulating the results. (A correction was made for the base line).

In the latest Rutherford target a fast sweep is used, following the ideas described above. However, a direct-coupled system is used following the detector, and the full integration $\int[(V_o - V)/V]\,dt$ carried out using a PACE analogue computer. The principle of this system (designed by J. Rice) is shown in figure 27. The voltage values at the beginning (V_i) and end (V_f) of each sweep are sampled, held and displayed on meters. This enables the tune of the proton resonant circuit to be checked continuously (when on tune, $V_i = V_f$). In calculating the above integral, the value V_o is taken as $(V_i + V_f)/2$ using the values from the preceding sweep. This compensates for small errors in the tune of the resonant circuit. Also, changes in the level of the whole r.f. system are automatically corrected by taking the full integral.

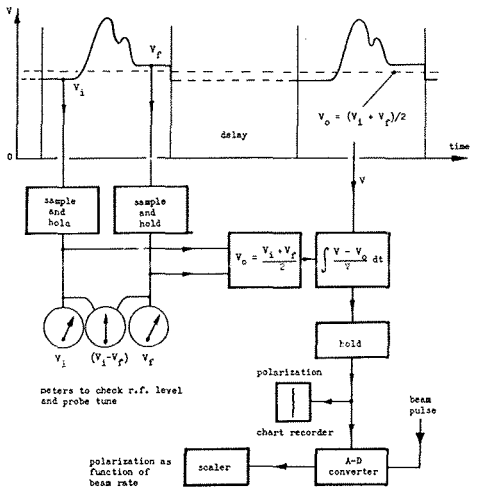

Fig. 27 Diagram showing principle of RHEL 2 analogue computer system.

The meter reading V_i is used to monitor the r.f. level in the system. The value of integral, which is directly proportional to the polarization, is periodically accumulated in a scaler at a rate determined by the arrival of beam particles, the correct average polarization resulting.

7.5 Constant voltage Q-meter

Ryter [49] has recently made a different type of Q-meter in which the admittance $Y = 1/Z$ of the LC circuit is measured, essentially by measuring the current flowing when a constant NMR voltage is applied across the circuit. By a calculation similar to that used for equation (7.8), Ryter obtains :

$$\frac{Y - Y_o}{Y_o} = \varphi'' + \frac{1}{2}\frac{\varphi'^2}{1 + \varphi''} \quad . \qquad (7.11)$$

Provided that the term in φ' can be neglected (this will give rise to the same errors as those given in section 7.2 for various values of φ''_{max}), then the polarization is given by :

$$P = \text{const.} \int (Y - Y_o)\,d\omega \quad . \qquad (7.12)$$

The advantage of the constant voltage Q-meter is that this integral is more easy to carry out than the integral $\int[(Z_o - Z)/Z]\,d\omega$ required for the constant current Q-meter. However, the electronic circuits required to measure Y are by no means simple***.

7.6 NMR coils

We now discuss one of the most important parts of the NMR system, the coils. Various types have been used. In general, the coil will not sample the polarization uniformly (see section 8.4). For example, a single turn coil wound closely round the target will produce an r.f. field which falls in strength towards the centre of coil. The coil will therefore average the target polarization unevenly, for the probability of the r.f. field inducing proton flips (and therefore the sampling function) is proportional to the square of the r.f. field.

The NMR coil design used at Berkeley [6,9] ensures that the r.f. field produced in the region of the crystal is uniform, by means of an ingenious double 8 configuration with copper septum, as shown in figure 18. Because of the phasing of the coils, the r.f. field takes the form of loops round the septum. The field has a uniformity of 5 % in the target material itself (measured by plotting the field lines using an analogue method), and so samples the polarization to a uniformity accuracy of 10 % (see fig. 28). The coil was insulated by Teflon (which contains no free protons) and tuned by a capacitor, external to the cryostat, connected to it by a coaxial cable of length 1.5 wavelengths. A similar coil arrangement was also used recently on a small target at CERN [18].

The Argonne target uses an arrangement in which the cavity itself, and a septum in it, form part of the inductance, which is resonated

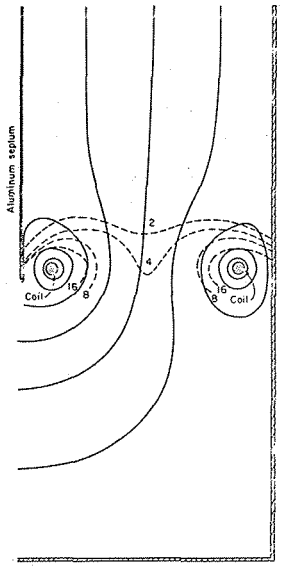

Fig. 28 Cross-section of half of the Berkeley cavity showing r.f. magnetic field lines (solid lines) and the lines of constant field [8].

by the capacitance formed by an extension of the septum and the cavity wall (see fig. 21). Final tuning is carried out using a small capacitor which is mounted near the cavity and adjusted mechanically from the outside. This arrangement gives naturally a high Q, and also a very high filling factor η. The Q has therefore to be artificially reduced to a low value to ensure that $|4\pi\eta Q\chi''|_{max} < 1$ to avoid instability.

The CERN 3 and RHEL 2 targets use simple coils of wirewound round the target crystals (e.g. see fig. 4). As these targets are quite long (50 to 74 mm), three coils are used to determine the uniformity of the polarization along the length of the target crystals.

In the RHEL 2 target each coil, although fed from a common oscillator, is provided with its own preamplifier and r.f. amplifier. Only one coil can be used at a time, the other two coils being detuned to prevent their coupling to the first coil. This detuning can be carried out remotely using a PIN diode in each preamplifier. (This diode can also be used to adjust remotely the Q-value of the LC circuit). Each NMR circuit can be tuned remotely using a varactor. (These last two features were the work of P.H.T. Banks).

8 GENERAL DISCUSSION

8.1 Operation of a target

A summary is given here of some important factors in operating a polarized target, most of which have been discussed in more detail in previous sections.

Basically, running conditions should be such that every paramagnetic centre in the target receives just sufficient microwave radiation at the correct frequency and amplitude to saturate the desired forbidden transition.

In practice, different parts of the target will require slightly different microwave frequencies to excite the required transitions, for the following reasons : the external magnetic field is not uniform in space or stable in time ; the local magnetic field is slightly modified by the field from the polarized protons themselves ; the LMN crystals will have small relative misalignments. To compensate for these irregularities, and also to obtain a more uniform microwave field distribution in the cavity, it is important to modulate the frequency of the microwave oscillator. Naturally the greater the FM required to overcome the above errors, the greater is the total microwave power required - and therefore the higher the temperature and the lower the mean polarization.

The initial values of field and microwave frequency must be set by trial and error. A suitable centre frequency should first be chosen (perhaps for optimum coupling to the cavity) and then the magnetic field adjusted for maximum polarization. Following this, increasing frequency modulation is applied till the polarization just begins to decrease. The level of microwave power should then be adjusted for maximum polarization. In a continuous-flow cryostat the helium flow valve is adjusted for minimum flow just to keep the cavity full. (A carbon resistor in the cavity is useful here as a level indicator). The polarization is reversed by changing the frequency or the field (or both).

Once these operating values of frequency and field have been established, it is most desirable to be able to maintain or repeat them without continual searching. This requires that both can be measured accurately - and preferably absolutely. As mentioned already, this is done on the second Rutherford target by measuring the field with an independent NMR probe just outside the cryostat, and the microwave frequency by reference to a harmonic of a crystal-controlled oscillator.

Polarization can be reversed in about 15 minutes, simply by setting field and frequency to the predetermined values. In reversing pola-

rization it may be necessary slightly to retune the NMR resonant circuit(s). A faster reversal of polarization direction (in < 1 second) can be accomplished by fast adiabatic passage [50].

Measurements of the enhanced lines should be made at intervals of time (of the order of minutes) much less than the proton relaxation time. The correct operation of the NMR system should be frequently checked by, for example, measuring the output voltage level of the system in the absence of a proton line (e.g. at the beginning of the frequency sweep) and also the gain of the PSD system (if used).

The whole NMR system should be recalibrated periodically, for example by measuring the thermal equilibrium proton line. The latter can be done quite rapidly with a continuous-flow cryostat by reducing the pumping speed, when the temperature can be adjusted quickly to a higher value (e.g. 1.8° K) at which substantially shorter proton relaxation times obtain. However, at low temperature thermal equilibrium can take a very long time to be established. For example at CERN, twenty four hours is required to reach equilibrium at 1.05° K ($T_{1p} \sim 120$ minutes) [18].

8.2 Polarization obtained

It is seen from Table IV that, for targets operating under the "standard" condition, 18-19 kG and ~ 1° K, the maximum polarizations range from 50 to 75 %, whilst the average values obtained over long periods range from 40 to 72 %. These variations cannot be explained simply in terms of variation in the theoretical maximum polarization P_e (equation (2.1)) in each case, for the values of P_e for all targets in the Table lie within the narrow range 87 to 93 % : nor can the variation be explained by non-uniformities in the field, since in the CERN magnets there are spatial variations of 4 to 7 G, together with time fluctuations of 1 to 2 G, yet polarizations of 75 % are obtained.

However, other things being equal, it is seen that the following promote high proton polarizations : pure crystals, perhaps grown from a solution with less than 1 % Nd/La ; small target (and cavity) volumes ; high helium pumping speeds. These conditions are particularly important because they lead to low temperatures, long proton relaxation times and small microwave power requirements (all of which are interrelated).

The influence of these factors can be seen in the high polarizations in recent CERN targets, and in the remarkable results for Dubna 2.

8.3 Errors in the NMR method

a. Errors in measuring relative polarizations.

Firstly, errors can arise due to changes in the characteristics of the electronic circuits used, and the LC circuit itself. These errors should be negligible if care is taken periodically to check the system as discussed in section 8.1. In this respect it is an advantage to use a system which automatically corrects for small changes in gain, for example as with the analogue computer arrangement on the latest Rutherford target.

Secondly, there are errors caused by limitations in the NMR system, for example : the finite output impedance of the NMR oscillator ; non-linearities in the amplifiers, detector and frequency sweep rate.

Thirdly, errors occur due to the mathematical approximations made in calculating the polarization from the measured voltages. Thus, neglect of the reactive effect of the target introduces an error which can, however, be reduced to the order of a few percent by using small values of ηQ (section 7.2). An error also arises due to uncertainty in the criterion for tuning the LC circuit with the proton line present, and hence in an ambiguity as to the position of the base line of the NMR signal.

All these errors should with care be reduceable to less than $\pm$ 5 %.

b. Errors in absolute calibration.

Errors arise here because of the small size of the "TE" signal, and because the target will not be exactly in thermal equilibrium with the helium bath. Also, the NMR field will at least slightly depolarize the protons. On the other hand, the temperature of the helium can be measured quite accurately ($\sim$ 1 %) by its vapour pressure, correcting for the thermomolecular effect [51].

Otherwise, errors arise as mentioned in (a) above, to which must be added an error due to the large change in the size of the signal from TE to enhanced conditions.

Borghini et al [18] measure the area of the TE line to about 1 %, and suggest that if sufficient care is taken, an accuracy of absolute polarization measurement of $\pm$ 3 % should be obtained.

The Argonne workers find fluctuations in the size of their TE signal of $\pm$ 8 % from day to day [15].

Betz et al [9] quote accuracies for the TE signal of $\pm$ 6 % and for the relative polarization $\pm$ 5 %.

c. Sampling uniformity.

A further error is introduced because the NMR coils do not sample the polarization uniformly. This effect is discussed below.

8.4 Uniformity of polarization

All the methods in section 6 measure in some way the average polarization over the whole target. However, different parts of the target may well not be equally polarized.

It would not matter if the polarization were non-uniform provided that the beam had a uniform current density, and at the same time the measuring system saw all parts of the target with equal weight. However, although the latter can be approximately achieved (for example, using the Berkeley coil, section 7.6), the beam will not usually be uniform unless its centre only is used, with consequent loss of useful beam.

In an early version of the Berkeley target the polarization was proved to be very non-uniform when the four crystals comprising the target were stuck together with Kel-F (hydrogen free) grease, making a solid cube of side 25 mm [8,10]. The distribution of polarization was determined by measuring the scattering asymmetry when a proton beam of diameter 6 mm from the 184" cyclotron sampled a number of different regions of the crystal. The relative polarization was found to range from 1 at the centre to 1.7 at the edge of the target. This effect was thought to be due to temperature gradients in the solid block of target crystals, from inside to periphery, due to release of energy from microwaves. When the target was rebuilt separating the four crystals to allow helium to flow freely between them, the polarization was found to be uniform over the whole cross-section of the target.

Ducros et al [28] have also used a probe beam in this way, demonstrating that their target was uniformly polarized in a radial direction.

In the case of long targets, the uniformity in the longitudinal direction can be determined using a number of NMR coils, as for the RHEL 1 and CERN 3 targets.

The uniformity can also be checked by seeing that the same average value of polarization is obtained from measurements made using two different methods which sample the polarization differently. In most of the comparisons of this sort which have been made, good agreement has been found between the different methods as, for example, in the case of the NMR and HEP methods (section 8.5). Similarly, target polarizations have been determined at Dubna both

by the NMR method and by measuring the polarization of a neutron beam transmitted through the target, satisfactory agreement again being obtained [36]. Also at Dubna there was good agreement in the polarization measured by the NMR and external field methods (section 6(b)).

Thus, it can be concluded that a reasonable degree of uniformity is usually achieved in practice, provided the target is carefully made and operated. The following conditions are important if good uniformity is to be obtained.

a. The target should be divided into a number of thin, well cooled slabs. The thickness of each slab should be such that the temperature gradient from inside to the surface is negligible, taking into account the thermal conductivity of the material and the heat dissipated in it. The slabs should be arranged so as to minimize the effect of any thermal gradients which may nevertheless occur, a good arrangement being to stack the slabs perpendicular to the beam.

b. The paramagnetic centres (Nd^{3+} in the case of LMN) should be uniformly distributed.

c. The frequency of the microwave oscillator should be modulated (section 8.1).

d. The NMR field must not be depolarizing (or at least should be uniformly depolarizing).

e. There must be negligible radiation damage from a non-uniform beam.

f. Beam heating must be negligible.

Whatever precautions are taken to obtain completely uniform polarization, it is hard to guarantee that this has been achieved in practice, unless detailed measurements have been made at different parts of the target, as for example in the probe beam measurements mentioned above (or unless the polarization is found to be near its theoretical maximum value). In view of this, the HEP method, where applicable, seems to be the best way of measuring the polarization, provided that the beam-line used for the main experiment can be adjusted to provide a beam of suitable particles which has the same shape as the main beam. As this method of measurement is time consuming, it would normally be used only to calibrate a secondary monitoring system, for example an NMR system [15,24].

8.5 Comparison of NMR and HEP results

A number of experiments have been carried out in which polarization has been measured both by the NMR method calibrated by the TE signal, and by the scattering of particles of known properties. The results of some of this work are summarized here.

a. Saclay.

Ducros et al [28] reported good agreement for p-p scattering at 720 MeV using Saturne.

b. CERN/Saclay.

Borghini et al investigated p-p scattering at 600 MeV, obtaining good agreement with the Berkeley results, but bad agreement with Dubna data at 635 MeV [16].

c. Argonne.

Esterling et al [15] have measured the absolute polarization of their target by two methods simultaneously : firstly, by the NMR method, calibrated by the proton TE signal ; and secondly by observing the asymmetry in the scattering from the target of protons of momentum 1 GeV/c at which the polarization parameter had previously been measured by double scattering experiments with an unpolarized target. The ratio of the target polarization calculated from the scattering result (P_{p-p}), to that from the NMR method (P_{NMR}) was found to be :

$$P_{p-p}/P_{NMR} = 0.92 \quad .$$

The difference between the two measurements is probably not significant, for the counting errors in measuring the asymmetry were ± 8 %, the error in the double scattering result ± 10 %, and the error in the TE signal ± 8 %.

d. Berkeley.

Chamberlain et al [11] found good agreement for p-p scattering at 720 MeV.

It is seen that, on the whole, there is good agreement between the NMR calibration of polarized targets and HEP results.

8.6 Conclusions

It is possible to obtain polarizations near the theoretical maximum in LMN targets of volume ~ 16 cm^3. Larger targets (~ 40 cm^3) have been successfully built, and there seems no reason why much bigger volumes could not be supplied if required.

With a continuous-flow cryostat, efficient operation of a target is possible : the maximum cooling effect is extracted from the liquid helium, and the target can be kept fully polarized for long periods of time, with only short breaks every day or two for dewar changes. Such cryostats allow the geometry of the target better to be arranged to fit the high energy experiment.

Iron-cored magnets can also be tailored to allow good access to the target itself. Superconducting magnets look especially useful for certain experiments in which the beam is parallel with the polarization direction. A magnet giving an access solid angle of 4π is not yet available.

Measurement systems based on the Q-meter are now convenient, giving immediate values of polarization. However, the external field method of polarization measurement has much to recommend it.

Thus, target technology is well developed, although targets are expensive both to build and to operate. Methods are likely soon to become available to reduce both costs substantially.

More fundamentally, however, what are now urgently required are target materials containing more free protons.

The author is most grateful to the following for supplying him with reports and other unpublished information, which have been of great help in the preparation of this paper : A. Abragam, M. Borghini, O. Chamberlain, M. Chapellier, Y. Ducros, C.D. Jeffries, R.V. Pound, L. Van Rossum, P. Roubeau, C. Ryter, J. Sanderson, G. Shapiro, F.L. Shapiro, M.A. Wigan, A. Yokosawa, and finally his colleagues at the Rutherford Laboratory.

Notes and References

* LMN. However, in this paper "LMN" should usually be taken to mean lanthanum magnesium nitrate doped with Nd.

** Fundamental aspects of the solid effect have been discussed by many authors, including Jeffries [3,30,31], Abragam and Borghini [2], Schmugge and Jeffries [32], Ramakrishna and Robinson [33], and Borghini [34,35].

*** Petricek and Odehnal reported at the Saclay Conference a comparison between the constant current and constant voltage Q-meters. They concluded that the polarization could be accurately deduced by applying calculated corrections to the measured values of $\int(Z_0 - Z)d\omega$.

1) A. Abragam, M. Borghini, P. Catillon, P. Roubeau and J. Thirion, Phys. Letters, 1962, 2, 310.
2) A. Abragam and M. Borghini, Progress in Low Temperature Physics (North-Holland Publ. Co., Amsterdam, 1964), 4, p. 384.
3) C.D. Jeffries, Dynamic Nuclear Orientation (John Wiley, New York, 1963).
4) O. Chamberlain, C.D. Jeffries, C. Schultz and G. Shapiro, Bull. Am. Phys. Soc., 1963, 8, 38.
5) O. Chamberlain, C.D. Jeffries, C.H. Schultz, G. Shapiro and L. Van Rossum, Phys. Letters, 1963, 7, 293.
6) C.H. Schultz, Ph.D. Thesis, University of California Radiation Laboratory Report N° UCRL-11149 (unpublished).
7) C.H. Schultz, O. Chamberlain and G. Shapiro, Bull. Am. Phys. Soc., 1964, 9, 95.
8) P.D. Grannis, Ph.D. Thesis, University of California Radiation Laboratory Report N° UCRL-16070 (unpublished).
9) F. Betz, J. Arens, O. Chamberlain, H. Dost, P. Grannis, M. Hansroul, L. Holloway, C. Schultz and G. Shapiro, Phys. Rev., 1966, 148, 1289.
10) P. Grannis, J. Arens, F. Betz, O. Chamberlain, B. Dieterle, C. Schultz, G. Shapiro, H. Steiner, L. Van Rossum and D. Weldon, Phys. Rev., 1966, 148, 1297.
11) O. Chamberlain, M.J. Hansroul, C.H. Johnson, P.D. Grannis, L.E. Holloway, L. Valentin, P.R. Robrish and H.M. Steiner, Phys. Rev. Letters, 1966, 17, 975.
12) A. Moretti, S. Suwa and A. Yokosawa, Int. Conf. on Polarization Phenomena of Nucleons (Karlsruhe, 1965).
13) S. Suwa, A. Yokosawa, T.K. Khoe and A. Moretti, V. Int. Conf. on High Energy Accel. (Frascati 1965), p. 564.
14) S. Suwa, A. Yokosawa, N.E. Booth, R.J. Esterling and R.E. Hill, Phys. Rev. Letters, 1965, 15, 560.
15) R.J. Esterling, R.E. Hill, N.E. Booth, S. Suwa and A. Yokosawa, EFINS 66-29 (Enrico Fermi Inst. for Nuclear Studies, University of Chicago, 1966).
16) M. Borghini, M. Odehnal, P. Roubeau, C. Ryter, G. Coignet, L. Di Lella and L. Dick, Proc. Int. Conf. on High Energy Physics (Dubna 1964), vol. II.
17) M. Borghini, P. Roubeau and Ch. Ryter, Helv. Phys. Acta, 1965, 38, 660.
18) M. Borghini, P. Roubeau and Ch. Ryter, CEN-Saclay Preprint (submitted to "Nucl. Instr. and Methods", 1966).
19) G. Coignet, D. Cronenberger, K. Kuroda, A. Michalowicz, J.C. Olivier, M. Poulet, J. Teillac, M. Borghini and Ch. Ryter, Nuovo Cimento, 1966, 43, 708.
20) M. Borghini, G. Coignet, L. Dick, L. Di Lella, A. Michalowicz and P.C. Macq, Phys. Letters, 1966, 21, 114.
21) V.I. Lushchikov and Yu.V. Taran, Sov. J. Nucl. Phys., 1965, 1, 609.
22) F.L. Shapiro, Private communication (1966).
23) R.V. Pound and J. Sanderson, Private communication (1966).

24) H.H. Atkinson, B.E. Belcher, B.F. Colyer and R. Downton, Proc. 10th Int. Conf. High Energy Accel. (Frascati 1965), p. 559.
25) P.J. Duke, D.P. Jones, M.A.R. Kemp, P.G. Murphy, J.D. Prentice, J.J. Thresher, H.H. Atkinson, C.R. Cox and K.S. Heard, Phys. Rev. Letters, 1965, 15, 468.
26) H.H. Atkinson, C.R. Cox, P.J. Duke, K.S. Heard, D.P. Jones, M.A.R. Kemp, P.G. Murphy, J.D. Prentice and J.J. Thresher, Proc. Roy. Soc., 1966, A289, 441.
27) H.H. Atkinson et al, to be published.
28) Y. Ducros, A. De Lesquen, J. Movchet, J.C. Raoul, L. Van Rossum, J. Deregel, J.M. Fontaine, A. Boucherie and J.F. Mougel, Int. Conf. Elementary Particles, Oxford (1965), (unpublished).
29) G. Shapiro, Progr. in Nucl. Tech. and Instrumentation, 1964, 1, 176. Also note : G. Shapiro, Sci. Am., July 1966, p. 68.
30) C.D. Jeffries, Proc. Phys. Soc., 1966, 88, 257.
31) C.D. Jeffries, Tech. Report UCB-34P20-T-1 (1966).
32) T.J. Schmugge and C.D. Jeffries, Phys. Rev., 1965, 138, A1785.
33) J. Ramakrishna and F.N.H. Robinson, Proc. Phys. Soc., 1965, 87, 945.
34) M. Borghini, Phys. Letters, 1966, 20, 228.
35) M. Borghini, Phys. Rev. Letters, 1966, 16, 318.
36) D. Draghicescu, V.I. Lushchikov, V.G. Nikolenko, Yu.V. Taran and F.L. Shapiro, Phys. Letters, 1964, 12, 334.
37) H.M. Rosenberg, Private communication.
38) J.C. Waldron, AERE-M 1666 (A.E.R.E., Harwell).
39) T.J. Schmugge and C.D. Jeffries, Phys. Rev. Letters, 1962, 9, 268.
40) C.N. Fallier Jr., Rev. Sci. Instr., 1961, 32, 342.
41) J. Sanderson, Private communication (1966).
42) T.W.P. Brogden, O.N. Jarvis, J. Orchard-Webb and M.R. Wigan, 2nd Int. Conf. on Polarized Phenomena in Nucleons (Karlsruhe 1965), p. 298.
43) M.R. Wigan, Private communication (1966).
44) Y. Ducros and L. Van Rossum, Private communication (1966). Note also : H. Desportes, Report N° CEA-R2606 (Saclay 1964).
45) P. Roubeau, Cryogenics, August 1966, p. 207.
46) P. Roubeau, Thesis, Docteur-Ingénieur (Grenoble, November 1966).
47) A. Abragam, Compt. Rend., 1964, 258, 1773.
48) A. Abragam and M. Chapellier, Private communication.
49) Ch. Ryter, CEN-Saclay Preprint (June 1966).
50) M. Chapellier, Private communication (1965).
51) T.R. Roberts and S.G. Sydoriak, Phys. Rev., 1956, 102, 304.

COMMENT ON PROTON RELAXATION IN Nd : LaMN AT HIGH FIELDS AND LOW TEMPERATURES

C.D. JEFFRIES
University of California, Berkeley

Recent measurements by T.E. Gunter [1] on the proton spin lattice relaxation rate T_{1p}^{-1} in a crystal of Nd:LaMN, grown from 1 % solution [2], are of interest to polarized target technology. Data were taken with $z \perp H$ over the range $10 < H < 50$ kOe, $0.5 < T < 3°$ K using a superconducting solenoid and a ^{3}He cryostat ; some results are shown in the figure 1. The data are well fit over wide ranges of H and T by the solid line, which is the sum of two terms :

$$\frac{1}{T_{1p}} = 2.1 \times 10^{-16} H^3 \coth\left(\frac{2.7\beta H}{2kT}\right) \operatorname{sech}^2\left(\frac{2.7\beta H}{2kT}\right)$$

$$+ 9.9 \times 10^{-8} H \coth\left(\frac{4.4\beta H}{2kT}\right) \operatorname{sech}^2\left(\frac{4.4\beta H}{2kT}\right)$$

the first, due to Nd^{3+}, completely dominating the second, due to a non-Kramers impurity, possibly Fe^{2+} of $\sim 10^{-5}$ concentration. Both are in good agreement with the prediction from the shell-of-influence model [3] :

$$\frac{1}{T_{1p}} = \frac{3}{10}\left(\frac{g_\perp \beta}{H}\right)^2 \frac{1}{r_1^3 \, r_2^3} \frac{1}{T_{1e}} \operatorname{sech}^2\left(\frac{g_\perp \beta H}{2kT}\right) \quad .$$

In particular, the factor $\operatorname{sech}^2(g_\perp \beta H/2kT)$ is well verified, showing that very long relaxation times may be achieved. From the measured value $T_{1p} = 40$ hours in 19.5 kOe, at 0.5° K, we predict $T_{1p} = 300$ hours at 0.4° K and several thousand hours at 0.3° K. This suggests the utility of semi-permanently polarized samples in certain configurations, e.g., in bubble chambers or in balloon flights.

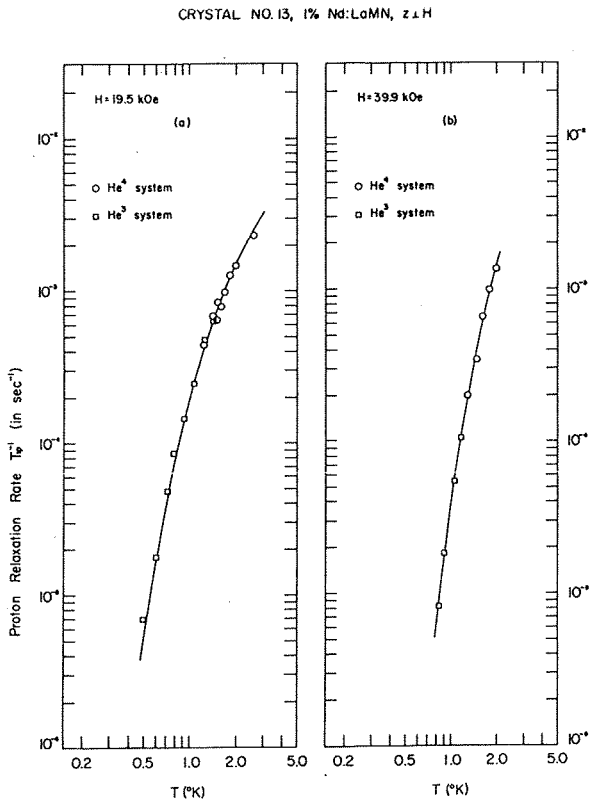

Fig. 1 Measured proton relaxation rate in Nd:LaMN.

References

1) T.E. Gunter and C.D. Jeffries, Bull. Am. Phys. Soc., 1966, 11, 906 (to be published in Phys. Rev.).
2) This is crystal N° 13 of reference 3.
3) T.J. Schmugge and C.D. Jeffries, Phys. Rev., 1965, 138, A1785, equation (14).

HIGH ENERGY PHYSICS EXPERIMENTS WITH POLARIZED TARGETS

O. CHAMBERLAIN

University of California, Berkeley

If we are to do a workmanlike job of studying the strong interactions it is imperative that we have knowledge of the spin dependence of the forces. This implies that polarization experiments are essential. Already Bareyre, Bricman, Stirling and Villet [1] have shown that pion-proton polarization experiments should be interpreted as indicating two new resonances not previously seen by other methods.

The present-day approach to determining detailed pion-proton scattering amplitudes is to use measured differential cross-sections, polarization measurements, dispersion relations, and isospin conservation rules. Further assumptions are unitarity of the S matrix and the short-range nature of strong interactions. In the more distant future I hope we may see the day when the scattering experiments will be sufficiently detailed that the dispersion relations will not be necessary to the interpretation of results. Then the dispersion relations may themselves be checked experimentally, rather than being assumed.

I see, then, an early period of polarization experiments followed by a later period in which more extensive experimental results will be called for. For the pion-proton system the first period seems well progressed, based on measurements of differential cross-section and P, the polarization. In the second period more complex experiments should be required, such as measurements of the parameters R and A. In R and A measurements, the protons have a known polarization before the collision takes place. After the pion scatters on the proton, one asks how much residual polarization the proton has.

The nucleon-nucleon (N-N) system is susceptible to similar analysis but there are more amplitudes to be determined, so more expe-

riments must be performed. The N-N system is less well analyzed at present than the π-N system.

Before describing in detail the experiments that have already been performed we review the definition of polarization, restricting our discussion to particles of spin 1/2. If a beam or target has random spin-axis directions it is said to be unpolarized. If all the spin axes are oriented in a particular direction it is said to be completely (or 100 %) polarized in that direction. For any beam or target we may imagine that we measure the component of spin along a particular direction for each particle, finding for each particle either +1/2 (spin up along the chosen direction) or -1/2 (spin down). The component of polarization in the chosen direction is then :

$$P = \frac{N_{up} - N_{down}}{N_{up} + N_{down}}$$

where N_{up} (or N_{down}) is the number with spin up (or down).

The first experiment performed with a polarized proton target was that of Abragam, Borghini, Catillon, Coustham, Roubeau and Thirion [2]. It was a measurement of the parameter C_{nn} for proton-proton scattering at 20 MeV. The parameter C_{nn} is a spin correlation coefficient expressing the dependence of the differential scattering cross-section on the relative spin orientation of two colliding protons. The subscripts n refer to the normal to the scattering plane. We imagine first that a proton beam completely polarized in a particular direction normal to its direction of motion impinges on a proton target completely polarized either parallel or antiparallel to the polarization direction of the beam. In either case let $I(\theta)$ be the differential cross-section for scattering in a plane perpendicular (normal) to the polarization direction at center-of-mass angle θ. The parameter C_{nn} would then be :

$$C_{nn}(\theta) = \frac{I_{parallel}(\theta) - I_{antiparallel}(\theta)}{I_{parallel}(\theta) + I_{antiparallel}(\theta)} .$$

If the beam polarization is P_B and the target polarization P_T then the equivalent expression is :

$$C_{nn}(\theta) = \frac{1}{P_B}\frac{1}{P_T}\frac{I_{parallel}(\theta) - I_{antiparallel}(\theta)}{I_{parallel}(\theta) + I_{antiparallel}(\theta)} .$$

A sketch of the experimental arrangement of Abragam et al is shown in figure 1. A beam of α particles was incident at the left on a hydrogenous foil, giving rise to knock-on protons highly polarized in a vertical direction (normal to the scattering plane at the hydrogenous foil, the first target). The highly polarized protons

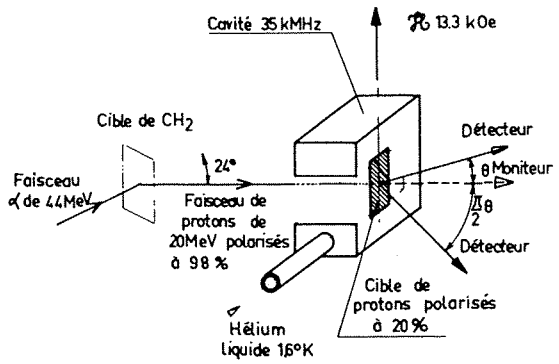

Fig. 1 Sketch of the apparatus of Abragam et al, that was used to measure the spin correlation coefficient C_{nn} for proton-proton scattering at 20 MeV. A highly polarized proton beam made by alpha-proton scattering is incident on the polarized proton target.

(of 20 MeV) impinged on a polarized proton target (of lanthanum magnesium nitrate (LMN)) and proton-proton scattering events were counted at center-of-mass angles between 60° and 90°. By measuring the rate of p-p scattering events with the target protons polarized parallel or antiparallel to the beam polarization, they could determine C_{nn}. For the proton-proton system the meaning of C_{nn} is particularly simple at 90° c.m. scattering angle : spins parallel means triplet spin state ; spins antiparallel means singlet. The experimental value of - 0.91 for C_{nn} corresponds to the fact that the p-p scattering at this energy is mainly in singlet states. However, as the scattering angle deviates from 90° (c.m.), the interpretation becomes more complicated.

Since I attribute to Professors Abragam and Jeffries the birth of polarized proton targets in usable form, it would be fitting if I next described work of which Professor Jeffries is a co-author. However, I want first to give the definition of the relevant parameter P and then to describe the older technique of measuring it.

The definition of the polarization parameter P is the final-state polarization after the scattering process providing the particles were unpolarized before the scattering. In fact, figure 2 shows a plan view of an experiment [3] to measure the parameter P by rescattering the recoil protons from a π-p collision. A pion beam strikes the (unpolarized) hydrogen target. The recoil protons are rescattered on a second (carbon) target, where any vertical component of polarization would result in a left-right asymmetry in the scattering at the carbon target. This is a tolerable way to measure P if no more convenient way is readily available. While some improvements on this basic method have been made with the introduction of spark

chambers [4], it is still better to use a different approach that involves a polarized proton target.

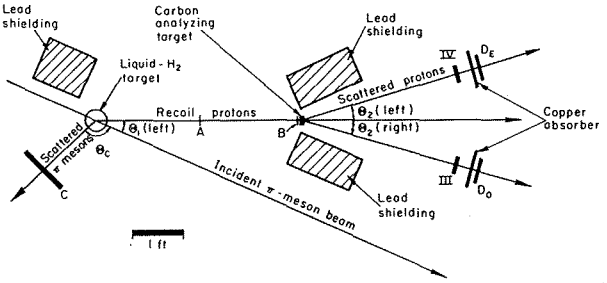

Fig. 2 Plan view of the apparatus of Foot et al, used to measure the polarization P in pion-proton scattering. The pion-proton scattering occurs at the first target. The polarization of the recoiling proton is measured by a second scattering on a carbon target. This technique has for the most part been replaced by polarized-target methods.

The use of a polarized target to measure P depends on the presumed facts that the strong interactions conserve parity and are invarian under the time-reversal transformation. We will not make the arguments here, but they may be found in a review paper of Wolfenstein [5]. The result is that for elastic scattering the left-right asymmetry ϵ of the scattering on a target completely polarized up is numerically equal to P :

$$\epsilon \equiv \frac{N_{left} - N_{right}}{N_{left} + N_{right}} = P$$

where N_{left} (or N_{right}) is the number of pions elastically scattere to the left (or right) at angle θ and P is the polarization in scattering at the same angle. If the target is not 100 % polarized this may be corrected for by using :

$$\epsilon = P_T \, P$$

where P_T is the target polarization. By measuring P_T and the asymmetry ϵ we may deduce P.

In practice one of the two configurations (let us say that of right scattering) can be rotated by 180° around the beam direction so tha the counter is on the left but the target polarized down. This has the advantage that the counter may be in exactly the same position for the two cases being compared, so there is no problem of making

a left scattering angle exactly equal to a right scattering angle. The desired asymmetry is then :

$$\epsilon = \frac{N_{up} - N_{down}}{N_{up} + N_{down}}$$

where N_{up} (or N_{down}) is the number of scattering processes detected in a counter to the left when the target is polarized up (or down). This is the method used by Jeffries, Schultz, Shapiro, Van Rossum and myself [6].

A further comment is necessary concerning the separation of pion-proton scattering events from other types of scattering such as pion scattering by protons bound in complex nuclei. When the target material is lanthanum magnesium double nitrate (LMN) the protons of hydrogen constitute only 3 % of the target weight. Accordingly, scattering by bound protons is much more common than scattering by free protons (hydrogen). To avoid having the interesting events overshadowed by unwanted scattering processes one must select elastic pion-proton scatterings from other scattering processes on the basis of the scattering kinematics.

The selection of elastic scattering processes on free hydrogen can be accomplished by steps as follows :

a. Observe whether a scattered pion is accompanied by a coplanar recoil proton, as required by the elastic scattering on hydrogen.

b. Observe whether the angle of emission of the coplanar recoil proton is that expected for elastic scattering kinematics.

c. Check whether the energy of the emerging pion is consistent with kinematics.

d. See whether the energy of the recoil proton is consistent with the kinematics.

If all of these checks were applied, the background would be small indeed, as witnessed by the very-high-momentum-transfer p-p scattering experiments at alternating-gradient synchrotrons [7]. In practice it is often sufficient to apply (a) and (b) only, and is much simpler. That is the way most of the π-p scattering experiments were done.

Figure 3 shows the apparatus. A coincidence between the pion telescope and some proton counter indicated a coplanar event (condition (a)), and a coincidence with the central proton counter indicated the proton angle was consistent with π-p scattering. Scattering by bound protons is rather like scattering from a moving nucleon, so the emergence angle of the proton is usually not that of elastic scattering on free hydrogen.

Figure 4 shows a further elaboration of the same method in which the scattered beam particle may be detected in any one of 10 coun-

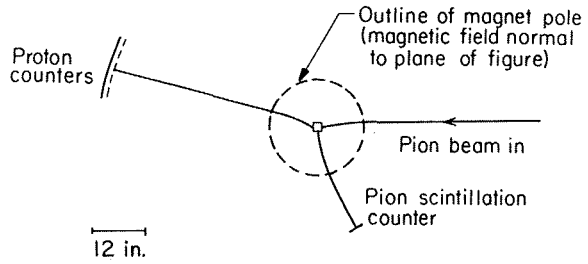

Fig. 3 Sketch of the rather simple experimental arrangement of Chamberlain, Jeffries, Schultz, Shapiro and Van Rossum as used to measure the polarization in pion-proton scattering. The polarized proton target is located at the center of the magnet.

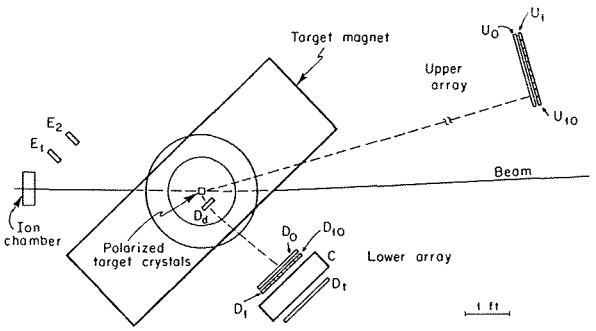

Fig. 4 Elevation view of a more sophisticated apparatus for measuring polarization in elastic scattering. The upper and lower counter arrays each have 10 counters. The beam is incident from the left. The Cherenkov counter C is used for monitoring the beam intensity on the polarized target. To be of interest a scattering event should count in counters U_o, D_d, D_o, one of U_1 to U_{10} and one of D_1 to D_{10}.

ters above the beam line, and the recoil proton detected in one of 10 counters below. Figure 5 shows a typical histogram constructed out of the scattered particles from a polarized target made of LMN. Each event that registered in a particular upper counter (number 6) has been entered in the histogram if it was coincident with a count in one of the ten lower counters so as to show the number of coincidence counts in each of the lower counters. The figure shows 3 sets of data : counts taken with the target negatively polarized (opposi-

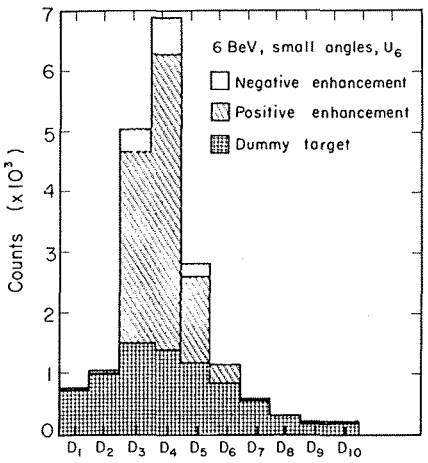

Fig. 5 Histogram of coincidence events between the upper counter U_6 and each of the lower counters D_1 to D_{10}, for the apparatus shown in figure 4. The peak in counters D_3 and D_4 represents elastic scattering on free target protons. The dummy target data show the unwanted contribution from heavy elements in the polarized target. The intensity difference between runs taken with negative and positive target polarization indicates an asymmetry of about 5 % for this particular scattering process.

te to the thermal equilibrium direction), counts taken with target positively polarized, and counts taken with a dummy target, chosen to be similar to LMN except having no hydrogen content. The polarized target data show a strong peak due to free hydrogen above a broad background from heavy elements in the LMN. The dummy-target data allow a reasonable subtraction of the background to be made. Notice that the size of the hydrogen peak is slightly different for the two signs of target polarization, indicating some asymmetry in the scattering process in this case.

Figure 6 shows the results of Betz et al [8] on the polarization in proton-proton scattering at 740 MeV, as an illustration of typical results. Figure 7 shows their results at 328 MeV, compared to earlier results at 310 MeV obtained without benefit of polarized target. The agreement is not perfect but, within the recognizable errors, indicates that we may have confidence in the measurement of the target polarization in this case.

Figure 8 shows results of Grannis et al [9] for polarization in p-p scattering at higher energy.

Figure 9 displays the largest value of polarization in p-p scattering as a function of the (laboratory) kinetic energy. After it reaches a peak value near 700 MeV it decreases monotonically at higher energy, in qualitative agreement with theoretical expectations.

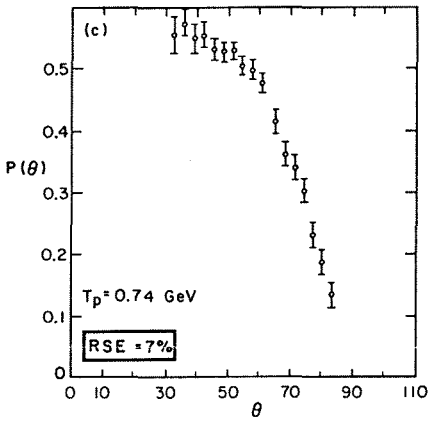

Fig. 6 Results of Betz et al for polarization in proton-proton scattering at 740 MeV (lab.) kinetic energy. The apparatus has been shown in figure 4. The relative systematic error, corresponding to uncertainty in the polarization of the polarized target, is 7 %. This means there is a 7 % uncertainty in the scale against which P(θ) is measured.

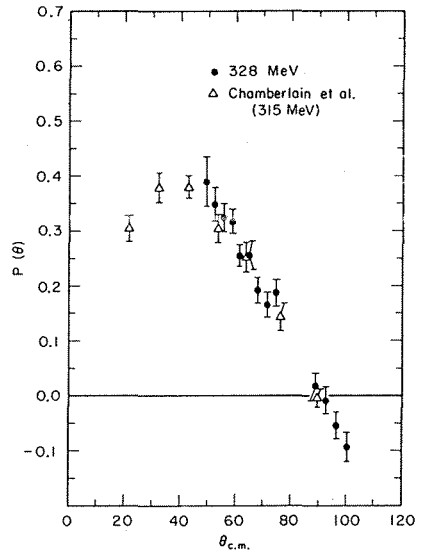

Fig. 7 Results of Betz et al for polarization in proton-proton scattering at 328 MeV, compared to 315 MeV results obtained without benefit of a polarized target.

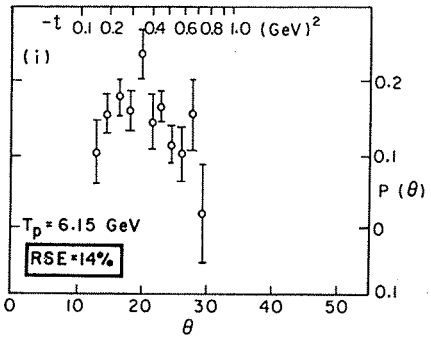

Fig. 8 Results of Grannis et al on polarization in proton-proton scattering for incident lab. kinetic energy of 6.15 GeV. The polarization scale is uncertain by 14 %. t is the invariant square of momentum transfer. θ is the center-of-mass scattering angle.

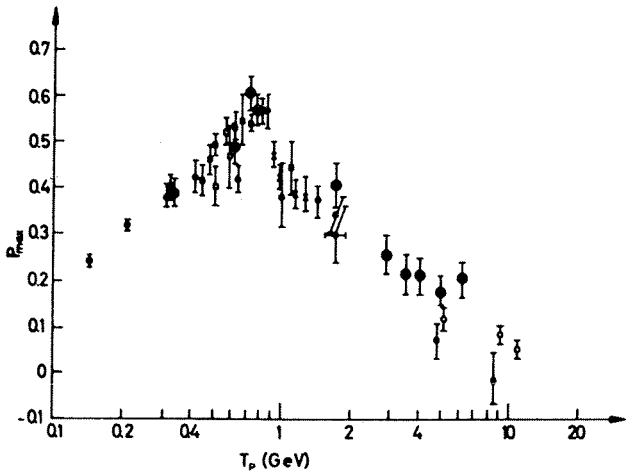

Fig. 9 Plot of the maximum polarization in proton-proton scattering as a function of lab. kinetic energy T_p.

When it is desired to use the polarized target for a measurement of polarization at a very small angle it may be impracticable to make the target thin enough that the recoil proton can emerge reliably. In this case one is restricted to making measurements only on the scattered beam particle to distinguish the scattering from free hydrogen. A case in point is taken from reference 6, where polarization in small-angle pion-proton scattering was attempted. The method consists in measuring the energy of pions scattered at a particular angle and selecting those whose energy is consistent with elastic scattering kinematics. In this case the range of the pions in a copper absorber could be used as a measure of their energy. Figure 10 shows differential range curves taken with LMN target and with dummy target. The difference shows the elastic scattering on hydrogen, but notice that for data taken at the appropriate value of copper absorber the LMN counts are only about 20 % due to hydrogen, the rest being background from heavy elements. This indicates the limitations on the use of a polarized LMN target when only one constraint can be applied to distinguish the scattering on free hydrogen.

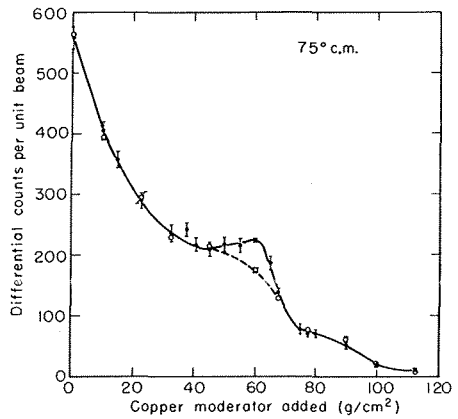

Fig. 10 Counting rate of scattered pions in a differential range telescope as a function of copper absorber thickness. The solid curve represents data taken with the polarized target in place but not highly polarized. The dashed curve represents dummy target. The difference near 60 g/cm^2 is due to elastic scattering on free protons in the target.

An arrangement for measuring C_{nn} in proton-proton scattering is shown in figure 11. It is the apparatus of Dost et al [10]. The 740 MeV external beam from the cyclotron is deflected by two magnets so as to impinge on the first target of liquid hydrogen either from above or from below the regular beam line. The protons that go in the forward direction are polarized in the scattering and may be focussed onto the polarized hydrogen target (of LMN). In order to determine C_{nn} without altering the counter positions

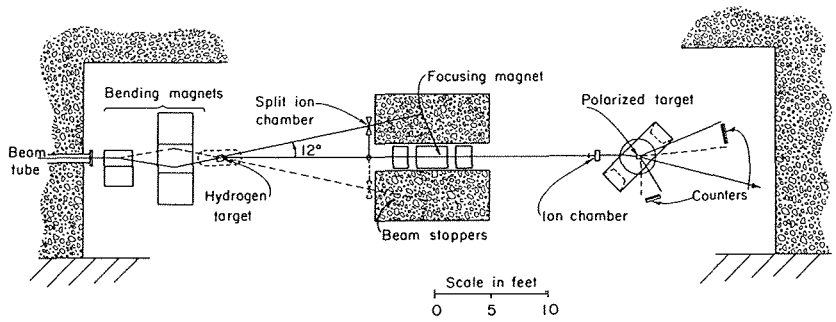

Fig. 11 Elevation view of the apparatus of Dost et al for measuring the spin correlation coefficient C_{nn}. The proton beam was polarized by a first scattering on a hydrogen target. The resulting polarized beam was incident on the polarized proton target.

one takes a 4-way difference involving both signs of beam polarization, by striking the liquid hydrogen target both from above and from below, and both signs of polarization in the LMN target. The expression is :

$$C_{nn} = \frac{1}{P_T}\frac{1}{P_B}\frac{N_{++} - N_{+-} - N_{-+} + N_{--}}{N_{++} + N_{+-} + N_{-+} + N_{--}}$$

where T indicates target (LMN), B indicates beam (incident on the LMN target) and the other subscripts refer to incident-beam polarization direction and polarized-target polarization direction. The results are shown in figure 12, along with three points obtained by Golovin, Dzhelepov, Zul'karneev and Wa-Ch'uang [11] without the benefit of a polarized target. The agreement between the two experiments is quite good. The fact that C_{nn} is nearly 1 at 90° indicates that the scattering there is mostly triplet scattering.

A very important series of measurements on pion-proton polarization has been made by Atkinson, Cox, Duke, Heard, Jones, Kemp, Murphy, Prentice and Thresher [12]. Their apparatus is shown in figure 13. It uses an extensive series of counters on each side of the beam. Figure 14 shows a view of their apparatus viewed along the beam direction. They have used an extensive array of counters to assure de coplanarity of the events they have used in their results. They have made measurements at a number of energies. Figure 15 shows typical results, for the case of incident pion momentum of 1080 MeV/c. These results have played a crucial part in the analysis of Bareyre, Bricman, Stirling and Villet [1].

Similar experiments have been carried out at a somewhat higher energy of π-p scattering by Suwa, Yokosawa, Booth, Esterling and Hill [14]. Their experimental arrangement is shown in figure 16

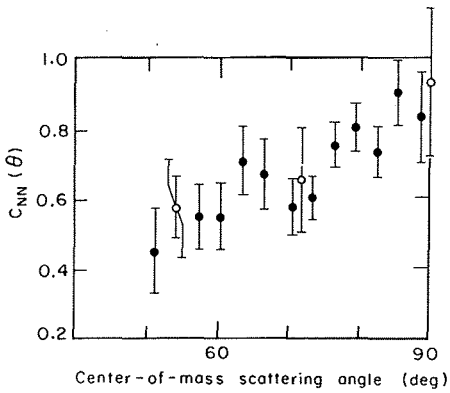

Fig. 12 Results of Dost et al on C_{nn} in proton-proton scattering at 680 MeV, along with 3 points (open circles) of Golovin et al at 640 MeV. The Golovin experiment was performed without a polarized proton target.

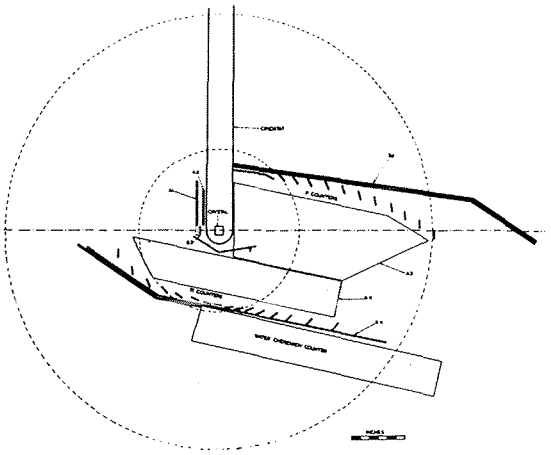

Fig. 13 Apparatus of Duke et al for measuring the polarization in pion-proton scattering. A3 and A4 are anticoincidence counters placed against the magnet pole faces.

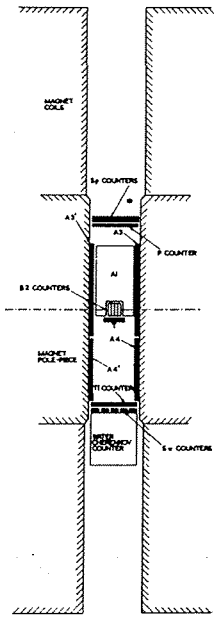

Fig. 14 Apparatus of Duke et al as seen from the beam direction. The series of counters B2, Sp and Sπ were used to select coplanar scattering events.

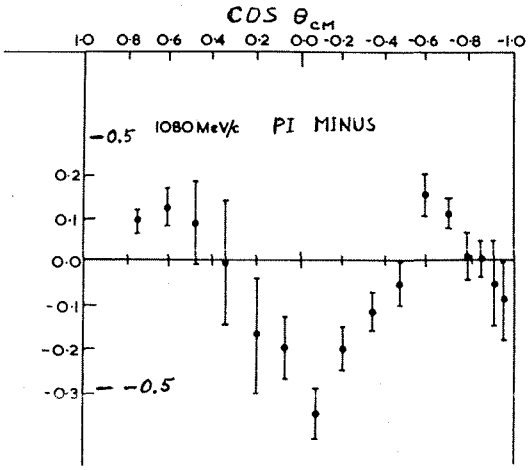

Fig. 15 Typical results by Duke et al. The momentum of the incident negative pion beam is 1080 MeV/c. The original scale shows the asymmetry observed. A suitable scale of polarization is indicated by markings at P = 0.5 and P = -0.5. The horizontal scale represents the cosine of the center-of-mass scattering angle.

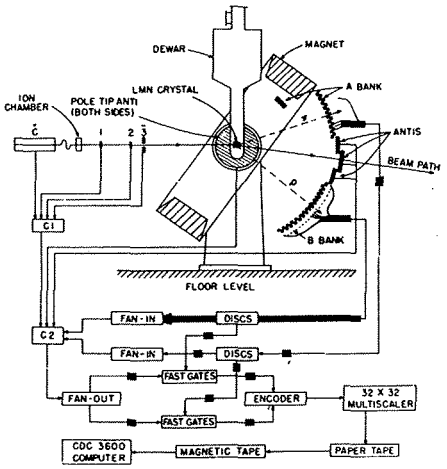

Fig. 16 Polarized target arrangement of Suwa, Yokosawa, Booth, Esterling and Hill.

and figure 17 shows their "hydrogen peak", in the histogram of coincidence counts between the counters of one array with a particular counter in the other array. An example of their results is shown in figure 18.

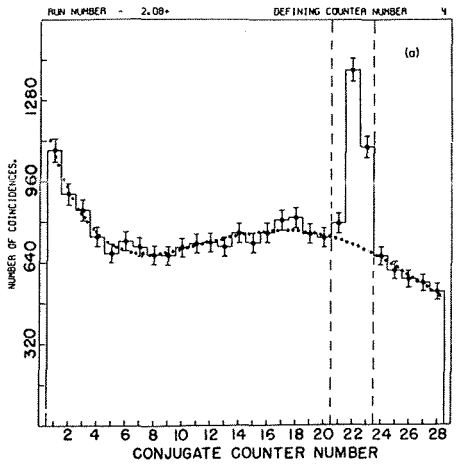

Fig. 17 Histogram of coincidence counts between one counter of one bank and each counter of the other bank. The peak near counter 22 is due to elastic pion-proton scattering. The apparatus is shown in figure 16.

A recently used arrangement of Hansroul et al [15] is shown in elevation view in figure 19. Some 30 counters above the beam partly overlap each adjacent counter so as to give some 60 "bins" of angle

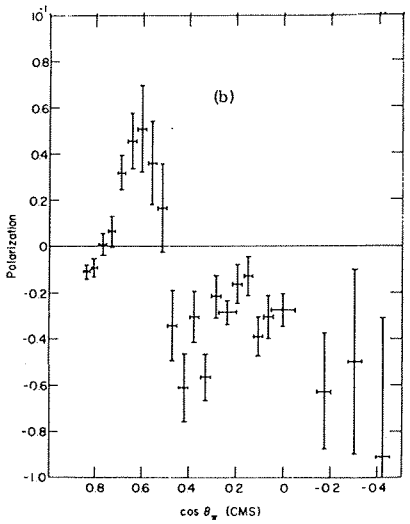

Fig. 18 Polarization results of Suwa, Yokosawa, Booth, Esterling and Hill for negative-pion-proton scattering. The momentum of the incident pions was 2.08 GeV/c.

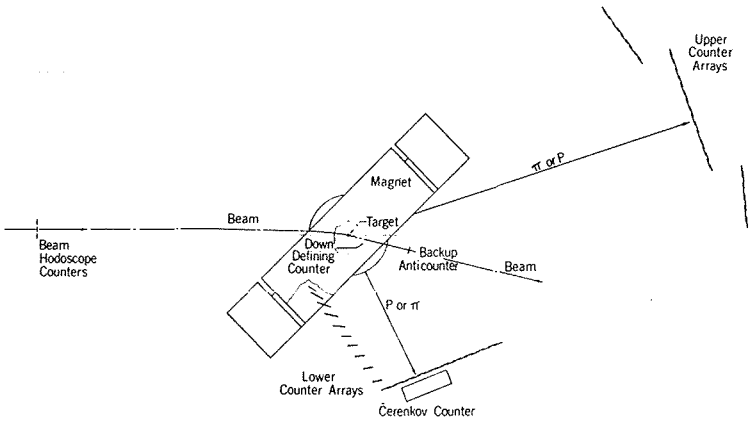

EXPERIMENTAL ARRANGEMENT

Fig. 19 Elevation view of the apparatus of Hansroul et al for measuring the polarization in pion-proton scattering. When the incident particles were positive pions it was necessary to use the Cherenkov counter at certain angles of scattering to determine whether the particle reaching the lower set of counters was a pion or a proton.

in the scattering plane. Counters below the beam line are similarly arranged. Not shown in the figure are like sets of counters running in a perpendicular direction so that when a particle strikes the plane of a counter array both its coordinates can be recorded. This system should combine good coplanarity determination and good angular resolution with a large solid angle for counting scattered particles. Some trouble was experienced with electrons in the pion beam. It was found that electrons may emit high-energy X rays in the first part of the LMN target and these X rays may then make electron-positron pairs in the latter part of the target. The pairs go almost directly forward, but the magnetic field of the polarized-target magnet deflects one member of the pair up into one counter array and the other down into the other counter array. Because these electron-pair events tend to satisfy the coplanarity requirement automatically, they can represent a troublesome background. It was also found that it is helpful to have the polarized target rather completely surrounded with anticoincidence counters in directions in which the desired events do not send particles. At high energy the anticoincidence counters help to suppress unwanted inelastic processes. Measurements were made at 10 energies for the π^--p polarization and 15 energies for the π^+-p. As an example of some of the better results, figure 20 shows the results for incident momentum 1.44 GeV/c.

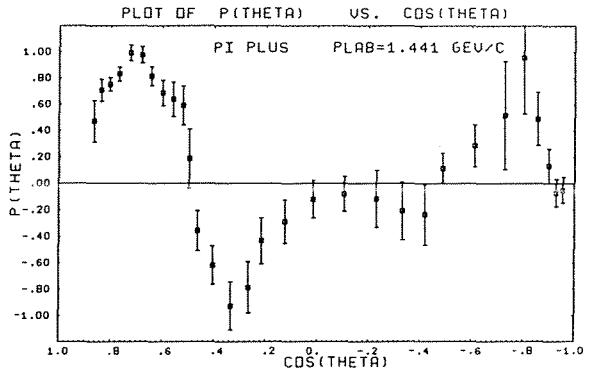

Fig. 20 Polarization in positive-pion-proton scattering as a function of cosine of center-of-mass scattering angle according to Hansroul et al. The incident beam momentum was 1.441 GeV/c.

We have said above that for elastic scattering the asymmetry observed in scattering on a polarized target is guaranteed by parity conservation and time-reversal invariance to be related to the polarization P in the same scattering process by :

$$\epsilon = P_T \, P \quad .$$

Bilen'kii [16] has pointed out that if the character of the particles changes in the scattering process we may have the more general relation :

$$\epsilon = \pm P_T P$$

where the plus sign applies if there is no change in the intrinsic parity of the particles involved in the scattering, the minus sign if the intrinsic parity changes.

As an example, consider the reaction :

$$\pi + p \rightarrow K^+ + \Sigma^+ \quad .$$

Both the pion and the K meson have zero spin and both proton and Σ hyperon have spin 1/2, so this is a suitable place to apply the Bilen'kii argument. If the product of π and p intrinsic parities is the same (or different) from the product of K and Σ intrinsic parities we will have a plus (or minus) sign in the relation :

$$\epsilon = \pm P_T P \quad .$$

P has already been measured in bubble-chamber experiments so a measurement of asymmetry ϵ in the reaction on a polarized target could check the product of intrinsic parities of K and Σ . (The π-p system is already known to have an odd product of intrinsic parities).

In spite of the fact that the K-Σ parity was believed demonstrated to be odd, on the basis of work by Tripp et al [17], Dieterle et al [18] in Berkeley decided to remeasure the K-Σ parity as a demonstration of the new method and as a further reassurance about the Tripp result. The apparatus used is shown in figure 21.

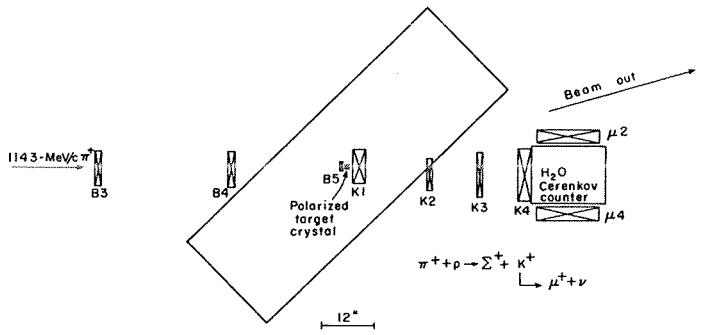

Fig. 21 Elevation view of the apparatus of Dieterle et al, used for the K-Σ parity determination. K^+ mesons were detected if they came to rest in the H_2O Cherenkov counter.

The incident pion beam was partially separated to suppress protons. Pion momenta were measured in spark chambers and magnets along the beam line. The desired reaction was selected by the observation of a final-state K^+ particle, detected in a somewhat standard K^+ detector involving K^+ that come to rest in a water Cherenkov counter. By observing the K^+ angle of emission (by spark chambers) and the K^+ energy (by range measurement) the authors could obtain a one-constraint selection of the desired reaction. Figure 22 shows more detail of the apparatus in the vicinity of the water Cherenkov counter. Two prior Cherenkov counters were required to show no pulse (the desired K mesons being too slow to produce Cherenkov light there) but the large water Cherenkov was required to show a delayed pulse (due to the fast decay products of the K^+). The range of the K^+ was determined by extrapolating forward the spark-chamber track of the entering K^+ particle and extrapolating backward the decay product as observed in the "μ" spark chamber.

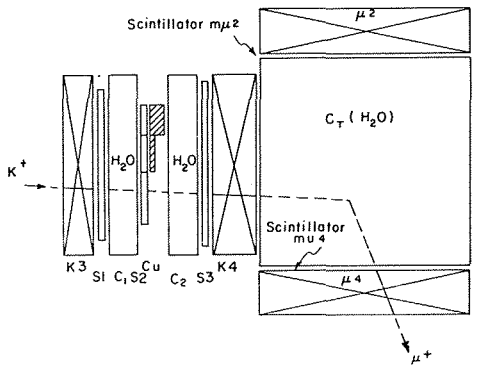

Fig. 22 Detail of the apparatus of Dieterle et al. K^+ ange was determined by extrapolation of spark-chamber tracks in the spark chambers K4 and any one of four μ spark chambers placed around the water Cherenkov counter.

For each stopping K^+ a parameter was calculated to compare the observed energy with that expected from kinematic relations for the desired reaction for a K^+ emitted at the angle observed for that event. To construct this parameter each stopping K^+ was treated as if it originated from free hydrogen but as if the unobserved particle were not necessarily a Σ particle, but some fictitious particle of mass m (missing mass). When this missing mass falls close to the mass of a Σ^+ the event is consistent with the desired reaction.

Figure 23 shows the distribution in missing mass for the observed events from the polarized target (of LMN). There is certainly no clear hydrogen peak in the vicinity of the Σ mass. Rather, there is a broad distribution more characteristic of the heavy elements in the target. When the LMN target was replaced with a CH_2 target

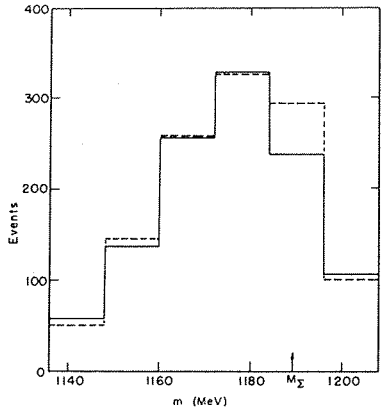

Fig. 23 Histogram of "missing mass" for the events of Dieterle et al obtained with the LMN target. Events on free hydrogen should show as a peak at the sigma mass, but they are here obscured by a large background due to collisions on heavy elements in the target.

the resulting missing mass distribution did show a hydrogen peak, as shown in figure 24. This indicated that the apparatus was performing as expected and allowed one to make a computation of the fraction of free-hydrogen events in the polarized-target data. On the basis of this analysis these data confirm the odd parity of the K-Σ system rather than even parity by odds of 40 to 1. The experiment indicated again the difficulties of working with one-constraint fits to separate the hydrogen effect in the LMN target.

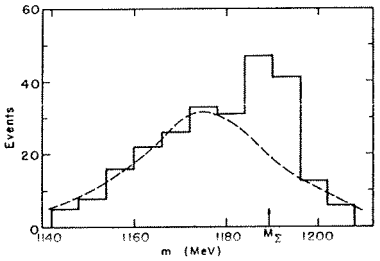

Fig. 24 Histogram of "missing mass" for the events of Dieterle et al when a CH_2 target was substituted for the LMN target. The peak at the sigma mass indicates the apparatus was adjusted as intended, and allows an estimate to be made of the fraction of LMN events near the sigma mass that are due to free hydrogen.

A conceptually similar experiment designed to measure the intrinsic parity of the Ξ hyperon is in the analysis stage at the CERN laboratory.

A valuable extension in the uses of a polarized proton target has been made by a Saclay-Orsay-Pisa collaboration, as reported by Sonderegger at the Stony Brook Conference. They have used a polarized target to measure the polarization in charge-exchange scattering :

$$\pi^- + p \rightarrow \pi^0 + n$$

particularly at high energy and small momentum transfer to the nucleon. Figure 25 shows their experimental arrangement. They observe the neutron and measure its velocity by time of flight in scintillation counters and they observe the gamma rays from the decay of the neutral pion in spark chambers. Their trigger is based on an incident negative pion, no charged particle emerging from the target, and the detection of a reasonably slow neutron. Their separation of a hydrogen peak is quite clear in figure 26. Their results are shown in figure 27, for incident pion momenta of 5.9 and 11.2 GeV/c. This process is quite interesting in that the polarization had been expected to vanish rapidly at high energy according to the simplest Regge-pole model.

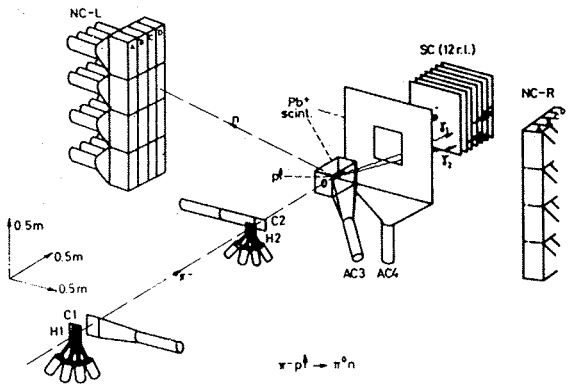

Fig. 25 Apparatus of the Saclay-Orsay-Pisa collaboration for measuring the polarization in charge-exchange scattering of negative pions on protons. The neutron counters are to the left and right of the beam. A spark chamber was used to detect the gamma rays from the neutral pion.

Extensive high-energy polarization measurements have been made for π-p and p-p scattering by a group of CERN authors consisting of Borghini, Coignet, Dick, Kuroda, Di Lella, Macq, Michalowicz and Olivier. They used incident momenta from 6 to 12 GeV/c. Because of the high incident energy the measurements are limited to the most forward directions of scattering. However, there is a great deal of interest in this near-forward scattering as it contains vital information on the limiting behaviour of scattering amplitudes at

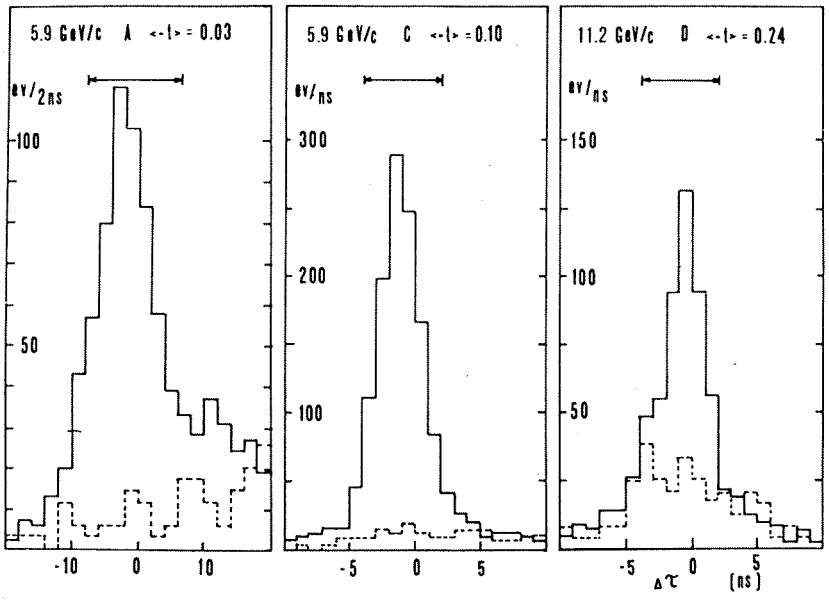

Fig. 26 The hydrogen peaks, clearly evident above the background (dashed line), of the Saclay-Orsay-Pisa collaboration.

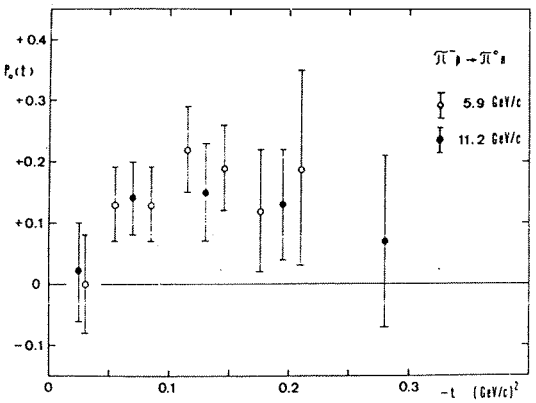

Fig. 27 Polarization results for pion-nucleon charge exchange, from the Saclay-Orsay-Pisa collaboration. t is the square of invariant momentum transfer. P_0 is the polarization.

high energy. In particular, it is important to decide whether Regge poles are sufficient to describe the high-energy scattering at small angles. Other more complex polarization experiments will also be needed but the measurement of P is a very important first step. One form of their experimental arrangement is shown in figure 28. They have used a counter hodoscope to determine the angle of scattering of the beam particle and have used an ingenious substitute, which I will not discuss here, to determine the angle of the recoil proton. Their hydrogen peaks are shown in part in figure 29. Their results for π-p polarization are shown in figure 30. In all cases the data for π^+-p polarization are positive at small angles, those for π^--p are negative at small angles. The curves are the theoretical values of Chiu, Phillips and Rarita [19] based upon a Regge-pole analysis. The agreement with the Regge analysis is not bad. The experimental results for p-p scattering are shown as solid circles in figure 31. At 6 GeV/c there is not perfect agreement with results obtained in Berkeley.

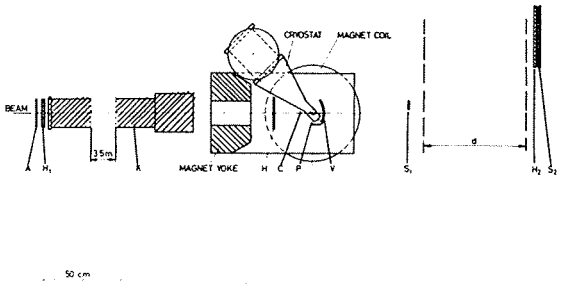

Fig. 28 Plan view of one arrangement used by Borghini et al to study polarization in pion-proton and proton-proton scattering. K is a Cherenkov counter in the beam used to distinguish pions from protons in the beam. V is an anticoincidence counter. H_2 is a hodoscope used to measure the angle of the scattered beam particle.

I have omitted descriptions of some other quite interesting applications of polarized proton targets such as their use to obtain relatively high-intensity polarized neutron beams, as reported by Dragicescu, Lushchikov, Nikolenko, Taran and Shapiro [20]. Incidentally, this work suggests that for targets of high polarization it may be practicable to measure the target polarization by measuring the transmission of the target to an initially unpolarized beam of slow neutrons.

Several other valuable polarized-target experiments are now under way. K-p polarization experiments are now well started at CERN and

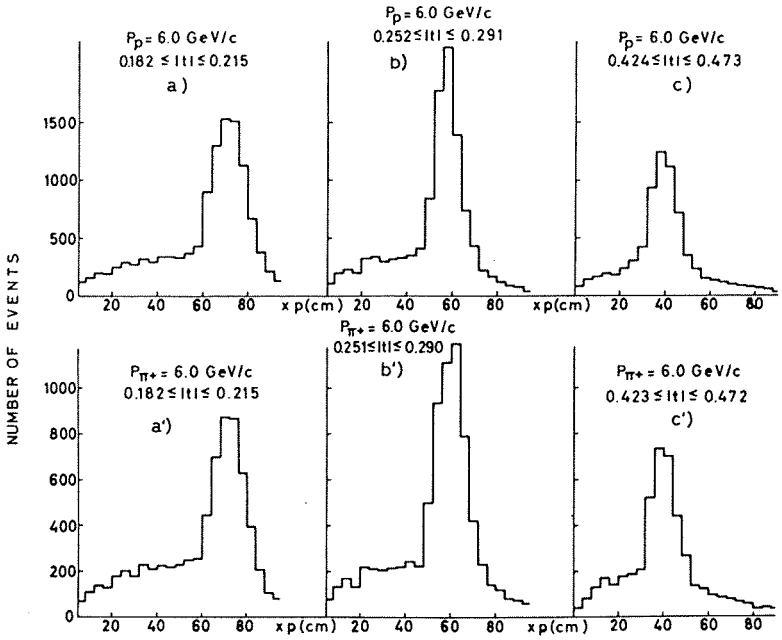

Fig. 29 Examples of the hydrogen peaks in the work of Borghini et al.

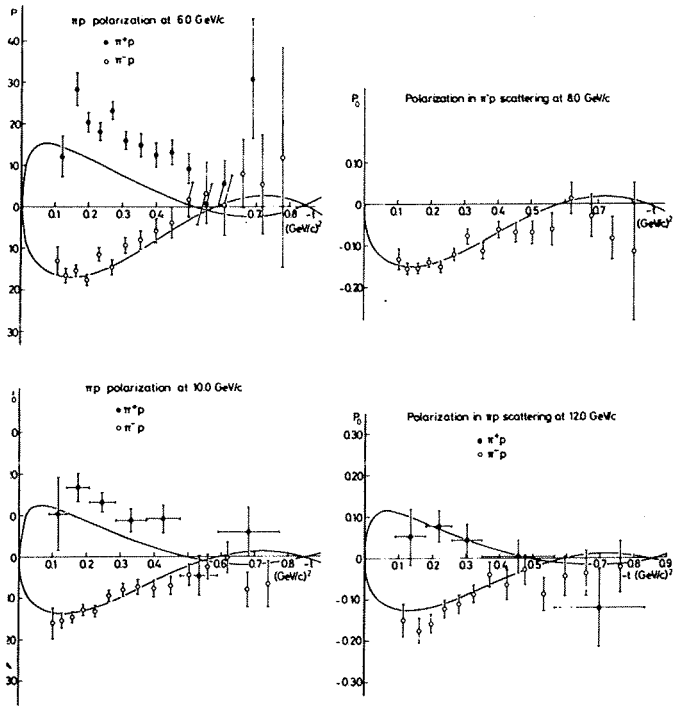

Fig. 30 Polarization results plotted against invariant square of momentum transfer for pion-proton scattering, from the work of Borghini et al. The curves show predictions of a Regge-pole model.

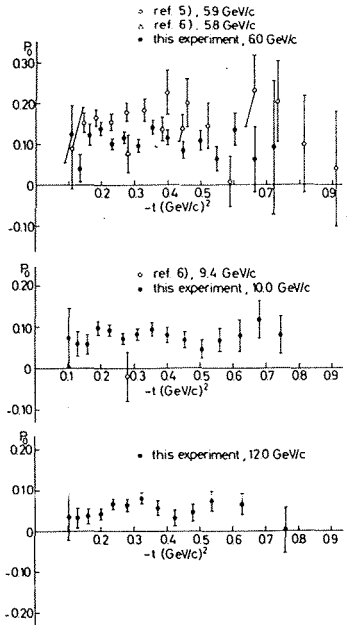

Fig. 31 Experimental proton-proton polarization results of Borghini et al (dark circles). The points indicated in the figure as reference 5) are Berkeley results. The points indicated as reference 6) are probably from the Soviet Union.

at the Rutherford Laboratory, and work is well progressed at Saclay toward measurements of the parameters A and R for π-p scattering. While many of the experiments previously mentioned could have been done, if necessary, without polarized proton targets, the measurements of A and R definitely require polarized targets. Here is an important aspect of scattering for which polarized targets are absolutely essential.

It is my expectation that we will hear during this conference about promising possibilities for target materials other than the presently predominant LMN. There is a particular need for polarized targets with a higher proportion of hydrogen, and for some experiments it will be important to have targets less susceptible to radiation damage than LMN. I look forward to hearing the current status of new target materials and I hope this conference will lead to further work toward finding superior new target materials.

References

1) P. Bareyre, C. Brickman, A.V. Stirling and G. Villet, Phys. Letters, 1965, 18, 342.

2) A. Abragam, M. Borghini, P. Catillon, J. Coustham, P. Roubeau and J. Thirion, Phys. Letters, 1962, 2, 310.
3) J.H. Foote, O. Chamberlain, E.H. Rogers, H.M. Steiner, C.E. Wiegand and T. Ypsilantis, Phys. Rev., 1961, 122, 948.
J.H. Foote, O. Chamberlain, E.H. Rogers and H.M. Steiner, Phys. Rev., 1961, 122, 959.
E.H. Rogers, O. Chamberlain, J.H. Foote, H.M. Steiner, C.E. Wiegand and T. Ypsilantis, Rev. Mod. Phys., 1961, 33, 356.
4) See, for example, P. Bareyre, C. Brickman, M.J. Longo, G. Valladas, G. Villet, G. Bizard, J. Duchon, J.M. Fontaine, J.P. Patry, J. Seguinot and J. Yonnet, Phys. Rev. Letters, 1965, 14, 198.
R.D. Eandi, T.J. Devlin, R.W. Kenney, P.G. McManigal and B.J. Moyer, Phys. Rev., 1964, 136, B536.
5) L. Wolfenstein, Ann. Rev. Nucl. Sci., 1956, 6, 43.
6) O. Chamberlain, C.D. Jeffries, C.H. Schultz, G. Shapiro and L. Van Rossum, Phys. Letters, 1963, 7, 293.
7) See, for example, G. Cocconi, V.T. Cocconi, A.D. Krisch, J. Orear, R. Rubinstein, D.B. Scarl and B.T. Ulrich, Phys. Rev., 1965, 138, B165.
8) F. Betz, J. Arens, O. Chamberlain, H. Dost, P. Grannis, M. Hansroul, L. Holloway, C. Schultz and G. Shapiro, Phys. Rev., 1966, 148, 1289.
9) P. Grannis, J. Arens, F. Betz, O. Chamberlain, B. Dieterle, C. Schultz, G. Shapiro, H. Steiner, L. Van Rossum and D. Weldon, Phys. Rev., 1966, 148, 1297.
10) H. Dost, University of California Lawrence Radiation Laboratory, Report UCRL-11877 (unpublished).
H. Dost, J. Arens, F. Betz, O. Chamberlain, M. Hansroul, L. Holloway, C. Schultz and G. Shapiro, Phys. Rev. (to be published) (UCRL-11877 ReV, September 1966).
11) B.M. Golovin, V.P. Dzhelepov, R.Ya. Zul'karneev and Ts'ui Wa-Ch'uang, J. Exptl. Theoret. Phys. (U.S.S.R.), 1963, 44, 142, Soviet Phys. JETP, 1963, 17, 98.
12) H.H. Atkinson, C.R. Cox, P.J. Duke, K.S. Heard, D.P. Jones, M.A.R. Kemp, P.G. Murphy, J.D. Prentice and J.J. Thresher, Proc. Roy. Soc., 1966, A289, 449.
13) S. Suwa, A. Yokosawa, N.E. Booth, R.J. Esterling and R.E. Hill, Phys. Rev. Letters, 1965, 15, 560.
14) A. Yokosawa, S. Suwa, R.E. Hill, R.J. Esterling and N.E. Booth, Phys. Rev. Letters, 1966, 16, 714.
15) O. Chamberlain, M.J. Hansroul, C.H. Johnson, P.D. Grannis, L.E. Holloway, L. Valentin, P.R. Robrish and H.M. Steiner, Phys. Rev. Letters, 1966, 17, 975.
16) S.M. Bilen'kii, Nuovo Cimento, 1958, 10, 1049.
17) M.B. Watson, M. Ferro-Luzzi and R.D. Tripp, Phys. Rev., 1963, 131, 2248.
18) B. Dieterle, J. Arens, O. Chamberlain, P.D. Grannis, M.J. Hansroul, L.E. Holloway, C.H. Johnson, C.H. Schultz, G. Shapiro, H.M. Steiner and D. Weldon, (to be published).
19) C.B. Chiu, R.J.N. Phillips and W. Rarita, Lawrence Radiation Laboratory, Report UCRL-16940 (1966, unpublished).
20) P. Draghicescu, V.I. Lushchikov, V.G. Nikolenko, Y.V. Taran and F.L. Shapiro, Phys. Letters, 1964, 12, 334.

RECENT RESULTS ON THE POLARIZATION PARAMETER IN π-p AND p-p ELASTIC SCATTERING FROM 6 TO 12 GeV/c

M. BORGHINI, G. COIGNET*, L. DICK, K. KURODA*,
L. di LELLA, P.C. MACQ**, A. MICHALOWICZ* and J.C. OLIVIER
CERN, Geneva

We present the final results of a measurement of the polarization parameter P_o in high-energy $\pi^{\pm}$-p and p-p elastic scattering, performed using a target which contained polarized protons. Data were taken at beam momenta of 6.0, 8.0, 10.0 and 12.0 GeV/c for π^-, and of 6.0, 10.0 and 12.0 GeV/c for π^+ and p, in the interval of invariant four-momentum transfer squared -t from 0.1 to 0.75 $(GeV/c)^2$.

---

* Institut du Radium, Laboratoire Joliot-Curie, Orsay (France).
** Present address : Centre de Physique Nucléaire, Université de Louvain, Louvain (Belgique).

THE PRODUCTION OF POLARIZED ELECTRON BEAMS BY SPIN EXCHANGE COLLISION

P. S. FARAGO and H. C. SIEGMANN*
University of Edinburgh

A method is described for obtaining a beam of polarized electrons by the transfer of polarization from a polarized atomic beam to a cross-fired initially unpolarized electron beam. The transfer takes place by spin exchange in elastic collisions and an appreciable degree of electron polarization can be obtained if low energy electrons are trapped in the atomic beam for a sufficient length of time.

The first experiments yielded 10 % polarization at a peak intensity of 0.01 μA in pulses of a few μ s length and 100 s^{-1} repetition rate. Details of this experiment will be described.

Progress of the experiments aimed at the improvement of the above results will be reported, and the feasibility of using this scheme as a source of polarized electrons for high energy accelerators will be discussed.

---

* On leave of absence from the "Laboratorium des Instituts für theoretische Physik der Universität, München".

POLARIZATION AT FORWARD ANGLES AND SCATTERING AMPLITUDES IN π-N ELASTIC SCATTERING

A. YOKOSAWA
Argonne National Laboratory, Argonne

I would like to discuss the rôle of polarization measurements in the π-N interaction below those energy regions (6 to 12 GeV/c) that the previous speaker just covered.

Based upon the polarization measured in π^--p elastic scattering from 1.0 to 2.5 GeV/c, partial-wave amplitudes were determined by a phase-shift analysis [1]. Let us evaluate the nonflip and spin-flip scattering amplitudes from the phase-shift solution. Figure 1 shows both the real and imaginary part of scattering amplitudes at 2.5 GeV/c, where the effect of resonances was least expected. Here we learn a striking feature of the diffraction pattern in the entire region of momenta transfer. At present, theories are confined to forward and backward regions, and it is hoped that the above mentioned fact is useful to develop a model that explains the scattering process in the entire region. Figure 1 suggests that the experimental data may be fitted with several parameters based upon an optical model [2] that was extensively used in nuclear physics. The results of such analysis at 2.5 GeV/c are shown in figure 2 in terms of phase-shifts, and they are in agreement with those obtained by the particle-wave analysis. The helicity nonflip, A_{++}, and helicity-flip, A_{+-}, amplitudes are also evaluated by making use of the phase-shift solution at 2.5 GeV/c and are shown in figure 3. Here we learn [3] that the imaginary part of helicity-flip amplitudes is responsible to the secondary peak appearing in the differential cross-section measurements [4].

Now let us look at the charge-exchange process in which the forward region is relatively well understood. In particular, by the application of a Regge-pole model to the differential cross-section data, trajectory parameters and pole residues were determined [5]. Since this process is dominated by one-pole exchange [6], the effect of resonances in π-N interaction becomes very sensitive to the polarization in the charge-exchange process. This pro-

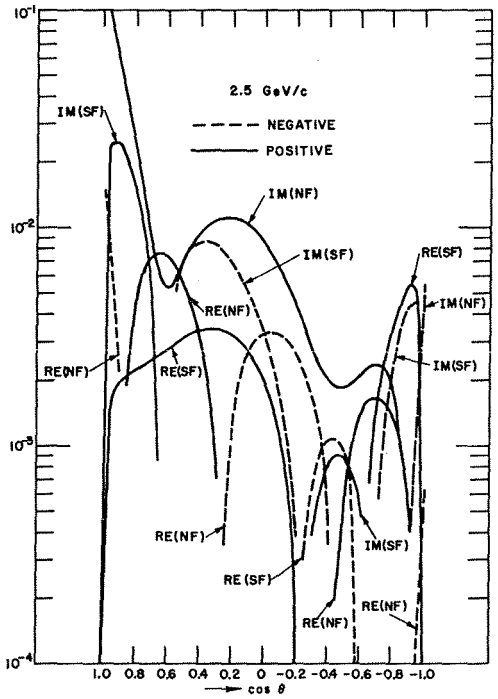

Fig. 1 Scattering amplitudes at 2.5 GeV/c.

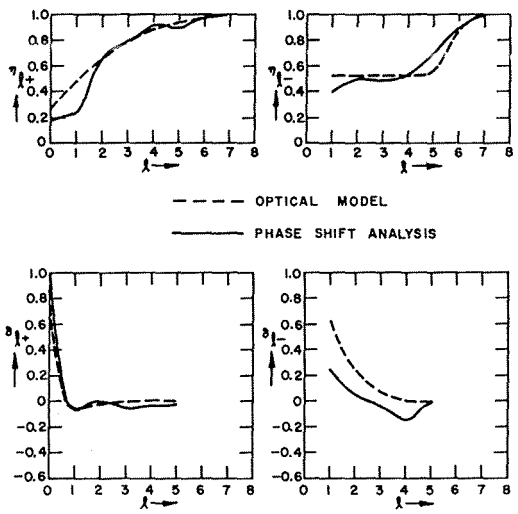

Fig. 2 Comparison of phase-shifts by optical model and phase-shift analysis.

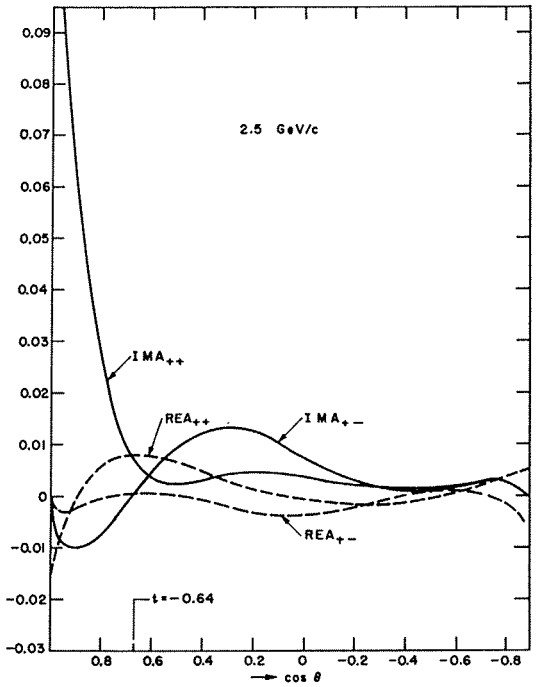

Fig. 3 Helicity scattering amplitudes at 2.5 GeV/c.

vides a strong tool to investigate resonances [7]. Figure 4 illustrates the effect of resonances [8] on the polarization. The pole-residues used in this calculation were obtained by two-parameter search with the differential cross-section data [9] without functionalizing parameters [10]. This was done by fitting data at small t intervals, where parameters were assumed to be constant, and by applying a continuity condition. The search started at $t = 0$, where the nonflip residue, b_1, was well determined from the total cross-section data. Both the nonflip, b_1, and spin-flip, ab_2, residues obtained by the above method are plotted with respect to t and are shown as curve I in figure 5. The results of applying a condition [5] to satisfy the cross-over effect are shown as curve II in figure 5. The calculated polarization by using curve II and resonances is shown in figure 6. The difference between figures 4 and 6 will be experimentally clarified.

Valuable discussions with Dr R. Arnold on a Regge-pole model are greatly appreciated.

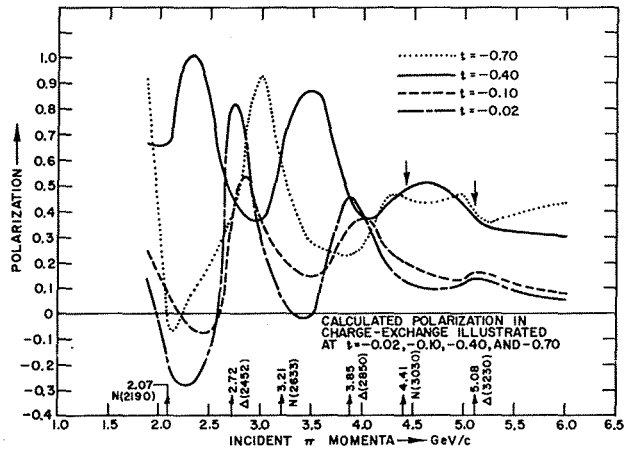

Fig. 4 Calculated polarization in charge-exchange process.

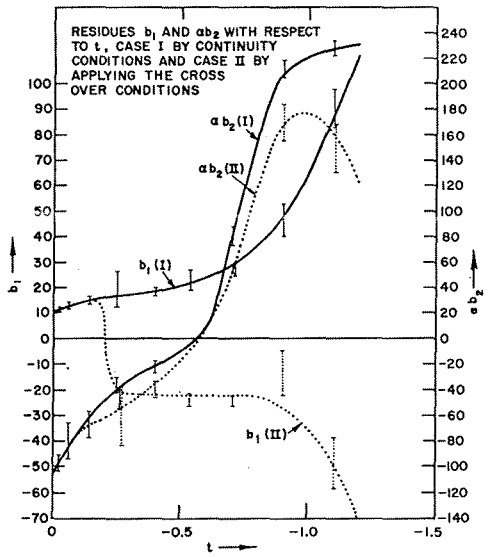

Fig. 5 Pole-residues in charge-exchange process.

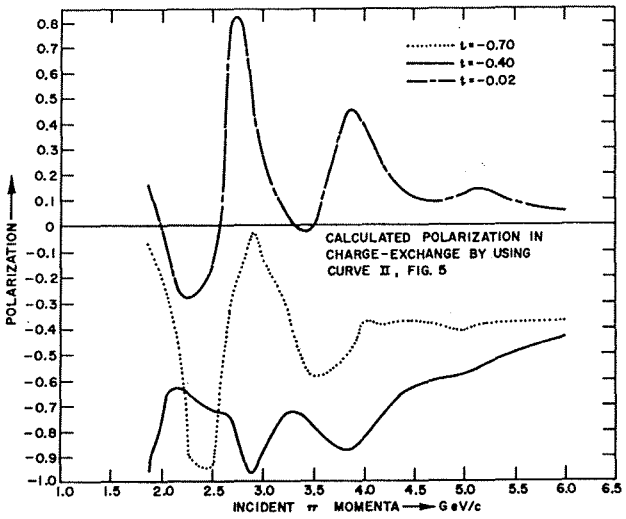

Fig. 6 Calculated polarization in charge exchange by using curve II, figure 5.

Notes and References

1) A. Yokosawa, S. Suwa, R.E. Hill, R.J. Esterling and N.E. Booth, Phys. Rev. Letters, 1966, 16, 714.
2) Professor M. Ross suggested to us this type of parameterization, which was described in reference 1.
3) This fact was pointed out by Professor Ross.
4) C.T. Coffin, N. Dikmen, L. Ettinger, D. Meyer, A. Saulys, K. Terwilliger and D. Williams, Phys. Rev. Letters, 1965, 15, 838.
5) R.J.N. Phillips and W. Rarita, Phys. Rev., 1965, 139, B1336.
6) This point is not quite certain because of the recent polarization measurements by Saclay-Orsay-Pisa group. However, the discussion that follows should qualitatively be valid.
7) Some of this aspect was described by A. Yokosawa, Phys. Rev. Letters, 1966, 16, 1019.
8) Resonance parameters used are from articles by V. Barger and D. Cline, Phys. Rev., 1966, 16, 913, and R.K. Logan and L. Sertorio, Phys. Rev., 1966, 17, 834.
9) A.V. Stirling, P. Sonderegger, J. Kirz, P. Falk Vairant, O. Guisan, C. Bruneton and P. Bongeaud, Phys. Rev. Letters, 1965, 14, 763.
P. Sonderegger, J. Kirz, O. Guisan, P. Falk Vairant, C. Bruneton, P. Borgeaud, A.V. Stirling, C. Caverzasio, J.P. Guilland, M. Yvert and B. Amblard, Phys. Letters, 1966, 20, 75.

10) The expression for the ρ-trajectory used is $a = 0.58 + 1.00\ t$.

Work performed under the auspices of the U.S. Atomic Energy Commission.

THEORETICAL ASPECTS OF NUCLEAR DYNAMIC POLARIZATION

M. BORGHINI
CERN, Geneva

1 INTRODUCTION

The basic facts involved in the principle of nuclear dynamic polarization by "solid effect" having been given in one of the preceding papers [1], we would like to enter here into some more details of the theory with the specific purpose of seeing why solid effect does not work in every case and what can be done to improve the present achievements that are presented in other papers [2,3] : we shall see for instance why solid H_2, solid HD and solid D_2 are not well polarized, and why the polarized targets of lanthanum magnesium nitrate (LMN) with longer nuclear relaxation times are better polarized than the other ones, as is apparent in reference 2. We shall be able to see also why the polarization of a LMN target decreases by a factor of about two when it is bombarded by a few 10^{12} incident ionizing particles. The solid effect being a method to increase the thermal equilibrium polarization of nuclear spins, it seems in order to begin by discussing this one.

2 STATIC POLARIZATION ("brute force" polarization)

The polarization of an assembly of protons placed in a magnetic field H and in contact with a thermal bath at a temperature T, is given by :

$$P_n = P_n(1/2) = 2 \coth\left(2 \times 10^{-7} \frac{H}{T}\right) - \coth\left(10^{-7} \frac{H}{T}\right) =$$

$$= \tanh\left(\frac{\mu_n H}{kT}\right) \simeq \tanh\left(10^{-7} \frac{H}{T}\right)$$

where H is expressed in gauss and T in degree Kelvin. However, this formula is valid only if there is no coupling between the spins of these protons and the orbital states of the molecules to which they belong : it is valid for instance for hydrogen atoms in lithium hydride LiH, in polyethylene $(CH_2)_n$, in the water of hydration of the lanthanum magnesium double nitrate LMN, and it is not valid, as is well known, for solid hydrogen : due to the exclusion principle, molecules of hydrogen, H_2, may exist only as para-molecules, with a total nuclear spin I = 0 and rotational quantum number J = 0, 2, 4, ... or as ortho-molecules with I = 1 and J = 1, 3, 5, ... The fundamental molecular rotational state being J = 0, then I = 0 ; in the solid, molecules retain enough of their individuality so that this fact remains true, and, as well-known, solid hydrogen converts to a pure para-state with zero total nuclear spin :

$$P_n = P_n(0) = 0, \text{ independently of H and T.}$$

Of course, as one knows how to produce nearly pure ortho-hydrogen, and if it were possible to keep it in that state, the proton system would keep a polarization given by :

$$P_n = P_n(1) = \frac{3}{2} \coth\left(3 \times 10^{-7} \frac{H}{T}\right) - \frac{1}{2} \coth\left(10^{-7} \frac{H}{T}\right) \text{ bigger than } P_n($$

but this does not seem possible. We would not have spoken of this problem if it were not to introduce another compound which presents just the opposite behaviour, and may become a good sample to use with the new advanced techniques for producing high magnetic fields and very low temperatures ; namely <u>methane</u>, CH_4. Here, again, in the molecular state, the exclusion principle connects the total nuclear spin and the rotational quantum numbers, but it is the state with <u>maximum</u> nuclear spin I = 2 (meta-methane) which is the fundamental state, thus excluding the poorer I = 1 and I = 0 ones. In the solid form, the fundamental state is not yet completely known [4], but contains more than the normal statistical weight of meta-methane, which means that the static polarization is higher than given by $P_n(1/2)$. For pure meta-methane :

$$P_n = P_n(2) = \frac{5}{4} \coth\left(5 \times 10^{-7} \frac{H}{T}\right) - \frac{1}{4} \coth\left(10^{-7} \frac{H}{T}\right) .$$

Figure 1 shows $P_n(0)$, $P_n(1/2)$, $P_n(1)$, $P_n(2)$ as a function of $H/T \times 10^{-7}$. With H = 100 kG and T = 0.02° K, the polarization of normal hydrogen is 46 % whereas it is 73 % for meta-methane. Expressed in another way, it would require a field about two times smaller or a temperature two times higher to obtain the same polarization as

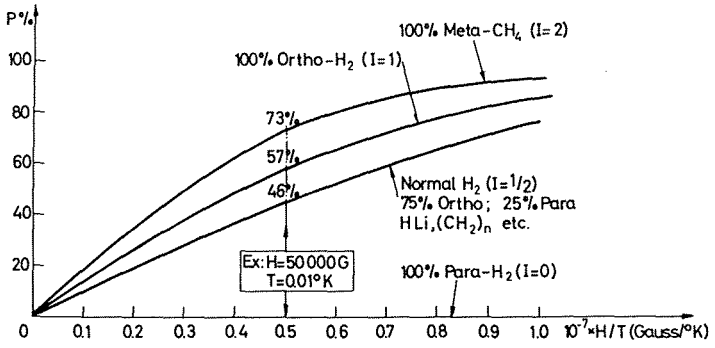

Fig. 1 Static polarization of protons in various samples (theoretical).

in normal hydrogen compounds.

Before we can obtain such polarized targets, we have to rely on dynamic polarization, with its unique feature that the direction of the polarization with respect to the magnetic field can be reversed by a slight change in the microwave frequency only.

3 DYNAMIC POLARIZATION

3.1 Notations

We deal with solid samples containing nuclear spins I and unpaired electronic spins S, placed in a static magnetic field H_o along a direction Oz and in a liquid helium bath at a temperature T_o. Let N_n and N_e be the respective numbers of nuclear and electronic spins per unit volume, ω_n and ω_e their Larmor pulsations ($\omega_n = 2\pi f_n = \gamma_n H_o$, $\omega_e = 2\pi f_e = \gamma_e H_o$, f_n and f_e being the Larmor frequencies), T_n and T_e their spin lattice relaxation times, P_n^o and $P_e^o \equiv P_o$ their thermal equilibrium polarizations. We shall have to introduce a special set of lattice vibration modes $M(\omega_e)$ interacting with the electronic spins S by one phonon exchange processes, with a frequency within the electronic resonance line ; let N_M be their number. We suppose also that the solid sample experiences a microwave magnetic field H_1, normal to H_o, with a pulsation ω .

We shall make the simplifying assumption that we are dealing with spins 1/2, both nuclear and electronic, although the consideration of higher spins presents a number of interesting features.

It has already been recalled [1] how, by inducing "flip-flips" or "flip-flops", one can polarize the nuclear spins, and how these "forbidden" processes are partially allowed by the action of the dipole-dipole interaction between the spins S and the spins I ; we have to introduce a parameter to describe this, the so-called dipolar mixing parameter ϵ : if we consider one spin S and one spin I^i, separated by a distance r_i, the ratio of the flip-flip or flip-flop probabilities to a pure electronic flip probability will be given by :

$$\frac{4\epsilon_i^2}{(1 + \Sigma_i \epsilon_i^2)^2}$$

where

$$\epsilon_i^2 = \frac{9}{16}\left(\frac{\gamma_e \hbar}{r_i^3}\right)^2 H_o^{-2} \sin^2 \theta_i \cos^2 \theta_i$$

θ_i being the angle between the direction Oz of the field and the direction of the vector joining S to I^i.

We have thus to introduce the relevant factor $f = \Sigma_i \epsilon_i^2$. The denominator $(1 + f)^2$ coming from the normalization of the wave function is not an aesthetical one, and will have an importance on some of the forthcoming conclusions.

3.2 Discussion

We may turn now towards the discussion of dynamic polarization : this can deal with the dependence of the dynamic polarization on the frequency ω and the amplitude H_1 of the applied microwave field with the maximum polarizations attainable in given conditions, and with the polarization time constants, but we shall mainly be interested in looking for the maximum steady state polarizations in given samples.

This theory can be divided into a few parts according to the nature and the width of the electronic resonance line : we are going to suppose here that this line is homogeneous, i.e. that the electron spins have all the same Larmor frequency, the broadening of their energy levels coming mostly from the electronic dipole-dipole interactions ; this case may be complicated enough so that we do not consider various inhomogeneous systems.

This homogeneous electronic line can be narrow or not with respect to the nuclear frequency, $\Delta\omega_e \ll \omega_n$. In the first case, the theory can be extended rather far into the description of actual situations in particular in the case of LMN, doped with neodymium. In the se-

cond case, one deals with a more complicated problem which involves the direct action of the microwave field H_1 on the electronic spins. This requires going into a rotating frame of reference [1] and attributing various temperatures to various parts of the transformed Hamiltonian : in this case, the theory of dynamic polarization has been derived [5] only under the so-called "high temperature" approximation, meaning in fact "low polarization" assumption. We are interested here, of course, in high polarizations only but, as the analysis of the general case, even with the above restriction, leads to an interesting physical insight into the situation, qualitative explanations or predictions can nevertheless be made and we are going to describe the general case here.

3.3 Narrow electronic resonance line

The spin system can be described by the expectation values of the z-components of the various spins only : with spins 1/2, the density matrix of the spin system reads :

$$\rho = \Pi_j (\frac{1}{2} + P_e S_z^j) \; \Pi_i (\frac{1}{2} + P_n^i I_z^i) \quad .$$

We have introduced only one P_e as the electronic system is homogeneous, and various P_n^i because we have not yet introduced nuclear spin diffusion. In some cases, spin diffusion is such that P_n^i is uniform at least in the major part of the sample, $P_n^i = P_n^{i'} \equiv P_n$, and P_n has a single relaxation time T_n ; in other cases, the various P_n^i may be different, but the mean value $P_n = \overline{P_n^i}$ has anyhow a single relaxation time T_n.

It can be shown that the maximum dynamic polarization is given by "something like" :

$$P_n^{max} = \frac{P_o}{1 + \frac{N_n}{N_e} \frac{T_e}{T_n}} \qquad (1)$$

where the relevant term $(N_n/N_e)(T_e/T_n)$ expresses the fact that the electrons should not be depolarized by having to polarize too many nuclei. We said "something like" because this formula is strictly valid in some very particular cases ; the exact formulation depends strongly on the precise character of spin diffusion, on the existence of "phonon bottle-neck" as we shall define it, on the presence of nuclear extra relaxation processes, etc, but formula (1) will give a sufficient basis for this general discussion.

We shall consider three different cases : i) where there is no extra relaxation processes (no "leakage"), i.e. no other electronic spins than the relevant spins S, and no intrinsic nuclear mechanisms ;

ii) where extra relaxation processes are present ; iii) where the electronic relaxation is limited by "phonon bottle-neck" as we shall see.

3.3.1 No "leakage", no "phonon bottle-neck".

We have to say something about the direct action of one spin S on one spin I^i : the electronic relaxation process with a rate $1/T_e$ induces a relaxation rate for I^i given by :

$$\frac{1}{T_n^i} = \frac{1}{T_e} \frac{4\,\epsilon_i^2}{(1+f)^2} (1 - P_o^2)$$

as discussed in reference 1 : ϵ_i^2 varies as r_i^{-6} so that $1/T_n^i$ is maximum for the nuclei close to the spin S, and decreases very rapidly. We suppose now that spin diffusion is fast with respect to the fastest $1/T_n^i$, so that at each time $P_n^i = P_n^{i'} \equiv P_n$, which has then a single relaxation time given by :

$$\left(\frac{1}{T_n}\right)_{fast} = \overline{\frac{1}{T_n^i}} = \frac{N_e}{N_n} \frac{1}{T_e} \frac{4f}{(1+f)^2} (1 - P_o^2)$$

so that

$$\left(\frac{N_n}{N_e} \frac{T_e}{T_n}\right)_{fast} = \frac{4f}{(1+f)^2} (1 - P_o^2) \leqslant 1 - P_o^2 \leqslant 1 \quad .$$

If spin diffusion is not so fast, then obviously :

$$\left(\frac{N_n T_e}{N_e T_n}\right) < \left(\frac{N_n}{N_e} \frac{T_e}{T_n}\right)_{fast} \leqslant 1 - P_o^2 \leqslant 1 \quad .$$

According to formula (1), P_n^{max} is thus never smaller than $P_o/2$. The exact solutions, taking into account the fact that $1 - P_o^2$ should be written in fact as $1 - P_o P_e$, are shown in figure 2 for the case of fast relaxation : one sees immediately the favourable effect of the factor $1 - P_o^2$ which goes quickly to zero as P_o approaches 1 [6].

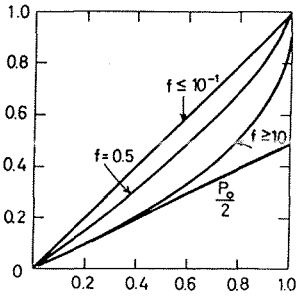

Fig. 2 Dynamic nuclear polarization P_n(max.) vs static electronic polarization P_o (no "leakage", no phonon bottle-neck)($f = \Sigma\, \epsilon^2$ dipolar parameter).

3.3.2 "Leakage", no "phonon bottle-neck".

We suppose now that there exist extra relaxation mechanisms for the nuclear spins, for instance their coupling with the rotation of the molecules, like for ortho-hydrogen, or simply their interaction with other paramagnetic centres, as for example with defects created by irradiation : one says that there is a "leakage". In that case the total nuclear relaxation rate $1/T_n^*$ can be much larger than in the preceding cases :

$$\frac{1}{T_n^*} \text{ possibly} \gg \frac{1}{T_n} \text{ and even} \gg \left.\frac{1}{T_n}\right)_{fast}$$

so that $(N_n/N_e)(T_e/T_n^*)$ can have any value smaller or bigger than one, and P_n^{max} may become very small.

This is the case in solid deuterium for example : electronic centres can be atoms produced in a gas discharge before condensation at low temperature [7] ; the density of such atoms is not very high and N_e/N_n is at most 2×10^{-6} ; T_e being about 1 ms whereas T_n^* is some 10 s :

$$\frac{N_n}{N_e}\frac{T_e}{T_n^*} \simeq 50 \quad ;$$

with $P_o = 50\ \%$ ($T_o = 1.2°$ K, $H_o = 8$ kG), formula (1) gives $P_n^{max} \simeq 1\ \%$ which is in agreement with experiment.

The same explanation holds for solid hydrogen where the rotation of ortho-molecules relaxes rapidly the nuclear spins, and in which even smaller concentrations of atoms can be obtained. In solid HD, nuclear relaxation times T_n as long as 10^4 s have been obtained [8], but the electronic relaxation times of impurities created by irradiation are of the order of 1 s ; their concentration remaining low, quite small polarizations are expected.

One should mention the fact that, if the "leakage" is due to paramagnetic impurities, $1/T_n^*$ is proportional to $1 - P_o'^2$ where P_o' is the polarization of these impurities and :

$$\frac{N_n}{N_e}\frac{T_e}{T_n^*} \sim 1 - P_o'^2$$

can be appreciably reduced by going to higher fields and/or lower temperatures.

3.3.3 No "leakage" but "phonon bottle-neck".

We come now to the "phonon bottle-neck" case : it happens sometimes, when N_e and $1/T_e$ are large, that the vibration modes $M(\omega_e)$ interacting with the electronic spins are not able to transfer rapidly enough the amount of energy that these spins have to release in the

presence of microwave fields ; $\langle Z_e \rangle$ being the electronic Zeeman energy and $\langle E_M \rangle$ the energy of these modes, σ the phonon bottle-neck parameter is defined as :

$$\sigma = \frac{\partial}{\partial t}\Big)_M \langle Z_e \rangle \Big/ \frac{\partial}{\partial t}\Big)_L \langle E_M \rangle$$

and may be very large compared to unity ; $\partial/\partial t)_M$ means the energy exchange rate between spins S and modes $M(\omega_e)$, $\partial/\partial t)_L$ the energy exchange rate between modes $M(\omega_e)$ and the rest of the lattice. It can be shown then that the effective electronic relaxation rate is smaller than $1/T_e$ and becomes :

$$\frac{1}{T_e^*} \simeq \frac{1}{T_e} \frac{1}{\sigma + 1} \simeq \frac{1}{T_e \sigma} \ll \frac{1}{T_e} \quad \text{if} \quad \sigma \gg 1$$

whereas T_n is generally not changed, because of the small energy of the nuclear spins, so that the factor $(N_n/N_e)(T_e/T_n)$ becomes :

$$\frac{N_n}{N_e} \frac{T_e^*}{T_n} \simeq \frac{4f}{(1 + f)^2} \sigma(1 - P_o^2)$$

which can be much larger than one when $f\sigma$ is larger.

In fact, the exact theoretical treatment is more complicated and involved evolution equations for P_e, P_n, and for the temperatures of the modes $M(\omega_e)$ as well as for the modes $M(\omega_e + \omega_n)$ and $M(\omega_e - \omega$ responsible for the relaxation by forbidden transitions [6], and some results are presented in figures 3 and 4 with $f\sigma'$ as a significa parameter ($\sigma = \sigma' P_o$).

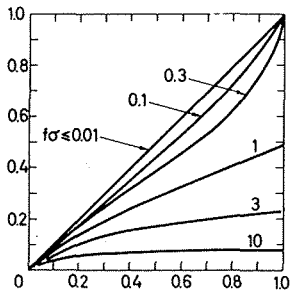

Fig. 3 Dynamic nuclear polarization vs static electronic polarization (no "leakage" but phonon bottle-neck) (f : dipolar parameter ; σ : phonon bottle-neck parameter).

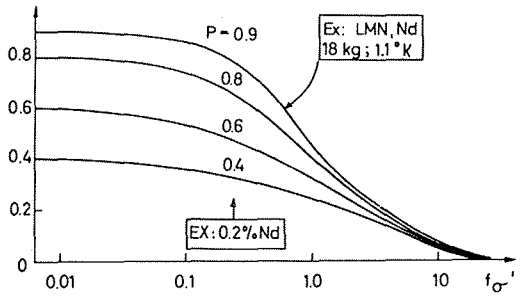

Fig. 4 Maximum proton polarization vs dipolar phonon bottle-neck parameter $f\sigma'$ (P_o : static electronic polarization).

As shown by C.D. Jeffries and collaborators [9], phonon bottle-neck exists in LMN,Nd at the fields and temperatures used for polarized targets : σ', deduced from electronic relaxation measurements, is roughly proportional to the Nd ion concentration and is of the order of a few hundreds ; f, deduced from nuclear relaxation measurements and the crystalline structure of LMN is of the order of 5×10^{-4} at 18 kG, so that $f\sigma'$ has typically values ranging from 0.1 to 0.5. One sees that the maximum polarization P_n^{max} is not far from P_o but is rather sensitive to the value of σ', i.e. of the neodymium concentration C ; as the nuclear relaxation time T_n is inversely proportional to C, one expects that the maximum polarization decreases when T_n is shorter, which is in fact observed in actual polarized targets [2]. We thus suggest that by having relaxation times of the order of 100 mn instead of 10-15 mn, the corresponding polarizations should become higher.

3.3.4 "Leakage" and "phonon bottle-neck".

We can now turn to the effect of radiation damage in LMN targets : it is easy to calculate the effect of an extra relaxation term $1/T_n'$ in a sample suffering from phonon bottle-neck as LMN,Nd ; $1/T_n'$ can in turn be related to a number of incident particles at minimum ionization hitting the target, by making use of nuclear relaxation measurements made in a 7 kG field on a LMN crystal irradiated by a source of strontium-90 [10] ; this was done for the curves presented in figure 5 and figure 6 ; the number N_i of incoming particles is of course not given with a high precision, as we have, in particular, in order to go from 7 kG to 18 kG supposed the relaxation rate of the paramagnetic defects to be proportional to H_o^3, which may not be absolutely correct. The right order of magnitude is nevertheless obtained. We should stress that, in order to compare irradiation effects in various targets, one has to use the complete set of equations and to take into account the relevant values of H_o, f and σ' which are generally different for these targets.

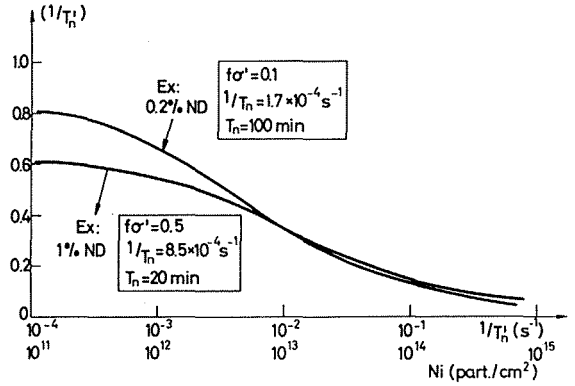

Fig. 5 Impurity effect (ex. radiation damage) on polarization in LMN,ND. Max. proton polarization vs extra relaxation rate or n° of incident particles (min. ioniz.).

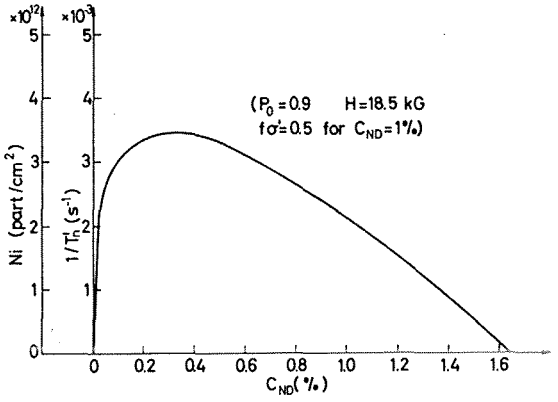

Fig. 6 Impurity effect (resp. radiation damage) reducing max. proton polarization to 0.5 vs ND concentration in LMN,ND.

We would like to end this section on the narrow electronic lines b; saying that we do not think that dynamic polarization works well i: rare earths salts because they have rather short relaxation times it is true that T_e is short, for example, 100 μs but, because of phonon bottle-neck, the effective T_e^* is much longer, 10 to 50 ms for example, which is of the same order as for other kinds of para· magnetic centres, like free radicals for instance. This has some consequence on the search for new polarized materials : one should

be more interested in having electron spins with a narrow resonance line, as in LMN,Nd, than having a particularly strong coupling with the lattice, provided their concentrations can be made large enough. For instance, polarizations in frozen liquids containing free radicals [11,12] are presently limited by the broadening of the electronic lines, and will be increased when narrower lines are found. This leads us to the case of an arbitrary electronic resonance line.

3.4 Arbitrary electronic resonance line

It has already been stated in reference 1 how solid effect can be viewed as a cooling of the electronic spins in a frame $R(\omega)$ defined by the transformation $U = \exp(i\omega t \sum_j S_z^j)$ rotating with the frequency ω of the applied RF field, and that this description, which gives trivial results when the electronic resonance line is narrow becomes necessary when it is not. Keeping to the assumption that we deal with spins 1/2, we are not only going to see why the nuclear dynamic polarization is reduced in the case of a broad resonance line, but also to show that this analysis can lead to a new polarization scheme, using two RF fields of different frequencies, which can give, at least in principle, nuclear polarizations higher than the electronic polarization P_0 which is the limit for the ordinary solid effect.

Let us start first with only one RF field with a frequency ω, and suppose that there is only a homogeneous system of electronic spins. When this field is applied within the electronic resonance line, the spin system can no longer be described by the electronic polarization alone, but rather by two different temperatures in the rotating frame $R(\omega)$: one for the effective Zeeman energy $Z_e^* = \sum_j \hbar(\omega_e - \omega) S_z^j$, another for the electronic dipolar energy, more precisely for the part $\mathcal{H}_{SS}^0$ of it which commutes with Z_e^*. Without entering into any details, let us just say that, because of energy conservation, the RF field provides a thermal contact between these two reservoirs : when a photon of energy $\hbar\omega$ produces a flip of an electronic spin with an energy change $\hbar\omega_e$, the remaining energy $\hbar(\omega - \omega_e)$ has to be exchanged with the dipolar interactions through a fast rearrangement of the relative orientations of all the spins. As a consequence, it can be shown that the cooling of the Zeeman part is smaller than the ratio $\omega_e/(\omega_e - \omega)$ corresponding to no contact with the dipolar part so that the electronic polarization is made smaller than its thermal equilibrium value P_0. When nuclei are present and when ω is near $\omega_e \pm \omega_n$, the RF field furthermore provides the necessary thermal contact between the two preceding reservoirs and the nuclear Zeeman energy Z_n which should be described by its own temperature in the rotating frame ; this contact cools Z_n, and as Z_n is not affected by the transformation U, the nuclear po-

larization is enhanced by the inverse ratio of the new temperature to the initial (lattice) one. The final results depend on the various heat capacities of these three reservoirs and on the strengtl of their interactions with the lattice (relaxation rates) as well as on the strength of the thermal contacts provided by the RF fiel

To be more specific, supposing again a fast nuclear spin diffusion, the enhanced nuclear polarization is given by :

$$P_n = \frac{P_o(W^+T_n - W^-T_n) + P_o \dfrac{\omega_n(\omega - \omega_e)}{a\omega_L^2} W_oT_e(W^+T_n + W^-T_n)}{\left[1 + (1+k)(W^+T_n + W^-T_n)\right]\left[1 + \dfrac{(\omega_e - \omega)^2 + a\omega_L^2 + k\omega_n^2}{a\omega_L^2} W_oT_e\right]}$$

with $k = (N_n/N_e)(T_e/T_n)$ and $\omega_L^2 = \gamma_e^2 H_L^2$, where H_L is a local field due to the electronic spin-spin interactions, related to the secon moment of the electronic resonance line by $H_L^2 = 1/3\ \overline{\Delta H^2}$; a is number representing the ratio of the relaxation rates for the dipolar energy and for the electronic Zeeman energy : it varies between 2 (when there is no correlation between the relaxation of two neighbouring electronic spins) and 3 (when there is a complete correlation) ; we shall take a = 2 in the following. W^+ and W^- are the transition probabilities for the forbidden transitions, W_o the probability for the pure electronic transitions ; with the hypothesis of a fast spin diffusion, one can write the "saturation" parameter WT as $W^+T_n = S^+ \sim f(\omega - \omega_n)$, $W^-T_n = S^- \sim f(\omega + \omega_n)$, $W_oT_e = S_o \sim f(\omega$ where $f(\omega)$ represents the shape of the electronic resonance line, having its maximum value for $\omega = \omega_e$.

We have introduced the factor $k = (N_n/N_e)(T_e/T_n)$ only for the sake of completeness and to discuss formula (2) we shall suppose that it is negligibly small. The first term of the numerator and the first factor of the denominator represent the ordinary solid effec if the electronic resonance line is narrow, and with a single RF field, only one of the saturation parameters S can be non zero ; then $P_n^{max} = P_o$ or $P_n^{max} = -P_o$ according to whether S^+ or S^- are larger than unity. If the electronic resonance line is broad, S^+, S^- and S_o are simultaneously non zero : with low RF power, P_n is smaller than P_o as a result of the competition between positive and negative polarizations described by the term $W^+T_n - W^-T_n$ (so-called "differential effect") ; in the limiting case of strong RF irradiation, S^+, S^- and S_o are much larger than unity and P_n is given by :

$$P_n = P_o \frac{\omega_n(\omega - \omega_e)}{(\omega_e - \omega)^2 + 2\omega_L^2}$$

with a maximum value as a function of ω equal to :

$$P_n^{max} = P_o \frac{\omega_n}{2\sqrt{2}\,\omega_L} \qquad (3)$$

and as we have supposed $\omega_L > \omega_n$, P_n^{max} again is smaller than P_o ; for instance, the polarization obtained in a field of 25 kG with a broad resonance line corresponding to a local field H_L of 50 G is given by $P_n^{max} \simeq 0.26\ P_o$.

We shall now remark that formula (3) would give a polarization P_n^{max} larger than P_o if $2\sqrt{2}\omega_L$ was smaller than ω_n but then the electronic resonance line would be narrow and $S_o(S^+ + S^-)$ would always be zero. However, by applying two RF fields, one with a frequency ω_1 near ω_e to produce the maximum cooling of the electronic spins in their rotating frame, the other one with a frequency $\omega_2 = \omega_e \pm \omega_n$ to provide the thermal contact between these spins and the nuclear ones*, one can reach polarizations given by equation (3) which could be higher than P_o**. To take a definite example, paramagnetic defects are produced in irradiated ^{6}LiH with a resonance line having a second moment $\overline{\Delta H^2} \simeq 210\ G^2$ so that $H_L \simeq 8.5$ G [13] ; with a static magnetic field of 25 kG, formula (3) gives :

$$P_n^{max} \simeq 1.6\ P_o \quad .$$

The extension of this spin temperature theory outside the "high temperature" approximation domain is difficult and has not yet been made : it is not clear how to define two different energy reservoirs, one corresponding to the Zeeman part Z_e of the Hamiltonian, the other one corresponding to the dipolar interactions $\mathcal{H}_{SS}^o$; the form of the dipolar energy relaxation equation when the electronic polarization is large has not been derived, and furthermore, cooperative phenomena between electronic spins may occur in the rotating frame of reference.

Many thanks are due to J. Dorleijn for having made some computations on the depolarization effect of radiation damage in LMN.

Notes and References

* One can also use one microwave source only with its frequency jumping continuously from ω_1 to ω_2 in a time short compared with the electronic relaxation time T_e.

** In the case of LMN,Nd at low temperatures, one has to take care of the fact that, in the case of a phonon bottle-neck with a parameter σ, the coefficient a should be multiplied by $\sigma + 1$ so that equation (3) becomes $P_n^{max} = P_o\omega_n/(2\sqrt{2(\sigma + 1)}\omega_L)$; this is because, whereas the relaxation rate of Z_e is lengthened by phonon bottle-neck, the relaxation rate of $\mathcal{H}_{SS}^{o}$ which has a much smaller heat capacity is not. As, in LMN,Nd, σ is of the order of a few hundreds, despite the smallness of ω_L, small polarizations would be produced by this method. The fact that high polarizations are obtained in LMN,Nd comes obviously from S_o remaining zero when S^+ or S^- are made non zero.

1) A. Abragam, "Polarized targets : how ?", these Proceedings, p. 27.
2) H.H. Atkinson, "Technology of present high energy targets", these Proceedings, p. 41.
3) D. Garreta, "Description of low energy targets", these Proceedings, p. 283.
4) For references, see for example, M. Borghini, "Choice of substances for polarized proton targets", CERN Report 66-3, 1966.
5) See A. Abragam and M. Borghini, Progr. in Low Temp. Phys. (C.J. Gorter, ed.), 1964, IV, chap. VIII.
M. Borghini, Phys. Letters, 1966, 20, 228.
6) M. Borghini, Phys. Rev. Letters, 1966, 16, 318.
7) G.A. Rebka Jr and M. Wayne, Bull. Am. Phys. Soc., 1962, 7, 538 and private communication.
8) W.N. Hardy and J.R. Gaines, to be published.
9) See C.D. Jeffries, "Dynamic nuclear orientation", (John Wiley and sons, New York, 1965).
10) W.N. Hardy and G. Shapiro, private communication.
11) R.J. Wagner and R.P. Haddock, Phys. Rev. Letters, 1966, 16, 1116
12) M. Borghini, S. Mango, O. Runolfsson and J. Vermeulen, these Proceedings, p. 387.
13) F.E. Pretzel, G.V. Gritton, C.C. Rushing, R.J. Friauf, W.B. Lewis and P. Waldstein, J. Phys. Chem. Solids, 1962, 23, 325.

THEORY AND OPERATION OF NUCLEAR SPIN REFRIGERATORS

C.D. JEFFRIES

University of California, Berkeley

I INTRODUCTION

The Berkeley type of high energy dynamically polarized proton target using Nd:LaMN [1], with improvements made at Saclay and CERN, is now in wide spread use. However the expense of the microwave system, helium consumption, uniform magnetic fields, and required operator skill and patience lead naturally to the question : isn't there a simpler method ? One suggestion was given by myself [2] and by Abragam [3] several years ago : one can polarize nuclei simply by rotating a suitable crystal in a magnetic field at low temperatures. This is an example of a spin refrigerator, which cyclically transfers a large paramagnetic polarization to nuclear spins without the use of microwaves. To fix ideas we immediately consider the crystal ytterbium yttrium ethyl sulfate $(Yb,Y)(C_2H_5SO_4)_3 \cdot 9H_2O$, containing ~ 1 % paramagnetic Yb^{3+} ions, denoted by Yb:YES. Figure 1 shows the experimental arrangement : the crystal is immersed in liquid He at $T \sim 1°$ K and is mounted to rotate in a field $H \sim 10^4$ Oe, so that $\theta = \angle H,c$ may take any value ; c is the crystal field symmetry axis. A fixed rf coil is used to measure the proton NMR signal, which is proportional to the proton polarization.

The crystal contains a number N_e of Yb^{3+} ions which we think of as Yb "spins" $S = 1/2$, meaning they constitute a two level system, figure 2(a), with a very anisotropic g-factor $g(\theta) = [g_{//}^2 \cos^2 \theta + g_{\perp}^2 \sin^2 \theta]^{1/2}$, where $g_{//} = 3.35$ ang $g_{\perp}$ is as small as the proton g-factor $g_n = 0.003$. Furthermore the Yb^{3+} spin-lattice relaxation time is very anisotropic : $T_{1e} \propto [\cos^2 \theta \sin^2 \theta]^{-1}$. There are N_n protons spins $I = 1/2$ in the water and ethyl groups, with energy levels independent of θ (fig. 2(c)). If θ is held at 45° for a few milliseconds, the Yb spins became highly polarized, the relative

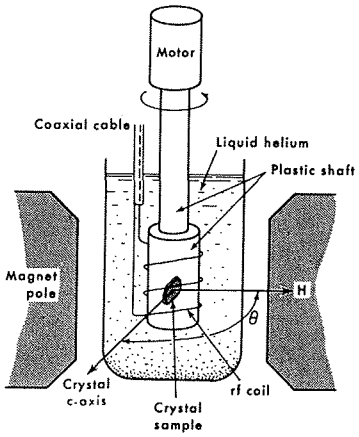

Fig. 1 Experimental arrangement of spin refrigerator.

Boltzmann populations being given in figure 2(a), where $\Delta = g(45°)\beta H/kT \approx 3$, typically, and β = Bohr magneton, and k = Boltzmann's constant. If we now rotate the crystal to $\theta = 90°$, quickly compared to T_{1e} but slowly compared to the Larmor period, the Yb spins will remain polarized along H ; the levels and populations are as shown in figure 2(b). A Yb spin now finds itself able to undergo a mutual spin flip with a neighbour proton through dipole-dipole coupling, the Yb flipping up, the proton down as shown by the dotted lines ; this polarizes that proton along H.

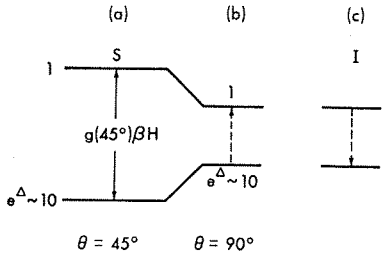

Fig. 2 a)Energy levels and populations of Yb spins at $\theta = 45°$; b) levels and populations of Yb spins after rapid rotation to 90° ; c) levels of protons.

Next the crystal is rotated to 135°, where the Yb spin again gets flipped to the lower state by fast lattice relaxation ; then to 180° where another proton is polarized, etc. After N_n/N_e cycles

all the protons are polarized ; more exactly, their polarization becomes :

$$p_n)_{ideal} = \tanh(\Delta/2) \approx g(45°)\beta H/2kT \qquad (1)$$

exceeding the static thermal equilibrium value $p_{no} = g_n\beta H/kT$ by $\sim 10^3$. The protons will be depolarized by relaxation, but at a much slower rate than the polarization process. This ideal spin refrigerator is thus potentially as effective as the dynamic microwave method in polarizing nuclei.

An alternative generalized description of the refrigerator using the concepts of spin temperature [4] and cross relaxation [5] is illustrated in figure 3, a thermal block diagram of the weakly interacting systems : proton spins, Yb spins, crystal lattice phonons, and helium bath. The protons have a common spin temperature T_n defined by $p_n = g_n\beta H/kT_n$; similarly T_e is the Yb spin temperature, and T is the phonon temperature, here assumed to be that of the helium bath. Thermal switch S_1 schematically represents the Yb spin-lattice relaxation, and is closed at roughly 45°, 135°, ... ; S_2 represents the cross relaxation between protons and Yb spins when $g(\theta) \approx g_n$, and is thus closed only at θ = 90°, 180°, ... The Yb spins are an anisotropic working substance cyclically transferring heat from the protons to the bath as θ takes on the successive values 45°, 90°, 135°, etc.

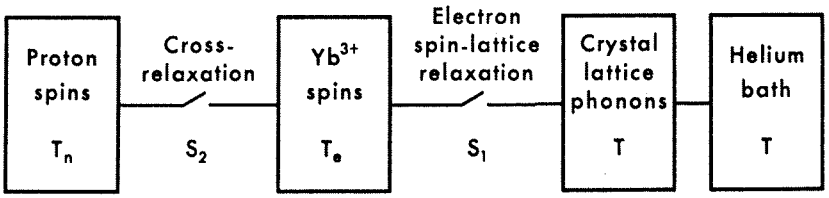

Fig. 3 Thermal block diagram of spin refrigerator.

At 45°, $T_e \rightarrow T \sim 1°$ K. Then as $\theta \rightarrow 90°$, S_1 opens and the Yb spins are isentropically cooled according to the relation :

$$\frac{g(45°)}{T_e(45°)} = \frac{g(90°)}{T_e(90°)} \qquad (2)$$

yielding $T_e(90°) \sim 10^{-3}°$ K. At 90°, S_2 closes, putting the cold Yb spins into thermal contact with the proton spins, initially at $T_n \sim 1°$ K. Conservation of energy leads to the common temperature T_c after mixing :

$$\frac{N_n}{T_n} + \frac{N_e}{T_e(90°)} = \frac{N_n + N_e}{T_c} \qquad (3)$$

which, for $N_n/N_e \sim 10^3$, yields $T_c \sim 0.5°$ K, i.e., the proton polarization is doubled. It is again doubled in the next cycle, etc, reaching after many cycles $T_n \approx T_e(90°)$, resulting in the enhanced proton polarization of equation (1). Continuous rotation instead of the discrete θ sequence, leads to only slightly smaller polarizations.

To generalize, the method is a solid state quantum mechanical spin refrigerator. One external parameter θ automatically operates the switches S_1 and S_2 and the isentropic cooling cycle, all in proper sequence. The switches are internal and microscopic in the sense that they operate by virtue of the dependence of the Yb^{3+} spin wave functions on θ. Energy is taken from the protons in quanta $g_n\beta H$ and exhausted as phonons of energy $\sim g(45°)\beta H$ which travel with the velocity of sound to the helium bath. The refrigerator can easily operate at 10^3 cycles per second, but only the spins not the lattice, are cooled. These features very clearly distinguish it from classical adiabatic demagnetization. Other nuclei in the crystal besides the protons could be similarly polarized. There are many possible varieties of spin refrigerators : e.g., one could operate S_1 not only by θ but by the magnitude of H, light, pressure, temperature, or electric fields ; the electron spin splitting can be varied by $g(\theta)$, by crossing levels, or by magnitude of H in 3rd order Zeeman splitting. One can also cross the Yb spin levels with a hyperfine system, thus cooling the nuclei in paramagnetic atoms ; another case of interest is to cross levels with a nuclear electric quadrupolar system.

Proton polarizations of $\approx$ 19 % have been achieved by Langley [6,7] upon rotation of a Yb:YES crystal at f_r = 60 rps in 10 kOe at 1.42° the limitation being due to insufficient rotation speed. In the same crystal McColl [8] has obtained polarizations of 35 % at T = 1.3° by rotation of a magnetic field of 20 kOe, rather than the crystal, at $f_r \approx 10^3$ cps. It is clear that Yb:YES is a favourable substance, and the bulk of this paper is a review of the work of Langley and McColl at Berkeley ; fuller details are given in reference 7.

Actually the first substance we considered was not YES but Ce:LaMN which also has both anisotropic relaxation rate and anisotropic g-factors ($g_\perp$ = 1.83, $g_{//}$ = 0). Rotation in 20 kOe at speeds up to 60 rps did not yield any significant proton enhancements [9] ; magnetic resonance experiments were then performed, yielding $g_{//} = 0.023 \approx 7\ g_n$. This is so large that cross relaxation to the protons does not occur in moderate fields. Subsequent rotation experiments at low fields by Robinson [10] yielded proton polarizations of $\sim$ 0.1 %, where there is some overlap in the tails of the proton and Ce^{3+} lines. Further experiments on Ce:LaMN by Schmugge and Langley, and by Combrisson, Ezratty and Abragam [11] and by

Luschikov, Neganov, Purfenov and Taran [12], did not yield proton polarizations greater than a few percent. Clark, Feher and Weger [13] obtained ≈ 1 % polarization of ^{27}Al by rotating a $Cr:Al_2O_3$ crystal. At about this time the first large dynamic proton polarizations (70 %) were obtained, by Schmugge [1] in Nd:LaMN at 70 Gc, which lead to the present high energy targets. This break-through caused most people to stop working on spin refrigerators ; however we hope to show that the discovery of the extreme anisotropies of Yb:YES makes spin refrigerators practical ; in fact, they may have several advantages over the present targets. Table I summarizes the measured nuclear polarizations obtained by spin refrigerators.

Nucleus	Substance	Polarization	Reference
^{1}H	2% Yb:YES crystal	10.5 %	6
^{1}H	2% ^{172}Yb:YES crystal	19	7
^{1}H	2% ^{172}Yb:YES crystal	35	8
^{1}H	2% ^{172}Yb:YES powder	17	26
^{1}H	2% Ce:LaMN crystal	0.12	10,9
^{1}H	2% Ce:LaMN crystal	0.48	11
^{1}H	0.2% Ce:LaMN crystal	2.4	12
^{27}Al	0.05% $Cr:Al_2O_3$ crystal	1.0	13

Table I Nuclear polarization achieved by spin refrigerators.

II PROPERTIES OF Yb:YES

Magnetic properties.

Single crystals of Yb:YES are easily grown from a saturated aqueous solution, the c-axis being parallel to a set of 12 generators, usually not fully developed. All the heavy atoms and probably even the hydrogens are in the $P6_3/m$ space group [14]. The Yb^{3+} free ion $4f^{13}$ has a $^2f_{7/2}$ ground state and a Landé g-factor $\Lambda = 8/7$. The spin-orbit interaction places the next multiplet $^2f_{5/2}$ higher by 10,200 cm^{-1}. Figure 4 shows the further splitting produced by the crystal field of C_{3h} symmetry in the ethyl sulfate, and by the applied dc field H. Only the lowest Kramers doublet $|a\rangle$, $|b\rangle$ is significantly populated at helium temperatures and forms the effective S = 1/2 Yb "spin" system introduced above. The wave functions $|J = 7/2, J_z\rangle$ shown in figure 4 are the eigenfunctions of the crystal field interaction [15] :

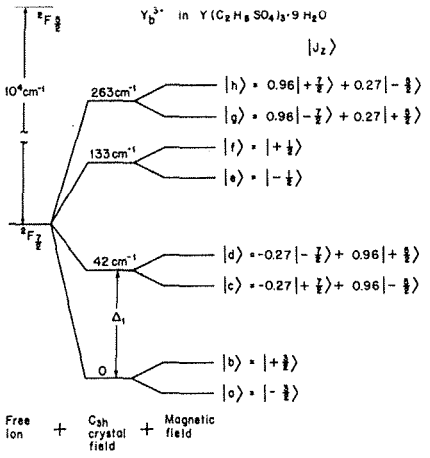

Fig. 4 Energy levels and zero order wave functions of Yb^{3+} in YES.

$$\mathcal{H}_c = A_2^0\langle r^2\rangle \alpha O_2^6 + A_4^0\langle r^4\rangle \beta O_4^0 + A_6^0\langle r^6\rangle \gamma O_6^0 + A_6^6\langle r^6\rangle \gamma O_6^6$$

with the values $A_2^0\langle r^2\rangle = 140$ cm^{-1}, $A_6^0\langle r^6\rangle = -29$ cm^{-1}, $A_6^6\langle r^6\rangle = 41$C cm^{-1}, obtained by an extrapolation procedure [16], and $A_4^0\langle r^4\rangle = -6$8 cm^{-1}, which best yields the measured value [17] $\Delta_1 = 42$ cm^{-1}. For the doublet $|a\rangle$, $|b\rangle$ these zero order wave functions yield $g_{//} = 3.4$ and $g_\perp = 0$; in agreement with susceptibility measurements [18,19] ($g_{//} = 3.40 \pm 0.07$, $g_\perp < 0.05$) and paramagnetic resonance [20] ($g_{//} = 3.35$, $g_\perp \approx 0$). That $g_\perp = 0$ follows from the fact that the lowest doublet is $|\pm 3/2\rangle$, which has no matrix elements for $J_\pm$. That the lowest doublet is pure $|\pm 3/2\rangle$ is a consequence of the relative magnitudes of the crystal field parameters and also the symmetry : for C_{3h} only states differing by $\Delta J_z = \pm 6$ are admixed by $\mathcal{H}_c$. Actually $g_\perp$ does not entirely vanish (otherwise paramagnetic resonance would not be observable) because the Zeeman perturbation $\mathcal{H}_z = \Lambda\beta\underset{\sim}{H}.\underset{\sim}{J}$ does admix the zero order states slightly, yielding at $\theta = 90°$ an estimated third order Zeeman splitting $E_3 \approx 4.5\ H^3 \times 10^{-}$ Mc/s, where H is in Oe ; this does not exceed the proton splitting for $H < 30$ kOe. At angles near 90° the total Yb spin splitting is $E = (E_3^2 + E_1^2)^{1/2}$ where $E_1 = g_{//}\beta H \cos\theta$, so that proton-Yb cross relaxation can always occur for $H < 30$ kOe . Although this theoretical prediction has not yet been experimentally confirmed, nevertheless our existing data indicate that Yb:YES is unusually favourable in this respect : it is exceedingly anisotropic, by a factor 10^3, even in sizeable fields.

Yb^{3+} relaxation.

Thermal vibrations of the crystal lattice add to the crystal field interaction a random time dependent term $\mathcal{H}_c' \sim \epsilon \mathcal{H}_c$, where ϵ is the thermal strain. This induces relaxation transitions between $|a\rangle$ and $|b\rangle$ at the rate T_{1e}^{-1} by three well understood processes [21,22]. At the upper helium temperatures the experimental results for concentrated Yb:YES are [19] :

$$T_{1e}^{-1})_{O+R} = 7 \times 10^{11} \exp(-60/T) + 1.5 \times 10^{-2}\, T^9 \ s^{-1} \quad (4)$$

due to the Orbach and Raman processes, which are independent of H and θ. At lower temperatures, $T < 1.5°$ K, where the spin refrigerator is operated, the direct process T_{1d}^{-1} dominates. We sketch its H, θ dependence, starting from the standard expression :

$$T_{1d}^{-1} \approx 2\pi\hbar^{-1}\, \rho(\nu) \left[\left| \langle a | \mathcal{H}_c' | b \rangle \right|^2 + \left| \langle b | \mathcal{H}_c' | a \rangle \right|^2 \right] \quad (5)$$

where $\rho(\nu)$ is the density of states, proportional to the number of lattice oscillators per unit frequency, i.e., to ν^2. In equation (5) the bracketed term will yield a factor $\nu \coth(h\nu/2kT)$ from the strain ϵ, and a factor $|\langle a | O_n^m | b \rangle|^2$ from $\mathcal{H}_c$, which vanishes by Kramers theorem unless $|a\rangle$ and $|b\rangle$ are admixed by the Zeeman perturbation to higher doublets $|i\rangle$ at Δ by an amount of order $\langle a | \Lambda \beta H (\cos\theta\, J_z + \sin\theta\, J_x) | i \rangle / \Delta$. From figure 4 it is evident that only J_x will admix, the overall result being :

$$T_{1d}^{-1} \propto \nu^3 \coth(h\nu/2kT)\, H^2 \sin^2\theta \quad . \quad (6)$$

Using :

$$h\nu = g_{//} \beta H \cos\theta \qquad \chi \equiv g_{//} \beta H \cos\theta / 2kT \quad (7)$$

we get :

$$T_{1d}^{-1} = A' H^5 \sin^2\theta \cos^3\theta \coth\chi \quad (8)$$

which takes the simpler form for $\chi \ll 1$:

$$T_{1d}^{-1} = A H^4 T \sin^2\theta \cos^2\theta \quad . \quad (9)$$

Theoretical estimates [7] give $A' \approx 1.38 \times 10^{-16}$ and a rate an order of magnitude greater than preliminary measurements by the microwave saturation-recovery method on 2 % Yb:YES. Figure 5 shows the measured rates [19] for the Orbach and Raman processes in Yb:YES, as well as the theoretical estimates [7].

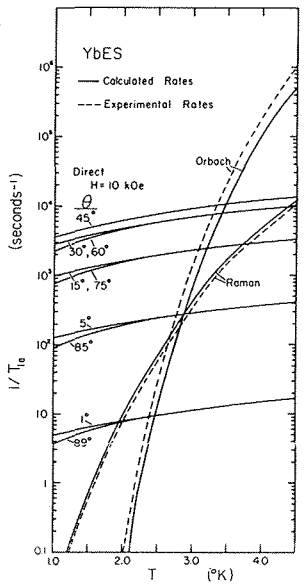

Fig. 5 Experimental values [19] and calculated values [7] for Yb^{3+} spin-lattice relaxation rate in the ethyl sulfate.

Proton relaxation in Yb:YES.

Neglecting other impurities, the relaxation of the abundant protons ($N_n/N_e \approx 1650$ for 2 % Yb:YES) is determined entirely by the Yb^{3+} ions. We recognize two cases : a) $\theta \neq 90°$, where the relaxation is predominantly through forbidden I_+S_- transitions, very analogous to proton relaxation in Nd:LaMN [1] ; and b) $\theta \approx 90°$, where relaxation is through energy conserving I_+S_- cross relaxation flips. To discuss case a) we use the shell-of-influence model [1] modified to include diffusion of proton polarization [23,24]. All the protons I are grouped into shells $r_1 < r < r_2$ about a typical Yb ion S in the sense that S is the course of their relaxation, and in the spin refrigerator, also the source of polarization. Radius $r_1 \approx 3.2$ Å is the minimum I-S in YES, from X-ray data ; $r_2 \approx (4\pi N_e/3)^{-1/3} \sim 20$ Å is half the average distance between Yb ions. Radius $r_2' \approx 10$ Å is the diffusion barrier within which rapid mutual proton flips are inhibited by the local field. Protons within r_2' do not contribute significantly to the NMR signal, however. The numerous distant protons n outside the diffusion barrier r_2' stay in internal spin temperature equilibrium via diffusion, i.e. mutual neighbour proton flips, and relax to the ion at the center of the shell by cross relaxation to relatively few n' near protons, which are relaxed directly by the ion at the rate $T_{1n'}^{-1}$. The observed spin-bath relaxation rate of the (distant) protons is just T_{1n}^{-1}, multiplied by the specific heat ratio :

$$\frac{1}{T_{1n}} \approx \frac{n'}{n} \frac{1}{T'_{1n}} \approx \left(\frac{r'_2}{r_2}\right)^3 \frac{1}{T'_{1n}} \quad . \tag{10}$$

Now T'^{-1}_{1n} can be calculated as previously but with the added complication $g_\perp = 0$. The result is :

$$\frac{1}{T'_{1n}} = \frac{1}{20} \left(\frac{g_{//}\beta}{H}\right)^2 \frac{7 - \cos^2\theta \, \mathrm{sech}^2\chi}{r_1^3 (r'_2)^3} \cdot \frac{}{T_{1e}} \quad . \tag{11}$$

Since $7 - \cos^2\theta \approx 6$, we find from equation (10) :

$$\frac{1}{T_{1n}} \approx \frac{3}{10} \left(\frac{g_{//}\beta}{H}\right)^2 \frac{1}{r_1^3 r_2^3} \frac{\mathrm{sech}^2\chi}{T_{1e}} \tag{12}$$

essentially the same expression as equation (14) of reference 1. We conclude that consideration of diffusion leads to a unique relaxation rate for the distant protons of the same magnitude as the average rate in the earlier shell-of-influence model. Although diffusion is important in establishing internal equilibrium of the distant protons it is so rapid that it does not enter explicitly into T_{1n}^{-1}, which is determined rather by the direct interaction of the nearest protons with the Yb^{3+} ion ; equation (12) is independent of the actual value of the diffusion barrier, if $r_1^3 \ll (r'_2)^3 \ll r_2^3$, a condition satisfied for 2 % Yb:YES.

In case b) at $\theta \approx 90°$, $g \approx g_n$, we assume all protons are coupled together by rapid diffusion and relax at the cross relaxation rate T_{12}^{-1} to the Yb spins, which themselves relax to the lattice at the rate T_{1e}^{-1}. The observed proton spin bath relaxation rate is now :

$$\left.\frac{1}{T_{1n}}\right)_{90°} \approx \frac{N_e}{N_n} \cdot \frac{1}{T_{1e} + T_{12}} \tag{13}$$

which may be several orders greater than equation (12).

To test the prediction of equation (12) T_{1n}^{-1} was measured for a 2 % Yb:YES crystal for $5° < \theta < 80°$ at H = 10 kOe and $1.4 < T < 4.2°$ K ; at 1.4° K data also were taken over the range $0.05 < H < 20$ kOe . The data are fit moderately well by the empirical expression :

$$T_{1n}^{-1} = 5.7 \times 10^2 \, H^{-2} \left[3.2 \times 10^{-17} \, H^5 \sin^2\theta \cos^3\theta \coth\chi + \right.$$

$$\left. + 7 \times 10^{11} \exp(-60/T) + 8 \times 10^{-2} \, T^9 \right] \mathrm{sech}^2\chi \quad s^{-1} \quad . \tag{14}$$

This is to be compared to the expression :

$$T_{1n}^{-1} = 13.5 \times 10^{2} H^{-2} \left[1.38 \times 10^{-16} H^{5} \sin^{2}\theta \cos^{3}\theta \coth x + 7 \times 10^{11} \exp(-60/T) + 1.5 \times 10^{-2} T^{9}\right] \operatorname{sech}^{2} x \quad s^{-1} ,$$

predicted from equations (12), (8) and (4). The fitted Raman process in equation (14) is ~ 5 x larger than that measured in Yb:YES, whereas the fitted direct process coefficient A' is ~ 4 x smaller than the theoretical estimate. In section IV we use $A' = 3.2 \times 10^{-1}$ in analysis of the spin refrigerator. Figure 6 shows the $T_{1n}^{-1}(\theta)$ data ; the dotted curve is the dominant direct process term of equation (14). The spike at 90° is due to cross relaxation, and the observed magnitude of $T_{1e}^{-1})_{90°}$ is within a factor 2 of that predicted by equation (13), assuming $T_{12} \ll T_{1e} \approx 0.3$ s from the Raman process, dominant at θ = 90° and 1.46° K. Actually the proton relaxation is not quite exponential at θ = 90°. The angular width 0.3° of the cross relaxation spike is probably due to a finite Yb^{3+} line width.

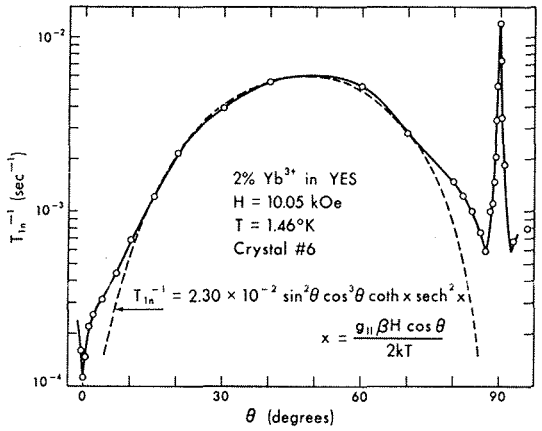

Fig. 6 Measured proton relaxation rate in 2 % Yb:YES.

To summarize, the magnitude of the proton relaxation rate, as well as its dependence on T, H, and θ is reasonably well understood for Yb:YES. Unfortunately the largest uncertainty is the magnitude A' of the direct process for Yb^{3+}, which is quite difficult to measure directly.

III SPIN REFRIGERATOR RATE EQUATIONS

Section II may be summarized as follows : at some given values of H, T, $\theta \neq 90°$, the Yb spin polarization p_e and the proton polarization p_n obey the effective relaxation rate equations :

$$\frac{dp_e}{dt} = - \frac{p_e - p_{eo}}{T_{1e}} \tag{16a}$$

$$\frac{dp_n}{dt} = - \frac{p_n - p_{no}}{T_{1n}} \tag{16b}$$

where $p_{eo}(\theta) = \tanh \left[g_{//} \beta H \cos \theta / 2kT \right]$, $p_{no} = g_n \beta H / 2kT$, and $T_{1n}(H,T,\theta)$ is given by equation (14), and $T_{1e}(H,T,\theta)$ by the bracketed terms in equation (14). At $\theta \approx 90°$, where the proton splitting Δ_n equals the Yb spin splitting Δ_e, we must add the cross relaxation terms [25,7] :

$$\left.\frac{dp_e}{dt}\right)_c = \frac{p_n - p_e}{T_{12}} (1 - \sigma) \approx \frac{p_n - p_e}{T_{12}} \tag{17a}$$

$$\left.\frac{dp_n}{dt}\right)_c = \frac{p_e - p_n}{T_{12}} \sigma \approx \frac{p_e - p_n}{T_{12}} \frac{N_e}{N_n} \tag{17b}$$

where we have assumed $N_e \ll N_n$, and introduced the cross relaxation rate T_{12}^{-1}, where :

$$\sigma \equiv N_e/(N_e + N_n) \approx N_e/N_n \tag{18a}$$

$$T_{12}^{-1} = \left(\frac{N_e + N_n}{N_e \quad N_n} \right) \sum_i^{N_n} \sum_j^{N_e} w_{ij} \tag{18b}$$

where w_{ij} is the transition probability of a mutual energy conserving spin flip between proton I_i and Yb spin S_j induced by the dipole terms $I_{i\pm} S_{j\mp}$. The overall behaviour of p_e and p_n is obtained by adding equations (16) and equations (17). Suppose that initially $p_e \gg p_n$; the solutions show that p_e drops to nearly p_n in a short time constant $\tau_f \approx T_{12}$, and p_e and p_n then decay together to $p_{eo} = p_{no}$ with the larger time constant τ_s given by :

$$\frac{1}{\tau_s} \cong \frac{1}{T_{1n}} + \frac{\sigma}{T_{1e} + T_{12}} \quad . \tag{19}$$

In a spin refrigerator we can break a cycle of operation into two regions : I, of duration τ_1 in which p_n and p_e are not coupled by cross relaxation, and p_e is built up to some large value ; and II, of duration τ_2, during which p_e and p_n cross relax, and p_n is built up. In region I of the next cycle p_n decays slightly at the rate $R_n = \langle T_{1n}^{-1} \rangle_{\tau_1}$, while p_e is built up again. Figure 7 shows schematically the overall behaviour of $p_e(t)$ and $p_n(t)$. After many cycles the values of p_e and p_n at the beginning of any region II, denoted by $\bar{p}_e$ and $\bar{p}_n$, do not vary but reach the steady state values denoted by $\bar{p}_{es}$ and $\bar{p}_{ns}$. Under the reasonable approximations $\tau_1 R_n \ll 1$, $\tau_2 \ll \tau_s$, and $(\tau_2/\tau_s) \ll \tau_1 R_n$, all valid for Yb:YES in our region of operation, it can be shown that the steady state proton polarization is :

$$\bar{p}_{ns} \approx \frac{\tau_1 R_n \, p_{no} + \sigma f \, \bar{p}_{es}}{\tau_1 R_n + \sigma f} \tag{20}$$

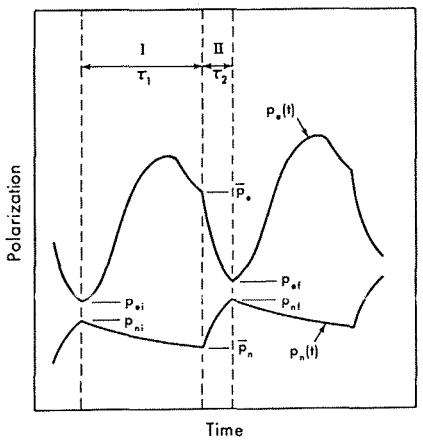

Fig. 7 Schematic diagram of time dependence of Yb polarization p_e and proton polarization p_n in region I, and in region II (cross relaxation) of a spin refrigerator.

where :

$$f \equiv 1 - \exp\left(-\tau_2/\tau_f\right) \tag{21}$$

is a measure of the completeness of cross relaxation. The build up of p_n is exponential at the rate :

$$\frac{1}{\tau_{on}} \cong R_n + \sigma \frac{f}{\tau_1} \quad . \tag{22}$$

At fast operation $\tau_1 \to 0$, and $\bar{p}_{ns} \to \bar{p}_{es}$, $\tau_{on} \to \tau_1 (N_n/N_e f)$, as expected from elementary considerations.

Equations (20) and (22) assume that cross relaxation occurs only if $\Delta_n = \Delta_e$, i.e. 1:1 proton-Yb spin flips. It is also energetically possible to have 2:1 flips if $2\Delta_n = \Delta_e$, etc, so we introduce the factor :

$$\epsilon \equiv \Delta_e / \Delta_n \tag{23}$$

to take into account multiple spin flips. We also introduce the factor :

$$K \equiv 1 - \exp\left[- \tau_1 / \langle T_{1e}^{-1} \rangle_{\tau_1} \right] \tag{24}$$

as a measure of the completeness of lattice relaxation of p_e in region I. In equation (20), $\bar{p}_{es}$ is the steady value obtained in the absence of the effect of the protons on p_e, i.e. assuming $K = 1$. With corrections for K and ϵ, equations (20) and (22) become :

$$\bar{p}_{ns} = \frac{\tau_1 R_n p_{no} + \dfrac{\epsilon \sigma f K \bar{p}_{es}}{K + f(1 - K)}}{\tau_1 R_n + \dfrac{\epsilon^2 \sigma f K}{K + f(1 - K)}} \tag{25}$$

$$\frac{1}{\tau_{on}} = \frac{1}{\tau_1} \left\{ \tau_1 R_n + \frac{\epsilon^2 \sigma f \left[\dfrac{K}{1 - K} - \tau_1 R_n \right]}{\dfrac{K}{1 - K} - \tau_1 R_n + f} \right\} \tag{26}$$

We note that for fast operation, $\tau_1 \to 0$, equation (25) predicts that $\bar{p}_{ns} \to \bar{p}_{es}/\epsilon$, showing that only multiple spin flips can prevent the proton polarization from reaching the value $\bar{p}_{es}$, the Yb polarization at $\theta = 90°$.

We now calculate $\bar{p}_{es}$ by integrating directly equation (16a). For simple rotation of the crystal $\theta = 2\pi f_r t$, and in the limit $f_r \to \infty$ one finds :

$$\bar{p}_{es}\Big)_{\infty} = \frac{32}{15\pi}\,\frac{g_{//}\beta H}{2kT} \qquad (27)$$

assuming $T_{1e}^{-1}(\theta) \propto \cos^2\theta \sin^2\theta$ as for Yb:YES. For finite rotation speeds a computor calculation gives the results of figure 8, $\bar{p}_{es}$ vs H, with the rotation speed as a parameter in the form f_r/A', where A' is the direct relaxation constant in equation (8). For given f_r, $\bar{p}_{es} \propto H$ up to a certain value and the decreases like $\bar{p}_{es} \propto H^{-1/3}$, as it turns out, because T_{1e} is becoming so short owing to the H^5 dependence in equation (8), that p_e tends to follow p_{eo} as $\theta \to 90°$.

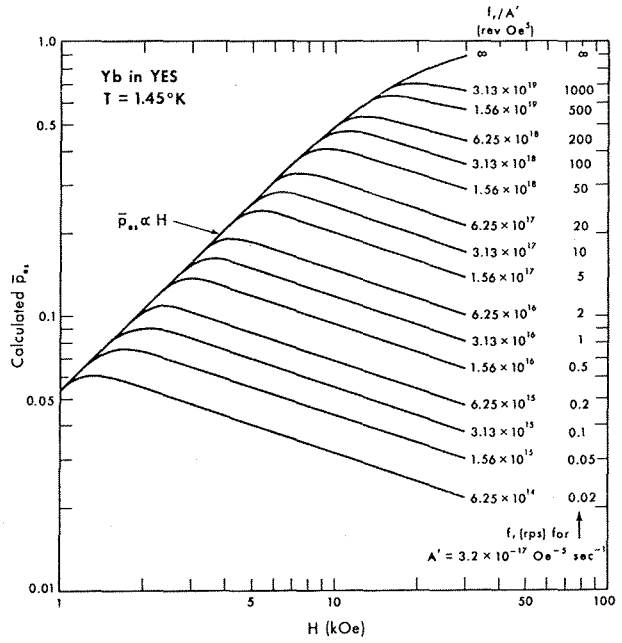

Fig. 8 Calculated steady state Yb polarization $\bar{p}_{es}$ at the beginning of the cross relaxation region, from integration of equation (16a).

Although we have implicitly assumed that the crystal c-axis is oriented as in figure 1, this is not strictly required for Yb:YES, or any other material in which $g_\perp = 0$. That is, if c is at some angle $\Phi < 90°$ with the vertical, this only reduces the maximum g-factor to $g_\perp \sin\Phi$, but still allows $\theta \to 90°$ at sometime during the rotation, since $g_\perp = 0$ in the whole plane perpendicular to c. For a single crystal the ideal proton polarization will be reduced by a factor $\sin\Phi$, and for a random powdered sample by $\pi/4$. At very high speeds the θ dependence of T_{1e} changes this slightly, and one predicts that a powdered sample will yield a polarization $10\pi/36 \approx 0.87$ of that of a single crystal, optimally oriented. This is of considerable practical significance, both in facilitating sample preparation and opening up the possibility of polari-

zing by a spin refrigerator the protons in a highly hydrogeneous medium (e.g., frozen organic liquids) in which crystallites of Yb:YES are dispersed. We further point out that paramagnetic ions in dilute liquid solutions often experience a reasonably well defined crystal field, and that highly hydrogeneous frozen solutions may exist in which $g_\perp \approx 0$, by virtue of the crystal field symmetry in the solid matrix. This has obvious application to polarized targets.

Our rate equation treatment of spin refrigerators should be valid if internal equilibrium is maintained in the proton and the Yb spin systems, respectively, and if changes in $\mathcal{H}$ are adiabatic, i.e., occur slowly compared to Larmor periods. The treatment seems to be adequate to give a semi-quantitative explanation of the data in section IV, although a more rigorous analysis using the density matrix may be necessary at higher speeds.

IV PROTON POLARIZATION RESULTS IN Yb:YES

Rotation of single crystals [6,7].

Langley's experiments were done in an apparatus like figure 1 for 0.5 %, 2 %, 10 % Yb:YES and 2 % ^{172}Yb:YES, the latter crystal being enriched to 98 % in the even isotope (I = 0) in an attempt to make negligible any residual width of the Yb line due to hyperfine structure. Experiments were done over the ranges $1 < H < 20$ kOe, $1.2 < T < 2.7°$ K and $0.5 < f_r < 60$ rps. The proton signal $p_{no}(H,T_o)$ was first measured at some given field H and temperature T_o; the crystal was then rotated as some constant speed f_r, while we observed the build up rate τ_{on}^{-1} and the final steady state enhanced proton signal $p_{enh}(H,T)$. Friction caused a slight rise in temperature to $T \approx 1.2\ T_o$, typically. The measured enhancement is $E = p_{enh}/p_{no}$, and the steady state polarization defined by $p_{ss} \equiv E\ p_{no}$ is essentially the polarization that would have obtained without heating. Figure 9 shows p_{ss} vs H in 2 % natural Yb crystal for various speeds and displays a behaviour like that of $\bar{p}_{es}$ in figure 8, except that p_{ss} is smaller by a factor ~ 3. The maximum in p_{ss} occurs at $H \approx 10$ kOe at the highest speed $f_r \approx 60$ rps, limited by friction and vibration. Figure 10 shows p_{ss} vs f_r at 10 kOe for a 2 % natural Yb crystal at $T_o = 1.45°$ K, and also a 2 % enriched ^{172}Yb crystal at $T_o = 1.23°$ K, yielding maximum values of p_{ss} of 12 % and 21.4 %, respectively. Since the temperatures rose from T_o to 1.65° K and 1.42° K, respectively, the actual proton polarizations achieved are 10.5 % and 18.6 % respectively, in crystals weighing ~ 200 mg ; the measured polarization build up was exponential, and in general exhi-

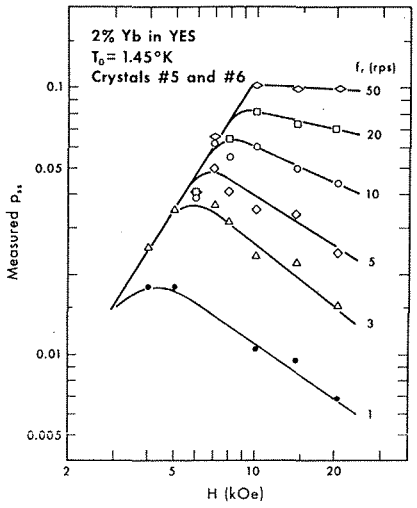

Fig. 9 Measured steady state proton polarization p_{ss} in Yb:YES spin refrigerator.

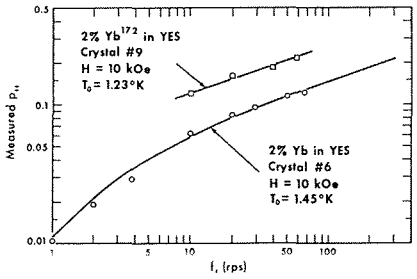

Fig. 10 Measured steady state proton polarization in Yb:YES spin refrigerator.

bited behaviour predicted by equation (22) : $\tau_{on}^{-1} \approx R_n + 2\sigma f f_r \rightarrow 2\sigma f$: at high speeds. The data roughly showed τ_{on}^{-1} to be 1) proportional tσ, i.e. to Yb concentration ; 2) independent of H and T ; 3) proportional to f_r. This means that $f = 1 - \exp(-\tau_2/T_{12})$ must be nearly unity, even at $f_r \approx 60$ rps, i.e. $T_{12} \lesssim 10^{-4}$ s, roughly. For the 2 % crystal, figure 9, $\tau_{on}^{-1} \approx 10$ s at $f_r = 60$ rps.

The data of figure 10 can be fit to equation (20) with $\tau_1 = (2f_r)^{-1}$ $R_n = \langle T_{1n}^{-1} \rangle_\theta \cong 3 \times 10^{-3}$ s from figure 6, $\sigma = 6 \times 10^{-4}$ for 2 % Yb:YES $f = 1$, and $\bar{p}_{es}$ from figure 8 only if we assume that $A' \approx 10^{-15}$ for the enriched crystal and $A' \approx 2 \times 10^{-16}$ for the natural crystal.

These values of A' are much larger than either the theoretical estimates or the preliminary measured values of the direct relaxation process in Yb:YES, and we feel that the failure to achieve ideal polarization is best explained by multiple spin flips. The data can be fit to equation (25) with f = 1 ; $\bar{p}_{es}$ from figure 8 with $A' = 3.2 \times 10^{-17}$; K calculated from equation (24) ; and $\epsilon = \epsilon_{eff}$, an adjustable parameter. The minimum value $\epsilon_{eff} = 1.9$ is found at 50 rps and 10 kOe for the enriched crystal and increases with decreasing field and decreasing frequency f_r. This is not unexpected since at low f_r more time is spent at orientations where multiple flips can occur, allowing more Yb spin polarization to leak to the protons at higher spin temperatures. And at lower H the fractional line width $\Delta H/H$ may be greater, allowing more overlap in the tails of the lines at a given θ.

Rotation of powdered samples [26].

McColl has obtained a proton polarization of 17 % in H = 10 kOe, T = 1.4° K by rotation of f_r = 60 rps of a powdered sample of 2 % ^{172}Yb:YES. This is to be compared to 18.5 % obtained in a single crystal under comparable conditions, and clearly establishes the feasibility of polarization by spin refrigerators of powdered samples. Experiments to polarize protons in a hydrogeneous matrix are in progress ; very preliminary results yield a few percent polarization for the protons in water, alcohol, glycerine frozen mixtures containing Yb^{3+} ions.

Rotation of field [8].

The experiments on rotating crystals (e.g., figure 10) clearly showed that higher rotation speeds are needed. This may be achieved by rotating the field electrically, rather than the crystal, as shown in McColl's apparatus, figure 11. The crystal is subject to a dc field $H_{dc} \sim 15$ kOe , and a pulsed field $H_p(t) \sim 15$ kOe produced by discharging a capacitor through a copper solenoid, cooled by the N_2 bath. The pulse has the approximate shape of a half sine wave of duration $\tau_p \approx 0.2 \times 10^{-3}$ s and pulse repetition period $\tau = 0.05$ s to 2 s. When the pulse is on, the net field is $\approx$ 22 kOe at $\theta = 45°$; this quickly polarizes the Yb spins. As the pulse turns off the net field rotates down to $\theta \approx 91°$, passing through the cross relaxation region in a time $\tau_2 \approx 10^{-5}$ s. Figure 12 shows the observed proton polarization vs pulse repetition rate τ^{-1} for 2 % ^{172}Yb:YES at 1.3° K. A proton polarization of 35 % at H_p = 20 kOe , H_{dc} = 15 kOe was observed at 10 pulses per second, with an exponential build up time of $\sim$ 10 minutes. This corresponds to an enhancement of 300. The data at H_p = 15 kOe give $(p_{ss})_{max}$ = 28 %, and are fit by the solid curve, which is equation (20) with $\tau_1 = \tau$, $\sigma = 6 \times 10^{-4}$ for 2 % Yb:YES, $R_n = 1.1 \times 10^{-4}$ s^{-1} $\approx$ measured value of T_{1n}^{-1} with $H_p = 0$, and the values f = 0.22, $\bar{p}_{es} = 0.29$, required to fit the data. This value of f is consistent with $\tau_2 = 10^{-5}$ s $\approx T_{12} \approx$ inverse proton linewidth. The fit-

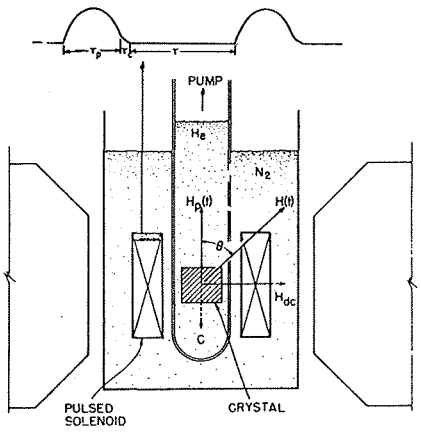

Fig. 11 Spin refrigerator apparatus for rapid rotation of magnetic field.

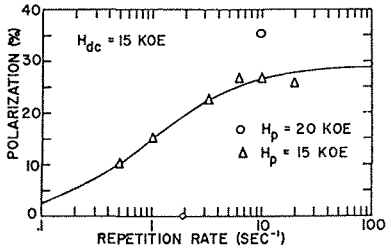

Fig. 12 Measured proton polarization in pulsed field spin refrigerator, yielding a polarization of 35 %.

ted value $\bar{p}_{es} = 0.29$ is to be compared to the value ~ 0.5 calculated by integration of equation (16a) using the measured pulse shape. Again, we feel that the failure to achieve theoretical ideal behaviour is due to multiple spin flips.

In very preliminary experiments on a deuterated Yb:YES crystal, deuteron enhancements of 30 were observed at 10 kŒ , 1.3° K. This small value is possibly because the minimum effective value of $g_\perp$ does not become small enough to cross relax at minimum spin temperature to the deuterons at $g_n = 0.00043$.

Additional rotating field experiments have been done by Langley [27] using an apparatus similar to the arrangement of figure 11, but with a vertical sinusoidal field $H_{ac} = H_o \sin 2\pi f_o t$ rather than a pulsed field, with $H_o = 3.5$ kOe, $f_o = 800$ rps. The net field oscillates between $\theta \approx 90°$ and $\theta \approx 45°$, approximately. Preliminary results in 2 % ^{172}Yb:YES yield a proton polarization of 12 % at $T = 1.17°$, $H_{dc} = 7.7$ kOe, with a build up time of 2 seconds. The measured polarization is 2.5 x smaller than theoretical prediction for the operating conditions, probably because of multiple spin flips. R. Ballard is constructing a similar apparatus to operate at much higher ac fields and higher frequencies.

V SUMMARY AND CONCLUSIONS

Using spin refrigerators, proton polarizations up to 35 % have been achieved at Berkeley in crystals of Yb:YES, which are 5.3 % hydrogen by weight. This is to be compared to Nd:LaMN, 3.1 % hydrogen, in which polarization of 70 % are achieved by microwave dynamic polarization. It is not unreasonable to expect that further spin refrigerator experiments underway at Berkeley at higher fields and higher rotation frequencies will yield polarizations of at least 50 %, thus making the spin refrigerator quite an acceptable method for polarized proton targets, with the following advantages. The short polarization time ($\tau_{on} \sim$ a few seconds in the best cases) and long relaxation time ($T_{1n} \sim 1$ hour in the best case) allows for scattering experiments in a small (~ 1 kOe) "holding" field produced by coils of open construction for good beam access, with brief periodic repositioning of the sample in the spin refrigerator rotating field for repolarization. No microwave resonance conditions are required, and spin refrigerator operation is semiautomatic. The helium consumption is an order of magnitude lower than in the microwave method ; initial construction costs are also much less, and should make polarized targets more widely available. The polarization should be quite uniform throughout the sample, since it is not dependent on microwaves. The absence of microwave heating may be a special advantage for low energy targets. The spin refrigerator may be operated in or near inhomogeneous magnetic fields, e.g., near a bubble chamber. A disadvantage is that only positive polarizations are produced by the simple rotation refrigerator ; however adiabatic fast passage can be used to rapidly reverse the polarization. The fact that polycrystalline samples with $g_\perp = 0$ may be used simplifies preparation of large samples, and also opens the possibility of polarizing the protons in a more hydrogeneous frozen matrix. Although proton polarizations achieved in Yb:YES are one to two or-

ders of magnitude greater than in other materials, it is not necessarily the ultimate material. Many refrigerator configurations are possible, e.g. : rotating samples, by motor drive, or preferably by cryogenic turbine ; oscillating plus static fields ; pulsed plus static fields ; or rotating field as in a 3 phase motor. It is not yet clear which configuration will be optimum.

The author is greatly indebted to K.H. Langley and J.R. McColl for their very major contributions to the work described here, and to the U.S. Atomic Energy Commission for continued support.

Notes and References

1) T.J. Schmugge and C.D. Jeffries, Phys. Rev. Letters, 1962, 9, 268 ; Phys. Rev., 1965, 138, A1785.
2) C.D. Jeffries, Cryogenics, 1963, 3, 41.
3) A. Abragam, Cryogenics, 1963, 3, 42.
4) A. Abragam and W.G. Proctor, Phys. Rev., 1958, 109, 1441.
5) N. Bloembergen, Proceedings of the VII International Conference on Low Temperature Physics (University of Toronto Press, Toronto, 1961), p. 36.
6) K.H. Langley and C.D. Jeffries, Phys. Rev. Letters, 1964, 13, 808.
7) K.H. Langley and C.D. Jeffries, Phys. Rev., December 1966, (to be published).
8) J.R. McColl and C.D. Jeffries, Phys. Rev. Letters, 1966, 16, 316.
9) We are indebted to Dr T.J. Schmugge for his helpful collaboration on these early experiments, described in Status Report, ONR Contract Nonr 222 (61), September 1, 1962 and December 1, 1962, University of California, Berkeley, (unpublished).
10) F.N.H. Robinson, Phys. Letters, 1963, 4, 180.
11) J. Combrisson, J. Ezratty and A. Abragam, Compt. Rend., 1963, 257, 3860.
12) V.I. Lushchikov, B.S. Neganov, L.B. Parfenov and Yu V. Taran, Soviet Phys. JETP, 1966, 22, 285.
13) W.G. Clark, G. Feher and M. Weger, Bull. Am. Phys. Soc., 1963, 8, 463 ; to be published in Phys. Rev.
14) D.R. Fitzwater and R.E. Rundle, Z. Kristallographie, 1959, 112, 362.
15) R.J. Elliott and K.W.H. Stevens, Proc. Roy. Soc. (London), 1952, A215, 437 ; 1953, A218, 553 ; 1953, A219, 387.
16) M.J.D. Powell and R. Orbach, Proc. Phys. Soc. (London), 1961, 78, 753.

17) E.Y. Wong, J. Chem. Phys., 1963, 39, 2781.
18) A.H. Cooke, F.R. McKim, H. Meyer and W.P. Wolf, Phil. Mag., 1957, 2, 928.
19) J. Van den Broek and L.C. Van der Marel, Physica, 1963, 29, 948 ; 1964, 30, 565.
20) T.J. Schmugge (unpublished) has observed a very weak paramagnetic resonance in Yb:YES and Yb:LaYES.
21) R. Orbach, Proc. Roy. Soc. (London), 1961, A264, 458.
22) P.L. Scott and C.D. Jeffries, Phys. Rev., 1962, 127, 32.
23) C.D. Jeffries, Proc. Phys. Soc. (London), 1966, 88, 257.
24) C.D. Jeffries, Technical Report N° UCB-34P20-T-1, University of California, Berkeley (1966).
25) N. Bloembergen, S. Shapiro, P.S. Pershan and J.O. Artman, Phys. Rev., 1959, 114, 445.
26) J.R. McColl and C.D. Jeffries, Bull. Am. Phys. Soc., 1966, 11, n° 7, 906.
27) K.H. Langley, Thesis, University of California, Berkeley, 1966 (unpublished).

Research supported in part by the U.S. Atomic Energy Commission, Contract AT(11-1)-34, Project 20.

^3He-^4He DILUTION REFRIGERATORS

E. VAROQUAUX

Institut d'Electronique Fondamentale, Orsay

For over thirty years, the only way to obtain very low temperatures has been to perform adiabatic demagnetization experiments.

An entirely new refrigeration cycle was suggested, in 1951, by Dr. H. London [1] ; more definite proposals were formulated, in 1962, by himself, G.R. Clarke and E. Mendoza [2]. Successful experiments were carried out almost simultaneously by H.E. Hall et al [3] at the University of Manchester and by B. Neganov and his coworkers [4] from the Institute for Nuclear Problems in Dubna.

This new method opens the way for new experiments in the very low temperature regions because it permits one to cope with fairly large amounts of heat and operates without magnetic fields.

The working principle of this refrigeration cycle rests on the properties of ^3He-^4He solutions and, more specifically, on the phase separation these solutions undergo below a certain critical temperature. The phase separation phenomenon is due to the large mass difference between ^3He and ^4He, which gives rise to large differences in zero point energies and anharmonic terms in the interaction potential. The phase separation curve, shown in figure 1, indicates that a given solution with a molar concentration in ^3He, x, larger than about 6 %, will separate below a certain temperature into two phases, the upper one richer than the other in ^3He.

Thus, at temperatures below a few tenths of a degree, there exist only very concentrated solutions and fairly dilute ones.

The thermodynamical properties of these solutions are, for our purposes, best described by means of the enthalpy H. The enthalpy diagram, shown in figure 2, is constructed from specific heat measurements for the rich phase and from a simple ideal gas model for the dilute phase. More details will be found in the appendix.

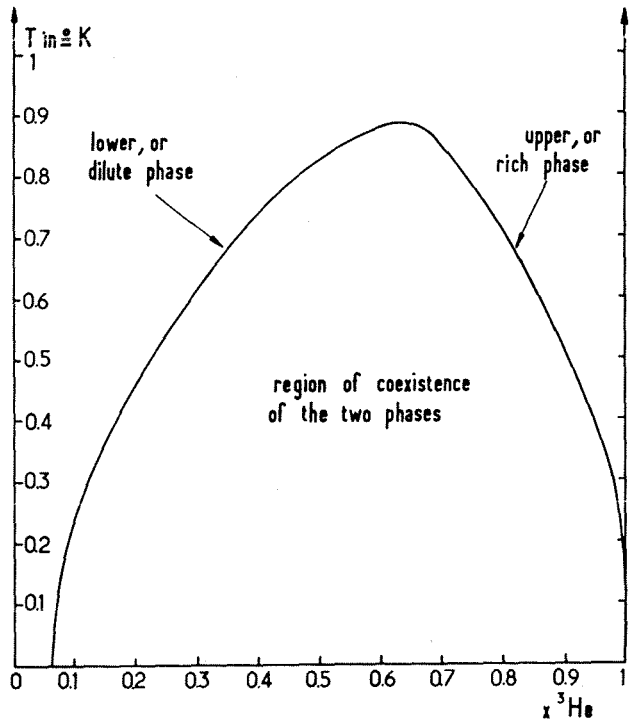

Fig. 1 Phase separation curve of helium solutions at satured vapour pressure.

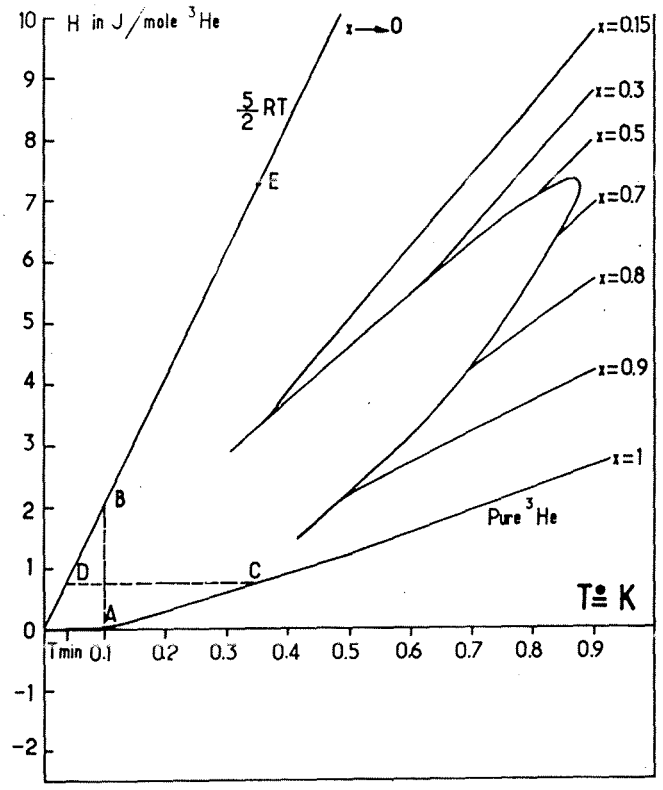

Fig. 2 Enthalpy diagram for ^{3}He pure and in solution. The straight line represents the enthalpy of an ideal classical gas with the same binding energy as pure ^{3}He.

In the rich phase, which is nearly pure ^{3}He, as can be seen in figure 1, the molar enthalpy is given by :

$$H_r(T) \simeq H_3(T) = - L_{03} + \int_0^T C_3 dT \qquad (1)$$

where H_3 is the enthalpy of pure ^{3}He, L_{03} its latent heat of vaporization at absolute zero, and C_3 its specific heat under constant pressure.

In the dilute phase, ^{4}He, being superfluid, plays no significant thermodynamical or hydrodynamical rôle at very low temperatures since it has zero entropy and zero viscosity ; it can be said to act merely as a filler to increase the volume occupied by ^{3}He. The dilute component of the solution behaves like an ideal gas, the molar enthalpy of which is given by :

$$H_d(x,T) = - E_{03}(x) + \frac{5}{2} RT \qquad (2)$$

where $E_{03}(x)$ is the binding energy of ^{3}He in the solution at absolute zero.

Therefore, upon mixing a number of moles n of ^{3}He in ^{4}He down to zero concentration, we can absorb a quantity of heat Q at the temperature T which is :

$$Q = n \left[L_{03} - E_{03} + \frac{5}{2} RT - \int_0^T C_3 dT \right] \quad . \qquad (3)$$

This isothermal process is represented on the enthalpy diagram (fig. 2) by the line AB. This line shows the maximum cooling power available at temperature T. However, heat exchangers cannot be made perfect and it is in practice not possible to achieve the ideal cycle so that a more realistic path is to cool ^{3}He down to point C for example and to perform the dilution adiabatically to point D, and then to absorb a certain quantity of heat, back to B.

D represents the point at which, with given heat exchangers, no cooling power is available anymore and sets the minimum temperature one can reach. One also sees on the H-diagram that a considerable cooling power is available above the temperature T, when going from B to E for instance ; this will help quenching the heat leaks in an actual apparatus.

From formula 3, at a temperature T = 0.1° K and with a circulation rate n = 10^{-4} mole per second, setting $E_{03}(x)$ nearly equal to L_{03}, we find a refrigerating capacity of the order of 2000 ergs per second.

The feasibility of a refrigerator working on the principle described rests on three essential facts : a) the very large cooling power of the dilution process ; b) the fact that it is possible to distil ^{3}He out of the solution in a very efficient way at a temperature of 0.6° K ; c) the fairly low heat conductivity of the

mixture that enables one to perform the dilution in the mixing chamber ① (fig. 3) and to extract ^{3}He in a distillation chamber ② at a much higher temperature through a duct ③.

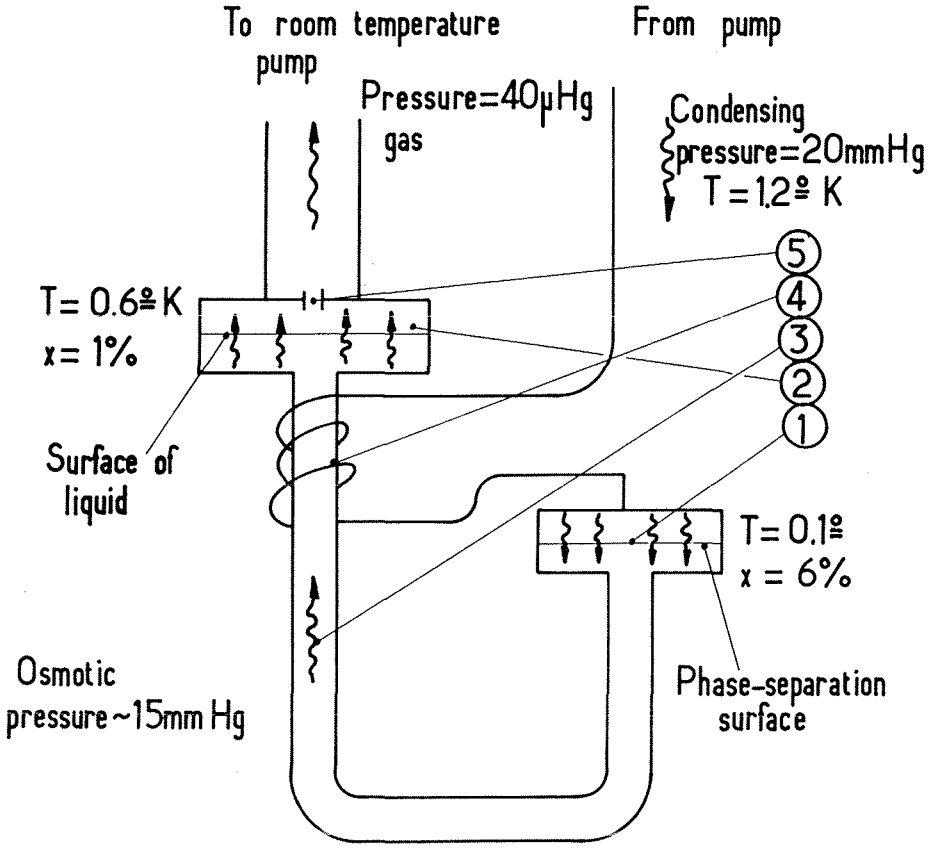

Fig. 3 Schematic description of a dilution refrigerator : ① mixing chamber, ② distillation chamber, ③ duct, ④ heat exchanger, ⑤ constriction on the pumping line. The direction of circulation of ^{3}He is indicated by the wiggly arrows to which are attached the relevant physical parameters of a typical working situation.

The problems met with in the construction of such a refrigerator are : a) the conception of efficient heat exchangers ④ to precool the incoming ^{3}He, to take advantage of fact a. b) the superfluid helium film creep along the wall of the distillation chamber, which has to be stopped by a constriction ⑤, to take advantage of fact b. c) the design of the duct ③ which must introduce adequate thermal isolation and a negligible osmotic pressure drop, by taking advantage of fact c.

Five such machines have been reported working at the 10th International Conference on Low Temperature Physics in September. Their performances are summarized in figure 4.

	Neganov Dubna	Hall Manchester	Wheatley Illinois	Zinov'eva Moscow	Leyden group
$\dot{n}$ circulation rate in mole/s	1.8×10^{-4}	3×10^{-5}	3×10^{-5}	1×10^{-5}	10^{-5} to 10^{-6}
Minimum temperature T_{min}	25 m° K	55 m° K	30 m° K	$\lesssim$ 0.1° K	88 m° K
Cooling power at 0.1° K $\dot{Q}$ (erg/s)	1800	40	200	0	-
Factor of merit $\dot{Q}/\dot{n}$ (erg/mole)	10^7	1.33×10^6	6.6×10^6	0	-

Fig. 4 Comparative table of performances.

APPENDIX

In a more sophisticated attempt to derive the H-diagram in the low temperature limit, we shall use the Landau-Pomeranchuk [5,6] model for dilute ^{3}He-^{4}He solutions which is confirmed by experiments [7,8] and according to which the Fermi excitations in the solution have the energy-momentum relation :

$$\varepsilon = - \frac{E_{03}(x)}{N_A} + \frac{p^2}{2m_3^*}$$

and the same number density as ^{3}He atoms in the solution. The effective mass m_3^* is independent of the concentration and equal to 2.4 times the real mass of ^{3}He [7]. The binding energy $E_{03}(x)$ is temperature independent and varies linearly with x [9]. The rich-phase is taken to be pure ^{3}He [10,11].

The condition for equilibrium at absolute zero is found by equating the chemical potentials of ^{3}He in the two phases :

$$- E_{03}(x_\ell) + RT_F(x_\ell) = - L_{03} \qquad (4)$$

where $RT_F(x_\ell)$ is 3/5 times the kinetic energy U of ^{3}He excitation gas and x_ℓ is the maximum stable concentration.

At finite temperature, this equation reads :

$$- E_3(x) + \mu_F(x,T) = - L_{03} - \int_0^T S_3 dT \qquad (5)$$

where μ_F is the kinetic part of the chemical potential and S_3 the entropy of pure ^{3}He. Equation 5 has been used by D.O. Edwards et al [9] to determine $E_{03}(x) - L_{03}$ knowing the phase separation curve $x_S(T)$.

The molar enthalpies in the two phases and the heat of dilution are given, in this quasi-particle theory, by :

$$H_d(x,T) = - E_{03}(x) + \frac{5}{3} U(x,T) \qquad (6)$$

$$H_r(T) = - L_{03} + \int_0^T C_3 dT \qquad (7)$$

$$\Delta H(T) = L_{03} - E_{03}(x_S) + \frac{5}{3} U(x_S,T) - \int_0^T C_3 dT \qquad (8)$$

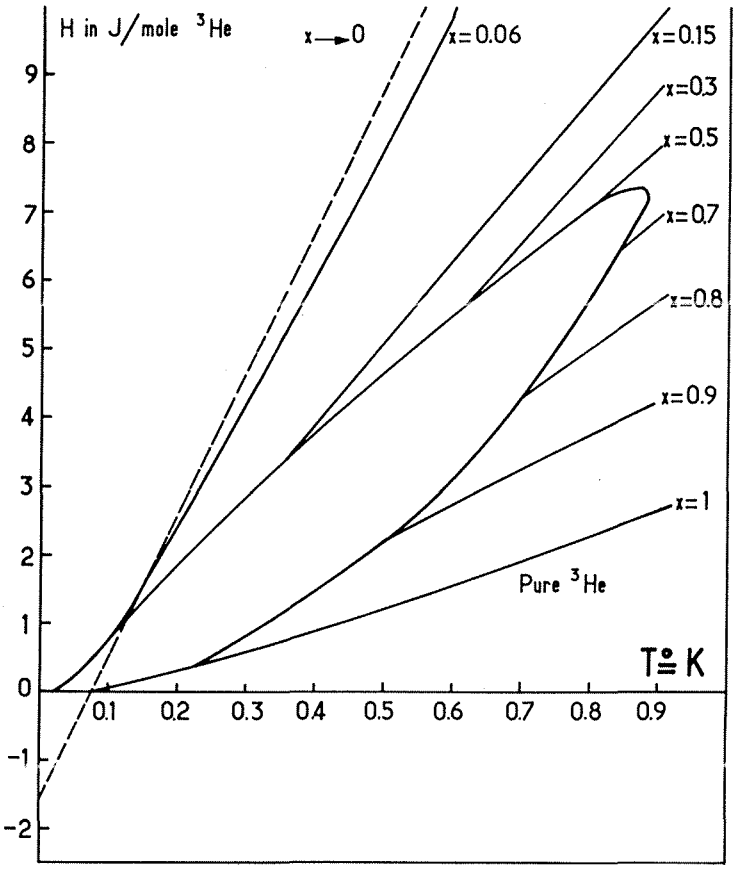

Fig. 5 Enthalpy diagram for ^{3}He pure and in solution in the quasi-particle model for an osmotic pressure equal to the zero-point pressure of the equivalent Fermi gas. The straight line represents the enthalpy of an infinitely dilute gas $\frac{5}{2}$ RT + L_{03} - $E_{03}(0)$.

C_3, the specific heat of pure ^{3}He at constant pressure, is known experimentally to a fair accuracy. The numerical evaluation of equation (8) can be easily performed with the help of the Fermi integral tables [12] and the results are plotted on figure 5.

In the case of a reversible dilution, the heat of mixing tends to zero as T^2, as already predicted by Peshkov [13] on other grounds. Finally, we wish to point out that the value we have derived for $\Delta H(0.1^\circ K)$ in the frame of the Landau-Pomeranchuk model differs from the one observed by Neganov [4], the predicted one being too small by 30 %.

References

1) H. London, Proc. Intern. Conf. Low Temperature Phys., p. 157 (Clarendon, Oxford, 1951).
2) H. London, G.R. Clarke and E. Mendoza, Phys. Rev., 1962, 128, 1992.
3) H.E. Hall, P.J. Ford and K. Thompson, Cryogenics, 1966, 6, 80.
4) B. Neganov, N. Borisov and M. Liburg, Zh. Eksperim. i Teor. Fiz., 1966, 50, 1455.
5) L.D. Landau and I. Pomeranchuk, Dokl. Akad. Nauk SSSR, 1948, 59, 669.
6) I. Pomeranchuk, Zh. Eksperim. i Teor. Fiz., 1949, 19, 42.
7) A.C. Anderson, W.R. Roach, R.E. Sarwinski and J.C. Wheatley, Phys. Rev. Letters, 1966, 16, 263.
A.C. Anderson, D.O. Edwards, W.R. Roach, R.E. Sarwinski and J.C. Wheatley, Phys. Rev. Letters, 1966, 17, 367.
8) R. De Bruyn Ouboter, K.W. Taconis, C. Le Pair and J.J.M. Beenakker, Physica, 1960, 26, 853.
9) D.O. Edwards, D.F. Brewer, P. Seligman, M. Skertic and M. Yaqub, Phys. Rev. Letters, 1965, 15, 773.
0) D.O. Edwards and J.G. Daunt, Phys. Rev., 1961, 124, 640.
1) D.F. Brewer and J.R.G. Keyston, Phys. Letters, 1962, 1, 5.
2) A.C. Beer, M.N. Chase and P.F. Choquard, Helv. Phys. Acta, 1955, 28, 529.
3) V.P. Peshkov, Proc. 10th Intern. Conf. Low. Temperature Phys., (Moscow, 1966), (to be published).
Also, O.E. Vilches and J.C. Wheatley (to be published) who give a precise experimental confirmation of equation (8) and have obtained an ultimate temperature of 20 m° K (13 m° K in transient regime) ; we are grateful to O.E. Vilches and J.C. Wheatley for sending a preprint to us.

POLARIZED ION SOURCES

R. BEURTEY
Département de Physique Nucléaire, Saclay
Present address : CERN, Geneva

1 INTRODUCTION

The question does not arise anymore whether it is necessary or possible to build sources of polarized ions. Such sources exist and are useful for physics, at least for low-energy physics. The remaining dilemma concerning the proton or deuteron sources (for ^{3}He, see G.C. Philips et al [1]) is today the following.

Should we build sources following the "conventional" atomic beam method, with a Stern-Gerlach separation followed by RF transitions, or the more recent method first used and improved by Donnally [2], which consists of producing two near resonant charge transfer processes via the (2S) state of atomic hydrogen :

$$H^+ \longrightarrow H(2S) \longrightarrow H^-$$

(unpolarized) (polarized) (polarized)

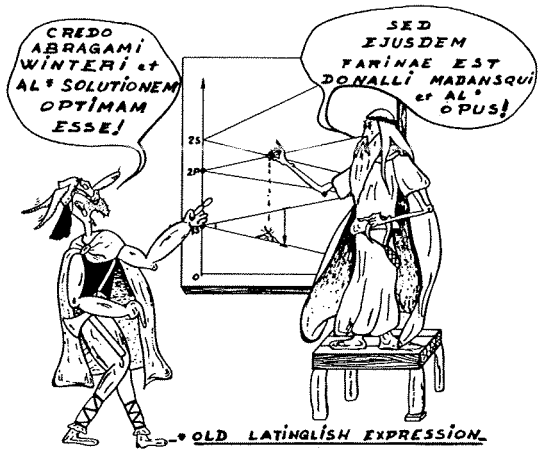

Fig. 1

(The figure 1 illustrates this dilemma).

This latter method is now fully developed and gives very encouraging preliminary results. As for the former method used by many laboratories, the basic "cookings" and the very numerous spices give styles as different from one source to another, as a French Bordeaux may be different from Bourbon, or a Sauce Béarnaise from Tomato Ketchup. For an observer outside the field, the situation is not clear, and the figure 2 indicates what he can hear from a "source man" during an informal "after drinking" discussion. But what the physicist really thinks when preparing his experiment is shown in the figure 3.

Fig. 2

Therefore, after a short inspection of the two fashionable methods, we shall examine the question : can we still improve existing sources and "marry" them with any definite accelerator ? We might incidentally ask ourselves whether it is of interest to generalize the use of polarized sources with all types of machines, and to increase their qualities. Let us indeed remember that there are so many theoretical papers beginning by "...let us suppose first that the particle has no spin...", and where it is said in the conclusion that "...a realistic calculation <u>should</u> have taken into account the <u>complications</u> due to the spin...", and never "...the enormous benefit due to the existence of spins and of kind experimentalists who use them to give us such fascinating results...".

To tell the truth, I shall correct this pessimistic assertion. All theoreticians and experimentalists are better and better "spin-players", for (as Leprince-Ringuet would say) "...the things become easier when they become familiar...".

Fig. 3

2 SOURCES USING METASTABLE (2S) HYDROGEN

This type of source has been developed essentially by Donnally [2] (Lake Forest), Drake [3] (Yale) and McKibben [4] (Los Alamos). The method is equally as good for protons as for deuterons.

2.1 Description of the method

The following steps are used to produce a beam of (H^-) in which the protons are polarized from a beam of unpolarized protons (H^+) (fig. 4).

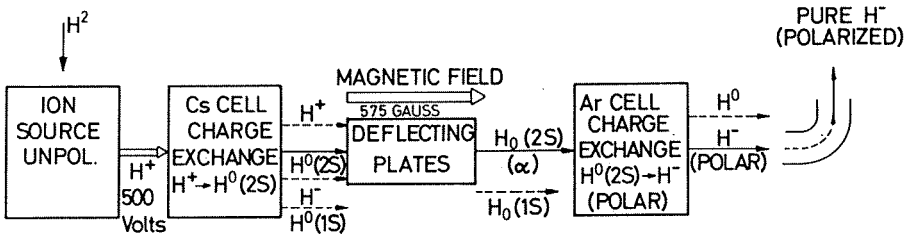

Fig. 4 Diagram of the double charge exchange method.

a. A beam of (500 ↔ 1000 eV) protons crosses a cesium cell in which a near resonant process of charge exchange takes place giving atomic hydrogen in the (2S) state with a high efficiency :

$$H^+ + Cs \leftrightarrow Cs^+ + H^o(2S) \quad .$$

b. The (2S) atoms are metastable and the polarizing process takes place (fig. 5) in a 575 G longitudinal magnetic field. In this field the lower state (β) ($m_J = 1/2$) crosses the (2P) state. The ratio of the lifetime τ_α/τ_β at this value of the magnetic field is ~ 1850. A low transverse electric field (mixing S and P states by Stark-effect) is enough to quench almost all (β) atoms to the ground state, losing a negligible quantity of (α) atoms. The same electric field is used : i) to eliminate the residual protons from the beam ; ii) eventually by increasing this field, to quench the (α) atoms, which is useful in order to measure the relative number of the remaining atoms in that state.

c. If now the magnetic field is decreased to a small value, the mean polarization of the (α) atoms will be 50 % (due to the cou-

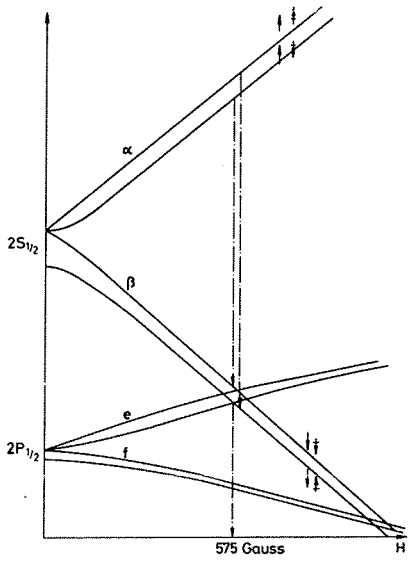

Fig. 5 Hyperfine structure of (2S) and (2P) states.

pling of the protons and electron spins). By adding an RF transition at 575 G, one can eliminate one more substate of the two hyperfine components of the (α) state and, if the ionization takes place in a high magnetic field, get a polarization ± 1 (but with a factor 1/2 for the intensity).

d. The remaining H_{2S}-(α) atoms (and H_{1S} arising from the quenching of the β-atoms) cross a new cell filled with argon, where the following process converts the H_{2S} atoms into H^- ions, preferentially by charge exchange :

$$H_{2S} + Ar \rightarrow Ar^+ + H^-$$

and the (H^-) ions are deflected by another electric field.

2.2 Benefit of the method

After a first look into this method, it seems very simple and promising. The two charge exchange processes are very efficient : an over-all efficiency of 2 % was already obtained by Drake and Krotkov [3]. The emittance of the H^+ is very little changed (of the order of, say, 0.1 cm x rad x $eV^{1/2}$). High intensity beams of polarized H^- may be hoped for by increasing the initial H^+ beam. And even for lower intensity beams used up to now, the method appears to be the best for machines accelerating H^- ions (tandem Van de Graaff and some cyclotrons).

2.3 Difficulties

If one desires to ionize in a low magnetic field, i.e. without RF transitions, the longitudinal decreasing magnetic field is such that small transverse magnetic components exist and in the proper reference system of an atom, such small but varying transverse magnetic fields can induce depolarizing transitions $\alpha \rightarrow \beta$. This effect is minimized by a smooth drop.

Problems involving very intense beams are more serious :

a. At such a low energy (500-700 eV) it is difficult to obtain intense H^+ beams with a good emittance. Currents larger than a few hundreds of microamperes (H^+) seem to require a neutralization of the space charge in the 500 V acceleration gap.

b. A similar problem takes place in the cesium cell where space charge due to positive remaining ions can produce electric fields high enough to quench the H(2S) atoms.

These problems are not of a fundamental nature, and successive improvements might qualify that type of source as the best for negative ion machines, and very competitive for others... if the intensities of the "classical sources" of polarized H^+ could not obtain in the near future a gain of an order of magnitude over the present situation.

3 CLASSICAL SOURCES (P AND D)

This type of polarized source is well known.

3.1 Description

The figure 6 shows a block diagram indicating the different components of such a source :

a. An atomic beam source consisting of a dissociator of molecular hydrogen and an injection system giving an atomic beam as intense as possible near the axis of the system and selecting a solid angle corresponding roughly to the acceptance of the following magnet.

b. A Stern-Gerlach magnet which selectively focuses the $m_J = 1/2$ ground state near the axis into the ionizer, and defocuses the $m_J = -1/2$ state, due to radial magnetic gradients and correspon-

dingly, radial forces of opposite signs.

c. An RF transition system, i.e. 0, 1, 2 or 3 transitions, depending on the desired final polarization states of protons or deuterons. The method generally used is the so-called "adiabatic passage" method, as suggested by A. Abragam and J.M. Winter [5].

d. An ionizer more and more of the "long-axial-strong-magnetic field type" [6].

e. If necessary, an injection system and if possible a machine.

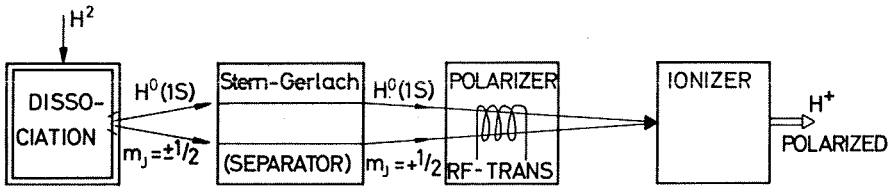

Fig. 6

The best way to match a source to a definite accelerator would be to build the equipment going from the accelerator to the hydrogen-dissociator. That is to say, after knowing the machine acceptance, to build first a well-adapted injection system and to infer the maximum emittance of the ionizer beyond which particles are no longer accepted by the machine. Then manoeuvre the ionizer to optimize the dimensions and efficiency. Finally, build a source giving in the useful volume of the ionizer the highest density of polarized atoms.

The opposite direction was generally followed by people who studied sources without making reference to an accelerator which often was not built or the acceptance of which was poorly known. It seems to me that we might express now the quality of a "polarized ion source" including the ionizer globally by the figure :

$$\frac{I \times P^2}{\text{Emittance}} \quad \text{(after the ionizer)}$$

better than by $I \times P^2$ itself.

I will not make a general review of existing sources. Excellent reviews exist in the literature [7]. I only will say between which broad limits the different components and results of sources vary. This variety is indicated by the next table (Table I).

Dissociator : Capillary - Nozzle - Hole - Ring - Slit			
Stern-Gerlach : Dipole - Quadrupole - Sextupole - Octupole			
	minimum	maximum	rapport
Dissociator { gas flow (cm^3/s)	0.2	9	45
Dissociator { frequency	14 Mc/s	200 Mc/s	14
Stern Gerlach { gradient (at pole tips) kgauss/cm	10	85	8.5
Atomic beam at the ionizer I/s	2×10^{12}	10^{16}	5000
Ratio $\frac{\text{I atoms}}{\sigma\ cm^2}$ at the ionizer (in $10^{15}/cm^2/s$)	.5	30	60
Ionizer efficiency	3×10^{-5}	2×10^{-3}	70
Ionization volume emittance	?	?	few orders of magnitude

Table I

Surely many sources might be improved, but let us not forget that the existing sources were built during a period of six years, and that it is difficult to improve something when physicists do not wish to stop experiments for the benefit of technology. It is the reason why I will not make comparisons. I prefer to make some general remarks, even if they resemble a science-fiction point of view, and try to define the best "classical" source we can obtain at the time being and what we could hope for in the near future. It is more a catalogue of questions than a recipe...

3.2 What is the "best" source ?

a. Concerning the polarization [8], I believe it is possible to find a unanimous point of view.

The protons can be 100 % ($\pm$) polarized by the adiabatic passage method using two RF transitions. It is the maximum we can do ! Only the problem of residual unpolarized protons remains, but it is less and less important...

The optimum solution for deuterons is found between : i) the possibility of obtaining the 3 pure states (0, +1, -1) ; ii) the pos-

sibility used in Saclay of obtaining :

$$\begin{cases} P_V = \pm\ 2/3 \\ \text{(2 states in} \\ \text{sequence)} \end{cases} \quad \text{or} \quad \begin{cases} P_{33} = \pm\ 1 \\ P_V = \pm\ 1/3 \\ \text{(4 states in sequence)} \end{cases}$$

Physically both choices seem equivalent.

For a primary atomic beam of intensity (I), the product IP^2 corresponds theoretically : i) in the first case to 2/3 I x 1 ; ii) in the second case to I x $(2/3)^2$.

But the necessity of using two Stern-Gerlach fields in the former will reduce the final intensity by chromaticity. The net results are equivalent but the second one is more flexible, and I shall not hesitate to say that our system is the best. Of course, more modest solutions can be used.

b. Another point is obvious concerning the Stern-Gerlach magnet. Sextupole fields seem to be a little better than others. We may be in disagreement concerning the best optics, but it is sure that, keeping all other parameters fixed, if we can increase the magnetic field at the pole tips, say by a factor k^2, then changing only the aperture radius by a factor k increases the entrance solid angle by k^2 and also the intensity.

Question : Magnetic fields at the pole tips (for usual dimensions) are limited to ~ 10 kilogauss. Can we hope to realize in the near future for instance, superconductive sextupole magnets with, say, 40 kG ?

c. Can we still improve the absolute intensity of the atomic beam and optimize the focusing properties of the separator ?

Concerning the dissociator, it seems that the upper pressure limit is not due to wall but to volume recombination. This limit would be around 5 torr, a value which has not been reached up to now. Pumping is not yet a limitation as we saw in Saclay around ~ 1 torr If stronger cooling is possible, some increase in intensity is obtainable.

The comparison between "nozzles" and "collimators" for the injectio: of the atoms does not indicate any great advantage of one system over the other (nozzles are a little more favourable at higher pressures, collimators at lower pressures). This "object" source is a part of the optical set - "injection - separator - useful volume of the ionizer" - for which optimization is complex. A detailed knowledge of the different parameters of the usual ionizers would be necessary. The adjustment between the atomic beam optics and the ioni·

zer is difficult, the final quality being a function of the number of atoms $dI/d\Omega$ emitted near the axis, of the separator solid angle $\Delta\Omega$ and magnification, chromatic dispersion, useful volume, and efficiency of the ionizer and of the ion extraction. Unfortunately all these parameters are only roughly known and interdependent.

d. The ionizers seem to be possibly improved according to the axial-strong magnetic field method [6,7], first used at Auckland, Rutherford and Birmingham. Ionization efficiencies near 10^{-3} can be reached, with beam emittances suitable for cyclotrons or Van de Graaff tandems.

If no large developments are made for the ionization, the maximum increase we can hope for the classical source "figure of merit", would not be more than an order of magnitude.

e. The injection of polarized protons or deuterons can also be improved in many cases. I think especially of circular machines for which this problem is not trivial.

The ionization in flight at the centre of the machine which seemed to be a few years ago the only safe way, is no longer suitable. Atomic density, ionization volume and efficiency are very small and the technology is not simple. Just now, the way is to ionize outside and to use one of the few methods suggested to inject the ions correctly at the centre. Essentially, two methods prove to be useful.

W.B. Powell [9] gave at Gatlinburg a very detailed paper on the so-called "axial injection", i.e. through a pole piece of the machine. The results obtained at Birmingham are quite good : a 6 % over-all efficiency is obtained from source to full radius. Let us point out by the way, the usefulness of the bunching already realized at Birmingham, which can increase the final intensity by a factor $2 \sim 3$ by concentrating the ions into the phase acceptance of the cyclotron.

Another method, the so-called "trochoidal injection", is used in our laboratory at Saclay. The particles are injected in the medium plane and the magnetic force is compensated at every point of the path by a transverse electric field [10]. Such a system (fig. 7) has good focusing properties. The measured efficiency in a magnetic model (9 kG over a length of 80 cm) was of the order of 30 %. The over-all efficiency (from source to full radius) should be comparable to the Birmingham one. The axis of the polarized source is now vertical. Ions are deflected into the medium plane.

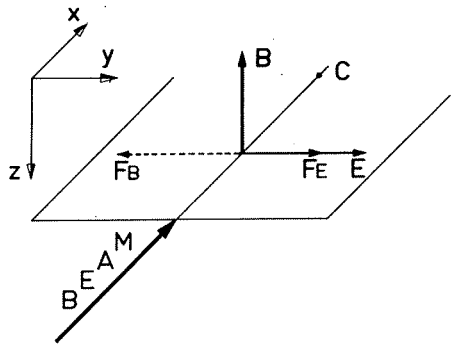

Fig. 7

3.3 Related topics and news from various laboratories

For people who desire to convert an H^+ polarized beam into a H^- beam, let us refer to the work originated in the laboratory of Donnally and carried on at Yale, which indicates an excellent efficiency of the charge exchange process $H^+ \rightarrow H^-$ using potassium or caesium vapours. The measurement of Donnally [11] for Cs and K give respectively 10 % and 11 % maximum efficiency (around 700 eV). Drake and Krotkov [3] at Yale have found an efficiency of ~ 25 % with Cs. This discrepancy is not yet explained to my knowledge.

Similar measurements were made recently by Donnally [11,12] with helium, indicating the possibility of charge exchanging $He^+ \rightarrow He^-$ with an efficiency of a few per cent by collisions with alkali atoms. This may be useful to convert $(^3He)^+$ polarized ions.

There are a few news items I received recently from various laboratories :

a. A new proposal is made by Donnally [12] to polarize ^3He by picking up polarized electrons from alkalis polarized by optical pumping.

b. Dickson sent me the "figure of merit" of the accelerated Rutherford-Linac polarized beam : 7×10^8 protons per second and 62 % polarization (best performance). This improvement is due essentially to their new ionizer.

c. At Zurich (ETH tandem) a polarized deuteron beam of 0.26 μA was observed after the ionizer (electron bombardment) with a measured tensor polarization $P_{33} \pm 0.77$. At Grenoble, 0.1 μA (D) was recently observed.

d. Craddock sent me from Vancouver the results they obtained at 4° K for ^{3}He. The measured beam is much lower than they expected. They are trying to optimize the "thermodynamics" of their system.

e. At Erlangen [13] a very good idea is being developed to measure the absolute polarization of a low energy H^+ beam. Using the Cs cell of Donnally, they propose to transfer $H^+_{(polar.)} \rightarrow H^0_{2S}$ and by selective quenching at different magnetic fields, the relative yields of polarized Lyman-α radiation can give with a good accuracy, the polarization of the initial beam.

f. I received just a few days ago a Progress Report from J.L. McKibben et al [14] which describes a more promising method to obtain polarized H^-, by using axially oscillating electric fields coupling (α) and (β) states (2S). This solution seems to be an elegant way to polarize protons or deuterons.

g. Concerning our system at Saclay, the last results obtained with the new ionizer is ~ 2.5 μA, but as they performed this measurement last friday, I do not know yet the emittance of this beam.

The figure 8 shows the new ionizer and figure 9 the new vertical set up of the source near the 29 MeV cyclotron.

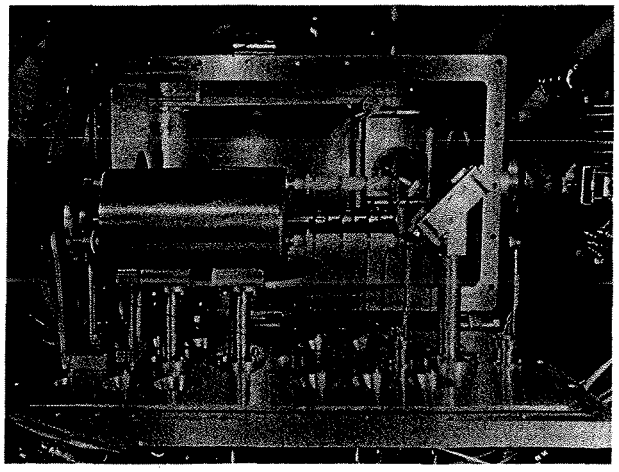

Fig. 8

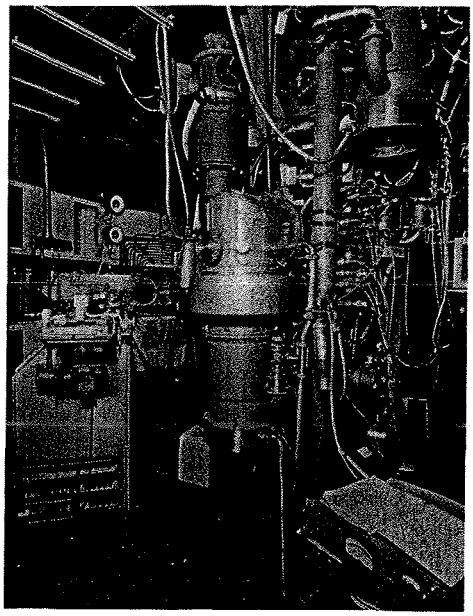

Fig. 9

4 DEPOLARIZATION

Is it necessary to investigate this question ? Nobody ever saw any depolarization effect in machines accelerating polarized particles [6]. Difficulties seem to appear for high-energy machines. But here arises another question : is it really useful to accelerate polarized protons up to very high energies ? One can compare roughly final intensities obtained by scattering (with a definite $\Delta p/p$ for the scattered beam) and by accelerating polarized particles by plotting two curves as functions of the final wanted energy : one is the ratio :

$$\frac{\text{Ejected ions}}{\text{Injected ions into the machine}}$$

which is strongly decreasing. For instance at CERN as high instantaneous proton currents as $\geq 10^{18}$/s are injected, and the final current is $\sim 3 \times 10^{11}$/s, at 20 GeV. From a polarized ion source, no more than $\sim 10^6$ protons/s can be expected at full energy. On the other hand the number of scattered protons with a definite $\Delta p/p$ increases with the energy, and beams of 10^8/s protons elastically scattered at 20 GeV can be obtained. There is a "crossing point" beyond which, at the time being, it is not useful to accelerate polarized protons if scattered protons at such high energies are polarized. The polarization measurements made by Borghini et al [14] indicate that polarization is ~ 10 % at 12 GeV in p-p scattering, and there are good theoretical arguments to expect more polarization in scattering protons on complex nuclei. Where the crossing point stays is not easy to be estimated. This point will be drifted to higher and higher energies as the ratio ejected/injected ions and (or) the polarized beams will be more and more increased.

For intermediate energies (100 MeV $\rightarrow$ few GeV), and especially for synchro-cyclotrons, the acceleration of a polarized beam remains of interest.

It is well known [16] that depolarization effects are of two kinds. In both cases one studies, in the proper reference system of the particle, the transverse oscillating components of the magnetic field which are able to induce some flipping of the spin by inducing resonances at the rotation frequency of the proton magnetic moment.

The first effect (so called imperfection resonances) is due to a lack of azimuthal homogeneity of the main magnetic field inducing oscillating components independently of the trajectories. Such defects must be (and can be) compensated to $\sim 10^{-4}$.

The second one (intrinsic resonances) is due to components seen by the particle which oscillates around the equilibrium orbit with intrinsic frequencies ν_Z, ν_R. The resonances are found by the formula :

$$\omega p/\omega c = \gamma \left(\frac{g}{2} - 1\right) = k + l\nu_Z + m\nu_R$$

where k, l, m are integers. The depolarization value is found by calculating the final component of P perpendicular to its initial value. I found recently a paper where a computation was made for the first resonance (around 110 MeV) for the CERN synchro-cyclotron. The author found a 24 % horizontal component and concluded that "...depolarization was not negligible and that it would be difficult to go through the many existing resonances...". But let us notice : i) that a (0.24) horizontal component corresponds to a vertical residual polarization of $1 - (0.24)^2/2 \sim 97.1$ % ; ii) that this value was calculated for an extreme oscillation amplitude. If we take the mean value over the amplitudes squared, the residue is $\gtrsim$ 99 %. Even if we have to go through many resonances, the situation is not catastrophic !

One can also improve things : i) by injecting fewer particles with a better emittance ; ii) by improving the machine itself, increasing for instance the Dee-voltage (shortening the transit time through the resonances), or the focusing near the centre of the synchro-cyclotron. Other computations [7] were made for synchrotrons. The situation is more complicated, but computations made for existing machines like those of Cohen (ZGS machine at Argonne) show that by improving the focusing system (i.e. adding pulsed quadrupoles) one can still conserve 70 % of the initial polarization at 12 GeV.

My conclusion is as follows. It is evident that low energy physics will demand more and more intense polarized beams. Intermediate energy machines could be equipped with polarized sources and provide for a renewal of interest (I am especially thinking of old machines). That this would be useful for very high-energy machines remains to be proved and the technical difficulties for such machines will delay the solution until physicists think of the high-energy polarized proton as a wonderful, powerful and strongly necessary physical instrument.

References

1) G.C. Phillips, these Proceedings, p. 215.
2) B.L. Donnally et al, Phys. Rev. Letters, 1964, 12, 502.

3) C.W. Drake, Jr and R.V. Krotkov, International Conference on Isochronous Cyclotrons, Gatlinburg (1966).
4) J.L. McKibben and G.P. Lawrence, Proceedings of the 2nd International Symposium on Polarization Phenomena, Karlsruhe (1965).
5) A. Abragam and J.M. Winter, Phys. Rev. Letters, 1958, 1, 325. A. Abragam and J.M. Winter, Compt. Rend., 1962, 255, 1099.
6) M.K. Craddock, International Conference on Isochronous Cyclotrons, Gatlinburg (1966).
7) J.M. Dickson, Progr. Nucl. Techn. Instr., 1965, 1, 105.
8) R. Beurtey, Proceedings of the 2nd International Symposium on Polarization Phenomena, Karlsruhe (1965).
9) W.B. Powell, International Conference on Isochronous Cyclotrons Gatlinburg (1966).
10) R. Beurtey et al, International Conference on Isochronous Cyclotrons, Gatlinburg (1966).
11) B.L. Donnally, Private communication.
12) B.L. Donnally et al, (to be published in Phys. Rev. Letters).
13) G. Clausnitzer and D. Fick, Nucl. Instr. Methods, 1967, 47, 171
14) J.L. McKibben et al, Private communication.
15) M. Borghini et al, (to be published in the Proceedings of the International Conference on High Energy Physics, Berkeley (1966
16) W.B. Powell, Proceedings of the 2nd International Symposium on Polarization Phenomena, Karlsruhe (1965).

SOME GENERAL PROBLEMS IN PRODUCING DENSE POLARIZED ^{3}He TARGETS

T.R. CARVER
Palmer Physical Laboratory, Princeton

In this conference which is concerned with the why and the how of polarized targets it is not clear why I should discuss a kind of target which hasn't yet been made -- a dense gaseous or liquid ^{3}He target suitable for high energy scattering physics -- when the next two contributors, Walters and Phillips, will discuss how to make a ^{3}He target suitable for low energy physics. Perhaps the best reason is that the problems and techniques to do with ^{3}He are so very different from those already discussed, involving dynamic polarization in crystals at low temperatures, that an introduction to the subject is useful and perhaps stimulating.

Why ^{3}He ? If the spin 1/2 nucleus of ^{3}He were polarized, what one would have is a polarized neutron with two unpolarized spectator protons. This is uniquely different from what has already been discussed. This nucleus is enclosed by two electrons in a $^1S_0$ configuration and is well protected from rapid nuclear spin relaxation, even at room temperature. The excited states of these atoms are so far above the ground state, at least 19 eV, that in collisions there is little spin-orbit interaction or polarization to cause nuclear relaxation. Since ^{3}He is an atom there is no rotational nuclear interaction such as is present in H_2 leading to an unfortunately short relaxation time in that gas. Finally, the light mass of ^{3}He results in very short correlation times for collisions and other interactions and therefore leads to very small effective fields for relaxation effects. As a consequence one may expect that the relaxation time arising from the Bloembergen, Purcell and Pound type of relaxation would be about 10^6 seconds for an STP gas (density 1 amagat) and about 600 seconds for the liquid at 1 atmosphere. These long times have not been observed, but relaxation times of about one order of magnitude shorter have been observed by our group and many others. Relaxation seems to come from wall and impurity effects. Thus, for such a slowly relaxing system, it is tempting to think that some

clever techniques for dynamic polarization might be employed to provide large scale polarization in a liquid, or especially in a compressed sample of room temperature gas. To employ such a target in an electron scattering experiment in the manner of Hofstadter [1], a sample of about 1 cm^3 or 1 in^3 at a density of 100 amagats would be very satisfactory. Or it is possible to imagine that a polarized ^3He bubble chamber is not completely unrealistic. Or perhaps the idea of a compressed flask of pre-polarized ^3He gas, which would not relax for a day or so. However the situation is not really so simple : the speaker will list some approaches that have been made to this problem.

1. The technique of brute force polarization must be mentioned in this case. Choosing a maximum convenient field of 100 kilogauss and a minimum convenient temperature of 1° K, it will be found that ^3He nuclei are polarized to about 1 %, or P = 0.01. It is presumably rather easy to reach a temperature at least 20 times lower than this. However, the Fermi-Dirac properties of ^3He place its degeneracy temperature rather close to this point, and any further reduction in temperature will only produce a maximum polarization of about 4 % [2]. This remains approximately true even if one considers the ^3He to be in a ^3He-^4He dilution refrigerator, and the advantages of polarization would, in any case, be mostly removed by this dilution with ^4He.

2. It was thought by several groups that one should be able to dynamically polarize the liquid in contact with paramagnetic materials. Such experiments were tried by Carver and Van der Ven [3], by Walters [4], and by Redfield while at Saclay using a variety of substances such as crystals of DPPH, coatings of DPPH, coatings of lithium metal on the walls and on glass wool, and charred sugar in which a narrow electron resonance line may be observed and saturated. The nuclear magnetic resonance of ^3He could be used as a most sensitive detector of any enhanced polarization and the experiment are in agreement that no effect at all is observed. In some cases it was not clear that the ^3He relaxation time was actually altered by these substances, in other experiments it seemed as though it must have been. None of us have had any definite ideas as to the cause of the lack of an effect. Whether a dipole-dipole interactio doesn't work because of a great distance from nuclei to paramagnet or whether an absorbed film of effectively solid ^3He blocks the interaction, or whether there is too little of adequately high frequencies of fluctuating thermal fields to cause transitions are po sible reasons. In addition to experiments of a conventional Overhaser type, there were also carried out experiments of the "effet solide", in conditions where the electron and nuclear lines could be resolved, but with equal lack of success.

3. The first successful dynamic polarization effect in ^{3}He was in the gas [5]. The paramagnetic impurity dissolved in the gas was the vapour of rubidium metal. Rather than saturating the paramagnetic resonance associated with the spin and Bohr magneton of the rubidium atom, the atom was polarized by optical pumping. Rubidium is particularly useful, as originally found from experiments at Princeton, for optical pumping because the isotope shifts of the isotopes 85 and 87 lead to a broader optical absorption line and the light of one isotope can be absorbed by the other, leading to much less trouble from self reversal. Moreover, the spin-orbit interaction is large and makes it convenient to employ a simple D_1 (reject D_2) interference filter which is needed for optical pumping in a high pressure of buffer gas. Thus rubidium may be pumped virtually to 100 % under ideal conditions, and to 20 or 30 % even with several atmospheres of helium, as a buffer gas.

It was found to be possible to increase the nuclear polarization of ^{3}He from the $1:10^8$ initial polarization to $1:10^4$ which is a most impressive enhancement of 10^4. However, the absolute polarization is .01 % which is not adequate for the purposes under discussion. This type of enhancement actually seemed to work best in the 4 atmosphere samples which were the maximum pressures tried, and the polarization times were between 1000 and 2000 seconds.

This mechanism was first thought to be smaller than expected, and then after further thought to be larger than expected. When finally the sign of the effect was correctly measured it also appeared to correspond, not to the I_+S_+ or I_-S_- or "flip-flip" type of interaction, but rather to the "flip-flop" interaction to be expected from an I.S scalar interaction. These problems were brought to a better resolution through the work of Herman [6] who had calculated the opposite process, the relaxation of optically pumped vapours by ^{3}He, and indeed there exists a scalar mechanism with a cross-section of about 10^{-25} cm^2 or larger, in contrast to the direct dipolar interaction between the nuclear moment of ^{3}He and the electron of Rb of 10^{-27} cm^2 [7].

It is easy to see why this very valid and potentially useful polarization interaction does not give sufficiently large polarizations. Instead of having about one rubidium atom to polarize about one million helium atoms, at the working range for optical pumping of 10^{-5} or 10^{-6} torr and a helium pressure of several atmospheres there is only one rubidium atom for each billion (10^9) helium atoms. It should not, in principle, be difficult to make this ratio more favourable, but unfortunately it is not possible to do optical pumping in a direct manner at higher pressures because, when the alkali vapour becomes more dense, the photons cannot be absorbed throughout the sample but only at the surface. Pumping at higher pressures has been found to be possible by mixing two alkalis such as rubidium or potassium with sodium. Optical pumping on the sodium results in the

transfer of polarization by spin exchange to the rubidium whose vapour pressure is two orders of magnitude higher [8]. We have tried preliminary experiments to use sodium and have made a most efficient Zeeman effect D_2 filter for the purpose [9], but the results in this case have been unsatisfactory because of the fact that the higher temperatures in the use of the sodium seem to result in browning of the glass sample cells and a drastic reduction of the ^{3}He nuclear relaxation time due to collisions with the presumably contaminated and paramagnetic Pyrex walls. It is clear that further work must be done in finding a suitable cell material for ^{3}He samples. Our experiments have shown that it is possible to coat the walls of a container with sufficient paramagnetic impurities so that the ^{3}He relaxation time becomes actually as short as the diffusion time of the atoms to the wall.

4. Since the next two speakers will deal in detail with the question of optical pumping of ^{3}He [10], I shall restrict my discussion to the possibilities of using this technique to produce a dense target. Suffice it to say that the $^3S_1(1s,2s)$ metastable state of He may be used as a "pseudo" ground state for optical pumping usin 10,830 Å light to couple to ^3P states. The resulting hyperfine-cou pled nuclear polarization of this state is left behind in the grou state after a collision of the type :

$$^3He(^3S_1)_{pol} + {}^3He(^1S_o)_{unpol} \longrightarrow {}^3He(^1S_o)_{nucl.pol.} + {}^3He(^3S_1)_{unpo}$$

which form of metastability exchange collision [11] is very similar to a spin exchange collision between two atomic hydrogen atoms, by virtue of the fact that these two helium states can form a $^3\Sigma_u$ molecule. Thus ^{3}He has been polarized in volumes of 100 to 2000 cm^3, at pressures from 100 microns to 5 torr, to polarizations from 10 to 50 %, in times ranging from 10 seconds to 10 minutes [10,7]. For example, we have polarized a 60 cm^3 sample at 1 torr to about 50 % polarization in 30 seconds and have polarized a 2 liter sample at 1.5 torr to 12-15 % polarization in about 800 seconds, which last figure was also the intrinsic relaxation time of that sample in the bulb and magnetic field used.

Can such samples be compressed or liquified ? Obviously yes, in principle. However, to achieve good polarization of the gas sample more than 100 seconds is required. Taken together with the fact that the liquid sample may relax in less than this time, and the large density ratio between liquid and gas, this would imply that about 10 liters of gas would be required to support 1 cm^3 of liquid in principle, and it is probable that diffusion difficulties and wall relaxation effects would actually result in the inability to have a polarization as great as 5 % anyhow.

A better bet would be compression of the polarized gas. Here the question is somewhat the same as for liquefaction. However, one must also find a simple high compression pump that doesn't add wall or bulk impurities whose effect (like that of pump oil, for instance) can reduce the nuclear relaxation time of the ^{3}He to less than 100 seconds in the high pressure sample. The use of mercury as a possible pump has been investigated at Princeton, and does not affect the relaxation time too severely at first if not dispersed as droplets. It can also be used in the optical pumping cell without causing quenching of the metastable atoms, providing it is kept at a temperature just above the melting point where the vapour pressure is less than 10^{-5} torr. However, these difficulties become greatly enlarged in practice, and are likely to prevent a practical continuously pumped operation, even though single shot compression may be satisfactory.

5. The effect of relaxation by field inhomogeneities is important in any aspect of ^{3}He gas polarization. It is somewhat unique since it is not observed in other more rapidly relaxing systems or in solids and liquids. Such a slowly relaxing system will find that the principle source of nuclear relaxation will be the inability of the moving nucleus to completely adiabatically follow the magnetic field in which it is placed -- sort of a gradual Majorana flip [12,13,7,10].

A useful derivation of this effect is so simple to make that it can be described here [7]. Imagine a nuclear spin travelling with velocity v more or less perpendicular to a field $\vec{H}$ which has a gradient $\partial H_\perp/\partial x$. As the nucleus moves it appears to see the field change its direction with a precession frequency $\Omega = v[(\partial H_\perp/\partial x)/H]$. In the frame of the nucleus this appears from simple mechanics of resonance as an effective field Ω/γ, where γ is the nuclear gyromagnetic ratio. The nucleus, of course, then precesses about the vector sum of $\vec{H}$ and $\vec{H}_{eff}$. All would be well were it not for the fact that the nucleus will change its direction of motion randomly and intermittently when it suffers collisions. Thus the effective field operates to cause a random loss of memory of precession direction. Using a random walk argument where the precession away from the H direction is $\theta = \Delta\theta\sqrt{N}$, where N is the number of steps, we take $\theta = 1$ for relaxation, $\Delta\theta = \gamma H_{eff} t$, where t is the time between collisions, and the number of steps, in a relaxation time, $N = T_1/t$. Introducing a mean free path by eliminating $t = \lambda/\vec{v}$, and combining all the simple foregoing relations, one finds that the relaxation rate is just :

$$1/T_1 = \vec{v}\,\lambda[(\partial H_\perp/\partial x)/H]^2 \quad .$$

Thus if one considers one atmosphere of ^{3}He which has a mean free path of 10^{-5} cm and a velocity of 10^5 cm/s, it would relax in one second if placed in a field with a "directional gradient" of 1 radian/cm. Indeed we have found that this is the case [7,12]. Obviously, the relaxation rate is 1000 times greater than this in the optical pumping range of 1 torr and considerable care must be exercised in the magnetic field environment of an optically pumped target.

A slightly more sophisticated classical argument, or a transition probability argument, shows that the relaxation rate is given in general by :

$$1/T_1 = \vec{v}\,\lambda\left[(\partial H_\perp/\partial x)/H\right]^2 \frac{2}{1+\omega_o^2 t^2} \quad ,$$

but the simpler upper equation describes the situation in the relevant range for optical pumping and compression.

Some thought was given to the idea that this inhomogeneous relaxation could be used like a ratchet [12]. That is, a pulsed field could be applied to a sample or a portion of a sample. While the field is on so are the accompanying gradients ; so the sample will rapidly relax to the volume averaged field that the sample sees weighted by the relaxation rate, which is, of course, greatest where the field and its gradient are greatest. Thus a pulsed field, which can be made larger than a static field, can be used and the sample will gradually achieve a Boltzmann polarization characteristic of the maximum field present during the pulse. However, tempting as this sounds, putting in practical numbers seems to indicate that it would not be possible to obtain more than about 1 % polarization at several atmospheres at room temperature and that compensating difficulties in going to lower temperatures would not increase this polarization appreciably.

6. The possibility that <u>discharges in a gas</u> of <u>^{3}He</u> might lead to dynamic polarization effects was considered earlier, and tried with some indications of success [7,12]. I report very recent and as yet unpublished experimental work carried out by Gene H. McCall which indicates a large, unexpected effect with some interesting features. In these experiments a Pyrex bulb of ^{3}He gas of volume of about 60-100 cm^3 and a pressure ranging from 2 to 35 cm of Hg pressure is placed between the poles of a fairly homogeneous electromagnet with a field ranging from 0 to 9 kilogauss. An electrodeless discharge is maintained using an RF generator, a Tesla coil discharge, a microwave diathermy discharge ; or in some bulbs a DC discharge is maintained between internal electrodes inside the bulb. After 10 to 100 seconds of discharge the bulb is removed to a low field sensitive nuclear resonance apparatus which is used, as in the other experiments reported here [5,7,10], to determine the nuclear polarization that is ultimately produced.

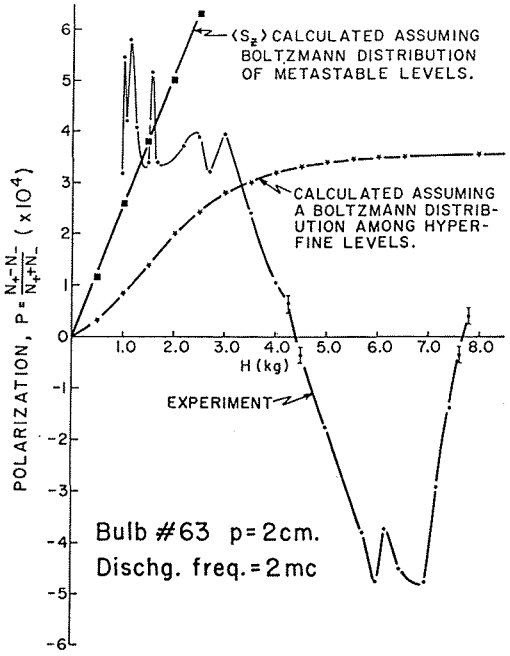

Fig. 1

Figure 1 shows the polarization which is achieved as a function of the magnetic field in which the bulb was placed while the discharge was maintained. There is some detailed and still unexplained structure in this curve which is reasonably reproducible. The polarization shown above the axis is enhanced nuclear polarization in the positive spin temperature sense, and the values below the axis represent an inverted or negative temperature polarization. The maximum polarization obtained of about 0.06 % occuring between 1 and 2 kilogauss represents an enhancement of more than 2000 times the nuclear polarization Boltzmann distribution at that field. Should it be true than an enhancement of nuclear polarization of that size would still appear at a field of 100 kilogauss and if it were still possible to produce such an effect at a temperature of 77° K, for example, then the resulting polarization would be in the range of 20 % and rather usefully interesting. However, we have not yet been able to avail ourselves of a suitably homogeneous superconducting solenoid of sufficient volume to carry out experiments at higher fields. It is particularly interesting to note that just below 8 kilogauss the spin temperature returns to the positive sense.

Shown on the graph are two other suggestive lines. The heavy line with solid squares shows the Boltzmann polarization of the electrons in the $^3S_1$ metastable state in the applied magnetic field.

The dotted line with stars shows the nuclear polarization in a hyperfine coupled $^3S_1$ metastable state of ^3He in thermal equilibrium with the magnetic field. At higher fields this curve flattens out in the region where the nucleus becomes decoupled from the electron spin. Specifically, if the discharge were to produce metastable states which come to thermal equilibrium with the magnetic field, and if the resulting nuclear polarization were transferred to the ground state by the same type of metastability exchange [11] which is important in the optical pumping process mentioned in 4, then this starred curve would represent the final nuclear polarization in the ground state. Obviously a more complicated mechanism is operating, but it is our belief that it is probably superposed upon the effect just described. We believe that the polarization mechanism is operating in some way through dynamic polarization or scattering polarization involving the metastable state. One reason for believing so is that the introduction of small amounts of impurities such as mercury vapour at 10^{-2} or ^{3} torr, which is known to quench out the metastable state and to spoil optical pumping in helium, also causes this discharge polarization to become very small. Also it is highly suggestive that the real peak in the polarization enhancement at 1.6 kilogauss occurs at the field in which there occurs a level crossing in the hyperfine structure of the $^3S_1(1s,2s)$ metastable state of ^3He.

At higher pressures, beyond 35 cm, there remains a similar effect in which there may still be an enhancement of as much as 800. However, the details of figure 1 become blunted and the sharp peaks are less in evidence. What type of discharge is used seems to make very little difference with one exception. At higher pressures a steady discharge always produces positive polarization. However, when a Tesla discharge characterized by sharp ringing bursts of power is used, then the higher pressure bulbs also show negative spin temperature above 4 or 5 kilogauss.

We have suggested that a resonance effect may be superposed on a normal thermalization of the metastable state polarization. It is also possible that different mechanisms operate in opposition. Some evidence for this is suggested by the fact that the use of a temperature of 77° has a pronounced effect on reducing the positive enhancement, but almost none on the negative temperature enhancement.

7. No work to my knowledge has been done on the question of dynamic polarization of solid ^3He. To the other difficulties intrinsic to low temperature dynamic polarization, it seems rather prohibitive to add the difficulty of maintaining the sample in a pressure cell at 40 or more atmospheres and still have a simple target. Another difficulty is that there is no clear way to add paramagnetic ions to the ^3He other than by radiation damage. However, it is

known that the relaxation time of the nuclei in the solid is very long, so that it should be investigated as a possibility.

In conclusion it can be seen that quite a number of interesting mechanisms for polarization of ^{3}He have been explored, and it is surprising that so much may be done with such a simple system. In spite of this description of failure to produce a really dense target, it should not be thought that other applications do not exist for this work, or that, as a consequence, little interesting physics has been developed.

References

1) H. Collard and R. Hofstadter, Phys. Rev., 1963, 131, 416.
2) W.M. Fairbank, W.B. Ard, H.G. Dehmelt and W. Cordy, Phys. Rev., 1953, 92, 208.
W.M. Fairbank, W.B. Ard and G.K. Walters, Phys. Rev., 1954, 95, 566.
3) N.S. Van der Ven, "Dynamic Polarization in Liquid Helium Three", Ph.D. Thesis Princeton University, 1962 (unpublished).
4) G.K. Walters, Symposium on Liquid and Solid Helium-3, Proceedings of the 2nd Symposium, p. 37 (Ohio State University Press, Columbus, Ohio, 1960).
5) M.A. Bouchiat, T.R. Carver and C.M. Varnum, Phys. Rev. Letters, 1960, 5, 373.
6) R.M. Herman, Phys. Rev., 1965, 137, A1062.
7) T.R. Carver and L. Gamblin, Phys. Rev., 1965, 138, A946.
8) M.A. Bouchiat and T.R. Carver, Proceedings of the Ann Arbor Conference on Optical Pumping (Ann Arbor, Michigan, 1959, p. 35).
9) T.R. Carver, F.R. Lewis, E. Pollock and G. Schrank, Rev. Sci. Instr., 1961, 32, 861.
10) F.D. Colegrove, L.D. Schearer and G.K. Walters, Phys. Rev., 1963, 132, 2561.
11) R.A. Buckingham and A. Dalgarno, Proc. Roy. Soc., 1952, A213, 327 and 506.
12) T.R. Carver and R.L. Gamblin, Bull. Am. Phys. Soc. II, 1964, 9, 11.
13) L.D. Schearer and G.K. Walters, Bull. Am. Phys. Soc. II, 1964, 9, 11 ; 1965, 10, 74.

POLARIZED ^{3}He TARGETS AND ION SOURCES BY OPTICAL PUMPING

G.K. WALTERS
Rice University, Houston

I INTRODUCTION

Since the original suggestion of Kastler [1], optical pumping methods have been used to orient the magnetic moments of a number of atomic species, including mercury and most of the alkali metals. These experiments have led to significant advances in precision atomic structure determinations, but the densities of the species so oriented are far too small (of order 10^{10} to 10^{12} atoms per cm^3) for practical nuclear targets.

In 1957, however, Dehmelt [2] demonstrated that optically-induced orientation can be transferred, during collisions involving electron exchange, from the optically-pumped species to other unpumped constituents of the sample. In the case of ^{3}He, the combination of optical pumping and electron exchange can be exploited to produce significant nuclear spin polarization in samples with densities several orders of magnitude greater than could be polarized by optical pumping alone [3,4]. In the following section, the principles of ^{3}He spin polarization by optical pumping and electron exchange are presented.

Section 3 deals with design criteria and fabrication techniques for polarized ^{3}He targets suitable for use in nuclear scattering experiments. Limitations of presently operational targets are discussed, as are prospects for improved higher-density gas and liquid ^{3}He targets.

Current experiments directed toward realization of a polarized ^{3}He$^+$ ion beam are described in section 4. Also discussed briefly is a feasibility study for possible exploitation of optical pumping in helium to produce high-intensity polarized electron beams.

II POLARIZATION OF ^{3}He GAS BY OPTICAL PUMPING

If a weak electrical discharge is maintained in helium gas at a pressure of a few torr, there results a steady state distribution in which the population of the metastable 2^3S_1 state (ground state of orthohelium) is about 10^{10} to 10^{11} per cm^3. Atoms in this state can be spin-polarized by optically exciting transitions to the 2^3P states with circularly polarized resonance radiation from a helium discharge lamp, the pumping cycle being completed by spontaneous decay from the 2^3P states back to one of the 2^3S_1 Zeeman sublevels. A weak magnetic field is applied along the pumping light axis to provide a unique axis of quantization. The pumping light introduces net angular momentum into the atomic system by virtue of the selection rule $\Delta m = +1$ (for right-hand circular polarization) on the change in magnetic quantum number in the $2^3S_1 \rightarrow 2^3P$ transitions.

Optical pumping of ^{4}He was first reported by Colegrove and Franken [5], and these studies were later extended by Schearer [6]. Because of the nuclear spin $I = 1/2$, the optical pumping process in ^{3}He is distinctly different from that in ^{4}He. In each case, the pumping light tends to produce spin-polarization of the 2^3S_1 atoms however, in the case of ^{3}He, collisions involving excitation transfer between 2^3S_1 atoms and ground state atoms :

$$He(2^3S_1) + He(1^1S_0) \rightarrow He(1^1S_0) + He(2^3S_1) \qquad (1)$$

are effective in transferring the optically induced polarization to the ground state. Spin angular momentum is well conserved in such a process, so that the incident and emerging ground-state ^{3}He atoms may have magnetic quantum numbers differing by ± 1, while the corresponding metastables differ in their magnetic quantum numbers by ∓ 1. (Clearly there is no counterpart to this process in the case of ^{4}He since the ground state is magnetically non-degenerate). As a result, the entire system of ground-state atoms, typically 10^6 times more dense than the 2^3S_1 atoms being directly pumped, become nuclear-spin polarized [3,4]. The attainable steady-state polarization is determined by balancing the angular momentum input from the pumping radiation against the angular momentum losses due to spin-relaxation processes in both the ground and metastable (2^3S_1) states. (The ground-state polarization $P = N_+ - N_-/N_+ + N_-$ where N_+ and N_- are the densities of spin-up ($m = +1/2$) and spin-down ($m = -1/2$) atoms, respectively). A schematic diagram of the angular momentum flow is shown in figure 1.

Figure 2 shows the pertinent ^{3}He energy levels and the transitions induced by the pumping light. The $2^3S_1 - 2^3P_2$ and $2^3S_1 - 2^3P_1$ transitions are spectroscopically unresolved, but the $2^3S_1 - 2^3P_0$ is

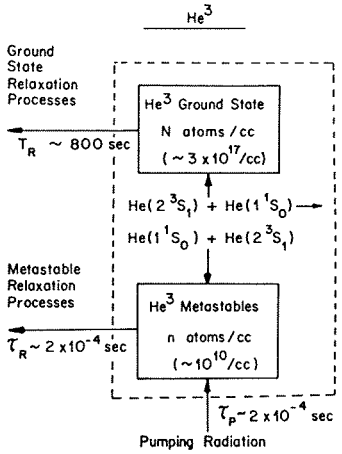

Fig. 1 Schematic diagram indicating the flow of angular momentum, via the 2^3S_1 atomic system, into the system of the ground state atoms. Angular momentum loss occurs as a result of spin-relaxation of ground state and/or metastable atoms.

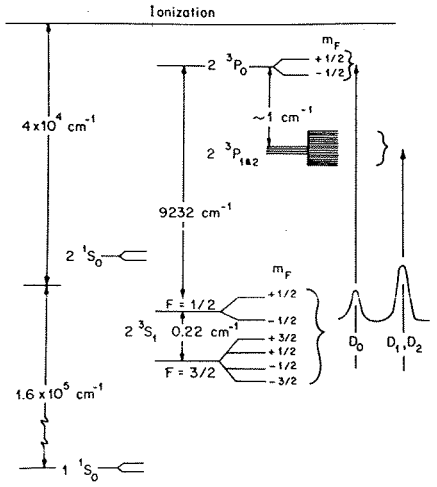

Fig. 2 Energy levels of ^{3}He atom in an external magnetic field (not to scale). Transitions labelled D_0 and D_3 connect the 2^3S_1 state to the 2^3P_0 and $2^3P_{1,2}$ (unresolved) states respectively.

well resolved from $2^3S_1 - 2^3P_{1,2}$. Thus the pumping transition consists of two components, designated D_0 and D_3 as shown in figure 2. An analysis of the pumping dynamics indicates that both D_0 and D_3 transitions are helpful in producing polarization for sample pressures sufficiently low that an atom excited by the pumping light to one of the 2^3P sublevels is unlikely to undergo a collision-induced transition to a different 2^3P sublevel before decaying back to the 2^3S_1 state. However at higher pressures, where such collisional-mixing in the P-states occurs, it can be shown that the D_3 component of the pumping light is actually detrimental to the polarization process [6]. Fortuitously, the isotope shift for the $2^3S - 2^3P$ spectral lines of helium is such that the D_3 transition in ^4He coincides with the D_0 transition in ^3He [7]. Thus a ^4He lamp pumps only the $2^3S_1 - 2^3P_0$ transition in ^3He, a desirable situation for relatively high ^3He sample densities. Figure 3 compares the pressure dependence of attainable polarization for ^3He and ^4He pumping lamps. The fall-off in attainable polarization at intermediate pressures using ^3He pumping suggests a P-state mixing cross-section of about 10^{-14} cm^2. Lamp pressure in the range 4 to 8 torr STP has been found to be optimum.

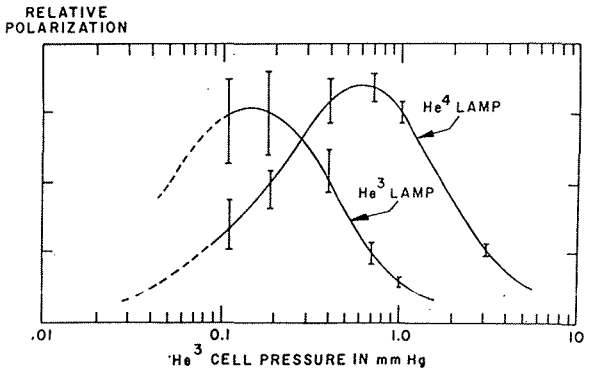

Fig. 3 Attainable ^3He polarization as a function of sample pressure for ^3He and ^4He pumping radiation. Sample is excited by 50 MHz electrodeless discharge.

The rapid polarization fall-off at higher pressures using ^4He pumping is not completely understood at present. This effect results from an increased rate of spin-relaxation in the ground state and/or in the 2^3S_1 metastable state, induced by collisions with undesirable constituents of the electrical discharge used to populate the 2^3S_1 state. The primary 2^3S_1 spin-relaxation mechanism is believed to be electron exchange collisions :

$$He(2^3S_1) + e^- \rightarrow He(2^1S_0) + e^- \qquad (2)$$

$$\text{or} \qquad \rightarrow He'(2^3S_1) + e^- \qquad (2')$$

where in the latter reaction the 2^3S_1 spin state is changed [8]. The visual appearance of the discharge changes markedly with sample pressure, and it is not unreasonable to suspect that both the electron density and energy distribution are pressure dependent. Also, it is observed at all pressures that the maximum polarization results when the discharge is run at the weakest level at which it can be sustained.

A possible ground-state relaxation mechanism results from conversion of atomic ions to molecular ions in the three-body reaction [9] :

$$He^+ + 2He \rightarrow He_2^+(^2\Sigma_u^+) + He \qquad (3)$$

followed by atom-ion interchange :

$$He_2^+(I,II) + He(III) \rightarrow He_2^+(I,III) + He(II) \qquad (4)$$

where I, II, III label the nuclear cores of the reactants. In the molecule, the nuclear spin is coupled to the electron spin, thence to the molecular rotation, by a combination of hyperfine and spin-rotational interactions ; the nuclear polarization presumably would be lost in rotational mixing collisions. Reaction 4) is thought to be responsible for the anomalously low mobility of the He_2^+ ion [10,11]. This spin-relaxation mechanism is currently being tested by adding small quantities of neon to the ^{3}He samples ; neon is known to be very effective in dissociating He_2^+ ions [12].

As a practical matter, we have observed a pronounced dependence of discharge character and of attainable polarization on the rf discharge excitation frequency. It can be seen from figure 4 that useful polarization can be maintained at considerably higher pressures using 500 kHz sample excitation rather than the 50 MHz used in our earlier studies [4].

The nuclear polarization P can be measured either by NMR techniques, using the thermal Boltzmann spin distribution of protons in water to provide a reference signal, or by optical methods. The NMR technique is more accurate and is generally used for most experiments ; however, this technique has not proven practical for use with operational polarized ^{3}He targets. Target polarizations can, however, be measured with about 20 % accuracy by the optical method.

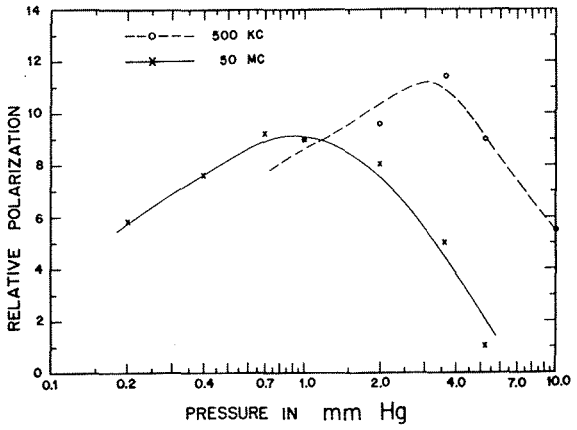

Fig. 4 Attainable ^{3}He polarization as a function of sample pressure for sample excitation by 50 MHz and by 500 kHz electrodeless discharge. Pumping radiation is from ^{4}He lamp.

The optical technique involves measurement of the change ΔI in light absorbed by the ^{3}He sample when it is polarized as compared to the absorption I_o when P = 0. The relation between P and I/I_o for ^{4}He pumping (D_o transitions only) is [4]:

$$\frac{\Delta I}{I_o} = \frac{P}{3 + P^2} \left\{ 6 - 2P - 3(1 - P)^2 \left[\frac{b + c - a}{a + b + c} \right] \right\} \qquad (5)$$

where a, b and c represent the relative absorption probabilities of the pumping light for the ($F = 3/2$, $m_F = -3/2$), ($F = 3/2$, $m_F = -1/2$) and ($F = 1/2$, $m_F = -1/2$) sublevels of the 2^3S_1 state, respectively. Though the pertinent electric dipole transition probabilities can be calculated with considerable confidence, there is uncertainty in the relative illumination of the $F = 1/2$ and $F = 3/2$ hyperfine components of the 2^3S_1 state by the ^{4}He pumping light. This problem is discussed in reference 4) and also in the paper by Greenhow [13]. Since the center-frequency and line breadth of the ($2^3S_1 - 2^3P_{1,2}$) ^{4}He spectral line used for pumping depends on such factors as the gas pressure in the lamp, method of excitation and lamp temperature, the appropriate weighting of the transition probabilities to give absorption probabilities a, b and c should ideally be established in each experiment by measuring the spectral profiles of the pumping radiation and polarized ^{3}He samples. Unfortunately, the high degree of spectral resolution required has so far precluded such measurements on polarized ^{3}He targets assemblies. However, the spectral profiles always fall between the limits corresponding to equal illumination of the $F = 1/2$ and $F = 3/2$ hyperfine components of 2^3S_1 on the one hand, and illumination of only the $F = 3/2$ component on the other hand. This places well defined limits on the a, b and c

factors, hence upon P. For equal illumination, a:b:c = 28:10:30, and for F = 3/2 illumination only, a:b:c = 28:10:o, so that :

$$P(15 - 10P + 3P^2)/(6 + 2P^2) \geqslant \frac{\Delta I}{I_o} \geqslant P(11 - 2P - P^2)/(6 + 2P^2). \quad (6)$$

Analysis of (6) shows that $P_{max}/P_{min} \leqslant 1.35$, so that if the polarization is taken to be the mean of the values P_{min} and P_{max} calculated from the two sides of equation (6), the uncertainty in P is always less than 20 %.

Experimental measurements of ΔI and I_o are made with a PbS photodetector that monitors the pumping light transmitted through the sample cell. Under typical operating conditions, only a small fraction (~ 2 %) of the pumping light is absorbed by the cell. I_o is determined by measuring the difference in light reaching the photodetector when the cell discharge is turned off (no 2^3S_1 absorbers) as compared to when the discharge is on and P = 0 (a small correction being made for the weak light emanating directly from the sample discharge). ΔI is the difference in light reaching the detector when the cell is polarized, as compared to when P = 0. The PbS photodetector incremental voltage output is approximately proportional to the change in light intensity in these measurements, so long as both I_o and ΔI are sufficiently small. The P = 0 condition can be established by applying a strong rf magnetic field at the ground state nuclear magnetic resonance frequency (ν = 3243 Hz/gauss), or, alternatively, simply by placing a small bar magnet in the vicinity of the sample cell. The latter method works because the extremely rapid ^{3}He spin-relaxation caused by magnetic field gradients effectively short-circuits the pumping process. Relaxation occurs because Brownian motion in the presence of gradients causes the moving ^{3}He atoms to experience randomly fluctuating magnetic fields. This mechanism has been studied in detail and is well understood on theoretical grounds [14,15]. As shall be seen in the following section, the gradient relaxation mechanism often presents a problem in polarized ^{3}He target cell design and construction.

III POLARIZED ^{3}He TARGETS

The optical pumping methods discussed in the preceding section have been applied successfully to construct polarized ^{3}He targets now routinely used in the T.W. Bonner Nuclear Laboratories at Rice University. In the following paper by G.C. Phillips, results

of these studies are presented. Here we shall be concerned only with target design and construction criteria, operational problems limitations, and possible future improvements.

A Presently operational targets

Targets for the study of elastic scattering of ^4He by ^3He [16], protons by ^3He, and the reaction $d + {}^3He \rightarrow p + {}^4He$ [17] over the range of energies provided by the Rice University tandem Van de Graaff accelerator have been successfully operated. Typical target polarization is about 15 % at a ^3He pressure of about 5 mm Hg (corresponding to ^3He number density of about 1.8×10^{17} per cm^3). This polarization is significantly lower than that attainable in spherical pyrex sample containers used in optical pumping studies ; the polarization loss presumably arises from design compromises and complications arising in making a cell simultaneously suitable for optical pumping and for nuclear scattering experiments.

Targets have been constructed both of brass and of pyrex, with foi windows for beam entrance and exit and for exit of scattered partic cles (at fixed scattering angles). In one experiment, solid-state particle counters were mounted inside the target cell, and in the $^3He(d,p)^4He$ experiment the scattered protons exited directly throu the pyrex walls, thus allowing easy variable positioning of extern counter telescopes and detectors to cover a wide range of scatteri angles.

Perhaps the most serious technical problem in making a usable targ cell is that of sample purity. The impurity level must remain belo about 10^{12} to 10^{13} per cm^3 or else the 2^3S_1 metastable atoms are lost in Penning collisions with impurities. Though the tolerable impurity level might appear quite easily attainable by current hig vacuum standards, a problem arises in cleaning and outgassing the sample cell, especially in the vicinities of the foils. Cells with foils are relatively easily cleaned by a combination of heating an ion and electron bombardment using intense rf discharges [4]. These techniques so far have not been as useful with target cells, becau the foils are sealed with indium O-rings or epoxies, neither of which can be heated appreciably. Improved foil-mounting techniques may eliminate this problem in the future. Despite the cleaning pro blem, sealed target cells have been operated for several days befo the impurity levels became intolerably high. In some cases it has proven useful to incorporate a getter that can be flashed periodic ly to remove impurities.

One must be extremely careful in target design and construction to avoid the use of any ferromagnetic materials or components, no mat how small or weakly magnetic they may be. Otherwise, gradient rela xation, discussed in the preceding section, completely precludes s

gnificant sample polarization. Care must also be taken that there are no ferromagnetic materials in the general vicinity of an operational target.

Current state-of-the-art in polarized ^{3}He targets can be summarized as follows. Polarization of about 15 % can be achieved at room temperature in ^{3}He targets of pressures at room temperature up to several mm Hg. Target cleanliness is something of a problem, but sealed targets have been used for several days before impurities start to degrade polarization. The targets and associated peripheral equipment are inexpensive, easy to operate, and are readily adaptable for use with most accelerators ; the set-up time is usually about an hour. The magnetic field used to provide a quantization axis need only be a few gauss, enough to overcome the earth's magnetic field ; hence there are no beam-deflection problems in the target environment.

B Possible target improvements

There appears to be little likelihood of significant increase in target density at room temperature without intolerable loss of polarization. Even if some of the spin-relaxation processes due to undesirable discharge constituents can be eliminated (as, for example, by addition of neon to dissociate He_2^+ ions), the target pressure could be raised only to about 20 mm Hg before 2^3S_1 de-excitation by the three-body reaction [18] :

$$He(2^3S_1) + 2He \rightarrow He_2(^3\Sigma_u^+) + He \qquad (7)$$

starts to degrade polarization.

There is perhaps some latitude for improvement in target polarization by using more intense pumping radiation and improved optics. We presently use a disk lamp excited by a 300 watt oscillator of design discussed by Gamblin and Carver [15]. Unfortunately, putting more power into the lamp would have little effect on the lamp surface brightness, since the lamp is already optically thick. As a crude estimate, one might hope to gain a factor of three or four in polarization by improved optics -- probably enough of an improvement to warrant the effort.

If the electrical discharge is turned off after a ^{3}He sample is optically polarized, the polarization decay time is observed typically to be several hours at room temperature [14,19]. This suggests the possibility of a cycle based on compression of the polarized gas for use as a dense target during the rather long decay period.

One might also consider the advantages of operating targets at reduced temperature. Gamblin and Carver [15] have shown that useful polarization can be extended to somewhat higher densities at 77° K, but the improvement is less than an order of magnitude. Our experiments indicate that optical pumping at still lower temperatures is infeasible because of the rapid fall-off in the excitation transfer cross-section (reaction 1) with decreasing temperature [20]. The fall-off results from a long-range repulsive interaction between 2^3S_1 and 1^1S_0 atoms, making excitation transfer a thermally-activated process [21].

Perhaps the most promising possibility for improvement involves the use of a cold finger extending from the optical pumping cell into a liquid helium bath (see fig. 5). This allows the optical pumping to be done at room temperature (or at 77° K) with diffusion transporting the polarized atoms to the extremity of the cold-finger where the density is greater by the ratio of pumping temperature to cold-finger temperature. H.H. McAdams and the writer have employed this technique in preliminary experiments to produce polarizations as high as 2 % in ^{3}He gas at 0.9° K and 4 mm Hg pressure (corresponding to atomic number density in excess of 4×10^{19} per cm^3).

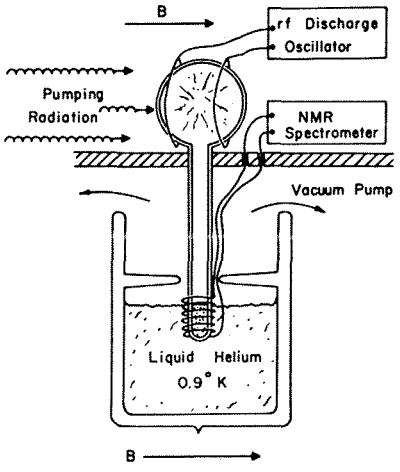

Fig. 5 Schematic diagram showing method for polarizing dense gas and liquid ^{3}He by combination of optical pumping at room temperature and polarization diffusion to the cold extremity.

By optically pumping the vapour (at room temperature) above a 20 mm^3 sample of <u>liquid</u> ^{3}He (atomic density $\sim 2 \times 10^{22}$ per cm^3), we have achieved liquid polarization as high as 0.2 %. These polarizations are achieved on an applied magnetic field of a few gauss achievement of the same polarizations thermally at 0.9° K would require a magnetic field of about 170,000 gauss in the case of the

gas experiment and 17,000 gauss in the liquid experiment. We believe that the polarization is at present limited by wall-relaxation in the vapour phase at low temperatures and by bulk relaxation in the liquid. The former loss might be reduced by improved geometry of the tube connecting the optical pumping cell to the cold finger and by introducing forced convection in the connecting tube ; the latter loss can be partially overcome by a larger ratio of optical pumping cell volume to liquid ^{3}He volume. To completely overcome polarization losses in the liquid, a ratio of order 10^5 would be required. Prospects appear to be good for dense ^{3}He targets of significant polarization by this technique.

IV POLARIZED $^3He^+$ ION SOURCE

Collaborative efforts of the Atomic Physics Group at Rice University with S.D. Baker and G.C. Phillips of the Bonner Nuclear Laboratories have led to successful extraction of a $^3He^+$ ion beam from an optically pumped source gas [22]. A schematic of the rf discharge ion source is shown in figure 6. Though ideal conditions for operation of an rf ion source on the one hand and for optical pumping on the other do not coincide, there is a sufficient area of overlap to allow the extraction of about 0.6 microamperes of well-collimated beam. The ion source operates at about 0.2 mm pressure, and the discharge provides both ions and the 2^3S_1 metastable atoms required for optical pumping. A 20 gauss axial magnetic field is provided by a large end-connected solenoid. (The field over the ion source must be quite uniform to avoid gradient relaxation). Using a 5 watt capillary ^{4}He lamp, the source polarization is about 3 % ; we are confident that the polarization can be improved by an order of magnitude or more merely by substituting our brighter 300 watt lamp, and by using ^{3}He rather than ^{4}He as the lamp gas. (At these low pressures, ^{3}He pumping is more effective than ^{4}He ; see fig. 3).

The ion polarization is expected to be between 50 % and 100 % of the source gas polarization. Ionization of polarized neutral ground-state ^{3}He atoms would give $^3He^+$ with 50 % of the neutral polarization. A somewhat higher figure would result from ionizing 2^3S_1 atoms ; the source of ionization in a helium discharge is unfortunately not known with any degree of confidence. Whatever the ionization mechanism, rapid electron exchange ($\sigma \simeq 5 \times 10^{-15}$ cm^2) with neutral atoms before extraction :

$$^3He^+ + {}^3He \rightarrow {}^3He + {}^3He^+ \qquad (8)$$

very likely would bring the ion polarization up to nearly 100 % of the source gas polarization.

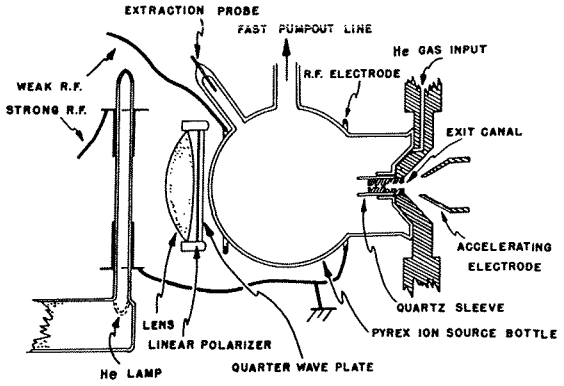

Fig. 6 Schematic diagram of optically pumped rf discharge $^3He^+$ ion source. Current of 0.6 μa has been extracted.

Though we are currently able to extract and focus $^3He^+$ ions that we believe to be polarized, direct measurement of ion polarization by means of a nuclear reaction has not yet been accomplished. Our ion-source test set-up accelerates the $^3He^+$ ions to a maximum of 300 keV. The beam polarization will be measured, hopefully within the next few months, by a double scattering experiment involving measurement of the polarization distribution of protons created in the reaction $^3He + d \rightarrow {}^4He + p$, using a deuterium target. This experiment is discussed in greater detail in the following paper by G.C. Phillips.

Experiments also are underway to determine the feasibility of extracting a polarized electron beam from an optically pumped source gas. As stated earlier, the source of ions and electrons in a helium discharge is not established ; certainly ionization of ground-state helium atoms would yield unpolarized electrons. However, considerable evidence exists suggesting that cumulative ionization processes involving excitation to the 2^3S_1 state with subsequent ionization predominate. Electrons derived from ionization of optically-pumped 2^3S_1 atoms would be expected to be spin-polarized. Regardless of the source of electrons, electron exchange collisions by reaction (2') should lead to electron polarization. We plan to use Mott scattering to measure the polarization of extracted electrons under a variety of ion source conditions to study ionization mechanisms in a helium discharge and, hopefully, to develop an intense polarized electron source.

V CONCLUSIONS

The combination of optical pumping and excitation transfer collisions in ^{3}He gas subjected to a weak electric discharge makes possible the attainment of sizeable polarization of the ^{3}He nuclei. Polarized ^{3}He targets based on these techniques have proven feasible for low-energy scattering experiments, and such experiments are now routinely conducted in the Bonner Nuclear Laboratories of Rice University. The targets are easy to operate, requiring no cooling and only weak applied magnetic fields, and the nuclear purity is very high. Present targets suffer from rather low atomic density, precluding their use in high energy experiments ; however, recent studies suggest a distinct possibility that useful liquid ^{3}He and/or dense gas targets can be developed by a combination of cryogenic and optical pumping techniques.

A 0.6 microampere $^3He^+$ beam has been extracted from an optically pumped ^{3}He ion source, and is believed to be polarized. Confirmation awaits the completion of nuclear scattering experiments designed to measure the beam polarization directly.

Work has been initiated on a possible intense source of polarized electrons.

VI ACKNOWLEDGMENTS

The author acknowledges with pleasure numerous stimulating discussions with S.D. Baker, G.C. Phillips, L.D. Schearer and E.B. Carter.

Notes and References

1) A. Kastler, J. Phys. Radium, 1950, 11, 255.
2) H.G. Dehmelt, Phys. Rev., 1958, 109, 381.
3) G.K. Walters, F.D. Colegrove and L.D. Schearer, Phys. Rev. Letters, 1962, 8, 439.
4) F.D. Colegrove, L.D. Schearer and G.K. Walters, Phys. Rev., 1963, 132, 2561.
5) F.D. Colegrove and P.A. Franken, Phys. Rev., 1960, 119, 680.
6) L.D. Schearer, Advances in Quantum Electronics (Columbia University Press, New York, 1961), p. 239-251.

7) M. Fred, F.S. Tomkins, J.K. Brady and M. Hamermesh, Phys. Rev., 1951, 82, 406.
8) R.A. Byerly, M.A. Thesis, Rice University, 1965 (unpublished).
9) E.C. Beaty and P.L. Patterson, Phys. Rev., 1965, 137, A346.
10) J.M. Madson, H.J. Oskam and L.M. Chanin, Phys. Rev. Letters, 1965, 15, 1018.
11) E.C. Beaty, J.C. Browne and A. Dalgarno, Phys. Rev. Letters, 1966, 16, 723.
12) H.J. Oskam, Philips Res. Reports, 1958, 13, 335.
13) R.C. Greenhow, Phys. Rev., 1964, 136, A660.
14) L.D. Schearer and G.K. Walters, Phys. Rev., 1965, 139, A1398.
15) R.L. Gamblin and T.R. Carver, Phys. Rev., 1965, 138, A946.
16) G.C. Phillips, R.R. Perry, P.M. Windham, G.K. Walters, L.D. Schearer and F.D. Colegrove, Phys. Rev. Letters, 1962, 9, 502.
17) S.D. Baker, G. Roy, G.C. Phillips and G.K. Walters, Phys. Rev. Letters, 1965, 15, 115.
18) A.V. Phelps, Phys. Rev., 1955, 99, 1307.
19) Recent studies by W.A. Fitzsimmons and the author indicate that the polarization relaxation time is highly temperature dependent reaching a maximum value of about 20 hours at 125° K, and fallin rapidly to the order of seconds as the temperature is decreased to 4.2° K. These results can be interpreted in terms of spin interactions with the container walls.
20) F.D. Colegrove, L.D. Schearer and G.K. Walters, Phys. Rev., 1964 135, A353.
21) R.A. Buckingham and A. Dalgarno, Proc. Roy. Soc. (London), 1952, A213, 327.
22) S.D. Baker, N.D. Stockwell, G.K. Walters, E.B. Carter and G.C. Phillips, Bull. Am. Phys. Soc., 1966, 11, 749.

Work supported by U.S. Atomic Energy Commission.

NUCLEAR REACTION STUDIES USING POLARIZED ^{3}He TARGETS AND BEAMS

G.C. PHILLIPS*

Rice University, Houston

I INTRODUCTION

This paper reports work at Rice University using polarized ^{3}He targets and beams. The ^{3}He is polarized by the optical pumping method described by G.K. Walters in the preceding paper [1]. Some of this work was reported last year [2] but for the sake of completeness, all of the nuclear studies made at Rice University using polarized ^{3}He will be reviewed.

The study of nuclear reactions with the target and/or the beam polarized are of basic importance because of the strong spin dependence of nuclear forces ; indeed, until a nuclear process involving particles with spins has been studied so as to ascertain the spin dependence, the processes are basically unknown. Thus, muchly studied reactions such as elastic and inelastic proton scattering from nuclei, and deuteron-nucleon "stripping" reactions, are really not yet completely studied for just this reason.

Two examples serve to emphasize this point. When protons are scattered from ^{3}He, the unstable nucleus ^{4}Li is formed as an intermediate, compound-nuclear system, and the experimental determination of the elastic scattering phase shifts for energies up to about 10 MeV gives information about the spins and parities of T = 1 states of the mass-4 system. If only elastic scattering with unpolarized beams and targets is available, along with spin measurements of the scattered proton, it is basically impossible to deduce a unique set of phase shifts. However, if the spins are also measured,

the degenerate solutions can be rejected, and a unique determination of phase shifts, resonance parameters, etc, becomes possible.

A second example of typical nuclear experiments that badly need spin determinations are (d,p) or (d,n) "stripping" reactions. Such processes typically produce strongly forward-peaked angular distributions of nucleons and polarization of the nucleons and are described in terms of an optical model potential that must contain spin dependent terms. If only angular distributions and nucleon spin determinations are available, it is impossible to deduce a unique spin dependence of the optical potential.

Both of the above problems have been studied at Rice using polarized targets and will be discussed later.

II EXPERIMENTAL REQUIREMENTS OF POLARIZED ^{3}He TARGETS

The preceding paper by Professor Walters has discussed the techniques for producing ^{3}He gas with useful nuclear polarization. Since some of these requirements are rather in conflict with the requirements for producing a polarized ^{3}He target useful in nuclear measurements, it is important to discuss these conflicts in detail.

To make a polarized ^{3}He gas target useful for nuclear experiments, it is necessary to admit a beam and perhaps to allow charged particles to emerge from the gas. This necessitates employing foils well sealed to the vessel with the resulting possibilities of damage to the electrical discharge properties of the cell, of introducing magnetic inhomogeneities and/or surfaces that serve to relax the polarization, and of introducing more possibilities for leaks and for outgassing. Indeed, the beam itself may introduce contaminants, cause leaks, and certainly increases outgassing.

To be useful for a nuclear physics experiment, a polarized target must be capable of being sealed off, attached to an accelerator or reactor, and operate with useful polarization for several hours or days. Thus, if detectors are placed internal to the target volume, they must not outgas and must not be significantly damaged or affected by the electrical discharge and light produced in the gas. Finally, it is necessary that the nuclear instrumentation not introduce magnetic gradients.

The most versatile ^{3}He target designed at Rice to date is shown in figure 1. This target attempts to eliminate all of the difficulties

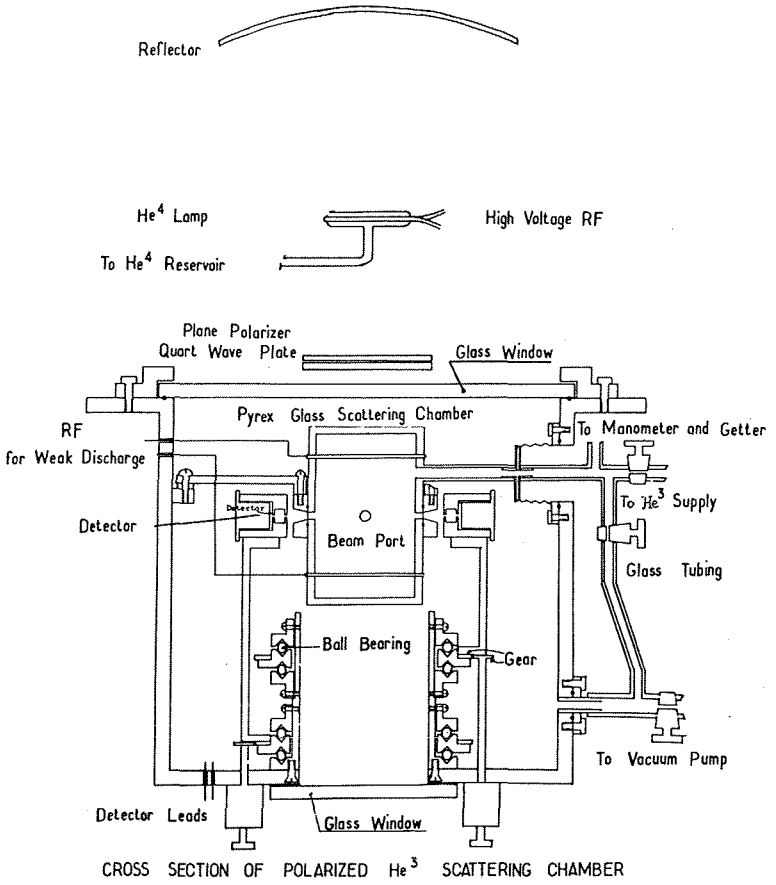

Fig. 1 A versatile ^{3}He polarized target arrangement. See text.

discussed above. To facilitate outgassing, the ^{3}He gas is contained in a precision ground glass cylinder through which the beam is passed via thin foils while reaction product charged particles can emerge through thin windows to either side in an angular range of 30° to 150°. The foils are sealed to the glass with indium "O"-rings and pressed against the glass by a precision retaining piece. This vessel is contained inside an evacuated vessel in which two silicon solid-state detectors and telescopes can be rotated. This feature allows very thin foils to be employed, and thus low-range particles detected, since the differential pressure across the foils cán be very small ; the design also eliminate leakage into the ^{3}He gas. Circularly polarized pumping light is admitted through the glass cover of the outer chamber and the flat top and bottom of the inner glass ^{3}He cell. Construction of this target system is now nearing completion. The cell and associated optical and electronic compo-

nents will be portable so that the target may be transported to other laboratories for use.

III SPECIFIC STUDIES USING POLARIZED ^{3}He TARGETS

Four nuclear processes have been studied to date using these targets ; three of these have been reported elsewhere [1] but will be summarized below. New data on proton-^{3}He scattering will be presented.

A ^{3}He(α,α)^{3}He

This reaction was the first use of a polarized ^{3}He gas target prepared by optical pumping and demonstrated the usefulness of the technique [3]. Figure 2 shows a schematic diagram of the apparatus which was employed with the Rice tandem Van de Graaff and α-particle beams of about 7 MeV energy. Earlier experiments had shown that a strong resonance for ^{3}He-α elastic scattering at about 7 MeV had $J^\pi = 7/2^-$ and allowed the extraction of unique phase shift fits near resonance which in turn predicted near 100 per cent ^{3}He polarization either side of resonance at certain angles. These predictions were checked by the apparatus of figure 2.

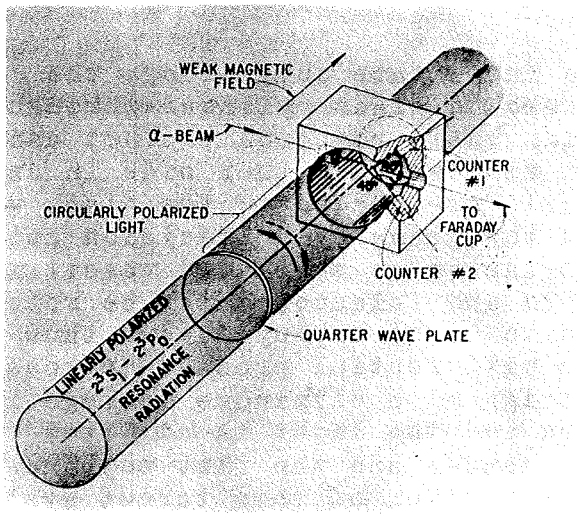

Fig. 2 Schematic diagram of the apparatus used to study the elastic scattering of alpha particles from polarized ^{3}He. See text and reference 3.

The expected left-right assymetry is $A = P_n P_t$, where P_n is the nuclear polarization of the ^{3}He calculated from the phase shifts and P_t is the target polarization measured optically [1]. The measured value of $A = (N_L - N_R)/(N_L + N_R)$, determined from the left or right counting rates N_L, N_R confirmed the predictions and demonstrated the usefulness of the method.

Several weaknesses of the design of this first target cell were apparent. These included the fact that the electrical discharge was very nonuniform in the partially metal cell, and that the cell which contained detectors outgassed and did not have a very long useful life, and a rather low polarization (about 8 per cent).

B ^{3}He(d,p)^{4}He

The study of this reaction with a polarized ^{3}He target has provided the first indication that optical model theories of "stripping" processes must include tensor interactions.

These measurements were carried out using a glass sphere ^{3}He cell with 1/4 mm walls. The beam passed through two 1/3 mil Al foils. The rather energetic protons could penetrate the glass and were detected in two thick Li-drifted silicon detectors operated in the air behind collimators [4]. Typical angular distributions of $A(\theta)$ are shown in figure 3. Also shown are $P(\theta)$, the proton spin polarization of the reaction when an unpolarized target is used [5].

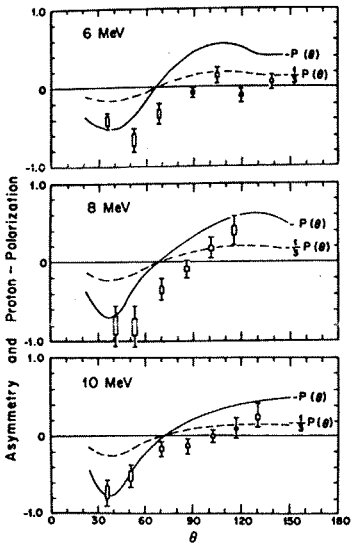

Fig. 3 ^{3}He(d,p)^{4}He angular distributions of the left-right asymmetry, $A(\theta)$ (see reference 4), using a polarized ^{3}He target, and the proton spin polarization, $P(\theta)$ (see reference 5) using an unpolarized target.

Note that at forward angles, where the cross-section is largest, that $A(\theta) \approx - P(\theta)$. Now ordinary optical model potentials that assume central plus spin-orbit forces, predict that $A(\theta) = - 1/3P(\theta)$, independent of the range and strengths of the potentials, a result deduced by Tanifugi [6]. Professor Ian Duck at Rice further demonstrated that the only way that departure from $A(\theta) = - 1/3P(\theta)$ can be obtained is for there to be large spin-flip amplitudes corresponding to strong tensor forces [7]. It is clear that other polarized target and beam studies need to be carried out for other "stripping" reactions to further define the spin dependence of optical potentials.

C $^3He(n,p)^3H$

This experiment was undertaken at the Materials Testing Reactor in collaboration with Dr Robert Spencer by using a beam of polarized neutrons obtained by Bragg scattering from a saturated Co-Fe single crystal. The large thermal capture cross-section (~ 5000 barns) was suspected to be due to a (virtual) resonance state in ^4He and thus should be detected for either the $J^\pi = 0^+$ or 1^+ configurations of the two spinors depending on the spin of the ^4He state involved. The measurements confirmed Brookhaven measurements [8] and showed that the capture is dominated by the singlet state and confirms that the ^4He first excited state (at near zero p-^3H energy) is a 0^+ state.

D $^3He(p,p)^3He$

The fundamental problem of the T = 1 excited states of the mass-4 nuclei can be studied by this elastic scattering process. The experimental determinations of cross-section and proton polarization using an unpolarized target have been phase shift analyzed by Tombrello [9] and more recently by Morrow and Haeberli [10].

The Rice measurements of the elastic scattering $A(\theta)$ using a polarized ^3He target have been carried out using a glass target cell with Al beam entrance and exit windows and with foils at 45° and 90° for left-right scattered proton detection which is shown in figure 4 [11]. The data were taken in the bombarding energy range of 4 to 11 MeV. The ^3He polarization was about 10 per cent and was measured optically.

Measurements of the asymmetry are shown in figure 5. These measurements may be compared to the calculation of Tombrello whose phase shifts predict asymmetries of 40 to 50 per cent at 90°. Since smaller asymmetries are observed, it is clear that the Tombrello

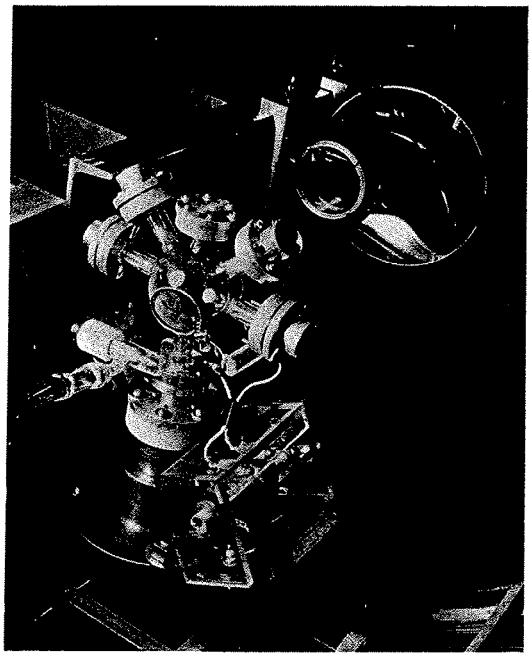

Fig. 4 Apparatus for the study of elastic proton scattering from a polarized ^{3}He target. Protons of 4 to 11 MeV bombard the cell and are scattered to detectors at 45° and 90°.

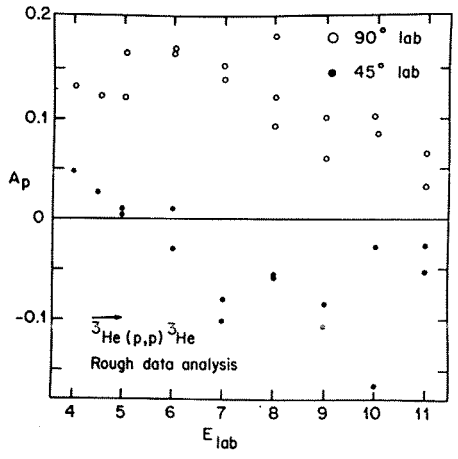

Fig. 5 ^{3}He(p,p)^{3}He left-right asymmetry, A(θ) (see reference 11), for θ = 45° and 90° in the proton energy range 4 to 11 MeV.

phase shifts are in error, although the size or nature of the discrepancy is as yet unknown.

Preliminary calculations by Morrow and Haeberli [10] yield two degenerate sets of phase shifts to fit earlier cross-section and polarization data. There is hope that one of these sets may describe the present asymmetry results and suggests that a unique determination of the p-wave, T = 1 states of ^{4}Li may be obtainable upon inclusion of all data in the fitting.

IV POLARIZED ^{3}He BEAM

An apparatus designed to produce $^{3}He^{+}$ polarized beams has been constructed. The polarized ion source is similar to a conventional R.F. ion source except that polarized pumping light is supplied to the discharge and great care is taken to provide for outgassing th ion-source and associated plumbing and to supply a flow of high purity ^{3}He gas. This apparatus has successfully produced several μA of $^{3}He^{+}$ ions over periods of many hours while simultaneous optical pumping of the discharge produced up to 20 per cent polarization of the gas [12].

The amount of polarization of the $^{3}He^{+}$ ions is, of course, related to the gas polarization, but in a complex and presently unknown way. Many factors should lower the polarization : for example, ionization of the atoms, collisions of ions with surfaces or impurities, and passage through magnetic gradients. One effect may restore some polarization to the $^{3}He^{+}$ ions : charge exchange collisions with polarized ^{3}He atoms. Thus, it is necessary to devise a method to measure the beam polarization.

The $^{2}H(^{3}He,p)^{4}He$ reaction has been chosen to measure the beam polarization, and an apparatus named a Demtan (Tandem backwards) has been constructed. The Demtan consists of the polarized ion source attached to an acceleration tube and elevated to + 150 kV above ground, with vacuum pumps at ground, and the deuterium target floating at - 150 kV off ground at the end of a second acceleration tube. In this way, the deuterium target can be bombarded with 300 keV $^{3}He^{+}$ ions. The apparatus is shown in figures 6 and 7.

The beam polarization will be measured by means of measurement of the spin polarization of the $^{2}H(^{3}He,p)$ protons. This will be accomplished by means of left-right scattering of the energetic protons from ^{4}He gas. A polarimeter has been constructed and tested that employs ^{4}He gas at 35 atmospheres with the protons being

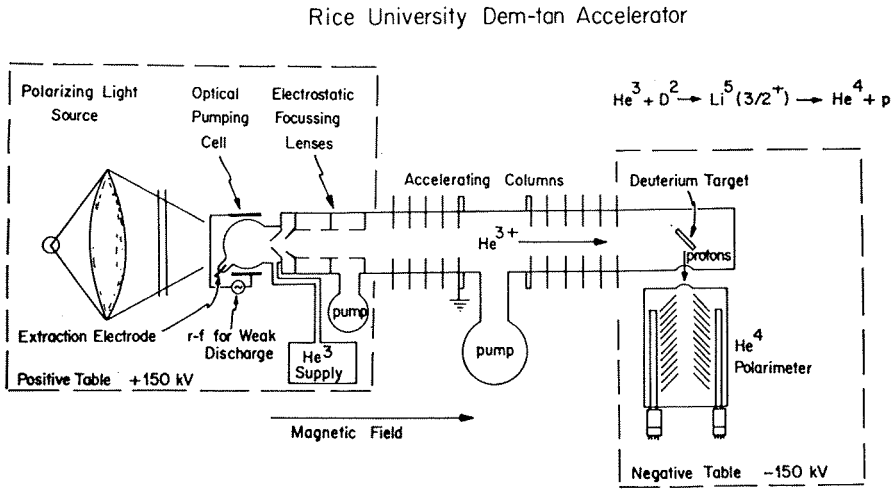

Fig. 6 Schematic of the Demtan accelerator to be used to test the $^3He^+$ ion beam polarization. See text.

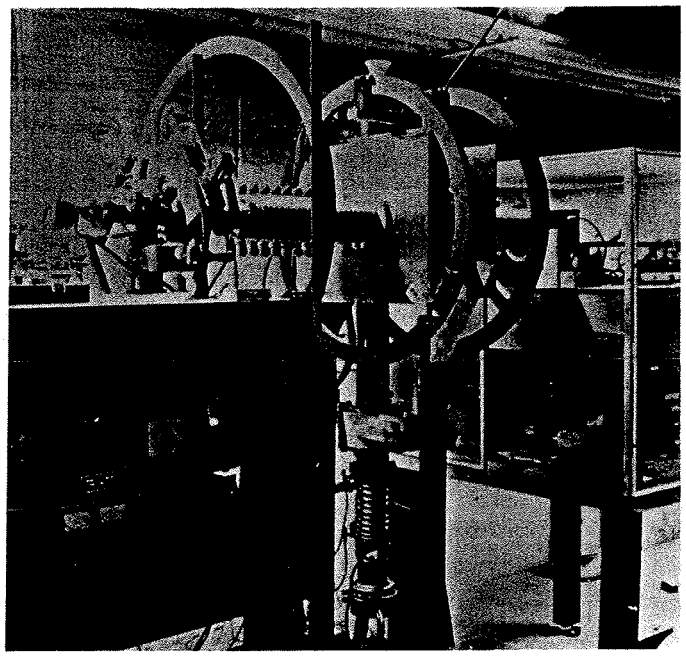

Fig. 7 Photograph of the Demtan.

scattered along a 19 cm path into collimated counters at about 60° to the proton direction, see figure 8. The protons will have energies of 6.5 to 11.1 MeV in the ^{4}He gas, and the p-^{4}He scattering asymmetry at those energies and angles is nearly 100 per cent for completely polarized protons. The beam polarization P_b is related to the proton polarization by $P_p = 2/3\ P_b$ for protons emitted perpendicular to the beam polarization.

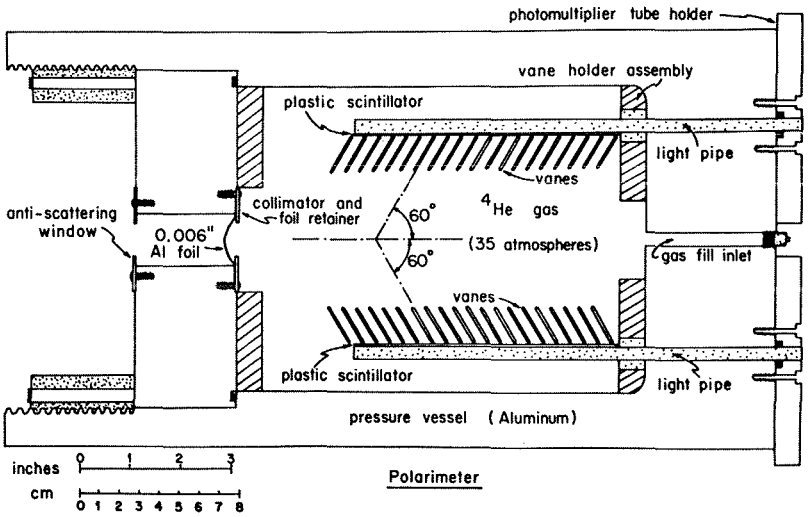

Fig. 8 Schematic of the proton-polarimeter. See text.

This apparatus is all built and tested [13] and the test of $^3He^+$ beam polarization will be carried out shortly.

V CONCLUSIONS AND ACKNOWLEDGMENTS

The use of polarized ^{3}He targets has materially aided studies of nuclear-structure and nuclear reactions. It has provided the first proof of the need for inclusion of tensor forces in optical models of stripping, has helped determine the spin and parity of the first excited state of the α-particle, and appears to be capable of deciding the proper phase shifts for p + ^{3}He scattering and determining the spins and parities of the T = 1 states of ^{4}Li. The extension of these measurements to lower and higher energies, to other projectiles, and especially to use with polarized beams should be very fruitful in providing additional new nuclear structure information.

I am indebted to many colleagues for help in preparing this paper. The work spans the last five years. For some of the earlier nuclear physics measurements I am indebted to Professor Pat Windham of North Texas State University and Dr Robert Spencer of Phillips Petroleum Company and to Dr Elmer Carter. In all the recent work, Professor Stephen D. Baker has taken significant responsibility and leadership.

The continuing close collaboration at Rice of the Nuclear Physics group with Professor Walters' Atomic Physics group has made the work possible and is also gratefully acknowledged, as is the close collaboration with members of the Nuclear Theory group, Professor Duck, and Dr Tanifugi.

Note and References

* On leave as NSF Senior Postdoctoral Fellow ; Brookhaven National Laboratory.

1) G.K. Walters, these Proceedings, p. 201.
2) G.C. Phillips, Proceedings of the 2nd International Symposium on Polarization Phenomena of Nucleons, Karlsruhe, September 6-11, 1965 (P. Huber and H. Schopper, Eds., Birkhäuser Verlag, Basel and Stuttgart, 1966), p. 113-125.
3) G.C. Phillips, R.R. Perry, P.M. Windham, G.K. Walters and L.D. Schearer, Jr, Phys. Rev. Letters, 1962, 9, 522.
4) S.D. Baker, G. Ray, G.C. Phillips and G.K. Walters, Phys. Rev. Letters, 1965, 15, 115.
5) R.I. Brown and W. Haeberli, Phys. Rev., 1963, 130, 1163.
6) M. Tanifugi, Phys. Rev. Letters, 1965, 15, 113.
7) I. Duck, Nucl. Phys., 1966, 80, 617.
8) L. Passel and R.I. Schermer, Bull. Am. Phys. Soc., 1965, 10, 587.
9) T.A. Tombrello, Phys. Rev., 1965, B138, 40.
0) L.W. Morrow and W. Haeberli, Private communication.
1) S.D. Baker, D.H. McSherry, D.O. Findley and G.C. Phillips, Bull. Am. Phys. Soc. (N.Y. Meeting, January, 1967).
2) N.D. Stockwell, E.B. Carter, G.C. Phillips and G.K. Walters, Bull. Am. Phys. Soc., 1965, 10, 156.
3) D.O. Findley, M.A. Thesis, Rice University, 1967 (unpublished).

Work partially supported by the U.S. Atomic Energy Commission.

TARGET OF ORIENTED ^{165}Ho NUCLEI FOR SCATTERING OF FAST ELECTRONS

R.S. SAFRATA*, J.S. Mc CARTHY, W.A. LITTLE,
M.R. YEARIAN and R. HOFSTADTER

Stanford University, Stanford

An experiment of scattering of 200 MeV electrons by oriented ^{165}Ho nuclei was performed at Stanford University, U.S.A. on the electron linear accelerator Mark III. The target was a plate (approximately 4 cm^2 square) 0.83 mm thick, cut out of a piece of holmium metal single crystal. This plate was placed in liquid ^3He between two windows made from 0.025 mm thick stainless steel foil. The primary electron beam had to traverse aluminium foils 0.05 mm thick at room temperature, 0.006 mm at liquid nitrogen temperature and 0.025 mm at 4.2° K on its way to the target in the ^3He chamber. The scattered electrons went through a similar set of windows to a magnetic spectrometer. The lowest temperature used was about 0.35° K at which temperature the alignment of the ^{165}Ho nuclei was about 45 %. The axis of alignment was perpendicular to the scattering plane. The maximum measured effect was about 10 %.

Work supported in part by the U.S. Office of Naval Research and the National Science Foundation.

* Present address : Nuclear Research Institute, Rez, Czechoslovakia.

SOURCE D'ELECTRONS POLARISES PRODUITS PAR IONISATION D'UN FAISCEAU D'ATOMES DE POTASSIUM ORIENTES

P. COIFFET et A. SEPTIER

Faculté des Sciences*, Orsay

On a repris l'expérience réalisée par Friedmann (1961) et refaite par Hughes en 1965.

Le potassium atomique est émis à partir d'un four porté à une température de 300° C ; le faisceau atomique traverse alors un champ magnétique très fortement inhomogène. On sélectionne ainsi les atomes de spin +1/2 focalisés à la sortie de l'aimant. Ils sont maintenus dans un champ magnétique longitudinal et ionisés par un rayonnement ultraviolet. Les électrons ainsi obtenus sont polarisés, l'ionisation s'effectuant sans transition. On les accélère. Après transformation de leur hélicité en polarisation transverse au moyen d'un filtre de Wien, on mesure leur polarisation par diffusion de Mott.

I LA SOURCE D'ATOMES POLARISES

a Le choix des atomes.

Les atomes utilisés doivent posséder un électron superficiel ayant une énergie de liaison faible. Le spin de cet électron doit être facilement découplable du spin du noyau. De plus, il faut pouvoir détecter le faisceau atomique. En examinant l'hamiltonien d'un atome alcalin :

$$H = \frac{p^2}{2m} + V(r) - \left(\frac{e\hbar}{2mc}\right)\vec{\sigma}\left(\vec{E} \wedge \frac{\vec{p}}{2mc}\right) + A\vec{I}.\vec{\sigma}$$

et en introduisant un champ magnétique externe, il suffit que :

$$A\vec{I}.\vec{\sigma} \ll \frac{e}{mc}\vec{\mathcal{H}}.\vec{\sigma}$$

pour que $[H,\sigma_x] = 0$ c'est-à-dire que σ_x soit une constante du mouvement.

Le calcul des champs équivalents de structure hyperfine fait apparaître qu'en utilisant des champs externes de 1 à 2 teslas, on peut considérer que le découplage entre spin nucléaire et spin électronique est complètement réalisé, au moins pour le lithium, le sodium et le potassium.

Le choix des atomes est aussi conduit par leur longueur d'onde d'ionisation. Elle va de 2300 Å pour le lithium à 3000 Å pour le césium suivant les alcalins. Il est difficile de fournir une puissance importante au-dessous de 2500 Å. Nous choisissons le potassium qui s'ionise à 2872 Å. Celui-ci se détecte aisément par ionisation de surface.

b Le champ magnétique.

Les pôles ont la forme donnée par la figure 1 ; c'est le cas limite de pôles circulaires où lignes de force et équipotentielles sont de cercles orthogonaux.

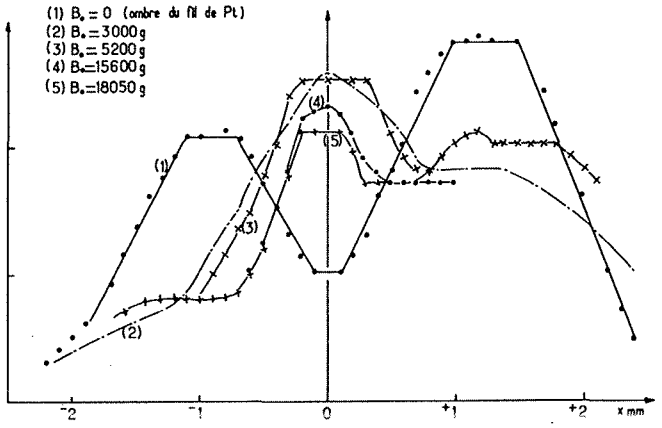

Fig. 1

Pour les atomes à mj = + 1/2, la matrice de transfert s'écrit, en appelant L la longueur de l'aimant :

$$\begin{vmatrix} x \\ x' \\ y \\ y' \end{vmatrix}_{\text{ortie}} = \begin{vmatrix} \cos\omega L/\bar{v} & (\bar{v}/\omega)\sin\omega L/\bar{v} & 0 & 0 \\ \frac{\omega}{\bar{v}}\sin\omega L/\bar{v} & \cos\omega L/\bar{v} & 0 & 0 \\ 0 & 0 & \mathrm{ch}\,\omega L/\bar{v} & \frac{\bar{v}}{\omega}\,\mathrm{sh}\,\omega L/\bar{v} \\ 0 & 0 & \frac{\omega}{\bar{v}}\,\mathrm{sh}\,\omega L/\bar{v} & \mathrm{ch}\,\omega L/\bar{v} \end{vmatrix} \begin{vmatrix} x \\ x' \\ y \\ y' \end{vmatrix}_{\text{entrée}}$$

Il y a focalisation en x et défocalisation en y. Pour mj = - 1/2 il y a défocalisation en x et focalisation en y.

Pour séparer les atomes émis par le four à travers une fente de 60 μ de largeur, on place, à l'entrée du champ, un diaphragme traversé en son milieu suivant Oy par un fil de platine de 0,1 millimètre de diamètre. Ainsi les atomes injectés suivant l'axe (donc non déviés par la suite) sont focalisés et se trouvent dans l'ombre du fil de platine à la sortie de l'aimant, les atomes à mj =-1/2 sont rejetés à l'extérieur de cette ombre.

Les pôles de l'aimant sont en acier Imphy AFK2 permettant d'atteindre plus de 1,8 tesla. Sa longueur est de 16 centimètres.

Le nombre d'atomes focalisés est d'environ 10^{12} par seconde pour T = 300° C. La figure 2 montre la répartition de ces atomes dans le plan focal.

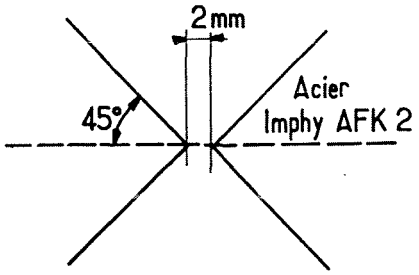

Fig. 2

2 LA SOURCE D'ELECTRONS POLARISES

Le champ directeur est réalisé à l'aide de bobines pouvant fournir un champ magnétique longitudinal compris entre 0 et 1030 gauss.

L'électrode H.T. (- 60 kV) se présente sous forme d'un cylindre revêtu intérieurement de nickel. Un miroir incliné à 45° sur l'axe de l'électrode et à l'intérieur de celle-ci permet de renvoyer le faisceau ultraviolet fourni par une lampe WHS 200 OSRAM. Le nickel a été choisi comme revêtement de préférence à l'argent car son seuil d'émission photoélectrique est plus éloigné de celui du potassium que ne l'est le seuil de l'argent. Il a aussi un bien meilleur coefficient de réflexion entre 2000 et 3000 Å.

Pour des valeurs du champ magnétique de 0, 420, 520, 780 et 1010 gauss, un effet de lentille élimine pratiquement tous les électrons photoélectriques. Il n'en rentre dans le transformateur de polarisation que moins de 10^{-14} ampère.

La mesure de la polarisation s'effectue par diffusion de Mott sur feuille d'or. On observe par réflexion à 90° du faisceau incident à l'aide d'un tube autocoupeur associé à un système de comptage.

RESULTATS

La chambre du four est séparée de l'enceinte. Les vides en fonctionnement sont de 10^{-5} mm de mercure pour la chambre du four et 10^{-6} mm de mercure pour le reste de l'enceinte.

L'alignement, très crucial, est assuré à l'aide d'un faisceau lumineux envoyé sur l'axe et l'on repère les positions des différents diaphragmes à l'aide d'une lunette de visée.

Le courant est mesuré à l'aide d'une cage de Faraday placée avant le transformateur de polarisation. Il varie entre 0,3 et 2 x 10^{-12} ampère suivant : i) les expériences (ceci est dû à des réglages différents ; rappelons que l'alignement est extrêmement délicat ; ii) la puissance U.V. envoyée (dans un rapport environ 3/2 dans la gamme de variation permise par la lampe utilisée, ce qui montre que l'efficacité d'ionisation dépend de la puissance U.V.

On constate que la polarisation dépend directement du champ magnétique directeur. Les erreurs dues à des asymétries expérimentales,

au bruit de fond du compteur, au fait qu'on observe tous les électrons arrivant sous un petit angle solide, s'élèvent à environ 10 %.

La courbe de la figure 3 montre la variation de la polarisation en fonction du champ magnétique directeur.

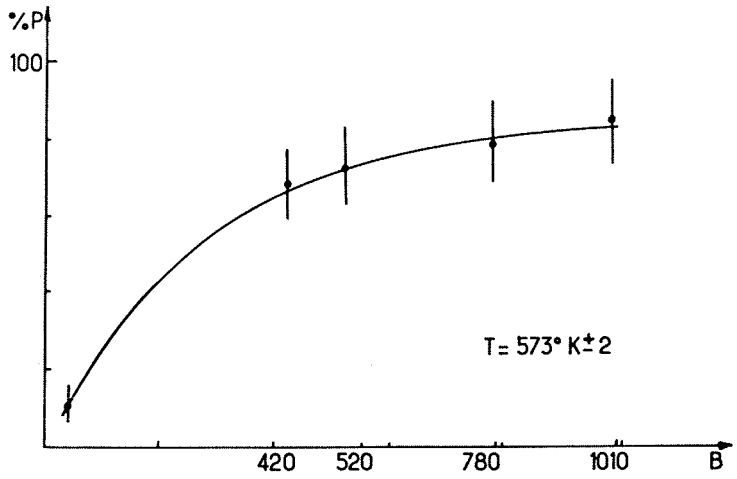

Fig. 3

Note

* Institut d'Electronique Fondamentale ; Laboratoire Associé au C.N.R.S.

DEFINITION AND DETERMINATION OF SPIN AMPLITUDES SOME APPLICATIONS OF POLARIZED TARGETS IN HIGH ENERGY PHYSICS

M. JACOB

Service de Physique Théorique, Saclay

INTRODUCTION

We must confess that the recent exploration of the strong interactions of elementary particles at high energy has presented us with several surprises. One of them is the population explosion of the strongly interacting particles, or hadrons, which, by sheer ignorance, we are bound to call elementary in our present framework. This discovery has taken us aback in our quest for still simpler constituants in the study of the structure of matter. It is a great satisfaction for our hellenic heritage that larger and larger symmetry groups can bring back this huge number of particles to a rather small number of multiplets. In order to do so a great effort has to be done to determine the quantum numbers of the many new candidates to the opening multiplets and, in particular, their spin and parity. We are then bound to face in considerable details the spin dependence of the production and decay mechanisms through which these new particles are discovered. In so doing polarized targets are already most precious tools [1,2].

An other, and more recent, surprise is that polarization effects do not cancel themselves out in some high energy processes, as they were expected to do, according to particular asymptotic behaviours. It was once thought that the pertinent regime would be already reached in the 10 GeV domain. There are now good reasons to think that the so-called complications due to spin are still a major effect there. Nevertheless, their presence is to be consider as a precious insight in the analysis of collisions at these high energies. Here again the use of polarized targets is most important [3].

Furthermore spin effects may be closely associated to the invariance properties which we need to test further and further and the use of polarized targets offers new and powerful techniques in our quest fore more refined tests.

It has been already shown by Prof. Jackson [4], how polarized target are extremely helpful devices in each of the three afore mentioned facets of high energy physics. The purpose of this talk is to come back on some of these applications but from a more technical point of view. I would like to present in a rather general way how polarization effects can be described in the analysis of reactions, and then show in some details, on a few particular examples, how the use polarized targets may bring further and most valuable information on reaction processes. In so doing, I shall select examples only in the field of high energy physics, many applications of polarized target to low energy reactions being presented in details by Prof. Noyes [5]. I shall further stay on a strict phenomenological basis. In particular I shall come back in some details on the full determination of the meson-baryon scattering amplitudes but leave to Prof. Phillips [6] to explain why their knowledge is so important in the framework of present theoretical model.

DEFINITION AND PROPERTIES OF SPIN AMPLITUDES

The exact invariance properties associated with the isotropy of space and time reduce the analysis of a collision process to the knowledge of a rather small number of independent amplitudes.

A two-body scattering of particles without spin is described by one amplitude. It is usually expended, in the center of mass frame, in terms of partial wave amplitudes. This reads :

$$F(W,\cos\theta) = 2 \sum_J (J + \tfrac{1}{2})\, f^J(W)\, P_J(\cos\theta) \qquad (1)$$

where W and θ are respectively the center of mass energy and scattering angle. J stands for the angular momentum (fig. 1).

If the particles have spin, it is necessary to introduce an amplitude for each spin arrangement or polarization state. It has presently become rather usual to label these states by the helicity of each particle. The helicity, λ, is defined as the component of the spin on the momentum*. Relation (1) is thus replaced by a set of $(2S_1 + 1)(2S_2 + 1)(2S_3 + 1)(2S_4 + 1)$ relations which we write :

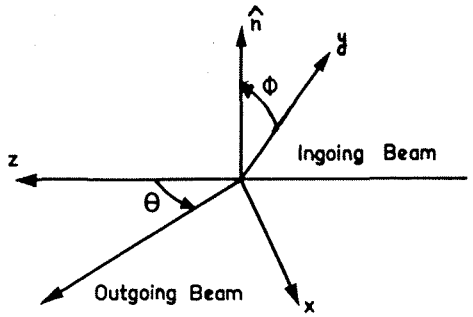

Fig. 1 Two body collision. $\hat{n}$ stands for the normal to the reaction plane. It is obtained from a fixed y axis through a rotation of angle Φ around the z axis. The final direction is obtained from the z axis through a rotation of angle θ around $\hat{n}$.

$$F_{\lambda_3\lambda_4,\lambda_1\lambda_2}(W,\theta,\Phi) = \sum_J (J+\tfrac{1}{2})\, f^J_{\lambda_3\lambda_4,\lambda_1\lambda_2}(W)\, d^J_{\Lambda_i\Lambda_f}(\theta)\, \exp\,(i(\Lambda_i-\Lambda_f)\Phi) \qquad (2)$$

It corresponds to the partial wave expansion of each helicity amplitude F. Φ denotes the azimuthal scattering angle. $\lambda_1\lambda_2,\lambda_3\lambda_4$ are respectively the helicities of the initial and final particles of spins S_1, S_2 and S_3, S_4. $\Lambda_i = \lambda_1 - \lambda_2$; $\Lambda_f = \lambda_3 - \lambda_4$.

Relations (1) or (2) incorporate all the simplifications brought by invariance under the Poincaré group and their difference in structure just translate the so-called complications due to spin. Such complications are sometimes referred to as unessential. What is meant by this qualification is that the theoretical description of reactions involving particles with spin does not seem to require new dynamical concepts besides those which provide the framework for our understanding of collisions between spinless particles. The introduction of spin brings as well known many complications which could be of a pure kinematical and computational nature.

The basic interest of relations (1) and (2) is that in many practical cases the series expansion is very quickly convergent and a reasonable number of partial wave amplitudes only actually matter. One therefore benefits from the simple unitarity properties of partial wave amplitudes.

Relations (1) and (2) also cover two body decays. In this particular case only one value of J is relevant and Λ_i runs across 2S + 1 values, according to the polarization of the initial particle.

Even though most inelastic collisions above 1 GeV involve more than

two final particles, many such reactions are in effect two body processes in which a resonant state, or two resonant states, are produced. These resonances quickly decay and most frequently do so into a two body state which might involve an unstable particle. Among such processes we may mention reactions such as :

$$\pi + N \rightarrow \rho + N^* \qquad (a) \qquad (3)$$

followed by :

$$N^* \rightarrow N + \pi \qquad (b) \qquad \text{and} \qquad \rho \rightarrow \pi + \pi \qquad (b')$$

or

$$\begin{aligned} K^- + N &\rightarrow K^0 + \Xi^*(1530) && (a) \\ \Xi^*(1530) &\rightarrow \Xi + \pi && (b) \\ \Xi &\rightarrow \Lambda + \pi && (c) \\ \Lambda &\rightarrow N + \pi && (d) \end{aligned} \qquad (4)$$

The detailed analysis of such many-steps processes extends the application of two body amplitudes such as (1) and (2) to a large and new domain [7]. This warrants our singling them out in the present discussion.

In order to use an expansion such as (2) it is important to state first the relations among the different spin amplitudes which follow from possible parity, P, and time reversal, T, invariance. It is obvious that the helicity changes sign through a space inversion and does not through a time inversion. A detailed calculation gives the following relations [8] :

$$f^J_{-\lambda_3-\lambda_4;-\lambda_1-\lambda_2}(W) = \eta_g \, f^J_{\lambda_3\lambda_4;\lambda_1\lambda_2}(W) \qquad (5)$$

with

$$\eta_g = \frac{\eta_3 \eta_4}{\eta_1 \eta_2} (-1)^{S_3 + S_4 - S_1 - S_2}$$

when parity invariance holds (η_i stands for the intrinsic parity of particle i), and :

$$f^J_{\lambda_3\lambda_4;\lambda_1\lambda_2}(W) = f^J_{-\lambda_1-\lambda_2;-\lambda_3-\lambda_4}(W) \qquad (6)$$

when time reversal invariance is satisfied.

A further relation holds for collisions between identical particles namely :

$$f^J_{\lambda_3\lambda_4;\lambda_1\lambda_2}(W) = f^J_{\lambda_4\lambda_3;\lambda_2\lambda_1}(W)$$

with a similar relation to translate charge conjugation invariance for reactions involving a particle and its anti-particle.

Phase conventions relevant for these relations as well as for the calculation of any polarization are defined a stated in details in reference 8**.

Relations such as (5) and (6) highly reduce the number of independent amplitudes when the pertinent invariance property hold. We illustrate this general property on the well known example of nucleon-nucleon scattering. The 16 different spin amplitudes are displayed on a 4 x 4 array according to the values of the helicities (+1/2 or -1/2). For each value of J, we thus obtain :

	$+\frac{1}{2},+\frac{1}{2}$	$+\frac{1}{2},-\frac{1}{2}$	$-\frac{1}{2},+\frac{1}{2}$	$-\frac{1}{2},-\frac{1}{2}$
$+\frac{1}{2},+\frac{1}{2}$	f^J_1	f^J_2	f^J_3	f^J_4
$+\frac{1}{2},-\frac{1}{2}$	f^J_5	f^J_6	f^J_7	f^J_8
$-\frac{1}{2},+\frac{1}{2}$	f^J_9	f^J_{10}	f^J_{11}	f^J_{12}
$-\frac{1}{2},-\frac{1}{2}$	f^J_{13}	f^J_{14}	f^J_{15}	f^J_{16}

(7)

Parity invariance implies a symmetry of the array with respect to its center, namely $f^J_i = f^J_{(17-i)}$, when time reversal invariance implies a symmetry with respect to the main diagonal. Parity invariance reduces by a factor 2 the number of independent amplitudes and their combination reduces it from 16 to 6. With two identical nucleons this number is further reduced to 5.

If we go back to (2) we see that relations (5) and (6) relate amplitudes which differ by the values of Λ_i and Λ_f being exchanged

or both changed into their opposite. The various $d^J(\theta)$ functions are very simply related under such transformations [9].

$$d^J_{\Lambda\Lambda'}(\theta) = (-1)^{\Lambda-\Lambda'} d^J_{\Lambda'\Lambda}(\theta) = d^J_{-\Lambda'-\Lambda}(\theta) \qquad (8)$$

these relations do not depend on J, thus, taking proper care of the trivial Φ dependence of the scattering amplitudes F, the equalities obtained among the members of each set of partial wave amplitudes are readily translated in terms of relations among the global spin amplitudes F. Parity invariance gives :

$$F_{-\lambda_3-\lambda_4;-\lambda_1-\lambda_2}(W,\theta,0) = \eta_g(-1)^{\Lambda_i-\Lambda_f} F_{\lambda_3\lambda_4;\lambda_1\lambda_2}(W,\theta,0) \qquad (9)$$

when time reversal invariance implies :

$$F_{\lambda_3\lambda_4;\lambda_1\lambda_2}(W,\theta,0) = (-1)^{\Lambda_i-\Lambda_f} F_{\lambda_1\lambda_2;\lambda_3\lambda_4}(W,\theta,0) \quad . \qquad (10)$$

These relations provide very strong constraints on the observed polarization effects. These constraints can be used either to highly simplify phenomenological analysis or to devise tests for the validity of the corresponding invariance properties. They hold irrespectively of the partial wave expansion (2). They provide basic tools for the determination of the relative phases of the different spin amplitudes, independently of a phase shift analysis rather complicate to carry forward at energies over 1 GeV.

POLARIZATION EFFECTS IN TWO BODY COLLISIONS

The scattering amplitudes, defined in any reference frame, are usually normalized in such a way that the differential cross-section reads :

$$\frac{d\sigma}{d\Omega} = \left| F_{\lambda_3\lambda_4,\lambda_1\lambda_2}(\theta,\Phi) \right|^2 \quad . \qquad (11)$$

This relation is however of little practical use as it stands. In order to reach easily measurable quantities a density matrix formalism is usually introduced. All polarization measurements made on a pure state written as :

$$\sum_{\lambda,\lambda'} C_{\lambda\lambda'} \, | \lambda,\lambda' \rangle$$

may be expressed in terms of a density matrix the elements of which are defined as :

$$\rho_{\lambda\lambda',\mu\mu'} = C_{\lambda\lambda'}\, C^*_{\mu\mu'} \quad . \tag{12}$$

The expectation value of any operator Ω , on such a state, is given by :

$$\langle \Omega \rangle = \sum_{\mu,\mu'} \sum_{\lambda,\lambda'} C^*_{\mu\mu'}\, \Omega_{\mu\mu',\lambda\lambda'}\, C_{\lambda\lambda'}$$

$$= \mathrm{Tr} \left| \Omega \cdot \rho \right| \quad . \tag{13}$$

If we do not have a pure state, but a statistical mixture, we may still describe its polarization properties in terms of an hermitian matrix ρ with is defined such as $\mathrm{Tr}|\rho| = 1$. One also has $\mathrm{Tr}|\rho^2| \leqslant 1$.

If the polarization of the initial state is given in terms of a density matrix $\rho^{(i)}$ the final state density matrix elements will read :

$$\frac{d\sigma}{d\Omega}\, \rho^{(f)}_{\lambda_3\lambda_4,\mu_3\mu_4} = \sum_{\lambda_1\lambda_2,\mu_1\mu_2} F_{\lambda_3\lambda_4,\lambda_1\lambda_2}\, F^*_{\mu_3\mu_4,\mu_1\mu_2}\, \rho^{(i)}_{\lambda_1\lambda_2,\mu_1\mu_2}$$

which gives in matrix notation :

$$\frac{d\sigma}{d\Omega}\, \rho^f(\theta,\Phi) = F(\theta,\Phi)\, \rho^{(i)}\, F^+(\theta,\Phi) \quad . \tag{14}$$

Combining (14) and (13), one readily expresses the result of any polarization measurement, in terms of the scattering amplitudes F and the initial polarization, described by $\rho^{(i)}$. The differential cross-section is the expectation value of an operator Ω , the matrix elements of which are :

$$\Omega_{\mu\mu',\lambda\lambda'} = \delta_{\mu\lambda}\, \delta_{\mu'\lambda'} \quad .$$

More complicated operators are further introduced to reach the polarization of each particle or correlation between polarizations. The polarization of one particle only, of spin S, will be obtained through operators of the type :

$$\Omega_{\mu\mu',\lambda\lambda'} = \omega_{\mu\lambda}\, \delta_{\mu'\lambda'}$$

where ω is a $(2S + 1) \times (2S + 1)$ matrix with zero trace. Our problem is to determine the scattering amplitude F from all feasible

such measurements, using all workable initial polarization states. We shall illustrate with a few examples how this may be practically achieved and how polarized targets can bring most needed and hitherto unaccessible information.

Our purpose here is just to indicate how this may be practically achieved. We refer the reader to the excellent review articles of Wolfenstein [10] and Bilenki, Lapidus and Ryndin [2] for a more detailed and comprehensive discussion. In order to do so we turn to the simplest but also top interesting case.

SPIN 0, SPIN 1/2 SCATTERING

We consider the case of a two body meson baryon reaction, where both initial and final meson have spin zero and both baryons have spin 1/2. We have in mind π-nucleon or K-nucleon collisions and therefore assume that invariance under parity holds. The number of independent amplitudes is thus reduced from 4 to 2 as it follows from (4). Time reversal invariance (5) does not give any further reduction in the case of elastic scattering. We may choose these two amplitudes as the helicity non flip, F_{++} and helicity flip, F_{-+} amplitudes.

Instead of parity invariance, one may use reflection invariance through the scattering plane. Under such an operation Y, the helicity states are transformed according to [8] :

$$Y|\lambda\rangle = \eta\,(-1)^{S-\lambda}|-\lambda\rangle \qquad . \qquad (15)$$

Relation (9) translates the pertinent symmetry property. It relates center of mass as well as laboratory amplitudes. Its consequences, which we now study, lead therefore to the same expressions when written in terms of center of mass or laboratory variables.

As already mentioned by Prof. Jackson, the scattering amplitudes may be written in a matrix form. We write*** :

$$M = f_1(W,\cos\theta)\mathbb{1} + f_2(W,\cos\theta)\ \vec{\sigma}.\hat{p}_f\ \vec{\sigma}.\hat{p}_i \qquad (16a)$$

when the initial and final state have the same intrinsic parity. One would write :

$$M = g_1(W,\cos\theta)\ \vec{\sigma}.\hat{p}_i + g_2(W,\cos\theta)\ \vec{\sigma}.\hat{p}_f \qquad (16b)$$

for the case of opposite intrinsic parity.

$\hat{p}_i$ and $\hat{p}_f$ are unit vectors along the baryon momentum in the initial and final states. (For meson nucleon scattering in the lab system, $\hat{p}_i$ is taken along the direction opposite to the incident beam).

We therefore write in either case :

$$\begin{aligned} F_{++}(\theta,\Phi) &= (f_1 + f_2)\cos\frac{\theta}{2} \\ F_{-+}(\theta,\Phi) &= -(f_1 - f_2)\sin\frac{\theta}{2}\, e^{i\Phi} \end{aligned} \qquad (17a)$$

or

$$\begin{aligned} F_{++}(\theta,\Phi) &= (g_1 + g_2)\cos\frac{\theta}{2} \\ F_{-+}(\theta,\Phi) &= -(g_1 - g_2)\sin\frac{\theta}{2}\, e^{i\Phi} \quad . \end{aligned} \qquad (17b)$$

Parity conservation implies the relations (9) :

$$F_{--} = \eta F_{++} \qquad ; \qquad F_{+-} = -\eta F_{-+}\, e^{-2i\Phi} \qquad (18)$$

where $\eta = +1(-1)$ for a final state with the same (opposite) parity as the initial one.

We define the polarization of the initial particle in terms of a 2 x 2 density matrix :

$$\rho^{(i)} = \frac{1}{2}\,(\mathbb{1} + \vec{\sigma}.\vec{P}^{(i)}) \qquad (19)$$

where $P_x^{(i)}$, $P_y^{(i)}$ and $P_z^{(i)}$ are defined as twice the expectation values of the initial baryon spin components, measured in its rest frame.

For simplicity matter, we take a scattering plane which corresponds to $\Phi = 0$ (fig. 1). The initial density matrix is defined with respect to a direct coordinate system x, y, z with z along the initial baryon momentum p_i, and y along the normal to the reaction plane $p_i \times p_f$ where p_f is the final baryon momentum. Its final density matrix, given by (14) is defined with respect to a different coordinate system x', y', z' with z' along p_f. The use of two separate coordinate systems is associated with our using of helicity states.

This has in effect some intrinsic interest since it provides an easy way to circumvent the technical complications associated with polarization when dealing with relativistic particles. The density matrix $\rho^{(f)}$ obtained from (14) describes just a well the polarization of the final baryon in its rest frame while $\rho^{(i)}$ also describes the polarization of the initial baryon in its rest frame, as they both do in the center of mass system.

Using (19), (14) and (13) one obtains expressions for the differential cross-section and the expectation values of the three components of the final baryon polarization, measured in its rest frame. They are :

$$\begin{aligned}
\frac{d\sigma}{d\Omega}(\theta,0) &= |F_{++}|^2 + |F_{-+}|^2 - 2\eta P_y^{(i)} \operatorname{Im}\{F_{++}F_{-+}^*\} \\
\frac{d\sigma}{d\Omega} P_{x'}^{(f)} &= \eta P_x^{(i)} (|F_{++}|^2 - |F_{-+}|^2) + 2P_z^{(i)} \operatorname{Re}\{F_{++}F_{-+}^*\} \\
\frac{d\sigma}{d\Omega} P_y^{(f)} &= -2\operatorname{Im}\{F_{++}F_{-+}^*\} + \eta P_y^{(i)} (|F_{++}|^2 + |F_{-+}|^2) \\
\frac{d\sigma}{d\Omega} P_{z'}^{(f)} &= -2\eta P_x^{(i)} \operatorname{Re}\{F_{++}F_{-+}^*\} + P_z^{(i)} (|F_{++}|^2 - |F_{-+}|^2)
\end{aligned} \tag{20}$$

These relations exhibit a very important result, already mentioned by Prof. Jackson. It is the simple connection between the polarized cross-section*+ and the polarization (normal to the reaction plane) observed with an unpolarized initial baryon. The relation holds for a well defined energy and scattering angle and reads [10,11,12] :

$$\frac{d\sigma}{d\Omega}(\theta,0) = \frac{\widetilde{d\sigma}}{d\Omega}(\theta,0)\,(1 + \eta P_y P'_y) \tag{21}$$

$\frac{\widetilde{d\sigma}}{d\Omega}$ is the differential cross-section, summed and averaged over polarization that is $|F_{++}|^2 + |F_{-+}|^2$. P is the polarization of the initial baryon. P' is the polarization of the final baryon when the initial baryon is not polarized. The observation of such a polarization - an a priori easy matter when the final baryon is a Λ, Ξ or Σ^+ hyperon - combined with the use of a polarized proton target, thus allows a possible determination of the K-nucleon-hyperon relative parity. It is at present under progress to reach the Ξ [13] and the Σ^+ hyperon parities [14]. We heard about this last experiment from Prof. Chamberlain.

This result is so neat and general that it is worth a simpler explanation.

One may consider an initial state with a "spin up" baryon that is fully polarized normal to a selected reaction plane. The differential cross-section, summed uncoherently over the "spin up" and "spin down" final states, reads :

$$\frac{d\sigma}{d\Omega}(\theta,0) = |g_{++}|^2 + |g_{-+}|^2$$

where g_{++} and g_{-+} are two scattering amplitudes without spin flip and with spin flip. These amplitudes depend on the scattering angles, and $\Phi = 0$ defines scattering to the left in the selected reaction plane. Scattering to the right, with the same polar angle θ, is equal to scattering to the left when the initial state is rotated through an angle π around the incident axis. This simply translates the rotational invariance of the S-matrix. The left right asymmetry therefore reads :

$$\Delta = \frac{L-R}{L+R} = \frac{|g_{++}|^2 + |g_{-+}|^2 - |g_{--}|^2 - |g_{+-}|^2}{|g_{++}|^2 + |g_{-+}|^2 + |g_{--}|^2 + |g_{+-}|^2}$$

were the polarization equal to P instead of 1 the pertinent result would be simply multiplied by P.

On the other hand the polarization, normal to the reaction plane, obtained with an unpolarized initial state is readily written in terms of the same amplitudes. Namely :

$$P^f = \frac{|g_{++}|^2 - |g_{-+}|^2 + |g_{+-}|^2 - |g_{--}|^2}{|g_{++}|^2 + |g_{-+}|^2 + |g_{+-}|^2 + |g_{--}|^2} \quad .$$

Let us then introduce a semi-classical argument. The orbital angular momentum $\vec{\ell}$ is normal to the reaction plane and since the spin is quantized along this axis, the total angular momentum is also normal to the scattering plane with values :

$$J = \ell \pm \frac{1}{2} \qquad \text{(figure 3)} \; .$$

Now J does not change when ℓ should not change or change by one unit ($\hbar$) whether the intrinsic parity of the final state is the same or different from that of the initial state. Therefore if the intrinsic parity does not change, there is no spin flip ($g_{-+} = g_{+-} = 0$) whereas if the intrinsic parity does change, there is only spin flip ($g_{++} = g_{--} = 0$). We therefore write :

$$P^f = \eta \Delta \quad .$$

Relations (16) also show that the information available on the scattering matrix is limited to the knowledge of $|F_{++}|^2 + |F_{-+}|^2$ and $\mathrm{Im}\,|F_{++}F^*_{-+}|$ if the initial baryon is not polarized. This is not exact since a phase shift analysis, which easily incorporates the further constraints given by unitarity may provide a complete determination of the amplitudes.

The center of mass scattering amplitude is usually expended in terms of partial wave amplitudes f_{ℓ_+} and f_{ℓ_-}, where the + (-) subscript is associated to a value of J which is equal to $\ell + \frac{1}{2}$ $(\ell - \frac{1}{2})$. It reads :

$$f_1 = \sum_\ell \left(f_{\ell_+} P'_{\ell+1}(\cos\theta) - f_{\ell_-} P'_{\ell-1}(\cos\theta)\right)$$
$$f_2 = \sum_\ell \left(f_{\ell_-} - f_{\ell_+}\right) P'_\ell(\cos\theta) \qquad (22)$$

P' stands for the first derivative of the Legendre polynomial of order ℓ.

In terms of the helicity amplitudes previously introduced, one has :

$$f_{\ell_+} = f^J_{++} + f^J_{-+}$$
$$f_{(\ell+1)_-} = f^J_{++} - f^J_{-+} \qquad (23)$$

As a matter of fact it is now much more convenient to observe an asymmetry using a polarized target than to determine the polarization of the recoil nucleon and we heard how important progresses have been thus made possible in the analysis of π-nucleon phase shifts [15]. We also heard about the very important polarization effects which have been observed in π-nucleon elastic and charge exchange scattering on a polarized target [3].

Such an analysis is however very difficult to carry out much above 1 GeV where many partial wave contribute and inelasticity is very large. Scattering on polarized targets is then a must to determine both amplitudes.

As seen on (16) the information obtained when the target nucleon is polarized normally to the reaction plane is formaly equivalent to what is obtained when the polarized cross-section is analyzed. We may further use initial polarization in the reaction plane. Four quantities may be thus measured. The x' polarization when the initial baryon is polarized along the z axis is written in terms of a parameter A defined by :

$$\frac{\widetilde{d\sigma}}{d\Omega} A = 2\mathrm{Re}\left| F_{++} F^{*}_{-+} \right| \qquad (24a)$$

R gives the x' polarization when the initial baryon is polarized along the x axis :

$$\frac{\widetilde{d\sigma}}{d\Omega} R = \eta \left(|F_{++}|^2 - |F_{-+}|^2 \right) \qquad (24b)$$

$$P^{(f)}_{x'} = A\, P^{(i)}_{z} + R\, P^{(i)}_{x} \qquad (24c)$$

The z' polarization respectively obtained with an initial polarization along the z or x axis provide two further quantities which are written as :

$$P^{(f)}_{z'} = A'\, P^{(i)}_{z} + R'\, P^{(i)}_{x} \quad . \qquad (25)$$

It is however obvious from (20) that in the particular case of π-nucleon scattering :

$$A' = \eta R \qquad \text{and} \qquad R' = -\eta A \quad . \qquad (26)$$

A still further quantity may be considered. The y polarization obtained from an initial y polarization. This relation defines another coefficient D :

$$P^{(f)}_{y} = D\, P^{(i)}_{y} + P_o \qquad (27)$$

which is equal to η in the case of spin 0, spin 1/2 scattering. P_o is the polarization obtained with an unpolarized target. More generally all five quantities are the non vanishing elements of the depolarization tensor introduced by Wolfenstein [10] (fig. 2).

Nucleon-nucleon scattering is the next complicated state. The discussion can be carried out along the same lines as what we just did for meson-nucleon scattering. Nevertheless, the larger number of independent amplitudes (5 for each isotopic spin state and 6 if we take into account isotopic spin violation) makes the algebra much more cumbersome if not more difficult to carry forward. We refer the reader to the review articles of Wolfenstein [10] and Bilenkii, Lapidus and Ryndin [2] for a comprehensive discussion. We merely list here the various typical experiments performed in this case, using polarized nucleon targets but also polarized nucleon beams.

The simplest one is of course the differential cross-section when no particle is polarized and when no polarization is observed.

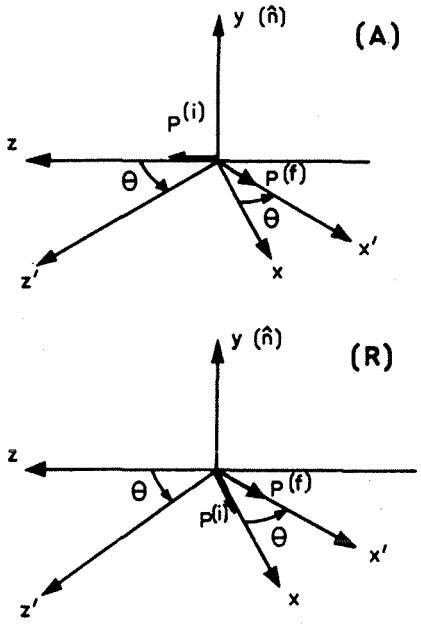

Fig. 2 Definition of the A and R parameters in spin 1/2, spin 0, two body scattering, z and z' respectively stand for the direction of the spin 1/2 particle in the initial and final state.

Next comes the polarization of either final particle when neither is initially polarized, or the polarized cross-section when one particle is polarized. There is of course a complete symmetry between both particles when charge independence holds (no singlet-triplet transition). The next complicated case is the determination of the depolarization coefficients when one nucleon is polarized in the initial state and the polarization of one nucleon only is measured in the final state. Here again one introduces the five Wolfenstein's parameters which are the non zero elements of the depolarization tensor D_{ij} : A, R, A', R' and D with now only one single relation among them [2,10].

The polarization of the other nucleon, observed with the same initial configuration is defined in an identical way through a polarization transfer tensor K_{ij}, with four independent elements also.

The next step involves a spin correlation in the initial or final state. The contribution to the cross-section which is associated to a correlation between the polarization of the beam and of the target (bilinear in the two polarizations) or the correlation between the two polarizations reached with an unpolarized beam and target are given in terms of the symmetrical "correlation tensor"

C_{ij} [2]. C_{nn} refers to both target and beam polarizations normal to the reaction plane.

More complicated experiments may be considered with polarization (polarization correlation) measurements as a result, of an initial polarization correlation (polarization). Nevertheless the afore mentioned quantities are already redondant to determine the five independent scattering amplitudes [2]. Prof. Phillips will show why some particular measurements are particularly important to make.

We now go back in some more details to the case of π-nucleon scattering.

PION-NUCLEON SCATTERING

In the particular case of π-nucleon collisions, $\eta = 1$, we go back to (20) and calculate the two scattering amplitudes f_1 and f_2 in terms of the parameters just introduced. This is straightforward procedure. One gets :

$$|f_1|^2 = \frac{\tilde{d\sigma}}{d\Omega} \frac{(1 - R \cos\theta - A \sin\theta)}{2 \sin^2\theta}$$

$$|f_2|^2 = \frac{\tilde{d\sigma}}{d\Omega} \frac{(1 - R \cos\theta + A \sin\theta)}{2 \sin^2\theta}$$

$$\mathrm{Re}\,|f_1 f_2^*| = \frac{\tilde{d\sigma}}{d\Omega} \frac{R - \cos\theta}{2 \sin^2\theta} \quad . \tag{28}$$

To which we ad :

$$\mathrm{Im}\,|f_1 f_2^*| = -\frac{P_o}{2 \sin\theta} \frac{\tilde{d\sigma}}{d\Omega}$$

the amplitudes f_1 and f_2 are often combined into a non spin flip G, and spin flip H amplitudes, with :

$$G = f_1 + f_2 \cos\theta$$

$$H = -f_2 \sin\theta \tag{29}$$

So that the scattering matrix (13a) reads : $M = G\,\mathbb{1} + iH\,\vec{\sigma}.\vec{n}$, where $\vec{n}$ is a unit vector along the normal to the reaction plane. Relations (22) and (23) are combined to give [2] :

$$|G|^2 = \frac{1}{2}\frac{\tilde{d\sigma}}{d\Omega}(1 + R\cos\theta - A\sin\theta)$$

$$|H|^2 = \frac{1}{2}\frac{\tilde{d\sigma}}{d\Omega}(1 - R\cos\theta + A\sin\theta)$$

$$\mathrm{Im}\,|GH^*| = \frac{1}{2}\frac{d\sigma}{d\Omega}P_o$$

$$\mathrm{Re}\,|GH^*| = -\frac{1}{2}(A\cos\theta + R\sin\theta) \quad . \qquad (30)$$

Both amplitudes are thus obtained in magnitude an sign*++ and we shall hear from Prof. Phillips [6] why such a determination is extremely important in view of the various models which are at present proposed to describe high energy meson nucleon scattering.

It may be of interest to describe an experiment in which the mere presence of the spin flip amplitude is determined. One may take a polarized target with polarization in the scattering plane and test a possible asymmetry in a plane normal to the reaction plane for the scattering of the recoil nucleon, when the events are chosen in such a way that the recoil nucleon flies off in the direction of the polarization of the target (fig. 4).

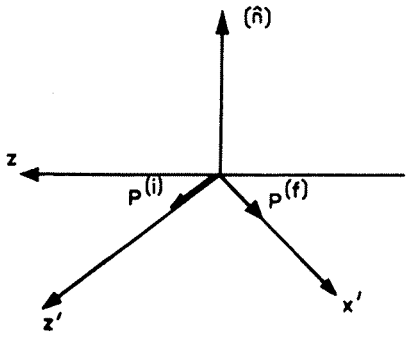

Fig. 4 A particular experiment sensitive to the spin flip amplitude.

In this case $P_x^{(i)} = P_o \sin\theta$, $P_y^{(i)} = 0$ and $P_z^{(i)} = P_o\cos\theta$. One obtains from (20) :

$$\frac{d\sigma}{d\Omega} P_{x'}^{(f)} = 2P_o \sin\theta(\cos\theta\ |f_2|^2 + \mathrm{Re}\ f_1 f_2^*)$$

$$= -\ 2P_o\ \mathrm{Re}\ |GH^*| \quad . \tag{31}$$

DETERMINATION OF SPINS AND PARITIES

We go back to a production and decay scheme such as the ones mentioned earlier and investigate the possible ways to determine the spin and parity of a new particle. The particle is assumed to be produced in a two body collision and in order to illustrate the general method we consider a reaction of the type (4) :

$$K + p \rightarrow Y^* + \pi$$

where Y* stand for an hyperon with two body decay :

$$Y^* \rightarrow Y + \pi$$

Y is a spin 1/2 baryon (Ξ , Σ or Λ), the polarization of which may be obtained from its decay asymmetry. Using (2) one readily derives the angular distribution and polarization distribution of Y in the Y* rest frame. They are both expressed in terms of the Y* density matrix, and read [16] :

$$I(\theta',\Phi') = |G|^2 \sum_{ij} \rho_{ij}^{Y^*}(\theta,\Phi)$$
$$\times\ e^{(i-j)\Phi'}\left(d^S_{i\frac{1}{2}}(\theta')\ d^S_{j\frac{1}{2}}(\theta') + d^S_{i-\frac{1}{2}}(\theta')\ d^S_{j-\frac{1}{2}}(\theta')\right)$$

$$I\ P_L(\theta',\Phi) = |G|^2 \sum_{ij} \rho_{ij}^{Y^*}(\theta,\Phi) \tag{32}$$
$$\times\ e^{(i-j)\Phi'}\left(d^S_{i\frac{1}{2}}(\theta')\ d^S_{j\frac{1}{2}}(\theta') - d^S_{i-\frac{1}{2}}(\theta')\ d^S_{j-\frac{1}{2}}(\theta')\right)$$

$$I\ P_T(\theta',\Phi) = \varepsilon(-1)^{S+\frac{1}{2}} |G|^2 \sum_{ij} \rho_{ij}^{Y^*}(\theta,\Phi)$$
$$\times\ e^{(i-j)\Phi'}\left(d^S_{i\frac{1}{2}}(\theta')\ d^S_{j-\frac{1}{2}}(\theta') + d^S_{i-\frac{1}{2}}(\theta')\ d^S_{j\frac{1}{2}}(\theta')\right) \quad .$$

The process is described with two sets of angles. The Y* direction is defined by the angles θ and Φ . The Y* polarization is described with respect to a set of axis associated with the production reaction. We may choose the z axis along the Y* momentum or along the normal to the production plane. The Y direction, in the Y* rest frame is specified by the angles θ' and Φ' defined with respect to this set of axis (fig. 5). The longitudinal and transversal polarization of Y are denoted by P_L and P_T. The spin and parity (relative to Y) of the Y* hyperon are denoted by S and ε . The set of relations (34) translates parity invariance in Y* decay. As a result of parity invariance there is only one decay amplitude, G. The transverse polarization of the decay baryon is the only decay parameter sensitive to the parity.

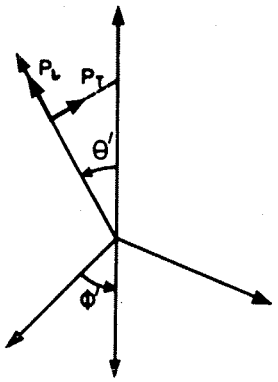

Fig. 5 Y* resonance two body decay. The Y direction is specified by the angles θ' and Φ'. P_L and P_T are its longitudinal and transversal polarizations.

In order to illustrate the types of tests available, and with little loss of generality, the relations just obtained (32) may be averaged over Φ'. It is obvious then that both P_L and P_T change sign with reversal of the vectorial polarization of the Y* hyperon ($m \leftrightarrow -m$) when the angular distribution does not. To see this just remember (8) :

$$d^S_{m\frac{1}{2}}(\theta') = (-1)^{m-\frac{1}{2}} d^S_{-m-\frac{1}{2}}(\theta')$$

$$d^S_{m-\frac{1}{2}}(\theta') = (-1)^{m+\frac{1}{2}} d^S_{-m+\frac{1}{2}}(\theta') \quad .$$

In order to observe a polarization of the daughter particle the Y* polarization must be not zero. Provided this is true one may obtain

the values of the spin and the parity by measuring the various moments of the decay and polarization distributions, as proposed by Byers and Fenster [17]. In particular one finds [16] :

$$R_1 = \frac{\langle P_L(\theta',\Phi')\ I(\theta',\Phi')\ \cos\theta' \rangle}{\langle P_T(\theta',\Phi')\ I(\theta',\Phi')\ \sin\theta' \rangle} = \varepsilon(-1)^{J-\frac{1}{2}} \frac{1}{2J+1} \qquad (33)$$

where the bracket symbol implies an averaged over the decay angles θ' and Φ'.

Such tests will be of little practical use if the Y* vectorial polarization is small, which might well be the case for high energy, mainly backwards, productions. Polarized targets may however be useful in order to provide the needed polarization. Present targets do not meet the required conditions but in view of their very rapid development such possibility are worth mentioning.

An other very interesting point is the simple connection which could be obtained between the particle and polarization distributions. This was pointed out by M. Gaillard [18]. As previously mentioned the angular distribution is obtained from the production parameters $\rho^{Y*}_{mm} + \rho^{Y*}_{-m-m}$ when the polarization distribution is obtained from the different set of parameters $\rho^{Y*}_{mm} - \rho^{Y*}_{-m-m}$.

It should be remarked however [18] that they may be both expressed in terms of a common set of parameters provided the initial proton is polarized. The key point is that parity invariance implies that transitions between a proton, with spin up along the normal to this plane, and a Y* are forbidden for half of the Y* spin state. This may be understood in a semi-classical way as shown on figure 3. $\vec{J}$ and $\vec{\ell}$ (orbital momentum) are classicaly parallel with $\vec{J} = \vec{\ell} + \vec{S}$. A change in ℓ by an odd number of $\hbar$ corresponds to a change in intrinsic parity when a change in ℓ by an even number of $\hbar$ is associated to no change in parity. The spin component along the normal follows the changes in ℓ.

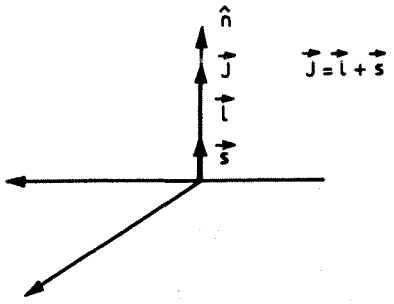

Fig. 3 Spin, orbital and total angular momentum in a semi-classical picture.

The calculation must nevertheless be done properly with the result [18].

$$\rho^{Y*}_{mm} = \frac{1}{2} |a_m|^2 \left(1 + \varepsilon(-1)^{m-\frac{1}{2}} P_o\right) \qquad (34)$$

where ε is the relative intrinsic parity between the initial and final states and P_o the proton polarization along the normal to the reaction plane. It follows that :

$$\rho^{Y*}_{mm} + \rho^{Y*}_{-m-m} = \frac{1}{2}\left[\left(|a_m|^2 + |a-m|^2\right) + \varepsilon(-1)^{m-\frac{1}{2}} P_o\left(|a_m|^2 - |a-m|^2\right)\right]$$

and (35)

$$\rho^{Y*}_{mm} - \rho^{Y*}_{-m-m} = \frac{1}{2}\left[\left(|a_m|^2 - |a-m|^2\right) + \varepsilon(-1)^{m-\frac{1}{2}} P_o\left(|a_m|^2 + |a-m|^2\right)\right]$$

$$P_o = \vec{P}.\hat{n} = P.\cos\Phi$$

All the production parameters may then be determined from the decay angular distribution alone with a well defined prediction for the polarization distribution, and this, for each proposed value of the spin and parity.

We refer the reader to reference [18] for a very detailed discussion of the method as well as its applications to the production of boson resonance (3). A similar analysis is possible. It involves the correlation between the boson decay distribution and the recoil baryon polarization.

The increasing importance of hadronic spectroscopy gives a great interest to such general methods.

TEST OF INVARIANCE PRINCIPLES

The symmetries postulated for the physical laws highly reduce the number of spin amplitudes. We have seen how parity invariance and time reversal invariance may be used to obtain many equalities among the different amplitudes. Conversely a more and more extensive analysis of polarization phenomena which are, as we have seen on some examples, much sensitive to these equalities, will provide further tests for the pertinent symmetry properties. In so doing polarized targets will offer a most interesting tool. Test for pa-

rity invariance are relatively easy to think of but are not expected to be practically interesting in the near future. On the other hand the recent observation of CP violating effects [19] has lead to question time reversal invariance in processes as important as the electromagnetic ones [20]. We will therefore consider in some details one such possible test which has already been mentioned by Prof. Jackson that is the electro-production of N* isobars on a polarized proton target [21]. Elastic scattering does not provide any test for time reversal invariance [20].

The principle of the experiment is the following. One scatters electrons off a polarized target and analyze their energy spectrum at a fixed production angle. The N* peak, due to production on the target proton will stand above a background produced by the target compound nuclei, and its magnitude should change with inversion of the polarization of the target, were time reversal invariance violated.

The electroproduction is known to proceed mainly through a one photon exchange (fig. 6) and the N*Nσ vertex (with a virtual σ-ray) involves 3 form factors which may be conveniently related to the matrix elements of the electromagnetic current between the various initial and final helicity states. We follow the choice of Christ and Lee [21] and define them as :

$$F_{\pm} = \pm \langle N^*, \tfrac{1}{2} \pm 1 | \, (J_x(0) \pm i \, J_y(0)) \, | N, \tfrac{1}{2} \rangle$$

$$F_z = \langle N^*, \tfrac{1}{2} \; J_z(0) \; | N, \tfrac{1}{2} \rangle \quad . \tag{36}$$

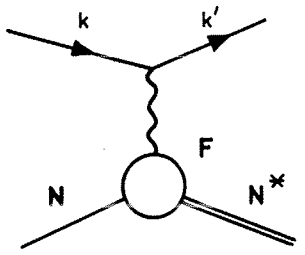

Fig. 6 N* electroproduction in the one photon exchange approximation.

We take the z axis along the isobar momentum and the y axis along the normal to the reaction plane. We obtain the other matrix elements through parity invariance (7). Namely :

$$\langle -\lambda' | J_z(0) | -\lambda \rangle = \eta (-1)^{S-\frac{1}{2}} (-1)^{\lambda-\lambda'} \langle \lambda' | J_z(0) | \lambda \rangle$$

$$\langle -\lambda' | (J_x(0) \pm i J_y(0)) | -\lambda \rangle = \eta (-1)^{S-\frac{1}{2}} (-1)^{\lambda-\lambda'} \langle \lambda' | (J_x(0) \mp i J_y(0)) |$$

where S is the N* spin and η stands for the NN* relative parity. W also use current conservation, namely :

$$p\langle N^*, \tfrac{1}{2} J_z(0) | N, \tfrac{1}{2} \rangle = -i(\sqrt{p^2+M^2}-m) \langle N^*, \tfrac{1}{2} | J_4(0) N, \tfrac{1}{2} \rangle$$

where p is the isobar momentum and where M and m are respectively the isobar and nucleon mass.

Any polarization effect will involve an interference between such amplitudes, and, in particular, it is easy to see that the contribution to the differential cross-section which is proportional to the nucleon polarization normal to the reaction plane, will involve only terms proportional to Im $\{ F_-^* F_z \}$. It should correspond to the same isobar helicity and correspond to an interference term between the +1/2 and -1/2 helicity states of the initial nucleon. Now if time reversal invariance holds all F's are relatively real and no such effect should be observed. Conversely the observation of the pertinent effect would be a direct proof of time reversal non-invariance in electromagnetic interactions*+++.

More precisely one finds that the isobar production cross-section reads :

$$\frac{d\sigma}{d \cos\theta} = \frac{2\pi \alpha^2 k'}{2k\, m^2 q^2} \frac{M^2 + m^2 + q^2}{1 + \frac{2k}{m} \sin^2 \frac{\theta}{2}} \left\{ 2R_1 + R_2 \cot g^2 \frac{\theta}{2} + P_o \frac{k^2 - k'^2}{m^2} R_3 \cot g \frac{\theta}{2} \right\} \quad (37)$$

P_o is the target proton polarization, normal to the reaction plane. k and k' are the initial and final electron momenta, θ is the scattering angle and q^2, the momentum transfer squared is given by :

$$q^2 = 4 kk' \sin^2 \frac{\theta}{2} \quad .$$

The electron mass has been neglected.

We have introduced three parameters :

$$R_1 = |F_+|^2 + |F_-|^2$$

$$R = \frac{q^2}{p^2} \left(|F_+|^2 + |F_-|^2 + \frac{4m^2 q^2}{(M^2 - m^2 + q^2)^2} |F_z|^2 \right)$$

and

$$R_3 = 2\varepsilon \, \mathrm{Im} \left| F^*_- F_z \right| \frac{4m^4 q^2}{p^2 (M^2 - m^2 + q^2)^2}$$

ε is the relative N*N parity time a factor + (-1) according to an even (odd) difference in spin between N and N*. For instance $\varepsilon = -1$ for the N* (1240) and $\varepsilon = +1$ for the N* (1520).

The interesting effect is the asymmetry obtained with up and down polarization :

$$\Delta = \frac{\sigma(\mathrm{up}) - \sigma(\mathrm{down})}{\sigma(\mathrm{up}) + \sigma(\mathrm{down})} = \frac{(k^2 - k'^2) \, R_3 \, \mathrm{cotg} \, \frac{\theta}{2}}{m^2 (2R_1 + R_2 \, \mathrm{cotg}^2 \, \frac{\theta}{2})} \quad . \qquad (38)$$

The hypothesis of a possible non invariance under T (or C according to PCT invariance) in electromagnetic interactions had already a short but hectic career. Recent results on η decays [22] show that if T invariance is violated (as compared to the present experimental accuracy) it is not likely so in interactions where the isotopic spin changes by one unit. Hence one should not expect any effect in N* (1240) electroproduction which would have seemed to be a few months ago, the best candidate for such a test. One should therefore consider at least N* (1520) or N* (1680) production which barely point out off the bremsstrahlung background, even in production on hydrogen [23].

This is probably not feasible at present and the same remark may also well apply to several of the applications previously mentioned. Nevertheless it is almost certain that the huge progresses made in polarized target techniques, which we have had the pleasure to witness here, may soon bring such experiments into the realm of possibility.

Notes and References

* The important thing is not that we use helicities but that the polarization of each particle is separately described. For a massive particle one readily shifts from helicity amplitudes to any set of amplitudes associated with a rest system description of the polarization.

** In particular, each helicity state with momentum direction θ and Φ is obtained from a standard state with momentum direction 0 and 0, through a rotation defined with the Euler angles Φ, θ and $-\Phi$.

*** 1 stands for the 2x2 unit matrix. The standard Pauli matrices denoted by σ_i are :

$$\sigma_x = \begin{pmatrix} 0 & 1 \\ 1 & 0 \end{pmatrix} \quad , \quad \sigma_y = \begin{pmatrix} 0 & -i \\ i & 0 \end{pmatrix} \quad , \quad \sigma_z = \begin{pmatrix} 1 & 0 \\ 0 & -1 \end{pmatrix}$$

*+ As seen on (17) changing Φ from 0 to π just adds an extra factor (-1) to η. One can therefore describe the polarized cross-section in terms of a left right asymmetry in a given reaction plane.
*++ Both amplitudes are determined up to an unobservable common phase. This ambiguity is associated with the fact that unitarity gives further constraints which involve much more than the elastic reaction which is singled out here.
*+++ The effect should of course be big enough so that the two photon exchange contribution could not be held responsible for it.

1) R. Omnes and R. Stora, "Sur les applications possibles d'une cible de noyaux polarisés en physique des hautes énergies", Saclay Report n° 646, 1960 (unpublished).
2) S.M. Bilenkii, L.J. Lapidus and R.M. Ryndin, Usp. Fiz. Nauk, 1964, 84, 243 or Soviet Phys. Usp., 1965, 7, 721. This review article contains a very large number of further references.
3) L. Dick et al, Proceedings of the Berkeley Conference (1966). P. Sonderegger et al, Proceedings of the Berkeley Conference (1966).
4) J.D. Jackson, Invited paper to this Conference.
5) P. Noyes, Invited paper to this Conference.
6) R. Phillips, Invited paper to this Conference.
7) See for instance J.D. Jackson, "Particle and polarization angular distribution in two and three body decays", Les Houches Lecture Notes (1965), (Gordon and Breach, New York, 1966).
8) M. Jacob and G.C. Wick, Ann. Phys. (N.Y.), 1959, 7, 404.
9) See for instance M.E. Rose, "Elementary theory of angular momentum", (John Wiley, New York, 1957).
10) L. Wolfenstein, "Polarization of fast nucleons", Ann. Rev. Nucl. Sci., 1956, 6, 43.
11) L. Wolfenstein and J. Askin, Phys. Rev., 1952, 85, 947.
12) R.H. Dalitz, Proc. Phys. Soc., 1952, A65, 175.
13) CERN experiment on Ξ parity.
14) Berkeley experiment on Σ^+ parity, O. Chamberlain, (This Conference).
15) S. Surwa et al, Phys. Rev. Letters, 1965, 15, 560. P.J. Duke et al, Nimrod Report (1966).
16) S. Berman and M. Jacob, Phys. Rev., 1965, 139B, 1023 and SLAC Report 43, 1965 (unpublished). M. Jacob, Hercegnovi Lecture Notes (1961).
17) N. Byers and S. Fenster, Phys. Rev. Letters, 1963, 11, 52.
18) M.K. Gaillard, Nuovo Cimento, 1964, 32, 1306 and CERN Report 64-33 (1964).
19) J.H. Christenson et al, Phys. Rev. Letters, 1964, 13, 138.

20) J. Bernstein, G. Feinberg and T.D. Lee, Phys. Rev., 1965, 139B, 1650.
21) N. Christ and T.D. Lee, Phys. Rev., 1966, 143, 1310.
22) Proceedings of the Berkeley Conference (1966).
23) For estimates of the different form factors for several isobars, we refer the reader to : J.D. Björken and J.D. Walecka, Ann. Phys. (N.Y.), 1966, 38, 35.

SOME POLARIZED TARGET EXPERIMENTS FOR ELEMENTARY PARTICLE PHYSICS

R.H. DALITZ

Department of Theoretical Physics, Oxford

1 INTRODUCTION

At the present stage in elementary particle physics, there are three major areas of phenomena where the use of polarized targets may lead to especially illuminating information.

a. High energy scattering, in the energy range where the dominant contributions to the processes observed may arise from Reggion exchange. The features of particular interest in these situations will be discussed at this meeting by Dr R.J.N. Phillips [1].

b. Tests of time-reversal (T) invariance for electromagnetic processes, following the suggestion by Bernstein et al [2] that the CP-violation observed in the weak decay of kaons arises from the existence of an electromagnetic interaction which strongly violates T-invariance. Evidence for this hypothetical T-violating electromagnetic interaction can be sought most directly in the study of electromagnetic processes from a polarized proton target, for example in the study of the electro-excitation process $e + N \rightarrow e + N^*$, as discussed by Christ and Lee [3]. The experiments proposed will be discussed at this meeting by Dr M. Jacob [4].

c. Hadron spectroscopy. Very many resonant states have been observed for mesonic and baryonic states. These hadronic states are believed to correspond to the patterns appropriate to unitary multiplets of states, and these unitary multiplets appear to be grouped in supermultiplet patterns. In our attempt to classify and understand all these hadronic states, our first need is for the determination of the spin and parity for each state. A general survey of the methods available for their determination will be given at

this meeting by Dr M. Jacob [4]. In this talk, we wish to discuss briefly some particular situations of interest, in order to illustrate the kinds of experiment which appear especially relevant at present.

2 RESONANCE FORMATION EXPERIMENTS

The additional information made available by the use of polarized targets is especially valuable in the case of resonant states which may be formed by direct collisions. Such "resonance formation experiments" are possible only for resonance states for which there is an entrance channel corresponding to a conveniently long-lived particle ($\pi^{\pm}$, $K^{\pm}$, K^{0}_{2}, p, n or $\bar{p}$) incident on a proton or neutron target. We shall discuss the situations briefly in turn.

The <u>πN system</u> has already been much studied in the resonance region. Polarized target experiments have been reported for $\pi^{+}p$ and $\pi^{-}p$ elastic scattering up to N* mass about 2200 MeV, as summarized by Dr O. Chamberlain [5] at this meeting. The πN scattering processes are described by two amplitudes :

$$S_I = f_I + i g_I \, \underline{\sigma}.\underline{n} \qquad (2.1)$$

for total isospin I = 1/2 and 3/2, and it is possible to carry out analysis on the basis of these $\pi^{\pm}$-p elastic scattering data alone. However it will also be desirable to have available the angular distribution and polarization data for the charge exchange process $\pi^{-}p \rightarrow \pi^{0}n$, which is governed by the difference $(S_{3/2}-S_{1/2})$, in order to allow a unique phase shift analysis for the πN system. Lovelace [6] has recently emphasized that these charge-exchange experiments would be of more immediate value for this purpose than the more difficult spin correlation experiments, involving measurement of the Wolfenstein R and A parameters.

Polarization studies of inelastic processes may also prove to be important, especially for those N* resonances which happen to have small partial width for the πN channel. The reaction $\pi^{-}p \rightarrow n\eta$ is a rather convenient example, which may be studied at the same time as the charge-exchange process ; at least one resonance, the $(1/2^{-})$ $N^{*}_{1/2}$ (1540) resonance which leads to the strong nη threshold production, is known to have particularly large partial width for the nη channel. Other reactions of the same kind are $\pi^{-}p \rightarrow \Lambda K^{0}$, which also selects I = 1/2 N* states, and the various reactions $\pi N \rightarrow \Sigma K$, especially the process $\pi^{+}p \rightarrow \Sigma^{+}K^{+}$ which se-

lects I = 3/2 N* states. The ΛK^0 and Σ^+K^+ reactions just mentioned are of particular interest in that a polarization analysis of the final state is readily available in consequence of the strong polarization dependence of the decay processes $\Lambda \to p\pi^-$ and $\Sigma^+ \to p\pi^0$. Some polarization analyses of these reactions have already been carried out on this basis, without the use of polarized targets, but these have not been sufficient for a unique analysis of the reaction amplitudes. Marked oscillations in the ΛK^0 polarization angular distribution have been reported in bubble-chamber data analysed by Schwartz [7], for pion momenta about 1500-1700 MeV/c, which are probably associated with an $N^*_{1/2}$ resonance not otherwise known [8]; however, the statistics available even from such large bubble-chamber experiments are not sufficient to determine the details of the phenomena with sufficient precision for a definite interpretation. An investigation of this reaction with a polarized target, together with polarization observations for the final Λ particle, would be of particular interest, in that this situation would allow a complete determination of the spin properties for this reaction. For the Σ^+K^+ reaction, polarization effects have been reported which are associated with the resonance $N^*_{3/2}$ (1920), although the statistics in these bubble-chamber experiments are relatively limited, and these have been interpreted by Holladay [9] in terms of interference between resonant and peripheral production amplitudes to give support for the assignment $(7/2^+)$ for the spin-parity of this state. A more adequate study of the polarization properties of this Σ^+K^+ reaction could be made also for the higher $N^*_{3/2}$ states, with the use of polarized targets.

For the $\bar{K}N$ system, there are two elastic amplitudes $\bar{S}_0$, $\bar{S}_1$ of the general form (2.1). The K^-p elastic scattering amplitude is $1/2(\bar{S}_0 + \bar{S}_1)$; the amplitude for the charge exchange process $K^-p \to \bar{K}^0n$ is $1/2(\bar{S}_1 - \bar{S}_0)$. Hence, a complete analysis for the $\bar{K}N$ system requires angular distribution and polarization data for both the elastic and charge exchange processes. Here, the knowledge of the charge exchange process is essential for an adequate analysis, and this process has received very little attention to date; there is some preliminary bubble-chamber data on angular distributions and total cross-sections, but no information at all on its polarization properties.

The inelastic process $K^-p \to \Lambda\pi^0$ is of particular interest, both because the final state has I = 1 and is therefore an indicator for Y^*_1 states and because of the polarization analysis possible for the Λ hyperon. Bubble-chamber studies of this reaction (or of the corresponding reaction $K^-n \to \Lambda\pi^-$) have already yielded much information on the Y^*_1 resonance states [10]. The inelastic reaction $K^-p \to \Lambda\eta$ similarly has special interest, in that the final state has I = 0 and is an indicator for Y^*_0 states; apart from the threshold studies, which indicate the existence of a Y^*_0 (1670) resonance with $(1/2^-)$, there is rather little data available on this reaction,

essentially none on its polarization properties. These reaction amplitudes are not closely related with the elastic $\bar{K}N$ amplitudes, except for the form of the Breit-Wigner amplitude for the resonant state, since the unitarity relations are complicated, owing to the large number of other competing channels. However, with polarized target and polarization observations for the final Λ particle, complete spin and partial-wave analyses are possible for these amplitudes alone. Of course, the study of these reactions with polarized targets is made difficult by the fact that the final mesons are neutral, unless targets are available with a very high proportion of polarized protons.

For the KN system, K^+p elastic scattering leads directly to the $I = 1$ amplitude S_1 of the form (2.1). Polarized target studies are needed for a partial wave analysis for S_1 and experiments are being planned by several groups. At present, these will be of particular interest in the neighbourhood of K^+ momentum 1250 MeV/c, where a small bump has been found recently in the K^+p total cross-section [11].

The $I = 0$ KN amplitude S_0 is more difficult to reach. One possibility involves the study of the charge exchange reaction $K^+n \to K_1^0 p$, whose amplitude is $(S_1 - S_0)/2\sqrt{2}$, and there has already been some study of its angular distribution from charge exchange observations in K^+d collisions [12]. At present there is particular interest in the study of the $I = 0$ amplitude in the neighbourhood of K momentum 1150 MeV/c in consequence of a rather marked bump which has been observed recently in the K^+d total cross-section [11] and which must be attributed to the $I = 0$ KN interaction. Polarization information on the $I = 0$ KN interaction is therefore much desired, in order to assign this bump to a definite spin-parity state for the KN system and to clarify its interpretation. This could be done with a polarized deuterium target, since the neutron within the deuterium will have polarization $(P_{+1} - P_{-1})$, where P_m denotes the percentage of deuterons with magnetic quantum number m along the polarization direction. The K_1^0 angular distribution observed requires rather substantial corrections at forward scattering angles for the effect of the Pauli principle, arising from the presence of two final protons in the reaction $K^+d \to K_1^0 pp$ (the differential cross-section necessarily vanishes for 0° scattering with full energy) ; the corresponding corrections to the polarization angular distribution would need to be looked into, since the Pauli principle effects are certainly spin dependent here. The polarization experiment could well be done using a polarized ^3He target, using the reaction $K^+ {}^3He \to K_1^0 ppp$. The Pauli principle corrections are much larger (and more difficult to evaluate convincingly, owing to the nuclear complications) for this situation than for the deuterium reaction, so that this is a very unfavourable situation for the determination of $d\sigma/d\Omega$ for the charge-exchange reaction ; however, since the two initial protons have total spin zero, the Pauli

principle corrections are spin-independent and the determination of the polarization angular distribution would not depend on their evaluation.

Another possibility for the study of the KN charge exchange reaction which should be mentioned here is the reaction $K_2^0 p \rightarrow K^+ n$, since this reaction has the advantage of a proton target. The difficulty is that the K_2^0 beams available to date are not monoenergetic, but have a rather broad momentum spectrum (typical spread of order ± 50 %). In this situation, there are no constraints on the K^+ momentum, so that it is exceedingly difficult (if not practically impossible) to separate out the charge exchange events occurring from the polarized protons in the target.

The $\bar{p}p$ system can lead to mesonic resonance states m* with Y = 0 and I = 0 or 1, for mass values above 1876 MeV. A number of such mesonic resonances (with $I \geq 1$) have been established recently by Focacci et al [13], the S^--meson at 1929 MeV, the T^--meson at 2195 MeV (a neutral meson of mass 2207 MeV has also been reported by Alles-Borelli et al [14]) and the U^--meson at 2382 MeV. The spins and parities of these states are not known ; it is speculated [15] that each of these mesonic states are associated with four nonets with total spins J = L + 1, L (twice) and L - 1, and parities $(-1)^{L+1}$, where L = 3 for the S-mesons, L = 4 for the T-mesons, L = 5 for the U-mesons, and so on. In principle, these mesons may be formed directly in $\bar{p}p$ collisions and their existence may therefore affect the polarization and angular distributions for $\bar{p}p$ elastic scattering. It is quite likely that these mesonic states m* may have small partial widths for the $\bar{N}N$ channels, since these channels have thresholds lying relatively close to the meson mass values. However, since these mass values appear quite accurately known and these resonances are rather narrow (upper limits typically $\Gamma \lesssim 35$ MeV), a search for their possible effect on $d\sigma/d\Omega$ and $P(\theta)$ for $\bar{p}p$ elastic scattering would be of considerable interest. Even though the amplitude for $\bar{p}p \rightarrow m^* \rightarrow \bar{p}p$ may be quite small, polarization effects do depend essentially on interferences between different partial wave amplitudes and can be sensitive to a small, rapidly-energy-dependent amplitude of relatively high orbital angular momentum. The determination of the spin-parity values for these high-lying mesonic states appears quite a difficult problem at the present moment.

3 RESONANCE PRODUCTION EXPERIMENTS

Here we refer to reaction processes in which the resonant state is observed as a final-state interaction among the particles re-

sulting from a multiparticle production process. The simplest examples of such processes are of the type :

$$m + p \rightarrow m' + B^* \quad , \quad B^* \rightarrow B + m'' \qquad (3.1)$$

where B and B* denote a baryon and baryonic resonance state, respectively, and m, m', m" denote various mesons.

First, we consider the semi-stable fermion states. For the spin-1/2 baryons for which the parities have not already been determined by other methods, there are experiments under way (at Berkeley for the Σ^+, at CERN for the Ξ^-) to determine their parities, using polarized proton targets and the result of Bilenky [16] that the differential cross-section for the reaction :

$$m + B \rightarrow m' + B' \qquad (3.2)$$

where the mesons m, m' are spinless and the baryons B, B' have spin 1/2, from a polarized B target with polarization $\underline{P}_t$ is given by :

$$\frac{d\sigma}{d\Omega}(\theta) = \left(\frac{d\sigma}{d\Omega}(\theta)\right)_0 \left\{ 1 + \epsilon\, \underline{P}_t \cdot \underline{P}(\theta) \right\} \qquad (3.3)$$

where $(d\sigma/d\Omega\,(\theta))_0$ and $\underline{P}(\theta)$ are the differential cross-section and B' polarization for the reaction from an unpolarized target and ϵ denotes the product of the intrinsic parities of all the particles m, m', B and B'.

The other semi-stable fermion known is the Ω^--hyperon, believed to belong to the $(3/2^+)$ decuplet. About ten examples have been found to date, from the production reaction :

$$K^- + p \rightarrow K^+ + K^o + \Omega^- \qquad (3.4)$$

at various K^- energies. The decay processes, $\Omega^- \rightarrow \Lambda K^-$ and $\Xi\pi$, occur through weak interactions which do not conserve parity, so that the Ω-parity cannot be determined from the study of Ω-decay distributions. In due course, it should be possible to determine the Ω spin value from the analysis of the Ω-decay distributions, and we may anticipate that the value $J = 3/2$ will be established. The problem is then how to determine whether $(3/2^+)$ or $(3/2^-)$ holds for the Ω^--hyperon.

Bilenky and Ryndin [17] have proposed a method for the determination of the Ω^--parity which represents an extension of the method for spin-1/2 baryons based on the relation (3.3). It will be instructive to consider the basis for this method in some de-

tail. It may be applied to reaction (3.4) in three situations : i) if there exists a 0^+ resonance m* with the decay mode $m^* \to K^+K^o$, so that attention can be confined to the reaction $K^-p \to \Omega^- m^*$; ii) if attention is confined to final states for which the K^+K^o c.m. momentum is sufficiently low as to ensure that $\ell = 0$ holds for the K^+K^o system ; iii) if attention is confined to events leading to Ω^-, K^+ and K^o momenta which are coplanar.

In each of these situations there is a unique production plane defined. The method proposed is based on the Bohr theorem [18] which expresses the invariance of the strong interactions with respect to reflection in this production plane. Since this reflection operation is equivalent to P x $R_{\underline{n}}(\pi)$, where P denotes the parity operation and $R_{\underline{n}}(\theta)$ denotes rotation of the axes by angle θ about the normal $\underline{n}$ to this plane, this invariance leads to Bohr's result :

$$(-1)^{\Sigma_i m_i} \Pi_i (\epsilon_i) = (-1)^{\Sigma_f m_f} \Pi_f (\epsilon_f) \qquad (3.5)$$

where m_α denotes the spin component of particle α along the normal $\underline{n}$ and ϵ_α denotes the intrinsic parity of particle α, and i, f refer to the initial and final particles, respectively. The special feature common to the three situations listed above is that the K-mesons do not contribute to the spin sums $\Sigma_\alpha m_\alpha$ in the relation (3.5). With this simplification, then, for initial proton spin $m_i = +1/2$ in reaction (3.4), the relation (3.5) allows only $m_f = +1/2$ and $-3/2$ for the Ω^--spin, for the case of negative Ω^--parity ; let us denote these amplitudes by $a_{1/2}$ and $a_{-3/2}$. For $m_i = -1/2$, negative Ω^--parity would allow only $m_f = -1/2$ and $+3/2$ for the Ω^--spin ; let us denote these amplitudes by $a_{-1/2}$ and $a_{3/2}$. For a completely polarized target with $m_i = +1/2$, then, the cross-section is :

$$|a_{1/2}|^2 + |a_{-3/2}|^2 = \sigma_0 + \sigma_1 \qquad (3.6)$$

where

$$\sigma_0 = \frac{1}{2} \left\{ |a_{3/2}|^2 + |a_{1/2}|^2 + |a_{-1/2}|^2 + |a_{-3/2}|^2 \right\} \qquad (3.7a)$$

$$\sigma_1 = -\frac{1}{2} \left\{ |a_{3/2}|^2 - |a_{1/2}|^2 + |a_{-1/2}|^2 - |a_{-3/2}|^2 \right\} \qquad (3.7b)$$

For positive Ω^--parity, initial proton spin $m_i = +1/2$ can lead only to $m_f = -1/2$ or $+3/2$ for the Ω^--spin ; again, these amplitudes are denoted by $a_{-1/2}$ and $a_{3/2}$. For $m_i = -1/2$, the final spin states are $m_f = +1/2$ and $-3/2$, with amplitudes $a_{1/2}$ and $a_{-3/2}$, respectively. In this case the cross-section for $m_i = +1/2$ target is

$\left| |a_{3/2}|^2 + |a_{-1/2}|^2 \right|$, leading to the result $(\sigma_0 - \sigma_1)$. To sum up, the production cross-section has the general form :

$$\sigma = \sigma_0 - \epsilon \sigma_1 \, \underline{P}_t \cdot \underline{n} \qquad (3.8)$$

where ϵ denotes the Ω-parity and $\underline{P}_t$ denotes the proton target polarization.

For unpolarized target, the reaction (3.4) leads to the Ω-spin state $m_f = +3/2$ with intensity $|a_{3/2}|^2$, $m_f = +1/2$ with intensity $|a_{1/2}|^2$, $m_f = -1/2$ with intensity $|a_{-1/2}|^2$, and $m_f = -3/2$ with intensity $|a_{-3/2}|^2$. The quantity σ_1 can be determined from the odd moments of the Ω-spin :

$$\langle \underline{S} \cdot \underline{n} \rangle = \left| \frac{3}{2} \left(|a_{3/2}|^2 - |a_{-3/2}|^2 \right) + \frac{1}{2} \left(|a_{1/2}|^2 - |a_{-1/2}|^2 \right) / N \right| \qquad (3.9a)$$

$$\langle (\underline{S} \cdot \underline{n})^3 \rangle = \left| \frac{27}{8} \left(|a_{3/2}|^2 - |a_{-3/2}|^2 \right) + \frac{1}{8} \left(|a_{1/2}|^2 - |a_{-1/2}|^2 \right) / N \right| \qquad (3.9b)$$

where

$$N = \left| |a_{3/2}|^2 + |a_{1/2}|^2 + |a_{-1/2}|^2 + |a_{-3/2}|^2 \right| .$$

In fact :

$$\sigma_1/\sigma_0 = \left| \frac{7}{6} \langle \underline{S} \cdot \underline{n} \rangle - \frac{2}{3} \langle (\underline{S} \cdot \underline{n})^3 \rangle \right| .$$

These spin moments can be determined unambiguously from the polarization angular distribution of decay processes $\Omega^- \rightarrow \Lambda K^-$ and $\Xi\pi$, as discussed in general by Byers and Fenster [19]. Hence, with this determination of σ_1, comparison of the observed cross-section for target polarization $\underline{P}_t$ with the expression (3.8) will lead directly to a determination of the Ω-parity ϵ . Bilenky and Ryndin give more general formulae, appropriate to arbitrary spin value for the Ω-hyperon, but the above discussion is sufficient for the expected value $J = 3/2$.

Typical examples of the resonance production process (3.1) are :

$$\pi^+ + p \rightarrow \pi^o + N^{*++} \quad , \quad N^{*++} \rightarrow p + \pi^+ \qquad (3.10a)$$

$$\pi^- + p \rightarrow K^o + Y_0^* \quad , \quad Y_0^* \rightarrow \Sigma + \pi \qquad (3.10b)$$

$$K^- + p \rightarrow \pi^- + Y_1^{*+} \quad , \quad Y_0^{*+} \rightarrow \Lambda + \pi^+ \qquad (3.10c)$$

$$K^- + p \rightarrow K^+ + \Xi^{*-} \quad , \quad \Xi^* \rightarrow \Xi + \pi \qquad (3.10d)$$

The spin and parity of the resonance state $B^* \rightarrow B + m''$ can be determined by the method of Byers and Fenster [19] when : i) B* is produced in a state of non-zero polarization (i.e. a state for which some spin tensor of odd rank has non-zero expectation value), and ii) all components of the polarization of the baryon B can be determined, as is the case especially for the Λ, Σ^+ and Ξ particles.

The statistics needed to establish these parameters naturally become very large as the degree of polarization available falls to zero, so that it is very desirable to know in advance under what experimental conditions the B* polarization will be large. Many of these production processes are dominantly peripheral in character. This is generally the case for reactions of types (3.10 a, b, c), for example ; the non-peripheral processes of the same general kind (for example, the process $K^-p \rightarrow \pi^+ Y_1^{*-}$ which requires a charge exchange of two units) generally have significantly smaller cross-sections, perhaps an order of magnitude smaller, than the corresponding peripheral processes. A purely peripheral process (i.e. whose reaction amplitude corresponds exactly to the exchange of a single meson, treated in first Born approximation) will not generate any B* polarization ; however some polarization may generally be generated as a result of absorptive corrections to the purely peripheral amplitude or as a result of interference of the peripheral amplitude with some non-peripheral amplitudes, which can still be quite appreciable.

Hence, although the Byers-Fenster procedure is completely adequate for a spin-parity analysis, one can see at least two ways in which the use of a polarized target may be of benefit for these spin-parity determinations :

a. by making a rapid search for energies at which the B* polarization effects are especially strong. This involves measuring the effect of the polarization of the target proton on the B* production angular distribution. Although, for spin $J > 1/2$, there is not a one-to-one correlation between this asymmetry and the B* polarization tensors (as exemplified by the above discussion for the Ω-particle), the observation of a strong asymmetry guarantees that there must be at least one substantial B* polarization tensor in the experimental conditions examined. However, Chamberlain [5] has already pointed out here the difficulties of polarized target experiments at present for reaction processes with no constraints. In these B* production reactions, there is the additional problem of the finite width for the B* resonance, together with the effects on the asymmetry of the inclusion of non-resonant background.

b. even for a purely peripheral process, polarization for the target proton can ensure that the B* resonance produced has non-zero polarization. This will be especially useful when the proportion

of highly polarized protons in the target can be made high and when a complete picture of the B* production and decay event can be obtained by means of a large magnetic spark chamber. In this situation, the Byers-Fenster analysis can then be used for the B* spin-parity determination. The spark-chamber study of multiparticle production reactions, including the production and decay of B* resonances, has already been under discussion for some time, although not yet with polarized targets.

If a polarized target can be used for a B* production experiment where B* polarization is already generated with an unpolarized target, then it is possible to obtain still further tests for the B* spin and parity. This has been discussed by Gaillard [20] for an instructive but relatively special situation. Consider a reaction of type (3.1), where m' is a spinless meson, and let us take together all B* decay events for a given B* production direction, taking no note of the azimuth of the decay (i.e. averaging the B* decay around the normal to the production plane). This reduces the B* density matrix to diagonal form, with respect to the axis $\underline{n}$ (which means giving up a large fraction of the information contained in these decay distributions).

The remaining elements of the B* density matrix are then :

$$\rho_{mm} = N|a_m|^2 \ (1 + P_t(-1)^{m-\frac{1}{2}})/2 \qquad (3.11)$$

where P_t denotes the target polarization along $\underline{n}$, N is a normalization constant such that $\Sigma_m \rho_{mm} = 1$, and a_m again denotes the amplitude leading from an initial proton spin state to B* state with spin component m. The structure of this expression (3.11) is determined by the Bohr relation (3.5). For $P_t = +1$, we have $m_i = +1/2$ for the target proton and the elements ρ_{mm} are zero for $|m - m_i|$ = odd integer when the B* parity ϵ has value +1, or for $|m - m_i|$ = zero or even integer, when the B* parity ϵ has value -1, as required by this relation. The density matrix-elements ρ_{mm}/N are linearly dependent on the target polarization P_t and therefore interpolate linearly between the values $|a_m|^2(1 + (-1)^{m-1/2})/2$ for $P_t = +1$, just given by the Bohr relation, and the values $|a_m|^2/2$ for $P_t = 0$.

As shown explicitly by Byers and Fenster, the B* decay angular distribution is determined by the spin tensors of even rank ; after averaging around $\underline{n}$, these spin tensors are completely determined by the even combinations $(\rho_{mm} + \rho_{-m,-m})$. The polarization distributions for the baryon B resulting from B* decay are determined entirely by the spin tensors of odd rank, which are determined entirely by the odd combinations $(\rho_{mm} - \rho_{-m,-m})$. These combinations are given by :

$$\rho_{mm} + \rho_{-m,-m} = \frac{1}{2} N \left\{ A_m + P_t(-1)^{m-\frac{1}{2}} B_m \right\} \qquad (3.12a)$$

$$\rho_{mm} - \rho_{-m,-m} = \frac{1}{2} N \left| B_m + \epsilon P_t (-1)^{m-\frac{1}{2}} A_m \right| \qquad (3.12b)$$

where $A_m = |a_m|^2 + |a_{-m}|^2$, $B_m = |a_m|^2 - |a_{-m}|^2$. From the P_t-dependence of the B* decay angular distribution, both the coefficients A_m and ϵB_m may be deduced from expression (3.12a). With expression (3.12b), this then leads to a prediction of the odd spin tensors, as function of P_t ; their absolute sign is proportional to ϵ . For a given set of odd spin tensors, the angular distribution of the longitudinal ($\underline{P}.\underline{k}$) and transverse ($\underline{P}_{tr} = \underline{P} - \underline{k}P.\underline{k}$) components of the polarization of the baryon B (momentum along the unit vector $\underline{k}$ in the B* rest frame) are definite (for given J), apart from their relative sign ; the observation of this relative sign constitutes the Byers-Fenster determination of the B* parity ϵ . With (3.12b), the observation of the absolute sign of the longitudinal polarization (and of its dependence on P_t) also constitutes an independent determination of the parity ϵ . Explicit expressions for these relationships have been obtained by Gaillard [20] for arbitrary J, and we shall not give the details here, since the qualitative conclusion that these polarized target observations allow independent determinations for the resonance parity is already clear. The observation of these polarized-target effects would be of interest, although it appears that whenever these effects are prominent, the Byers-Fenster method is necessarily also available and adequate for the spin-parity determination desired.

Most of the Y* resonances can be studied by the resonance formation experiments, with the use of polarized targets. Only the Y_0^* (1405) (spin-parity not yet established directly but believed to be $(1/2^-)$ from other considerations) and Y_1^* (1385) (spin-parity $(3/2^+)$ established) are energetically inaccessible in this way, lying below the $\bar{K}N$ threshold. There may also be a number of exceptional cases (for example, Y_1^* (1660)) where the amplitude for direct formation happens to be particularly small (i.e. with small $\bar{K}N$ partial width) and where spin-parity analysis by the Byers-Fenster procedure in a resonance production experiment is therefore particularly advantageous. On the other hand, the Ξ^* (and Ω^*) resonances are accessible only through resonance production experiments. The observation and analysis of the Ξ^* resonances especially will be of great importance for our understanding of the B* unitary multiplets. Many Ξ^* resonances are expected to exist, in fact there will be one Ξ^* resonance expected corresponding to each N* resonance established. So far, long bubble-chamber experiments have given rather little information about these Ξ^* resonances, beyond Ξ^* (1530), Ξ^* (1820) and Ξ^* (1930), owing to the extreme smallness of their production cross-sections. It seems quite likely that the complete study of Ξ^* resonances will require counter experiments, with selection of the Ξ^* mass value by momentum selection for the K^+ in the production reaction (3.10d) and with the use of a large magnetic spark chamber system for the analysis of the Ξ^* decay products and their polarization properties. If polarized targets are available with a high

proportion of highly polarized protons by that time, their use might be rather well justified in such Ξ^* studies, in order to obtain the most efficient indications of the Ξ^* spin and parity for the rather limited number of events which will be available.

References

1) R.J.N. Phillips, Polarization questions in high energy scattering, Proc. Conf. on Polarized Targets and Polarized Ion Sources (Saclay, 1966).
2) J. Bernstein, G. Feinberg and T.D. Lee, Phys. Rev., 1965, 139B, 1650.
3) N. Christ and T.D. Lee, Phys. Rev., 1966, 143, 1310.
4) M. Jacob, Definition and determination of spin amplitudes : some applications of polarized targets in high energy physics, Proc. Conf. on Polarized Targets and Polarized Ion Sources (Saclay, 1966).
5) O. Chamberlain, Experiments with polarized targets in high energy physics, Proc. Conf. on Polarized Targets and Polarized Ion Sources (Saclay, 1966).
6) C. Lovelace, Pion-nucleon phase shifts, Proc. 1966 Intern. Conf. on High Energy Physics (Berkeley, September 1966), (in press).
7) J.A. Schwartz, Associated Production from 1.5 to 2.4 BeV/c, Lawrence Radiation Laboratory Rept. UCRL-11360 (June 29, 1964).
8) G.J. Hoff and R.B. Hoff, Evidence for a T = 1/2, S = 0 resonance near 1.5 BeV/c (Enrico Fermi Institute preprint EFINS 66-6, January, 1966).
9) W.G. Holladay, Phys. Rev., 1965, 139, B1348.
10) W.M. Smart, A. Kernan, G.E. Kalmus and R.P. Ely, Phys. Rev. Letters, 1966, 17, 556.
11) R.L. Cool, G. Giacomelli, T.F. Kycia, B.A. Leontic, K.K. Li, A. Lundby and J. Teiger, Phys. Rev. Letters, 1966, 17, 102.
12) W.E. Slater, D.H. Stork and H.K. Ticho, Phys. Rev. Letters, 1961, 7, 378.
13) M.N. Focacci, W. Kienzle, B. Levrat, B.C. Maglic and M. Martin, Phys. Rev. Letters, 1966, 17, 890.
14) V. Alles-Borelli, B. French, A. Frisk, L. Michejda and E. Paul, Antiproton-proton annihilations into five pions at 5.7 GeV/c, CERN Rept. TC 66-25 (October, 1966).
15) R.H. Dalitz, Symmetries and the strong interactions, Proc. 1966 Intern. Conf. on High Energy Physics (Berkeley, 1966), (in press
16) S.M. Bilenky, Nuovo Cimento, 1958, 10, 1049.
17) S.M. Bilenky and R.M. Ryndin, Phys. Letters, 1965, 18, 346.
18) A. Bohr, Nucl. Phys., 1959, 10, 486.
19) N. Byers and S. Fenster, Phys. Rev. Letters, 1963, 11, 52.
20) M.K. Gaillard, Nuovo Cimento, 1964, 32, 1306.

POLARIZATION QUESTIONS IN HIGH ENERGY SCATTERING

R.J.N. PHILLIPS
A.E.R.E., Harwell

1 ASYMPTOTIC EXPECTATIONS

Until recently, most people supposed there was no spin-dependence in high energy elastic scattering. This came from simple ideas about diffraction.

In the diffraction picture, inelastic processes are the essential dynamics. The interaction may be roughly represented by a black or grey disc, absorbing the incident beam into inelastic channels ; elastic scattering follows as a shadow effect. In Feynman diagrams, an absorption like figure 1a gives scattering through figure 1b. At high energy, many inelastic channels are open and we expect -statistically - that absorption will not favour one spin state over another.

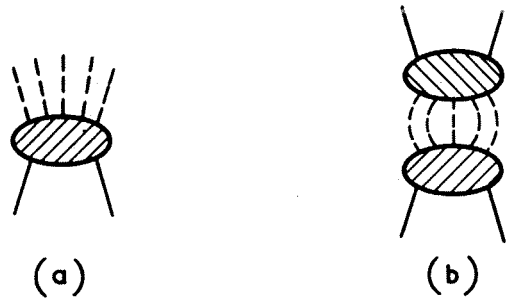

Fig. 1 Feynman diagrams for an absorption (a) and consequent shadow scattering (b).

In fact this notion of spin-independence is not as precise as it sounds. The "natural" definition depends on the spin formalism, as we shall see. Though we may believe the spin-dependence is trivial, which trivial form it takes is still an interesting question.

However, the spin-dependence may not be trivial, after all. Regge pole theory [1] allows this. (For the uninitiated, let me describe it as a new version of the old idea that scattering comes from particle exchanges). Regge poles have explained a lot of data, phenomenologically [2]. A full theoretical justification is still lacking, but at least some classes of Feynman diagrams, like figures 2a and 2b, have Regge-pole properties [3]. These diagrams look like diffraction scattering - so what is wrong with our previous argument ? Presumably the sum over intermediate states is not as "statistical" as we supposed.

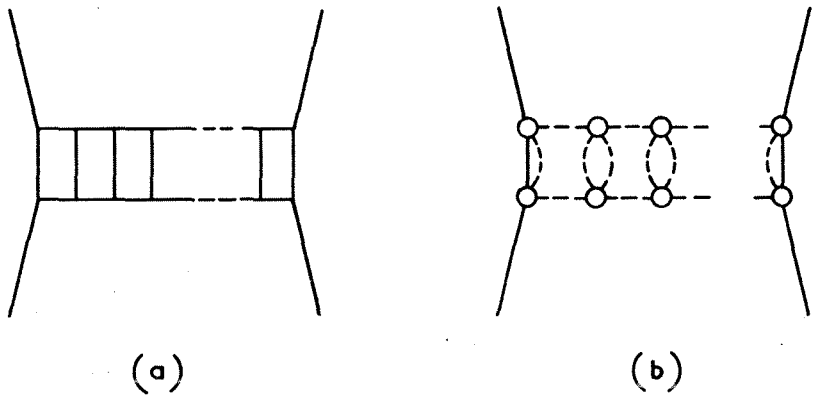

Fig. 2 Classes of ladder (a) and multiperipheral (b) diagrams that have Regge-pole properties.

The phase of scattering amplitudes are important for polarization. From general theorems [4], the energy-dependence of each term plus its behaviour under crossing (i.e. under the change from ab to $\bar{a}b$ scattering) determine its phase asymptotically. In any particular process, at fixed momentum transfer, we may expect a single term to dominate asymptotically - barring accidental degeneracies. Then the asymptotic amplitude, including spin-flip parts if they survive, has a common overall phase.

2 PION-NUCLEON SCATTERING

For a simple example, take πN scattering. The c.m. scattering amplitude T is an operator on the nucleon spin. How we write it depends on whether we describe spin by a Pauli spinor in the rest frame [5], or by a Dirac spinor [6], or by helicity states [7] :

$$T = G + iH\, \underset{\sim}{\sigma}.\underset{\sim}{N} \tag{1a}$$

$$T = - A + iB\, Q_\mu\, \sigma_\mu \tag{1b}$$

$$T = (f_{++}, f_{+-}) \quad . \tag{1c}$$

The natural definitions of spin independence in these three formalisms are that H, or B, or f_{+-} vanishes : they are not identical. In terms of G and H they are :

$$H = 0 \tag{2a}$$

$$H = G\sqrt{\frac{-t}{4m_N^2}} \tag{2b}$$

$$H = - G\sqrt{\frac{-t}{s}} \tag{2c}$$

in the high energy limit. Here s is the total c.m. energy squared, and t is the (negative) square of momentum transfer. These definitions coincide only at $t = 0$ (scattering angle $\theta = 0$). Elsewhere, (2b) always differs from (2a). (2c) could be written $H = - G \tan \theta/2$ and differs from (2a) at fixed θ ; but the usual case of interest is fixed t, so $\theta \to 0$ as $s \to \infty$ and (2c) ultimately agrees with (2a).

What are the possible measurements ? Measuring no spins, we get the unpolarized cross-section I_o. Measuring the spin in either the initial or final state gives the polarization parameter P. Measuring the spin both initially and finally gives the depolarization tensor D_{ij}, with two independent elements called D_{KK} and D_{KP} [8].

$$\left.\begin{aligned} I_o &= |G|^2 + |H|^2 , \\ I_o\, P &= 2\, \mathrm{Im}\, GH^* , \\ I_o\, D_{KK} &= |G|^2 - |H|^2 , \\ I_o\, D_{KP} &= 2\, \mathrm{Re}\, GH^* \quad . \end{aligned}\right\} \tag{3}$$

We expect G and H to have the same asymptotic phase, so $P \to 0$ anyway. To measure H, we are forced to the second-rank experiments. A technical complication is that the non-trivial elements of D_{ij} require initial target polarization in the scattering plane ; P only requires normal polarization. If H is not trivial, P gives a check on the phase rule.

As illustrations, figure 3 compares D_{KK} and D_{KP} for the three definitions of spin-independence (2a), (2b) and (2c), at 10 GeV/c. Figure 4 shows predictions for a case of non-trivial spin-dependence, a Regge pole model [9], at 5, 40 and 320 GeV/c.

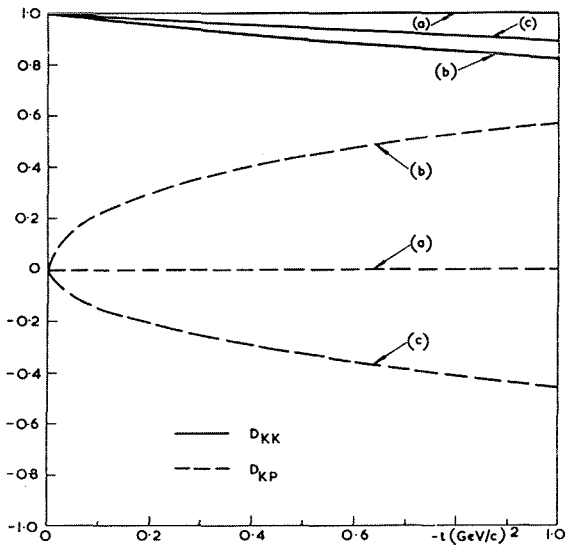

Fig. 3 Comparison of πN depolarization D_{KK} and D_{KP} at 10 GeV/c for the three definitions of spin-independence. Curves marked (a), (b), (c) correspond to eqs. (2a), (2b), (2c).

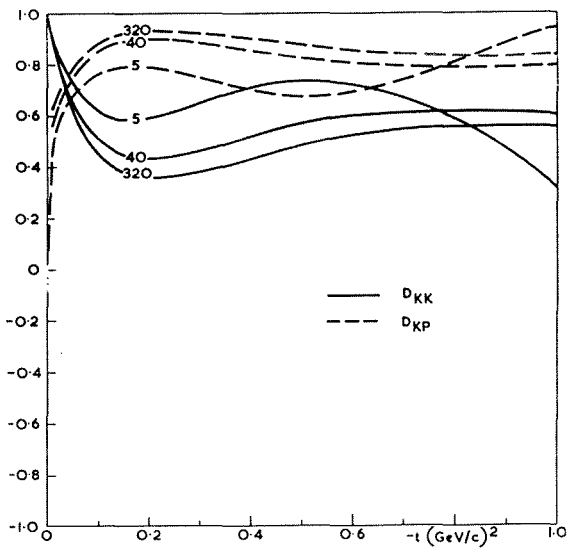

Fig. 4 Predictions of D_{KK} and D_{KP} for π⁻p scattering at 5, 40 and 320 GeV/c, for solution (a) of reference 9.

To summarize the conclusions so far :

a. The question of asymptotic spin dependence is interesting.

b. To investigate it, we need D_{ij} (D_{KP} being most sensitive to small H).

c. Target polarization in the scattering plane is needed.

d. P gives a phase rule test.

These rest on general arguments. We go next to a specific theory. But first we note that present accelerator energies are not asymptotic : asymptotic limits must be inferred by extrapolation. The way the limit is approached will also be interesting, however.

3 REGGE POLES

A Regge pole in high energy scattering is something like a particle exchange ; it can be represented by a similar graph and gives a term of the form [1,10] :

$$T_{ab\longrightarrow ab} = \frac{s_o}{8\pi\sqrt{s}} \frac{\eta_a(t)\,\eta_b(t)}{\sin \pi\alpha(t)} \left[1 \pm e^{-i\pi\alpha(t)}\right] \left(\frac{s}{s_o}\right)^{\alpha(t)} \quad . \qquad (4)$$

η_a and η_b are vertex functions, characterizing the coupling to particles $\underline{a}$ and $\underline{b}$: when there is spin, they are spin operators. The "trajectory function" $\alpha(t)$ fixes the s-dependence and also the phase, via the "signature factor" in square brackets. If there are several poles, the one with the highest $\alpha(t)$ dominates asymptotically.

The factorization property of Regge amplitudes* is important, but hard to test in unpolarized scattering. It gives predictions like $T_{\pi\pi}T_{NN} = (T_{\pi N})^2$, which brings in $\pi\pi$ scattering. However, this property includes <u>factorization of spin dependence</u> which can be tested via polarization effects.

Consider a Regge pole that contributes to πN, KN and NN scattering. Then all spin dependences come from the nucleon vertex function :

$$\left.\begin{aligned} T_{\pi N} &\sim \eta_\pi \left[\eta_N + i\Phi_N \underset{\sim}{\sigma}\cdot\underset{\sim}{N}\right] \\ T_{KN} &\sim \eta_K \left[\eta_N + i\Phi_N \underset{\sim}{\sigma}\cdot\underset{\sim}{N}\right] \\ T_{NN} &\sim \left[\eta_N + i\Phi_N \underset{\sim}{\sigma}^{(1)}\cdot\underset{\sim}{N}\right]\left[\eta_N + i\Phi_N \underset{\sim}{\sigma}^{(2)}\cdot\underset{\sim}{N}\right] \end{aligned}\right\} \qquad (5)$$

(suppressing irrelevant factors), where $\underset{\sim}{N}$ is the normal to the scattering plane.

Before discussing the tests, a few words about N-N scattering. In general T_{NN} has five independent terms [11] :

$$T_{NN} = a + ic(\underset{\sim}{\sigma}^{(1)} + \underset{\sim}{\sigma}^{(2)})\cdot\underset{\sim}{N} + m\underset{\sim}{\sigma}^{(1)}\cdot\underset{\sim}{N}\;\underset{\sim}{\sigma}^{(2)}\cdot\underset{\sim}{N} + (g+h)\,\underset{\sim}{\sigma}^{(1)}\cdot\underset{\sim}{P}\;\underset{\sim}{\sigma}^{(2)}\cdot\underset{\sim}{P} + (g-h)\,\underset{\sim}{\sigma}^{(1)}\cdot\underset{\sim}{K}\;\underset{\sim}{\sigma}^{(2)}\cdot\underset{\sim}{K} \qquad (6)$$

where $\underset{\sim}{N}$, $\underset{\sim}{P}$ and $\underset{\sim}{K}$ are unit vectors along $\underset{\sim}{k} \times \underset{\sim}{k}'$, $\underset{\sim}{k} + \underset{\sim}{k}'$, $\underset{\sim}{k}' - \underset{\sim}{k}$; $\underset{\sim}{k}$ and $\underset{\sim}{k}'$ are initial and final relative momenta [12]. The Regge poles that can couple to π and K contribute only to a, c and m ; such terms are thought to dominate elastic scattering. What about NN experiments ? Measuring no spin and one spin gives the unpolarized

cross-section I_o and polarization P. Measuring the spin of one nucleon both initially and finally gives the depolarization tensor D_{ij}. Measuring the <u>other</u> nucleon finally, instead, gives the polarization transfer tensor K_{ij}. Measuring both spins together, either before or after, gives the spin correlation tensor C_{ij}. (We ignore more complicated possibilities, with three or four spin determinations). Keeping only a, c and m in eq. (6), these observables are :

$$\begin{aligned} I_o &= |a|^2 + 2|c|^2 + |m|^2 \\ I_o P &= 2\,\mathrm{Im}\left[(a+m)c^*\right] \\ D_{NN} &= 1 \\ I_o D_{KK} &= I_o D_{PP} = |a|^2 - |m|^2 \\ I_o D_{KP} &= -I_o D_{PK} = 2\,\mathrm{Re}\left[(a-m)c^*\right] \\ I_o K_{NN} &= I_o C_{NN} = 2\,\mathrm{Re}\left[a\,m^*\right] + 2|c|^2 \end{aligned} \tag{7}$$

All other components vanish. Observe K_{ij} and C_{ij} have only one component left.

Now the factorization tests [8,13,14]. Asymptotically, if a single "Pomeranchuk" Regge pole dominates πN, KN and NN scattering, P = 0 for all three and the D_{ij} become identical :

$$\begin{aligned} D_{KK}(\pi N) &= D_{KK}(KN) = D_{KK}(NN) \\ D_{KP}(\pi N) &= D_{KP}(KN) = D_{KP}(NN) \quad . \end{aligned} \tag{8}$$

Factorization also gives $c^2 = -\,a\,m$ in NN scattering, so that :

$$K_{NN} = C_{NN} = 0 \quad . \tag{9}$$

Furthermore, at t = 0 we have c = 0 for invariance reasons, so m = 0 also and no spin-dependence remains. In this Pomeranchuk limit, by the way, KN and $\bar{K}N$ scattering are equal : so are NN and $\bar{N}N$.

At sub-asymptotic energies, several Regge poles take part. T no longer factorizes, but individual pole terms still do, and the latter can be separated approximately. The consequences are less simple than before, but still powerful. Take for instance the contri-

bution to polarization P from two poles interfering ; if at some t and s it vanishes for any one of πN, KN or NN scattering, it must vanish at this t-value for all three, for all s [15].

We have spoken only of factorization so far, but there are other properties to probe also.

In some reactions [2], one postulates a single Regge pole even at present accelerator energies, because only one suitable pole is known. The prediction $P = 0$ can then be tested.

For NN scattering, the Regge poles that contribute to g and h are believed to be weak. This can be tested in various ways ; for example, via D_{NN}, for which the full expression is $D_{NN} = 1 - 4(|g|^2 + |h|^2)/I_o$.

In general, it is argued [16] that beside Regge poles there will be branch cut terms ; the latter look like continua of Regge poles, but no-one knows how strong or weak they are. One sign of their presence would be factorization failure. Another would be g and h terms in NN scattering. The question of branch cuts adds interest to both these possibilities.

To summarize, we add to the conclusion of § 2 :

e. Factorization is most easily tested via polarization effects.

f. Asymptotic tests include $C_{NN}(NN) = K_{NN}(NN) = 0$ and :

$$D_{ij}(\pi N) = D_{ij}(KN) = D_{ij}(NN)$$

g. Sub-asymptotic tests require pole terms to be separated.

h. One-Regge-pole assumptions imply $P = 0$.

i. g and h terms in T_{NN} are interesting ; tests include D_{NN}.

For more specific examples, see references 2, 4, 8, 13, 14 and references therein.

Appendix

FACTORIZATION IN THE QUARK MODEL

In this model, N is made of three quarks, π and K of quark-antiquark pairs, in S-states. Asymptotically, we suppose all quark-quark and quark-antiquark amplitudes are the same, with general form like eq. (6) :

$$T_{qq} = \alpha + i\beta(\underset{\sim}{\sigma}^{(1)} + \underset{\sim}{\sigma}^{(2)}).\underset{\sim}{N} + \sigma\, \underset{\sim}{\sigma}^{(1)}.\underset{\sim}{N}\, \underset{\sim}{\sigma}^{(2)}.\underset{\sim}{N} + \delta\, \underset{\sim}{\sigma}^{(1)}.\underset{\sim}{P}\, \underset{\sim}{\sigma}^{(2)}.\underset{\sim}{P} + \epsilon\, \underset{\sim}{\sigma}^{(1)}.\underset{\sim}{K}\, \underset{\sim}{\sigma}^{(2)}.\underset{\sim}{K} \quad . \qquad (A.1)$$

Then a simple impulse approximation gives :

$$T_{\pi\pi} = T_{KK} = 4\alpha$$

$$T_{\pi N} = T_{KN} = 6\alpha + 2i\beta\, \underset{\sim}{\sigma}.\underset{\sim}{N}$$

$$T_{NN} = q_{\alpha} + 3i\beta(\underset{\sim}{\sigma}^{(1)} + \underset{\sim}{\sigma}^{(2)}).\underset{\sim}{N} + \sigma\, \underset{\sim}{\sigma}^{(1)}.\underset{\sim}{N}\, \underset{\sim}{\sigma}^{(2)}.\underset{\sim}{N} + \delta\, \underset{\sim}{\sigma}^{(1)}.\underset{\sim}{P}\, \underset{\sim}{\sigma}^{(2)}.\underset{\sim}{P} + \epsilon\, \underset{\sim}{\sigma}^{(1)}.\underset{\sim}{K}\, \underset{\sim}{\sigma}^{(2)}.\underset{\sim}{K} \quad . \qquad (A.2)$$

Hence an approximate factorization rule $T_{NN} = (T_{\pi N})^2/T_{\pi\pi}$ gives the first two terms correctly but not the rest, in general. We can devise combinations of NN parameters that depend on α/β alone, and are therefore related to πN and KN scattering, but nothing simple comes out.

Of course, if T_{qq} were itself dominated by the Pomeranchuk Regge pole, we would have full factorization again.

Notes and References

* The quark model also gives some factorization, but weaker. See Appendix.

1) G.F. Chew and S.C. Frautschi, Phys. Rev. Letters, 1961, 7, 394.
S.C. Frautschi, M. Gell-Mann and F. Zachariasen, Phys. Rev., 1962, 126, 2204.
V.N. Gribov, Soviet Phys. JETP, 1962, 14, 478.

2) For a recent survey, see R.J.N. Phillips, "Regge poles in high energy scattering", Proceedings of the 1966 Erice Summer School, (to be published by Academic Press).
3) B.W. Lee and R.F. Sawyer, Phys. Rev., 1962, 127, 2266, 2274.
D. Amati et al, Nuovo Cimento, 1961, 22, 569 ; 1962, 26, 896 ; 1963, 27, 913.
4) A.A. Logunov et al, Ann. Phys. (N.Y.), 1965, 31, 203.
S. Bilenkii et al, Soviet Phys. JETP, 1964, 19, 744.
A. Bialas and E. Bialas, Nuovo Cimento, 1965, 37, 1686.
A. Bialas and B.E.Y. Svensson, Nuovo Cimento, 1966, 42A, 672, 908.
5) H.P. Stapp, Phys. Rev., 1956, 103, 425.
6) G.F. Chew et al, Phys. Rev., 1957, 106, 1337.
7) M. Jacob and G.C. Wick, Ann. Phys. (N.Y.), 1959, 7, 404.
8) See for example R.J.N. Phillips and W. Rarita, UCRL-16185 (1965).
9) C.B. Chiu, R.J.N. Phillips and W. Rarita, UCRL-16940, Phys. Rev., (in press) : the case illustrated is solution (a) of this paper.
10) M. Gell-Mann, Proceedings of High Energy Physics Conference at CERN (1962), p. 533.
D.H. Sharp and W.G. Wagner, Phys. Rev., 1963, 131, 2226.
11) See for example M.J. Moravcsik, "The two-nucleon interaction", (Clarendon Press, Oxford, 1963).
12) Unfortunately, N, P and K also have to stand for nucleon, polarization and kaon : I hope there will be no confusion.
13) V.N. Gribov and I. Ya. Pomeranchuk, Phys. Rev. Letters, 1962, 8, 412.
14) E. Leader, Rev. Mod. Phys., 1966, 38, 476.
E. Leader and R. Slansky, Phys. Rev., 1966, 148, 1491.
15) The interference term vanishes only if both poles have the same ratio η_N/Φ_N, or the same phase. Either condition applies at once to all three processes, and to all s.
16) S. Mandelstam, Nuovo Cimento, 1963, 30, 1127, 1148.

DESCRIPTION OF LOW ENERGY TARGETS

D. GARRETA

Département de Physique Nucléaire, Saclay

This talk will be a report on the present situation in the field of the polarized proton targets used in low energy physics. I will first point out what are the specific problems encountered in their design, then give a description of the three targets already built and having been used in nuclear physics experiments. I will finish by giving a short description of the targets that are planned to be built or are already in a preliminary stage of construction. I will not mention the proton and deuteron targets of Dubna used with very low energy neutrons because, actually, their characteristics are very similar to those of high energy targets and will be described in the talk of Dr Lutchikov.

All the problems specific to low energy polarized targets derive from the drastic limitations on the quantity of material acceptable around the target. They are imposed by the necessity of getting the beam into the target and properly detecting the scattered particles with a high rate of background rejection.

The most important limitation is where the particles have the lowest energy, that is, between the place where the scattering occurs and the detectors. It implies a limitation on the thickness of the walls of the target but also on the thickness of the target itself. This limitation exists also, but generally not so strong, on the beam path in order to limit the background and, in case of charged particles, not to degrade the beam energy by a too large factor. These limitations bring three sorts of problems :

First : The handling problem on which I will not insist but of which the description of the target arrangements will give you an idea.

Second : The problem of cooling the crystal : in fact, when it is possible to have helium in the cavity it is all right, but, when

it is impossible, the crystal has to be cooled by contact and the cooling can be very critical, especially when you need a rather thick crystal.

Third : The polarization measurement problem : the crystals are small, from a fraction of cubic centimeter to a fraction of cubic millimeter. Then it is very difficult to have a NMR signal having a sufficient signal to noise ratio at thermal equilibrium and being at the same time equally sensitive to all parts of the crystal.

A last problem, specific to charged particle beam, comes from the small thickness of the targets and the high statistics wanted in low energy physics, it is the radiation damage effect. It makes that, after a relatively small number of charged particles have passed through the crystal, its polarization drops down and it has to be changed.

I now come to the description of the targets already built and used at Los Alamos, Harwell and Saclay. I will describe them in that order which corresponds to decreasing sizes of the crystal. I will try to point out for each case how critically the different problems mentioned above were encountered and the way they were resolved. The three targets use crystals grown from LMN solutions with 1 % of neodymium.

LOS ALAMOS TARGET [1,2,3]

The target of Los Alamos was designed for neutron proton scattering experiments with a beam of 23 MeV neutrons. This corresponds to recoil protons of 20 and 23 MeV at the scattering angles where the experiments were performed. It has to be noticed that this neutron energy is below the (n,p) threshold on helium-4, then, having helium on the beam path does not produce any background. In order to get a rather clean proton spectrum, for being able to substract the background, the thickness of the crystal was limited to 1.6 mm which corresponds to an absorption of the order of 8 MeV.

The target is cooled with a conventional cryostat to a temperature of 1.2° K and is polarized with a microwave klystron generator giving 400 mW at a frequency of 54 GHz in a multimode cavity (fig. 1) The 14.2 kilogauss magnetic field is perpendicular to the plane of that cross-section. The neutron beam comes from the left at an angle such that the scattered proton is always detected in the direction perpendicular to the plane of the crystal what gives a minimum

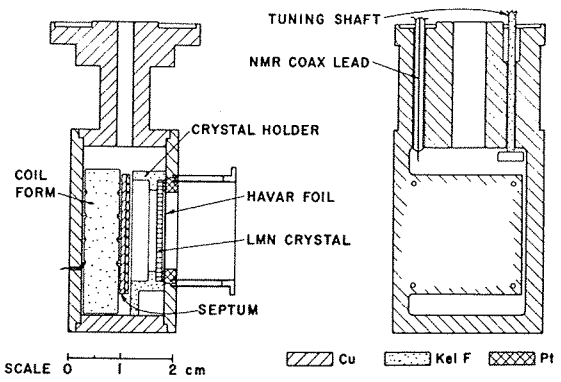

Fig. 1

path through it. By placing the crystal just beside the exit wall, it is possible to have liquid helium in the cavity as long as it does not require a too thick exit wall. This one, shown here by a heavy line, is made of an 8 microns thick Havar foil soft soldered on a platinum ring, which in turn is hard soldered to a tube with flange, which I call the "foil insert". The final stage of assembly is completed when the crystal is in place and the "foil insert" is located and sealed by soldering at its flange. This is remarquably thin for a mounting leakproof to superfluid helium.

The cavity resonates on very complicated modes and the tuning paddle just helps getting the maximum absorption.

Notice the NMR coil beside the copper septum faced with platinum that divides the cavity. The purpose of the platinum plate is to cut down the background coming from (n,p) reactions.

We see that the cooling problem is resolved.

We now come to the problem of measuring the polarization. Due to the large volume of the crystal, which is 2 cm^2 in surface, it is impossible to get a constant intensity of the microwave on all its parts. Then there is a possibility that the polarization is not constant throughout the crystal. It is why the NMR coil is located on the opposite side of the septum from the crystal. This provides a uniform sensitivity for all parts of the crystal to the NMR signal and gives the measurement of an average polarization equal to the average polarization seen by the neutron beam. Unfortunately this gives also a small filling factor, then a poor signal to noise ratio at thermal equilibrium which accounts for about half of the estimated relative error of 15 % on the measurement of the polarization.

P. Catillon will show that this accuracy, which seems poor compared to what is obtained with large targets, is more than sufficient for the experiments performed.

The polarization obtained with that target is of the order of 35 %.

No radiation damage effect was observed. The maximum number of neutrons that passed through a single crystal being only of the order of $10^{11}/cm^2$ we will see, by comparison with a proton beam effect, that this is normal.

HARWELL TARGET [4,5]

I now come to the target built at Harwell. It was designed for spin correlation experiments with a proton beam in the energy range of 143 MeV down to 70 MeV at the laboratory scattering angle of 45° and, at the energy of 143 MeV, at an angle up to 62°. This latter experiment done with an unpolarized beam provides a way of measuring the target polarization. Then this difficult problem is resolved. This energy region seems to be one where the cooling problem is fairly critical. In fact (p,2p) reactions are not negligible, this, with the necessity of detecting protons scattered at large angles would make rather difficult to have helium in the cavity, and, at the same time, you need, to get a reasonable counting rate, a crystal rather thick, then difficult to cool.

For limiting the energy spread of the scattered protons the crystal has a thickness of 1 mm. It is placed in the median plane of a cavity resonating, at a frequency of 35 GHz, on a TE_{012} mode. Its dimensions are 6.25 x 7.0 x 11.6 mm, these of the crystal are 7 x 6.25 x 1. mm. Figure 2 is a schematic drawing of the cavity showing the crystal in the median plane, the 9.3 kilogauss magnetic field horizontal and parallel to that plane, the beam perpendicular to that plane. It shows that this arrangement insures a rather high and constant intensity of the microwave field on the center part of the crystal which is the useful part for the experiment. The entrance and exit walls of the cavity on the beam path are made of 0.1 mm thick copper foils, the exit windows for the scattered protons are made of 0.05 mm thick copper foils.

Figure 3 is a drawing of the target assembly. The cavity is split into two parts that are connected by two tubes that allow the circulation of liquid helium in the bottom part and insures a proper cooling of that part. The crystal fits into groves made in the median plane. Then the two parts are put together and the connecting

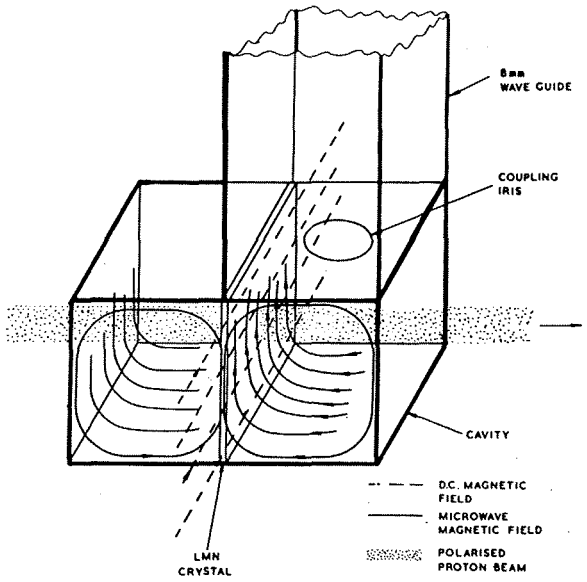

Fig. 2 Target cavity resonant in TE012 mode at 35.0 GHz.

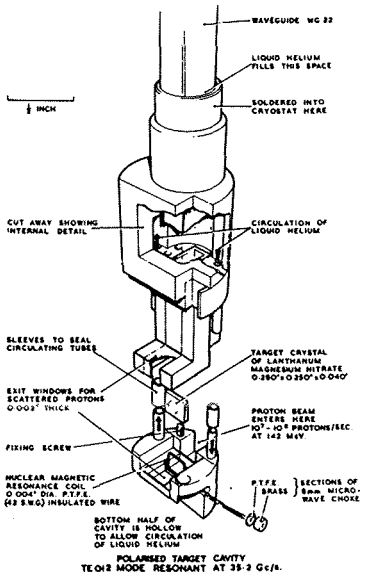

Fig. 3 Polarized target cavity TE012 mode resonant at 35.2 Gc/s.

tubes soldered leakproof to superfluid helium. The NMR coil is placed along the walls just beside the crystal. It has therefore a very non-uniform sensitivity to the different parts of the crystal. The crystal is cooled by contact of its edges with the thick walls of the cavity cooled to 1.35° K with a conventional type cryostat. The contact was made first with Kel-F grease which has the advantage of being non hydrogeneous and easy to handle but seems to have a rather bad thermal conductivity. The temperature of the crystal was going up rapidly as the microwave power was increased and even the energy loss of the beam, calculated to be only of the order of a few microwatts, was noticeable. Then the varnish GE 7031 was used, insuring a better cooling but having many handling disadvantages. It also contains hydrogen what is a reason more for making impossible the polarization measurement by NMR technics.

A polarization of the order of 35 % is obtained with that target.

A very interesting point is that the forbidden and doubly forbidden satellites of the electronic line were observed with that target [6]. The forbidden satellite was used for setting the correct field for "solid effect". The decrease of its intensity, while the polarization is growing up, was seen well enough to be used as a continuous polarization monitor.

An other interesting point is that it is with that target that, for the first time, the decrease of the polarization due to radiation damage was observed. Figure 4 shows the way the polarization drops down when the protons pass through it. It is fitted on this figure by a straight line but could as well be fitted by an exponential. It is characterized by a decrease of a factor of two when 2×10^{12} protons per squared centimeter have passed through the crystal. Brogden [7] reports that, after irradiation, the decay of the NMR signal, when the microwave is switched off, is no longer exponential. It is initially much faster than before irradiation and slows down later. He thinks that an explanation of that phenomenon could be the inhibition of the spin-diffusion mechanism. The protons standing near a neodymium ion would relax fast and their depolarization could not be slowed down by polarization diffusion from the rest of the protons. Those ones could then only relax slowly. In the process of building the polarization it would be the other way. The polarization of the protons sitting near a neodymium ion could grow up rapidly but could not be transmitted to the rest of the protons. We will see that, at Saclay, we have made observations on the Lorentz field that are consistent with that explanation.

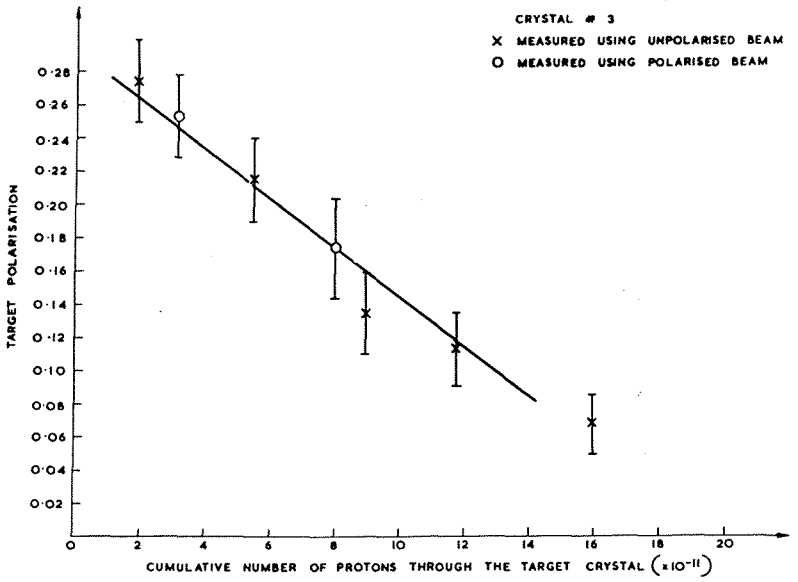

Fig. 4

SACLAY TARGET [8,9]

I now describe the target built at Saclay. It was designed for spin correlation experiments with a proton beam in the energy range of 10 to 26 MeV at the laboratory scattering angle of 45°. P. Catillon will show that the measurement made at 11 MeV provides a way of continuously measuring the product of the beam and target polarizations. This dispenses us with the necessity of measuring the polarization and even of continuously monitoring it. In that energy region, (p,2p) reactions are negligible then the background comes only from accidental coincidences. For measurements with 11 MeV protons the thickness of the crystal is limited to 0.1 mm.

A horizontal cross-section of the target is shown on figure 5. The 18.5 kilogauss magnetic field is vertical, then perpendicular to the plane of that cross-section. The exit wall has to be as thin as possible to allow very low energy protons to get through. It is made of a one micron thick copper foil. It is then impossible to have helium in the cavity. The crystal has to be cooled by contact. We thought that it would be better cooled if that contact is made on all its surface. The entrance wall has been chosen thick enough to provide a good cooling, thin enough for not increa-

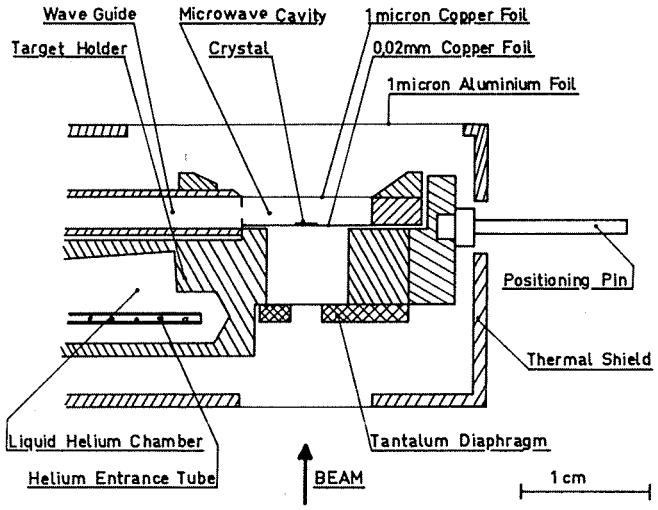

Fig. 5 Horizontal cross-section of the target.

sing too much the background. It is made of a 0.02 mm thick very pure copper foil. The crystal is glued on it with a non hydrogeneous grease similar to Kel-F.

The necessity of detecting the protons at an angle of 50° imposes that flat shape for the cavity. It resonates at a frequency of 70 GHz on a TE_{011} mode. Its dimensions are 10 x 10 x 2.2 mm. The flat shape of the cavity also provides a very constant intensity of the microwave power along the crystal, then a uniform polarization what is important for the experiment. The microwave generator is a klystron giving 100 mW.

A Roubeau type cryostat is used for cooling the copper block supporting the target to a temperature of 1.15° K. By outgazing carefully the grease before using it and, due to the very small thickness of the crystal, we had no cooling problem.

The NMR coil is made of a single wire placed beside the crystal. It is shown on figure 6 where you see the crystal glued on the entrance wall and the NMR coil beside the crystal. Its filling factor is very poor, only the enhanced signal can be seen and the sensitivity to the different parts of the crystal is very non uniform. But it could be used to measure the polarization by the Lorentz field method [10].

The effect of radiation damage on the polarization was similar to the one observed at Harwell. The decrease of the polarization by

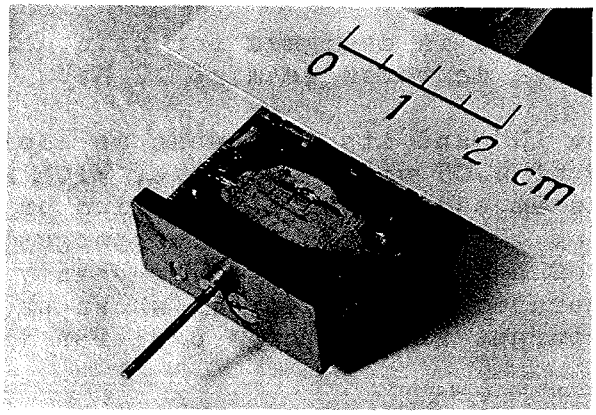

Fig. 6

a factor of two was obtained after about 10^{12} protons per square centimeter have passed through the crystal. We observed that the decrease of the Lorentz field was much smaller than the one of the average polarization which is consistent with the explanation of Brogden. We also noticed that the electronic line intensity was decreasing faster than the polarization.

I would like to make a remark about the Lorentz field method. In the case of a crystal not yet irradiated, with a uniform polarization and temperature, it seems that it could be a way of measuring the polarization of very small volume targets with some accuracy when no nuclear scattering method is available. It consists in measuring the local field created by the polarized protons at the place where are the neodymium ions. This is done by measuring the magnetic field shift of the electronic line when the target is depolarized rapidly. We observed shifts of more than 1.5 gauss and, with the overall stability of our microwave frequency and magnetic field which is, over a short period of time, of the order of 25 milligauss, it could be measured with a relative accuracy of better than 3 %. Unfortunately, at the present time, the coefficient relating the shift to the polarization has not been measured. But this measurement could be done in good conditions when the polarization of the target can be obtained with accuracy by nuclear scattering.

I now give a short description of the targets that are under a preliminary stage of construction and will briefly mention the targets for which the design is not yet started but that are planned to be built.

BIRMINGHAM TARGET [11]

The target of Birmingham is designed for spin correlation experiments with a polarized deuteron beam of 12 MeV.

The crystal will be LMN and its thickness is limited to 0.1 mm and should even be of 0.05 mm if possible. With such a low energy deuteron beam it is impossible to have helium on the beam path. The field will be of 18 kilogauss and the target would be polarized at the center of a multimode circular cavity with a carcinotron microwave generator. The cavity is shown on figure 7. The window around the target is made of a 6 micron thick silver plated mylar.

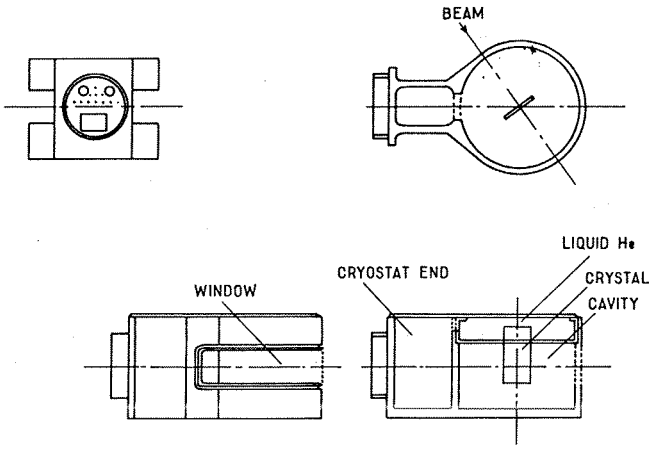

Fig. 7 Polarized target cavity.

It is very interesting to see the way the crystal will be cooled. The part of it used for scattering is in the vacuum while the other end will be in direct contact with liquid helium in a compartment located above the cavity. The sealing will be made with low temperature Araldite. A Roubeau type cryostat will be used.

With deuterons there is no easy way of measuring the polarization by nuclear scattering then it will have to be measured by NMR technics. Due to the possible polarization inhomogeneity coming from non uniform microwave intensity or temperature gradient between the top and bottom part of the crystal, a difficult problem will be of measuring an average polarization similar to the average polarization seen by the deuteron beam. But it has to be noticed that the crystal, being far from metallic walls, is in the most

favourable situation to give a good NMR signal. This one will be detected with a marginal oscillator.

ERLANGEN TARGET [12]

This target could be used with 10 MeV protons. It will use a LMN crystal cooled with a cryostat conventional but using a needle valve to depressurize the helium between the reservoir at atmospheric pressure and the copper block containing the target resonator and a small reservoir where liquid helium will be at a pressure of a few torr. The cavity is of rectangular shape resonating at a frequency of 70 GHz on a TE_{101} mode, its dimensions are : 2.19 x 10.12 x 10.12 mm.

KYOTO TARGET [13]

Designed for 52 MeV protons experiments. The LMN crystal will be cooled directly with helium in the cavity, this one being a multimode cavity. The cryostat is conventional but also uses a needle valve.

NEW SACLAY TARGET

A new target is in a very preliminary stage of development at Saclay. The idea would be to get a thin target with uniform polarization and at the same time, a good NMR signal.

In a cavity it is difficult to have, at the same time, a crystal properly cooled, far from metallic walls and in a microwave field of uniform intensity. Figure 8 is a schematic drawing of the target arrangement. The crystal would be cooled by contact with a quartz plate which has a good thermal conductivity and no inconvenient for the radiofrequency. A microwave horn would radiate a

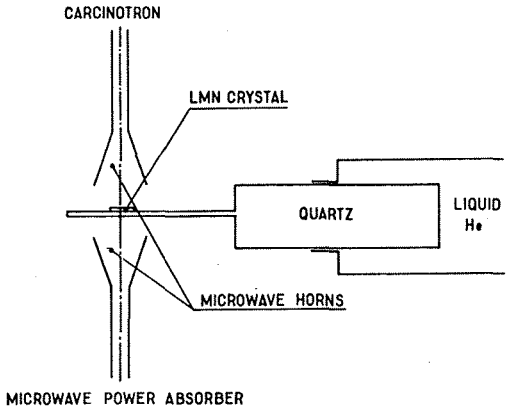

Fig. 8

travelling plane wave through the crystal, the microwave power would be received on an other horn, transmitted and dissipated outside the target.

A target will be built at Prague [14] to be used with low energy neutrons.

A target will be built at Davis [15] to be used with neutrons in the energy range of 30 to 50 MeV.

They will both use a Roubeau type cryostat but their design is not yet started.

A target using toluene doped with DPPH is planned to be built at Los Angeles [16]. It would be used with 52 MeV protons. It is interesting to notice that it would be the only one using an other material than LMN. Toluene could help from the radiation damage point of view, but if it is impossible to have helium in the cavity it could be very difficult to cool.

References

1) P.J. Bendt, J.J. Malanify, T.R. Roberts and J.E. Simmons, Karlsruhe Conference (1965), p. 293.
2) J.J. Malanify, P.J. Bendt, T.R. Roberts and J.E. Simmons, Phys. Rev. Letters, 1966, 17, 481.
3) J.E. Simmons, Private communication.
4) T.W.P. Brogden, O.N. Jarvis, J. Orchard-Webb and M.R. Wigan, Karlsruhe Conference (1965), p. 298.

5) J.P. Scanlon, Private communication.
6) T.W.P. Brogden and J. Butterworth, Proc. Phys. Soc., 1965, 86, 877.
7) T.W.P. Brogden, "A polarized proton target for proton scattering experiments", (not published).
8) M. Chapellier, D. Garreta and J. Kirsch, Karlsruhe Conference (1965), p. 126.
9) P. Catillon, M. Chapellier and D. Garreta, Rapport CEA, n° 3193, 1967.
10) A. Abragam, M. Borghini and M. Chapellier, Compt. Rend., 1962, 255, 1343.
11) N. Berovic, Private communication.
12) H. Kuiper, Private communication.
13) R. Kajikawa, Private communication, (Information can be obtained about that target from K. Nisimura, Kyoto University, Japan).
14) M. Odehnal and F. Lehar, Private communication.
15) J. Jungerman, Private communication.
16) R.J. Wagner, Private communication.

EXPERIMENTS AT LOW ENERGY

P. CATILLON

Département de Physique Nucléaire, Saclay

Until now three experiments have been done at low energy using polarized targets. The subject of each of them is the nucleon-nucleon interaction.

The spin correlation parameters can be measured without polarized targets. After scattering an unpolarized beam from an unpolarized target, the spins of scattered and recoil nucleons are detected in coincidence with two secondary scatterings called polarimeters. Depending on the direction of the spins in the outgoing channels, the spin correlation parameters are C_{nn}, C_{kp}, C_{pp}, C_{kk}. For these two last a magnetic field is necessary between the first target and one of the two polarimeters.

By time reversal invariance, equivalent parameters can be measured in polarized beam-polarized target experiments. Depending on the direction of the spins in the incoming channels, these parameters are A_{xx}, A_{yy}, A_{zz}, A_{zx}.

The relations connecting the $C_{\mu\nu}$ and A_{ij} have been given by J. Raynal [1]. The most important ones are :

$$A_{yy} = C_{nn}$$

$$A_{xx} = - \sin\theta\, C_{kp} + \cos^2\frac{\theta}{2}\, C_{kk} + \sin^2\frac{\theta}{2}\, C_{pp}$$

LOS ALAMOS

The neutron-proton A_{yy} measurement at 23.1 MeV has been done at Los Alamos by J.J. Malanify, P.J. Bendt, T.R. Roberts, J.E. Simmons [2].

The neutron beam is provided by the reaction $T(d,n)^4He$ with a deuteron beam of 7 MeV at the scattering angle of 30° lab (fig. 1). The neutron energy is 23.1 MeV and the polarization p_b = 49 % ± 6 %. The scattering plane is vertical. The polarized proton target is at a distance of 25 cm from the neutron source and the recoil protons in the vertical scattering plane are detected by a ΔE counter and a plastic E counter which gives the scattering angle.

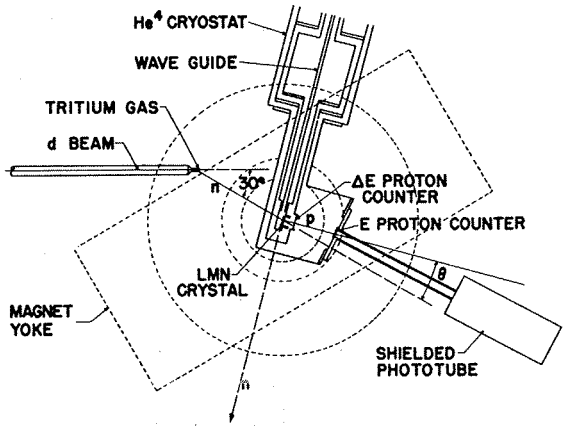

Fig. 1

Proton target polarization is typically 30 % ± 5 %. This polarization is reversed by changing the magnetic field of 35 gauss. For every run the neutron beam is integrated as carefully as possible by integration of the deuteron beam current, elapsed time and auxiliary monitor counter.

The relation between A_{yy}, the beam polarization p_b, the target polarization p_t and the so-called asymmetry ε, which is the difference between triplet cross-section and singlet cross-section over the total cross-section is :

$$A_{yy}(\theta) = - \frac{\varepsilon(\theta)}{p_t} \left[\frac{1}{p_b} + P_{np}(\theta) \right] - \frac{P_{np}(\theta)}{p_b}$$

where P_{np} is the polarization parameter in n-p scattering.

The results are given on the figure 2 and in the table below :

θ_{cm}	130°	140°	150°	174°
$A_{yy}(\theta)$	+ 0.13 ± 0.04	+ 0.074 ± 0.024	+ 0.05 ± 0.02	- 0.014 ± 0.011

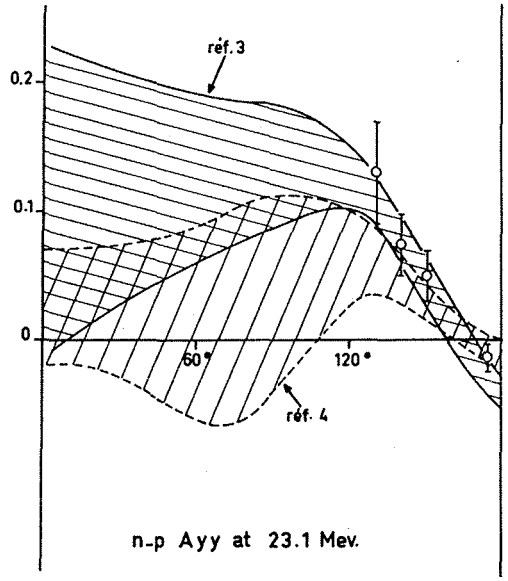

Fig. 2

The two regions are the corridors of error for the Livermore phase shift analysis solution C [3] and the new Dubna analysis [4]. The Livermore solution is close to the values given by models such as the Hamada-Johnston or the Yale potentials.

It would be interesting to measure a point for a smaller scattering angle and this is the reason why the same group will attempt to measure A_{yy} at 90° cm next year ; they will use a neutron detector in coincidence and evidently the counting rate will be reduced by an order of magnitude because of the neutron detector efficiency. For this reason they want to increase their target polarization toward 50 %.

HARWELL

This proton-proton A_{yy} measurement has been done by T.W.P. Brogden, O.N. Jarvis and M.R. Wigan [5].

The proton beam is provided by scattering from a primary aluminium target. The energy is 143 MeV but can be degraded to several lower energies. The beam polarization is 47.2 % ± 0.4 % and can be rotated by passing down a solenoid.

Scintillation counter telescope are used at 90° and 60° c.m. detecting both recoil and scattered protons.

The beam intensity monitor is a secondary scattering from a thick polythene target with a pair of detectors recording the protons at ± 45° lab.

The main difficulty of this experiment has been to measure the target polarization taking into account the large decrease of this polarization by radiation damage. The A_{yy} measurements have been interposed between runs using an unpolarized beam. During these runs the asymmetry gave the target polarization (crosses on the fig. 3) and an interpolation gave this polarization during the A_{yy} runs (circles on the fig. 3). This method cannot give the target polarization with a relative accuracy better than 5 %. This is probably the most crucial and delicate point of this experiment.

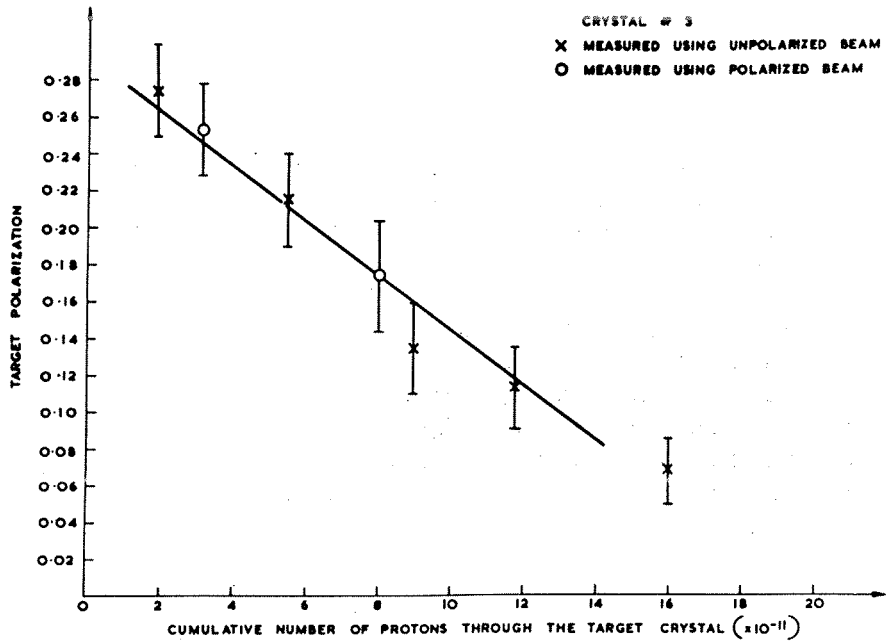

Fig. 3

The results are in the table below :

E_{MeV}	73.5	98	143
$A_{yy}(90°\ cm)$	+ 0.25 ± 0.06	+ 0.69 ± 0.04	+ 1 (± 0.05)
$A_{yy}(60°\ cm)$			+ 0.83 ± 0.03

In fact this table gives the ratio of the different parameters over the value of $A_{yy}(90°)$ at 143 MeV. The normalization coefficient is therefore (1 ± 0.05).

SACLAY

This proton-proton A_{xx} and A_{yy} experiment has been done by D. Garreta, M. Chapellier and myself [6].

The polarized proton beam is provided by the polarized proton beam of the cyclotron [7]. Its polarization is about 70 % and can be flipped from up to down five times a second by a radiofrequency transitions in the source. Thus we do not have to monitor the beam.

The target polarization is about 70 % but decreases by radiation damage during the run. The detectors (fig. 4) are solid state surface barrier detectors, 25 mm from the target inside the pole pieces of the magnet. They are at the scattering angle of ± 45° lab in horizontal and vertical scattering planes. Therefore the measured parameters are A_{xx} and A_{yy}. The so called asymmetries $p_b \cdot p_t \cdot A_{xx}$ and $p_b \cdot p_t \cdot A_{yy}$ are measured at the same time, with the same $p_b \cdot p_t$ product at two energies, the beam energy and the energy degraded by means of the degrader (5 on fig. 4) interposed on the beam path every five seconds. The knowledge of A_{xx} at 11.4 MeV (close to -1) gives the value of the product $p_b \cdot p_t$ and overcomes the difficulty of an accurate measurement of these polarizations.

The results are shown on the figure 5 taking - 0.984 as the best value of A_{xx} (11.4 MeV) [8]. The figure shows the results of C_{nn} by conventional experiments at Boulder [9] and Copenhagen [10]. The full line is the value of the last Yale potential called Y IV.

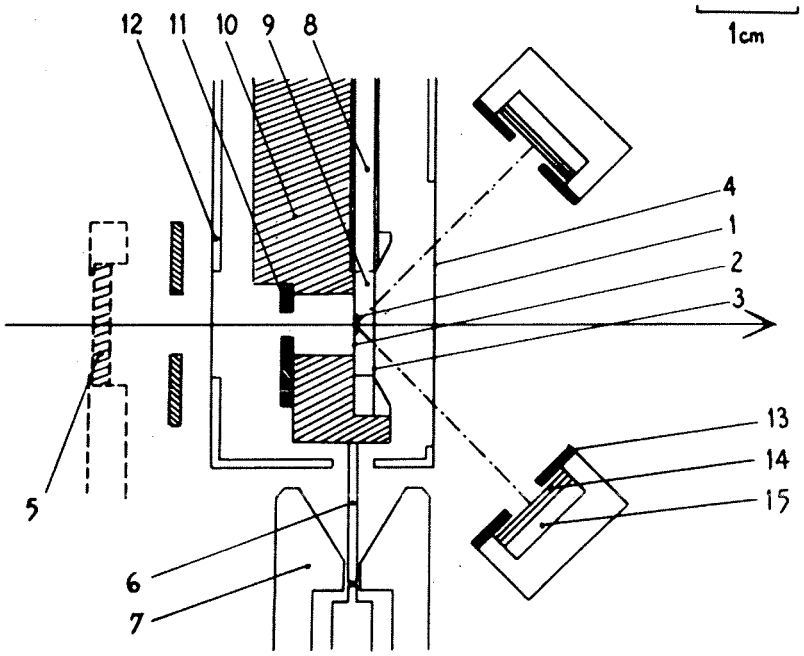
12
11
10
9
8
1cm
4
1
2
3
13
14
15
5
6
7

Fig. 4

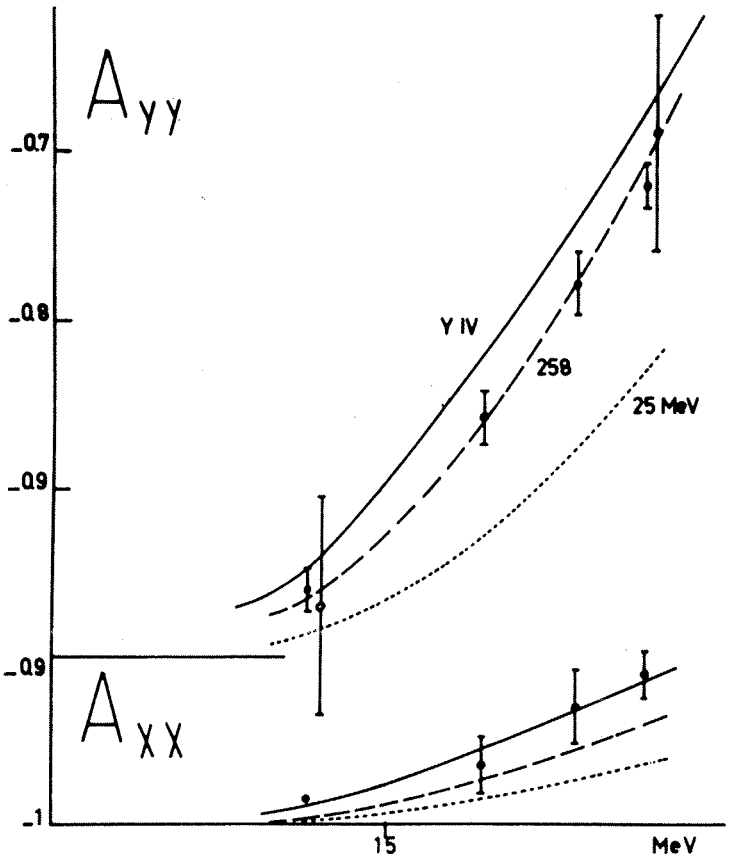
Ayy
-0.7
-0.8
-0.9
-0.9
-1
Axx
Y IV
258
25 MeV
15
MeV

Fig. 5

The dashed line "258" is an energy dependent phase shift analysis from Livermore combining n-p and p-p data from 20 MeV to 345 MeV. The dotted line "25 MeV" is an energy independent phase shift analysis from Livermore using n-p and p-p data around 25 MeV only. These two analyses have been done before the experiment and the results show the interest of the energy dependent phase shift analyses.

The table below gives the results with $A_{xx}(11.4) = -1$. It would be necessary to multiply every parameter by the true value of $A_{xx}(11.4)$, - 0.984 being a first approximation [8].

E_{MeV}	11.4 ± .2	19.5 ± .15	23.45 ± .15	26.5 ± .1
A_{xx}	- 1	- .981 ± .017	- .945 ± .022	- .926 ± .014
A_{yy}	- .976 ± .013	- .872 ± .016	- .791 ± .019	- .732 ± .013

In general what are the specific difficulties or advantages of the low energy experiments with polarized targets ?

It is impossible to have a thick target, the range of protons being small in the crystal, and this is the main difficulty for the target polarization measurement. Secondly, the required accuracy in low energy physics needs good statistics, that means a high counting rate and consequently severe radiation damage.

On the other hand, an advantage of the low energy experiments is that, as long as the Q value of the La(p,2p) reaction, about 6 MeV, is small with regard to the energy, the detection can select the protons scattered by free protons. That means that, at low energy, LMN is interesting for its high polarization, its small ratio of hydrogen over other nuclei being unimportant except for the counting rate.

But the main advantage of low energy physics is the possibility to measure the target polarization by nuclear scattering.

This can be done with an auxiliary scattering recorded from time to time, namely the asymmetry of an unpolarized proton beam scattered by the polarized target in the Harwell experiment. It could be the asymmetry of the recoil protons in the scattering of an α particle beam by the target. These asymmetries are well known and the accuracy can be good. But the difficulty is to make an interpolation between these test runs to obtain the target polarization during the real runs. It is also necessary to have a homogeneous.

polarization and, in case of radiation damage, a homogeneous decrease of this polarization.

Otherwise the averages of the target polarization during test and real experiments could be different if the detection efficiency for a specific point of the target is different for the two kinds of experimental set up. For instance, if the target polarization is measured from time to time with an unpolarized beam and if this beam is well focused on a small spot in the center on the target, each of these test runs will depolarize this center only by radiation damage. The measured polarization will decrease quickly but the polarization of the edges of the target will remain higher.

Consequently it is interesting to measure the target polarization continuously by nuclear scattering during the experiment itself. Something similar has been done at Saclay where one of the measured parameters is known and allows us to know the $p_b \cdot p_t$ product.

Still better an observable can be measured without any knowledge of the polarizations except for the size of the error bar, for instance the ratio A_{yy}/A_{xx} which is an observable as interesting as A_{xx} alone.

It is interesting to see that the effect of the accuracy of the polarization on the accuracy of the measured parameter is very different depending on whether this parameter is large or not. In the case of the Los Alamos experiment at 174° the error is chiefly due to the statistics, the asymmetry being close to zero.

And thus the characteristics of a target are very different according to the experiment and the expected value of the measured parameter.

I would like to insist now on the interest in measuring A_{yy} and A_{xx} in the p-p scattering.

The scattering matrix has been written by J. Raynal [1] in the helicity formalism as :

$$\begin{vmatrix} a & 0 & 0 & 0 \\ 0 & & & \\ 0 & & (b\ c\ d\ e) & \\ 0 & & & \end{vmatrix}$$

where a is the singlet scattering amplitude and bcde the triplet scattering amplitudes. At 90°c.m., b and d vanish and :

$$2\sigma(1 - A_{yy}) = |a|^2$$

$$2\sigma(A_{yy} - A_{xx}) = |c|^2$$

$$2\sigma(1 + A_{xx}) = |e|^2$$

Then, with a measurement of the cross-section, A_{xx} and A_{yy} at 90° c.m.,it is possible to determine the value of these three scattering amplitudes.

At an energy low enough to use an SPD approximation, e and c give directly the P wave splittings :

$$k^2 |e|^2 = 4(\delta^3P_2 - \delta^3P_0)^2$$

$$k^2 |c|^2 = 9(\delta^3P_2 - \delta^3P_1)^2$$

In Born approximation we can take for these P phase shifts.

The Gammel and Thaler expansion [11] :

$$\delta^3P_0 = \Delta_c + 4\Delta_T - 2\Delta_{LS}$$

$$\delta^3P_1 = \Delta_c - 2\Delta_T - \Delta_{LS}$$

$$\delta^3P_2 = \Delta_c + \frac{2}{5}\Delta_T + \Delta_{LS}$$

where Δ_c, Δ_T and Δ_{LS} are the contributions of the central, tensor and spin-orbit interactions, and then we can measure directly Δ_T and Δ_{LS}.

The figure 6 shows the experimental values of A_{xx} and A_{yy} in proton-proton scattering. The curves are from an old energy dependent phase shift analysis [12], a better fit can be obtained with new sets of phase shifts. But they show that :

1) the singlet amplitude |a| is close to zero at about 150 MeV and there $A_{yy} = +1$.

2) the triplet amplitude |e| is close to zero at about 120 MeV and there $A_{xx} = -1$.

Owing to the fact that at 90° $A_{yy} - A_{zz} = 1 + A_{xx}$, we have $A_{xx} = -1$ if $A_{yy} = A_{zz}$.

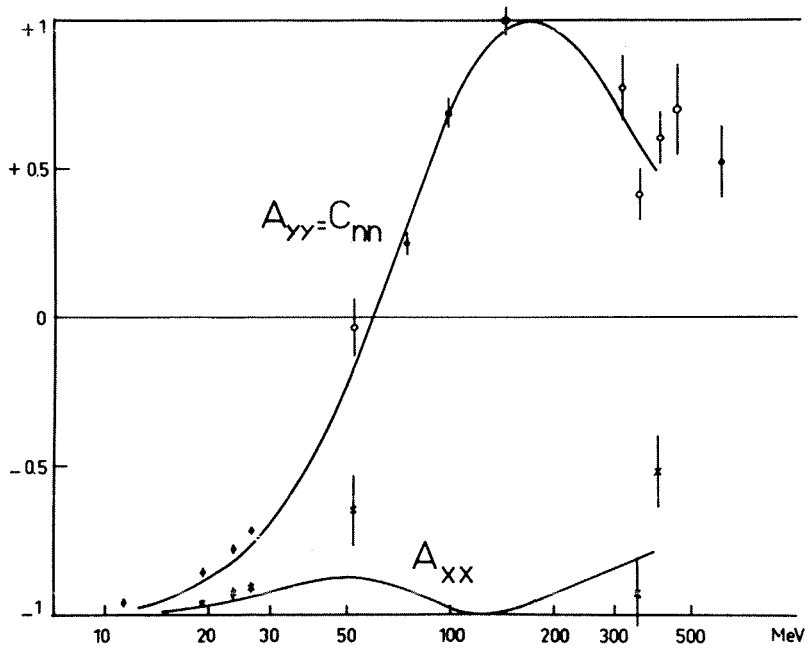

Fig. 6

If it is not too difficult to measure the asymmetry with the beam line making a 45° angle with the beam spin and a 135° angle with the target spin, then, at the energy where this asymmetry is zero, $A_{xx} = -1$, and this can be done without polarization measurements.

These two energies, where A_{xx} (90°) = -1 or A_{yy} (90°) = +1 could be taken as references for measurements of the parameters at other angles or energies.

Another experiment can be made without polarization measurements. It is the measurement of the energy where A_{yy} goes across zero (at about 55 MeV).

It would be very interesting to measure A_{xx} at about 50 MeV where $(1 + A_{xx})$ is maximum. This is directly connected to the maximum of the $^3P_0$ phase shift which is a contested point until now.

References

1) J. Raynal, Nucl. Phys., 1961, 28, 220.
2) J.J. Malanify et al, Phys. Rev. Letters, 1966, 17, 481.
3) R.A. Arndt and M.H. McGregor, Solution C, UCRL 70075 (1966).
4) Z. Janout, Yu Kazarinov and F. Lehar, El.2952 - Dubna (1966).
5) T.W. Brogden et al, Karlsruhe Conference (1965), p. 298.

6) P. Catillon, M. Chapellier and D. Garreta, Rapport CEA 3193 (1967).
7) R. Beurtey, Thesis, Rapport CEA R.2366 (1964).
8) From H.P. Noyes, (to be published).
9) N. Jarmie, (to be published).
10) R.L. Burman et al, Congrès de Paris (1964) 1/C 180.
11) J.L. Gammel and R.M. Thaler, Phys. Rev., 1957, 107, 291.
12) R.A. Arndt and M.H. McGregor, Phys. Rev., 1966, 141, 873.

INFORMATION ABOUT THE TWO AND THREE NUCLEON SYSTEMS OBTAINED AND OBTAINABLE FROM THE USE OF POLARIZED TARGETS AND BEAMS

H.P. NOYES

Stanford University, Stanford

I INTRODUCTION

It has been customary for a number of years in nuclear physics conferences to discuss the three-nucleon system together with 4, 5, ... n (n small) nucleon systems, and to consider the two-nucleon system, if at all, either as an isolated topic, or in conjunction with elementary particle physics. I believe the time has come to change this pattern. In fact, one of the main things I hope to convince you of in this talk is that the three-nucleon system will have to be treated as a problem in elementary particle physics, if we are to reach any fundamental understanding of its characteristic features, and that the theoretical and experimental techniques for such a treatment have reached a promising stage of development. A second reason for treating these two topics together is that the work on the two-nucleon system has reached a certain stage of completion (although there is much important work still to be done) and it may well prove profitable to aim future experiments at those features of the two-nucleon system which we will need to know better for three-nucleon calculations ; in a very real sense, I believe the frontier of the two-nucleon problem has become the three-nucleon system. A third point I wish to emphasize is that there is more than a superficial similarity between the current state of development of work on the three-nucleon system and the problems which faced us ten years ago in trying to understand nucleon-nucleon scattering. We should, therefore, be able to profit, if we are wise, from the lessons learned in that arduous and difficult development. In particular, I have learned to my cost that every complexity allowed by the conservation laws is in fact

present in the two-nucleon system, and that many mistakes were made by ignoring this possibility. The three-nucleon system is bound to be at least as complicated, and we should be correspondingly cautious about introducing simplifying assumptions into the analysis before we have a firm grasp on the dynamics. This line of thought leads me to discuss the work on the three-nucleon system first ; the recent experimental work on the two-nucleon system can then be described in what I believe to be the appropriate context.

At first sight, the problem of experimentally determining the three-nucleon scattering matrix for n-d scattering looks formidable. If we write the independent terms in this matrix as coefficients of rotationally invariant tensors, we find 12 invariant amplitudes for elastic scattering and 24 for inelastic scattering. A priori we therefore expect that we need 72 different experiments at each energy and angle to determine these 36 complex numbers ; this is an underestimate, since the observables are bilinear combinations of the amplitudes, and further experiments are required to resolve sign ambiguities. If full angular distributions are measured, or enough information obtained for a phase shift analysis, unitarity should bring the total number of experiments needed somewhat below 72, which is small comfort. Since there are 648 non-zero elastic scattering observables, and 2304 inelastic ones, there are plenty of experiments to choose from ; it is also clear that care should be exercised in the choice so that (except for purposes of increasing precision) experiments are not picked which simply give the same bilinear combinations of amplitudes already determined by earlier experiments.

With this large number of possibilities available, it is not surprising that so far only a few types of observables have been measured. These are : differential and total cross-sections (both elastic and inelastic), polarization of either protons or neutrons, vector and some of the tensor polarization coefficients of the deuteron, and one measurement of D and R'. It is clear from what has just been said that progress will be much more rapid once a comprehensive theory of the process exists, and we have some idea of which amplitudes are the most dynamical significance. Unfortunately this theory is only just beginning to be worked out.

II THREE-NUCLEON POLARIZATION EXPERIMENTS

Since this subject was reviewed by Barschall at Karlsruhe, I have attempted only to survey the literature published this year very cursorily, and have contacted groups at Berkeley, Dubna, Los Ala-

mos, Rutherford, Saclay and Wisconsin about recent work. It is very likely that I have overlooked significant papers and preprints, and wish to state explicitly that any omissions are unintentional, and to apologize for them. It should also be noted that, because of the specialized nature of this conference, I have made no attempt to survey differential cross-section, total cross-section, or break-up data.

An illustration of how far we have to go in exploring the three-nucleon system is the fact that prior to this year we had no experimental way of choosing between the two alternative choices for the doublet and quartet n-d scattering lengths allowed by the total cross-section measurements. The corresponding ambiguity between singlet and triplet scattering lengths in the n-p system is easy to resolve theoretically, since we know from effective range theory that the smaller of the two scattering lengths must go with the system that has the bound state, and as the deuteron has a quadrupole moment, we know that this must be the triplet state ; of course the ambiguity was also resolved experimentally long ago. Since we still lack a rigorous low-energy theory for the n-d system, the theoretical situation here is less clear. Many theoretical arguments have been advanced favouring the set in which the doublet scattering length, a_2, is smaller than the quartet scattering length, a_4, but it was still possible last year to argue for the alternative choice [1]. However, by measuring the transmission of polarized neutrons through a polarized deuteron target, Alfimenkov, Luschikov, Nikolenko, Taran and Shapiro [2] have shown conclusively that a_2 is less than a_4, as will be discussed in the paper to be presented this afternoon by Luschikov.

Granted this choice, the values of a_2 and a_4 which have been accepted for a number of years are [3] $a_2 = 0.7 \pm 0.3$ F, $a_4 = 6.38 \pm 0.06$ F. However, in a paper to be presented at the Stanford Meeting of the American Physical Society at the end of this month, Seagrave [4] provides a re-evaluation of recent measurements of the coherent and incoherent scattering of "cold" neutrons, including corrections due to residual binding effects of as much as 7 %, and reaches the preliminary conclusion that $a_2 = 0.1 \pm 0.2$ F, $a_4 = 6.2 \pm 0.1$ F, assuming a free cross-section of 3.2 ± 0.1 b, and the value of the incoherent cross-section obtained by W. Gissler [5] of 2.25 ± 0.04 b. If one accepts the unpublished value of the coherent scattering length of 6.17 ± 0.06 F obtained by R.E. Donaldson [6], one finds $a_2 = 0.11 \pm 0.07$ F, $a_4 = 6.14 \pm 0.06$ F and predicts $\sigma_{free} = 3.14 \pm 0.06$ b, which is consistent with this analysis. It is perhaps significant that, according to A.C. Phillips [7], it is easier to achieve consistency between these new values and the binding energy of the triton in the separable approximation to the three-body problem to be discussed below, than to fit the older values together with $\epsilon_{^3H}$.

I would like to emphasize that what is needed here for efficient analysis of the experiments is a model-independent theory of low

energy n-d scattering, analogous to effective-range theory for the two-nucleon system, taking full account both of the spin-structure of the three-nucleon system, and of the low-lying inelastic threshold. Working out the complications due to Coulomb interactions will be still more difficult but again is needed if we are to exploit the high experimental precision available in low energy p-d measurements.

Early work on p-d polarization at low energy has been summarized by Chalmers, Cox, Seth and Strait [8] in comparison with their results at 1.50, 2.02, 2.52 and 4.1 MeV, and more recent results by Grübler, Haeberli and Extermann presented at Karlsruhe have since been published [9]. Still more accurate results from Wisconsin at 4.0, 6.0, 8.0 and 10.0 MeV covering the angular range from 30° to 150° were presented by H.B. Clegg at the Washington meeting of the American Physical Society this spring [10], and unpublished results at 12.0 MeV from the same author were submitted to me for this conference. Clegg's results are everywhere positive in this angular range, and show a maximum at slightly below 120° at 4 MeV which moves to slightly above 120° as the energy increases. The value of the polarization at the peak is 0.072 ± 0.012 at 4.0 MeV, rising to 0.140 ± 0.010 at 10.0 MeV ; the 12.0 MeV data continue this trend. There is a partial overlap between these experiments and a measurement at 10.5 MeV over the range 30-100° made by McKee, Clark, Slobodrian and Tivol [11], and the same authors have also made available to me unpublished results at 12.5, 16.5 and 19.5 MeV. By 16.5 MeV the peak has moved out to about 145° and risen to a value of about 0.18, and at 19.5 MeV a minimum around 100° is also clearly shown. In the region of overlap, there is generally speaking reasonable agreement with Clegg's data, except that at 10.5 MeV, the Berkeley group find two negative values for the polarization below 40°, and that the 30° point at 12.5 MeV is also slightly negative.

The general trend of the polarization data is illustrated in figure 1, which gives my own free-hand curves through Clegg's data at 12 MeV, the data of Conzett, Igo and Knox [12] at 22 MeV, of Conzett, Goldberg, Shield, Slobodrian and Yamabe [13] at 40 MeV, of Hall, Johnston and Griffiths [14] at 30 MeV, and of Johnston, Gibson, Megaw, Griffiths and Eisberg [15] and Johnston, Gibson, McClatchie, Megaw and Griffiths [16] at 50 MeV. By making use of a double focusing magnetic spectrometer, Gibson, Johnston, McClatchie, Megaw and Griffiths [17] have recently extended the angular range of the 30 and 50 MeV measurements to both smaller and larger angles, and this new, unpublished data has also been drawn on in constructing my free hand curves.

It is clear that the polarization exhibits much interesting structure : the backward peak which develops at very low energy and gradually moves outward with angle as the energy increases, but which seems to saturate at about + 0.2, the very deep negative mi-

nimum which appears already below 20 MeV as noted above, and goes to large negative values at higher energy, and the small forward positive peak. The impulse approximation gives no indication of this structure, even when off-shell scattering corrections are included [18]. Hüfner and de-Shalit [19] have shown that this type of polarization structure can be correlated with the differential cross-section in a diffraction model, and obtain a qualitative fit to both at 40 MeV using a single parameter, but this hardly provides a dynamical explanation. It appears that the region around 50 MeV will provide an interesting challenge to detailed three-nucleon theories.

Since low energy n-d polarization results were reviewed by Barschall at Karlsruhe [20], I will mention only the 22.7 MeV measurement of Malanify, Simmons, Perkins and Walter [21] which has now been published. You will note in figure 1 that I have indicated that the large-angle p-d polarizations measured at 22 and 40 MeV apparently go to much higher values than the value of 0.2, which now appears to be accurately measured at 30 and 50 MeV.

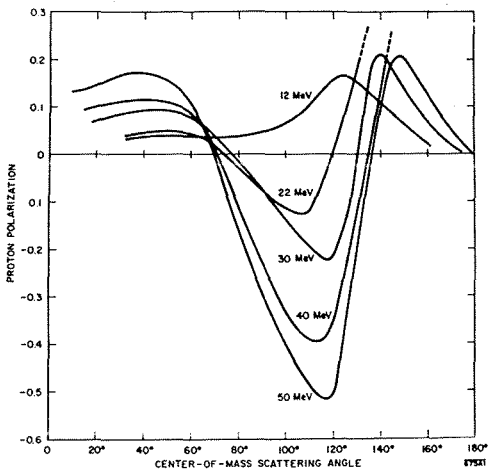

Fig. 1 General behaviour of proton polarization in p-d scattering up to 50 MeV.

If we compare the 22 MeV experiment with the n-d results, in figure 2, we see that the n-d experiment favours the smaller value found at 30 and 50 MeV. Since the proton experiment was at the end of its angular range, and the statistical errors, particularly at 40 MeV are large, while the neutron experiment is most accurate in this angular range [22], it would appear that in this instance the neutron work is more reliable. Of course, at these large angles we expect charge-independence to be directly applicable, and hence that n-d and p-d experiments should give the nearly same result,

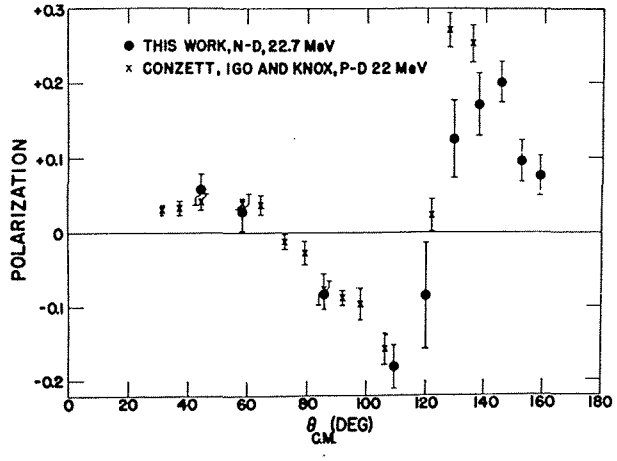

Fig. 2 Comparison of 22.7 MeV neutron polarization in n-d scattering with proton polarization in p-d scattering at 22 MeV, as given in reference 21.

but until we have a rigorous three-body theory including Coulomb interactions, we cannot be absolutely sure that this is true.

The only triple scattering experiments of which I am aware are measurements of D and R' at 135 MeV by Poulet, Michalowicz, Kuroda, Cronenberger and Coignet [23]. These show very qualitative agreement with an impulse approximation calculation using known nucleon-nucleon phase-shifts, but detailed theoretical analysis is again lacking.

The existence of tensor polarization components T_{20}, T_{21} and T_{22} for elastic p-d scattering in the energy range of 3-10 MeV for the deuteron has been demonstrated by Young and Ivanovich [24] and Young, Ivanovich and Olsen [25]. In a recent preprint from Wisconsin, P. Extermann [26] gives the energy variation of the vector polarization of the deuteron T_{11} at angles between 107° and 120°, and finds this roughly linear between 4 and 12 MeV. He also gives angular distributions of the vector polarization and of the combination $T_{22} + 0.41\ T_{20}$ at 8 and 11 MeV. Comparable preliminary results by Arvieux, Beurtey, Goudergues, Lechaczynski, Mayer, Mikumo, Papineau and Thirion were presented at Karlsruhe [27] last year, and are now being prepared for publication [28]. Since the experimental techniques differ considerably, and even the definitions used for the tensor components are not identical, it is suggested that the authors be contracted for details.

I have gained the impression from this cursory survey of the experimental material already available that rapid progress is being made in achieving results of reasonable precision, resolving experimental discrepancies, determining accurate parameters for a low

energy theory, and that on the experimental level the possibility of much more sophisticated spin-dependent experiments already exists. But it also will become clear in a moment that the number of experimental possibilities is so rich that it is hopeless for the time being to think of a direct empirical determination of the complete scattering matrix for many years to come, and that theoretical guidance will be needed to select crucial experiments. I will now attempt to indicate what has been done theoretically, and what I believe is still needed in order for progress to be made.

III THEORETICAL STRUCTURE OF THE THREE-NUCLEON SYSTEM

Since we start experimentally with an n-d or p-d system, and the density matrix for the spin-1/2 particle requires 4 numbers for complete specification, while the density matrix for spin-1 requires 9 numbers, there are 36 possible independent initial states. For elastic scattering there are 36 independent final states, and hence 36 x 36 = 1296 possible independent elastic scattering experiments. Since we can form no pseudoscalar from the initial and final momenta, and the scattering matrix is linear in the (pseudoscalar) spins, parity conservation requires half of the rotational invariants we can form to vanish identically leaving only 648 non-zero elastic scattering experiments*, which is not much help. If the interaction leaves three free nucleons in the final state, the final density matrix has 4 x 4 x 4 = 64 independent elements, so there are 36 x 64 = 2304 independent break-up experiments. If the three final momenta are coplanar (in the lab system), we can again form no pseudoscalar, and roughly half of these amplitudes will vanish in that plane, but not out of it. Since the determination that the momenta are non-coplanar necessarily requires coincidence measurements, we can conclude immediately that the angular distribution of coincidence measurements and not just of single-particle energy spectra will be essential in exploring the full structure of the three-nucleon system. It is by no means premature to start thinking about the experimental techniques needed for such measurements.

If we now add the requirement of total angular momentum conservation the number of independent amplitudes is drastically reduced. This is illustrated in table I. For elastic scattering ($1/2 + 1 \rightarrow 1/2 + 1$), we see that there are 18 possible transitions, but that time-reversal invariance reduces these to 12. For break-up, all 18 transitions are allowed, and in addition we have 6 possible transitions of the type $1/2 + 1 \rightarrow 1/2 + 0$, making 24 inelastic amplitudes. At this stage we, therefore, have

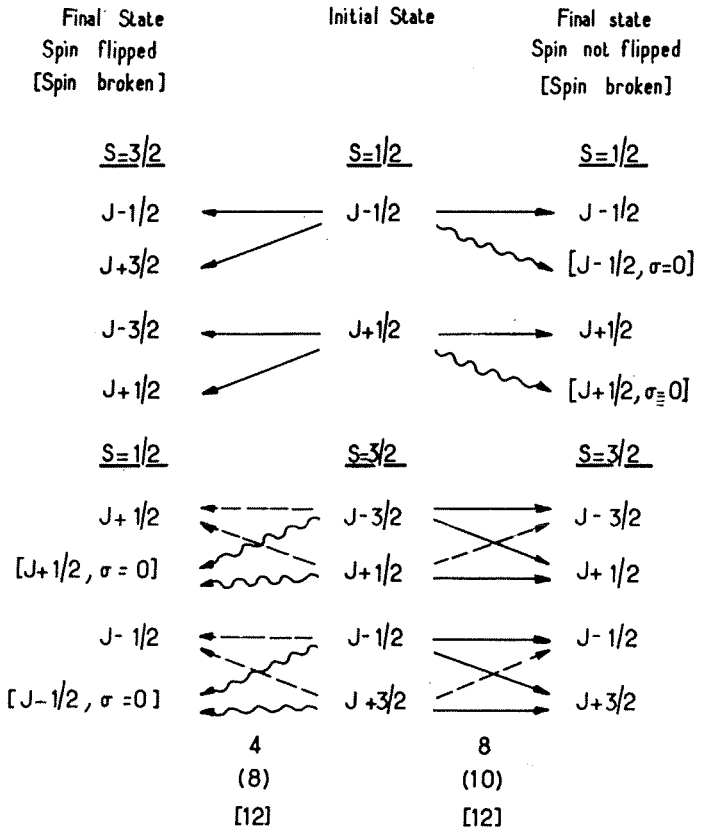

Table I Elastic scattering and break-up transitions for n-d scattering which conserve total angular momentum J and parity in the J, L, S representation. Solid arrows (→) indicate elastic scattering transitions ; dotted arrows (- - →) transitions which are independent in break-up, but known in terms of the solid arrow transitions from time-reversal invariance in elastic scattering ; wavy arrows (⇝) indicate transitions which occur only in break-up. Each entry gives the value of total orbital angular momentum L (= J ± 1/2 or J ± 3/2) ; final states where two of the nucleon spins add to zero are designated by $\sigma = 0$.

12 + 24 = 36 complex functions of energy and angle to be determined, less one overall phase, or 71 numbers in all. As we know from familiar analyses of elastic scattering with open inelastic channels, the 12 elastic amplitudes can be parametrized in terms of 12 real phase parameters, and 12 absorption parameters lying between 0 and 1. In principle, these 12 absorption parameters can be determined in terms of the 24 inelastic amplitudes by means of unitarity, giving a modest reduction to 60 phase parameters for each value of J. However, so far as I know, no one has yet worked out the unique parametrization which automatically guarantees unitarity in this case,

comparable to the phase shift analysis in two-particle reactions. Since no real progress in unscrambling the two-nucleon dynamics was made prior to the development of that formalism, it is clear that this task should have high priority for theorists interested in the three-nucleon problem.

The general non-dynamical structure for the cases $1/2 + 1 \rightarrow 1/2 + 1$, and for $1/2 + 1 \rightarrow 1/2 + 0$ have been published in a paper by Csonka, Moravcsik and Scadron [29], together with the machinery needed to reduce this to a phase-shift parametrization for two-particle final states, but the generalization to three-particle break-up is not transparent. Comparable formulae have been sent me by D. Fick [30], together with the evaluation of many possible observables in terms of the invariant amplitudes. The next step along this line is to work out which classes of observables lead to the same combinations of invariant amplitudes ; the usefulness of such an analysis is illustrated for the simpler case of $1/2 + 1 \rightarrow 1/2 + 0$ in a recent paper by Csonka, Moravcsik and Scadron [31] and applied to the reaction $^3He(d,p)^4He$. I have decided not to reproduce the formulae for T in terms of invariant amplitudes here, since they do not yet include the parametrization mentioned in the last paragraph, and since they also do not give the composition of these invariant amplitudes in terms of the Faddeev subchannels, the necessity for which I will discuss below.

Of more direct relevance to this Colloquium is a communication from Raynal and Arvieux which is reproduced as the Appendix to this talk (q.v.). They discuss all possible polarized-target polarized-beam elastic scattering experiments starting with n-d (or p-d), and show these can give 18 independent numbers. If there are no doublet-quartet transitions, there are 8 relations among these numbers, and a specific test of one of these relations is proposed. I would like to inject a work of caution at this point about making the assumption that only 10 experiments are needed even if this first test succeeds. We know both that the deuteron is a very loose structure, and that there are strong exchange and spin-flip forces between two nucleons. Consequently, I would personally be quite surprised if, even at quite low energy, we do not find double-quartet transitions in the n-d system, and would accept the simplified analysis only in energy regions where all 8 restrictions have been shown to hold <u>experimentally</u> to reasonable precision. This is just the type of simplifying assumption which got us into trouble in the early days of analysing the two-nucleon system.

In designing spin-dependent experiments it is important to keep in mind a point that Raynal has made before, but which cannot be repeated too often. This is that if one starts from a polarized-target polarized-beam system, important information is contained in the azimuthal variation other than that given by a left-right measurement in one plane, and an appropriate counter arrangement can greatly increase the information obtainable with no increase in

running time. A good illustration is the Saclay measurements of A_{xx} and A_{yy}, where by having counters in the planes both perpendicular and parallel to the plane containing the beam and target polarizations, both the accuracy and the usefulness of the experiment was greatly increased. When one adds the possibility of tensor polarization components, the azimuthal variation is still more complicated, and it is very important to make sure all appropriate azimuthal ranges are covered.

As we saw above, the non-dynamical structure of the three-nucleon system is quite complicated, and it will be a long time before we can hope to see a direct experimental determination of the transition matrix at any energy ; it is therefore clear that it will be essential to make use of a dynamical theory of this system before we can hope for much progress. Let me remind you that in the much simpler case of p-p scattering, where only five invariant amplitudes need be determined, and the phase shift parametrization was completely understood, the direct empirical approach failed. It was only after the dynamical assumption that the highest partial waves could be computed from one-pion-exchange (OPE) [32,33] was included in the data analysis that unique phase-shift analyses became possible, and the detailed transition matrix I will discuss below emerged from the experiments.

Thanks to the work of Faddeev [34], a well-defined mathematical theory of the non-relativistic three-body quantum mechanical problem now exists, and I am convinced it is only a matter of time, and a lot of hard work, before it can be made into a practical tool for the analysis of three-nucleon experiments. The basic difficulty with earlier approaches to the three-body problem was that, starting from the Schroedinger equation, no one knew how to formulate the scattering boundary conditions in a way that allowed solutions to be defined, while starting from the Lippmann-Schwinger equation $T = V + V\, G_0\, T$, again ambiguous and infinite terms were obtained. The physical origin of these difficulties is that even though one of the particles always separates from the other two if we wait long enough, the other two can continue to interact, either as a bound state or as a correlated continuum state of the two-particle subsystem, long after the three-particle interaction has ceased, and that this can happen in three different ways which must be correctly connected in order to preserve unitarity. The Faddeev approach is to split the three-body transition matrix into these three subchannels, in which the i^{th} particle is asymptotically free, that is $T = T^1 + T^2 + T^3$. It is then shown that these three amplitudes satisfy the coupled equations :

$$T^i(Z) = t^i\delta + \sum_{s=j,k} t^i\delta\, G_0(Z)\, T^s(Z) \quad (i,j,k \text{ cyclic}) \quad .$$

Here t^i is the fully off-shell two-body transition matrix for the jk pair expressed as an operator in the three-body Hilbert space, the δ function insures that the i^{th} particle retains the energy not available to this jk interacting pair, and $G_o(Z)$ is the Green's function for the three-body system having extended energy Z.

If we now represent these operator equations as integral equations, the operators T^i become functions of (for example) nine variables representing the nine momentum components of the three particles in the final state, nine parameters determined by the momentum components in the initial state, and the extended energy Z. The physical transition matrix is then obtained by solving these equations and taking the limit $Z \to E + i0$, E being the total energy of the three-body system ; that is $E = \omega_1 + \omega_2 + \omega_3 = \omega_1' + \omega_2' + \omega_3'$ where $\omega_i(\omega_i')$ is the energy of the i^{th} particle in the initial (final) state. Faddeev has shown that if these equations are iterated a sufficient number of times, the apparent singularities from the δ functions and the Green's function disappear leaving Fredholm equations posing a well-defined mathematical problem, although not exactly an easy one to solve. By taking out the total momentum, and taking as variables the three final energies ω_i', together with a magnetic quantum number representing the projection of the total angular momentum on an axis fixed in the plane of the triangle determined by the three c.m. momenta (i.e. a body-fixed axis), Omnes [35] has reduced this system to coupled integral equations in three continuous variables with $3 \times (2J + 1)$ components.

If one makes the further assumption, which is appropriate to the three-nucleon problem if one ignores the Coulomb complication in p-d scattering (which may prove troublesome at a later stage), that the interactions are of short range, and hence that only interactions for orbital angular momenta less than L in the two-body subsystems need be included, Ahmezadeh and Tjon [36], and independently Osborn and I [37], have shown that this system can be still further reduced to coupled integral equations in only two continuous variables for functions with $3 \times (L + 1) \times \min(2J + 1, 2L + 1)$ components. Since these two variables are the total three-body energy E defined above, and (in each Faddeev subchannel) the energy ω_i' of the particle which is asymptotically free, bound-state and resonance singularities of the three-body system occur only in E, and are cleanly separated from the bound-state and resonance singularities of the two-body subsystems which are reflected in the variables ω_i'. This suggests that a powerful phenomenology for three-particle final states capable of testing the assumption that only pairwise interactions of the two-body subsystems are important without detailed dynamical assumptions will be possible, but this has yet to be worked out. Specific numerical solutions of these two-variable equations have yet to be obtained, but Osborn has by now pushed the development of practical computer techniques for this purpose to the point where I am confident that these will soon become available.

The remaining question to ask is whether we know enough about the two-nucleon interactions which provide the driving terms in the Faddeev equations to believe the solutions (a) well enough to call agreement with experiment significant, or (b) if there is disagreement with experiment, to believe that this is evidence for actual three-body forces in the three-nucleon system. The quantities we need for the Faddeev equations are now the two-nucleon partial-wave amplitudes $t_\ell(q,p,z)$ (with $0 \leqslant \ell \leqslant L$) for the scattering from a state of relative c.m. momentum p to a state of relative c.m. momentum q at an extended energy z. If we examine the kinematics of the three-particle system, we find that the values needed are for $p^2/2\mu_i = E - r_i\omega_i$, $q^2/2\mu_i = E' - r_i\omega_i'$, $z = Z - \omega_i'$; here $\mu_i = m_j m_k/(m_j + m_k)$, and $r_i = (m_j + m_k)/m_i$. The ranges of E and ω_i are such that the values of p^2 and q^2 so defined are always positive or zero ; this is fortunate since p and q are radial variables in the Schroedinger equation for the two-particle system, and we would have difficulty in giving a physical interpretation to them outside this range. However, since in the Faddeev equations, ω_i ranges up to $+\infty$, we find that we must be able to interpret t_ℓ when the energy value in the Schroedinger equation ranges from $-\infty$ to Z. A further difficulty is that, from two-nucleon scattering experiments we can only directly determine $t_\ell(k,k\ ;\ k^2/2\mu_i) = \tau_\ell(k) = e^{i\delta_\ell} \sin\delta_\ell\ /k$, while the uncertainty principle allows this connection between free-particle momentum and energy to be broken independently in all three variables in the three-body dynamical equations.

The solution to this problem can be made in two steps. As has been shown elsewhere [38], it is possible to factor the half-off-shell transition matrix $t_\ell(p,k\ ;\ k^2/2\mu_i) = \tau_\ell(k)\ f_k(p)$ with $f_k(k) = 1$; as noted above $\tau_\ell(k)$ is directly determinable from two-nucleon scattering experiments. Further, it was shown that the function $f_k(p)$ is simply the representation in momentum space of the difference between the exact wave function in configuration space and the usual asymptotic form $n_\ell(kr) - \mathrm{ctn}\ \delta_\ell\, j_\ell(kr)$. It is, therefore, smooth and finite, the structure in energy as one moves off the energy shell occurring only over regions of order kR, where R is some average range of forces ; rapid variations in energy are confined to the bound states and resonances as reflected in the experimentally knowable $\tau_\ell(k)$. If we know the off-shell Born approximation for the potential in momentum space, $V_\ell(q,p)$, then it was shown [38,39] that $f_k(p)$ can easily [40] be computed from a non-singular Fredholm integral equation. On the other hand, if we know $f_k(p)$ experimentally from, for example, e-d scattering, photodisintegration of the deuteron, p-p bremsstrahlung, etc, $V_\ell(p,q)$ can be computed from the relation :

$$2\mu_i V_\ell(p,q) = \frac{2}{\pi}\int_0^\infty dk\ \frac{\sin^2\delta_\ell(k)\left[f_k(p)\ f_k(q) - f_q(p)\right]}{q^2 - k^2}$$

$$= \frac{2}{\pi}\int_0^\infty \frac{\sin^2\delta_\ell(k)\left[f_k(p)\ f_k(q) - f_p(q)\right]}{p^2 - k^2}$$

The two different forms come from the time-reversal invariance requirement, $V_\ell(p,q) = V_\ell(q,p)$ and are the only a priori restrictions on the off-shell extension function $f_k(p)$. Of course the interaction so constructed will in general be non-local as well as ℓ-dependent, a point I will return to below.

The full off-shell extension required for the Faddeev equations can then be constructed from the Lippmann-Schwinger equation $T(z) = V + VG_0(z)\,T(z)$ as follows : recall that if the full Hamiltonian $H = H_0 + V$, the free Green's function $G_0^{-1} = Z - H_0$ the exact Green's function $G^{-1} = Z - H$, and $G_0 t = GV$, or $T(z) = V + VG(z)V$. If we now introduce the plane-wave states $|k\rangle$, the exact scattering states $|\psi^+(k)\rangle$, and the usual result that $T_\ell(p,k\,;\,k^2/2\mu_i) = \langle p|V|\psi^+(k)\rangle$, the completeness relation :

$$1 = \frac{2}{\pi}\int_0^\infty k^2 dk\,|k\rangle\langle k| = \frac{2}{\pi}\int_0^\infty k^2 dk\,|\psi^+(k)\rangle\langle\psi^+(k)| + \sum_b |b\rangle\langle b|$$

gives us immediately that :

$$\langle q|t_\ell(z)|p\rangle = -2\mu_i V_\ell(q,p) - \sum_b \frac{\gamma_b(q)\,\gamma_b(p)}{z+\epsilon_b} + \frac{2}{\pi}\int_0^\infty k^2 dk\,\frac{\langle q|t_\ell|\psi^+(k)\rangle\langle\psi^+(k)|t_\ell|p\rangle}{k^2 - 2\mu_i z - i\epsilon}$$

or

$$t_\ell(q,p\,;\,z) = -2\mu_i V_\ell(q,p) - \sum_b \frac{\gamma_b(q)\,\gamma_b(p)}{z+\epsilon_b} + \frac{2}{\pi}\int_0^\infty \frac{dk\,\sin^2\delta_\ell\, f_k(p)\, f_k(q)}{k^2 - 2\mu_i z - i\epsilon}\,.$$

As we noted above, the off-shell potential can be computed from $f_k(p)$, and the residues of the bound state terms γ_b are also in principle experimental quantities (reduced widths). The current extent of our knowledge of $\sin^2\delta_\ell$ and $f_k(p)$ for nucleon-nucleon interactions will be discussed below.

So far, we have ignored spin in the above equations. A priori, we would expect the number of coupled equations to increase by a factor of 36 when we include spin, but this is much too pessimistic. For instance, including $^1S_0$, $^3S_1$ and $^3D_1$ states with both tensor and central forces, Sitenko and Karchenko [41] needed only three coupled equations for three functions in order to compute the triton binding energy and the doublet scattering length, if they also assume the interaction separable. Also Aaron, Amado and

Yam [42] found that even though values of J up to 10 or so are needed to fit 14 MeV n-d scattering, only the J = 0 and 1 states required any sophisticated techniques for the solution of the integral equations [43] ; for higher values of J, iterative solution of the equations converged rapidly, and this poses few problems for modern computers. This also suggests that it may be possible to exploit the loose structure of the deuteron to compute the higher J states in the n-d system in terms of the deuteron wave function in a reasonably model independent way, and hence reduce drastically the number of parameters which need be determined from experiment at low energy, in much the same way that the known OPE interaction simplifies the analysis of nucleon-nucleon scattering.

The calculations mentioned above [41,42] as well as the earlier work of Mitra and Bashin [44], and the comparable work of A.C. Phillips [45] all make the apparently drastic assumption that the interaction is separable (i.e. $V(p,q) = F(p)\,F(q)$), which reduces the Faddeev equations to coupled equations in a single variable. Until we have exact solutions of the two-variable equations for comparison, the physical justification of this approximation will remain dubious, but in the meantime this gives an interesting phenomenology. As is to be expected in calculations which include only pure attraction in S states, these calculations overbind the triton. Since, in the quartet state the exclusion principle keeps the neutron in the long-range region, the quartet scattering length comes out about right ; the doublet scattering length is sensitive to the details of the calculation, but of the right order of magnitude. Differential cross-sections for elastic n-d scattering and total cross-sections for break-up are reasonable well represented up to 14 MeV. The triton electromagnetic form factors are not so well represented [46,47].

I believe several theoretical tasks should be vigorously attacked in order to allow for the maximum fruitful interaction between theory and experiment : 1) Complete representation of the invariant amplitudes of the three-nucleon system in terms of (a) a unique unitary parametrization, and (b) the contribution to each of these from the Faddeev subchannels (two-nucleon amplitudes). This will allow calculation of observables, tests of simplifying assumptions, and guides to interesting experiments. 2) Complete formal development of the Faddeev equations for this system including spin, and the simplifications at (a) low energy, and (b) high J. This will allow the development of the analogs to effective range theory and OPE in the two-nucleon system, and hence cut down the number of parameters which need be measured experimentally. 3) Detailed investigation of the region of validity of various separable approximations so that they can be used with confidence in the regions where they are justifiable.

IV TWO-NUCLEON POLARIZATION EXPERIMENTS

A preliminary analysis of the A_{xx} and A_{yy} Saclay experiments on p-p scattering near 25 MeV, together with the n-p C_{nn} measurement from Los Alamos at a similar energy was presented at Karlsruhe [48]. Following a suggestion of Catillon's, it has proved possible to give an absolute normalization [49] to the Saclay experiments [50], and these, together with existing work in this energy region now define the 25 MeV p-p phase shifts to high precision. The Los Alamos n-p C_{nn} experiment, which originally gave a value only at 180°, has been pushed to smaller angles [51], and a new analysis completed by Arndt and MacGregor [52]. This analysis differs in important respects from an earlier work presented by the Dubna group [53], but the discrepancies have been resolved as due to differences in data selection, energy dependence assumed for the phase shifts or observables measured at different energies, and the complications due to a genuine solution ambiguity in the n-p analysis. The ambiguity allows two values of $^3S_1$, one greater than 90°, and the other less. Since we know from Levinson's theorem and effective range theory that $^3S_1$ starts from 180° at zero energy and falls monotonically, passing through 90° below 20 MeV, there is no doubt that the latter is the physically correct solution, but the existence of the spurious possibility makes the error analysis unreliable. However, one can use the correlated errors to compute observables and their uncertainties in order to determine which additional experiments will be most useful for increasing the accuracy of the analysis. This is illustrated for C_{nn} in figure 3. We see that extending the measurements to still smaller angles will not remove the solution ambiguity between C and C', but if comparable precision to the existing experiments is achieved, will reduce the uncertainties in the phase shift determinations. On the other hand, D and D_T, as shown in figures 4 and 5, if measured to even modest accuracy at the right angle, would eliminate the spurious solution. I think it is important to realize that this type of analysis can always be carried through whenever a theoretically reliable parametrization of the experiments exists, and should always be carried out in advance of designing new experiments, both to insure maximum usefulness of the results and to avoid spending a couple of years on an experiment that, even if successful, will not give any essentially new information.

I have spent this much time discussing the 24 MeV experiments because it is important to finish up this job in order to obtain a reliable experimental value for the $^3S_1$-$^3D_1$ coupling parameter ϵ_1. Because of the strong OPE tensor force in this state, and the loose structure of the deuteron, recent models of the deuteron obtain most of the binding from this tensor force, leaving room for only a rather weak central force. Blatt [54] claims, on the basis of variational calculations, that these models then cannot give the observed 8.49 MeV binding energy for the triton, but only 4 or 5 MeV

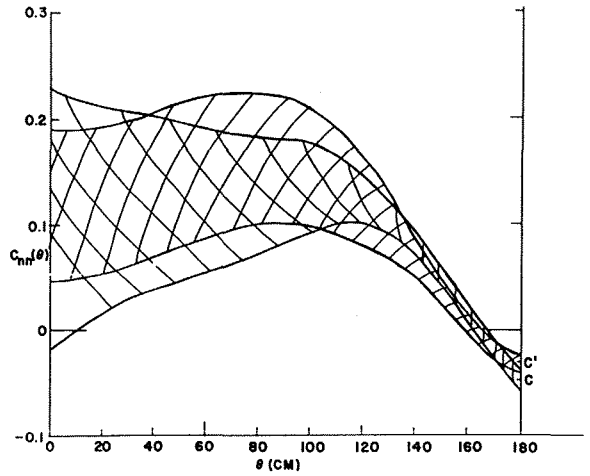

Fig. 3

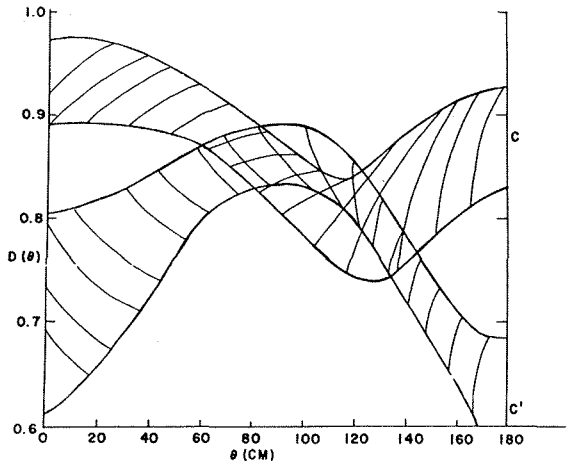

Fig. 4

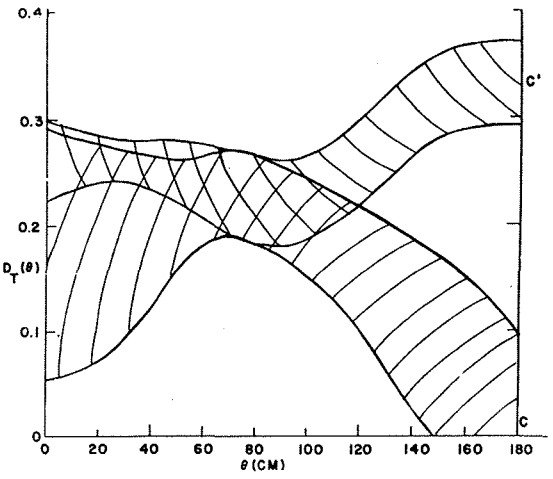

Fig. 5

Fig. 3, 4, 5 Predictions of C_{nn}, D and D_T for 25 MeV n-p scattering as given in reference 52. Error bands indicate the precision needed to improve the precision of the phase parameter determination ; the two bands show which measurements would resolve the solution ambiguity discussed in the text.

binding. As noted above, separable models with purely attractive central, S-wave interactions overbind the triton by about 3 MeV, but when the Yamaguchi tensor force is added, the triton is overbound by only about 1 MeV (41). However, the Yamaguchi tensor force corresponds to a 4 % D-state probability rather than the usually accepted 7 %, and also does not have the OPE range, so the physics of this calculation is not clear. Further, when the calcula-

tions are extended to include short-range repulsion, it is quite possible that the binding will turn out too small, in agreement with the variational calculations. It is, therefore, important to know experimentally that the OPE-tensor force is actually present in the $^3S_1$-$^3D_1$ state, and one way to do this is to improve the precision of the 25 MeV analysis to the point where a clean test of Wong's prediction [55] of ϵ_1 from OPE becomes possible. I should also note that Perring [56] has also carried through a new analysis of the 25 MeV data, and differs on some points of detail with Arndt and MacGregor.

Now that a differential cross-section at 50 MeV will soon be available [57], it is to be hoped that a similar analysis at that energy can be completed, and the n-p experiments needed to complete the picture to reasonable precision both pin-pointed and performed. This would again give interesting information about ϵ_1. So far as work at other energies is concerned, I believe that n-p experiments are the most important and should be given priority, simply because of the much greater uncertainties which still exist in the n-p phase shift analyses. If it can be shown in advance that a p-p measurement will resolve an uncertainty, or actually improve the precision to which some set of parameters is measured, then it is obviously worth doing, but my feeling is that the time is approaching when p-p experiments in the elastic scattering region should be attempted primarily when needed to supplement some n-p measurement or when it can be shown that the p-p scattering matrix at that energy is needed to higher precision for some specific purpose.

I will not attempt to review experiments above meson production threshold (280 MeV), since this brings in a new three-body problem ($NN\pi$), which not only has all the complications discussed above, but also lands us squarely in the middle of the still unsolved problem of connecting relativity and quantum mechanics in a theory containing only a finite number of particles, or some other approach which one is willing to follow into the battlegrounds of elementary particle theory.

V THEORETICAL STRUCTURE OF THE TWO-NUCLEON INTERACTION

We have seen in our discussion of the theory of the three-body problem that what we require as input, assuming only pairwise interactions, is (a) the on-shell amplitude $\tau(k)$ which we can get immediately from a phase-shift analysis of nucleon-nucleon scattering, and (b) the half off-shell extension function $f_k(p)$ which requires additional theoretical or experimental information to obtain. p-p phase shifts are now known with considerable precision over the entire

elastic scattering region, and n-p phase shifts are also falling into place. The first question is, therefore, whether we can obtain the function $f_k(p)$ from this information by a theoretical argument. Sticking for the moment to non-relativistic quantum mechanics (which means in practical terms that we assume the details of how $\tau(k)$ and $f_k(p)$ go to zero as k goes to infinity will not significantly affect three-nucleon calculations at low energy), the Gelfand-Levitan theorem tells us that if we know the phase shift for a single partial wave at all energies, and there are no bound states in that partial wave, we can construct uniquely the corresponding static, local potential ; the function $f_k(p)$ and all other partial waves can then be calculated theoretically. Including spin, we must do this for five amplitudes for each of the two isospin states, and for the $^3S_1$-$^3D_1$ state must also know the asymptotic normalization of the S and the D wave functions, but these two additional parameters are also in principle experimentally determinable.

We consider first the singlet state with I-spin one. The $^1S_0$ low energy behaviour is determined to a good approximation by the scattering length and effective range, and it has been shown [58] that the small deviations from this behaviour are accounted for by the same one-pion-exchange (OPE) interaction which fits the highest partial waves. A third parameter is provided by the change in sign of the $^1S_0$ phase shift near 250 MeV, which shows that (in a static, local model) there is also short-range repulsion. Since we know, both experimentally and theoretically that the longest range part of the interaction is given by OPE, we must adjust two parameters in the intermediate range attraction to fit the scattering length and effective range and, as the effective radius of the short-range repulsion is fixed by the energy at which the phase shift changes sign, about the only freedom left in the model is how we treat the short-range repulsion. One extreme assumption is that this is due to an infinitely repulsive hard core, which gives an essential singularity to $\tau(k)$ as k goes to infinity, and an oscillating phase shift ; a more physical assumption is to postulate a repulsive Yukawa potential with the ω-meson mass, which gives a phase shift that falls smoothly to zero at high energy ; the truth should lie in between. Because the attraction must have a range less than 2 pion Compton wavelengths, and the repulsion be still shorter, protons with wavelengths corresponding to energies up to 300 MeV cannot explore the details of this structure, and both models give reasonable agreement with observed $^1S_0$ phase shifts. The crucial test is then to see whether both models give the same $^1D_2$ and $^1G_4$ phase shifts over the same energy range, and is shown in figure 6. In fact the two predictions lie on top of each other, so are labelled "LOCAL", indicating that they are the unique prediction of a static, local potential fitted to the $^1S_0$ phase under the above assumptions. We also see from the experimental points that the predictions are too high by several standard deviations, demonstrating conclusively that the singlet nucleon-nucleon interaction

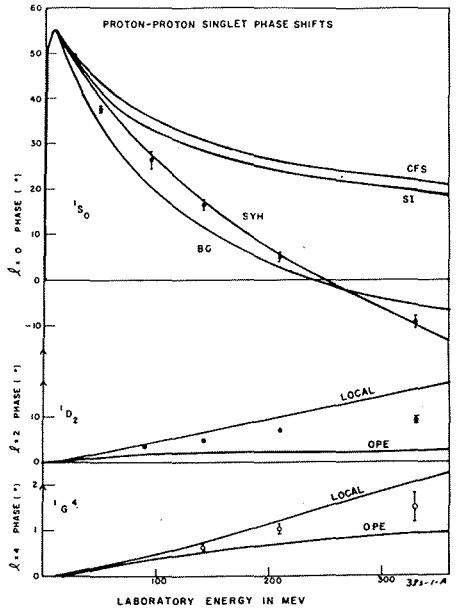

Fig. 6 (from reference 48) $^1S_0$ curves compare the prediction from a hard-core model (SYH) with the shape-independent approximation (SI), low energy dispersion theory including one-pion-exchange (CFS), and boundary condition model (BC). The three Yukawa potential model using π, "σ" and ω masses agrees with SYH at low energy and differs by less than 2° at all energies shown. Both the SYH (hard core) and the three Yukawa models predict the same $^1D_2$ and $^1G_4$ phase shifts shown by the "LOCAL" curve. Experimental points are from R.A. Arndt and M.H. MacGregor, Phys. Rev., 1966, 141, 873.

is non-local, and hence that the off-shell extension function $f_k(p)$ cannot be reliably computed from this assumption.

Since we cannot compute $f_k(p)$ from the local potential assumption, the next question is whether we can obtain it from some new type of experiment. We saw above that $f_k(p)$ is directly related to the two-nucleon wave function, so what is required is a measurement of this wave function inside the range of forces. Since the electromagnetic structure of the proton and neutron have been accurately measured by electron scattering, if we are willing to make the assumption that the electromagnetic charge and current distribution in the two-nucleon system follows the motion of the proton and neutron, we could do this from experiments such as e-d scattering, photodisintegration of the deuteron, p-p and n-p bremsstrahlung, etc. However, this also fails. For example, it is a straightforward matter to calculate the capture of epithermal neutrons by protons via the magnetic dipole process $n + p \rightarrow \gamma + d$, and to show that we know enough about nuclear forces to make this calculation to high precision [59]. The calculation fails by 10 %, with a theoretical limit of uncertainty of only 1.2 %, showing conclu-

sively that even for zero relative energy between the two particles there are sources of current in the two-nucleon system other than those due to the motion of the proton and the neutron. Presumably these are due to meson currents, so we find that in order to obtain the information needed for a physical solution of the three-nucleon problem, even in the non-relativistic region, we are forced to understand the coupling of the neutron and the proton to other elementary particles, and cannot simply treat them as non-relativistic mass-points interacting via a phenomenologically determinable potential.

Fortunately, the devoted experimental work of the last ten years on the spin structure of the two-nucleon system, using first triple-scattering and spin-correlation techniques, and now the powerful combination of polarized targets with polarized beams, has given us sufficiently detailed information so that we can make the interpretation of the two-nucleon interaction as due to the coupling to the nucleons to known bosons and boson resonances with some confidence. Turning first to the singlet p-p interaction, the phase shifts shown in figure 7 give us a great deal of information. As already noted, the longest-range interaction is correctly predicted by OPE, but this is both too long range and too weak to explain quantitatively the observed $^1S_0$ scattering length and effective range, so there is in addition an intermediate range attractive interaction.

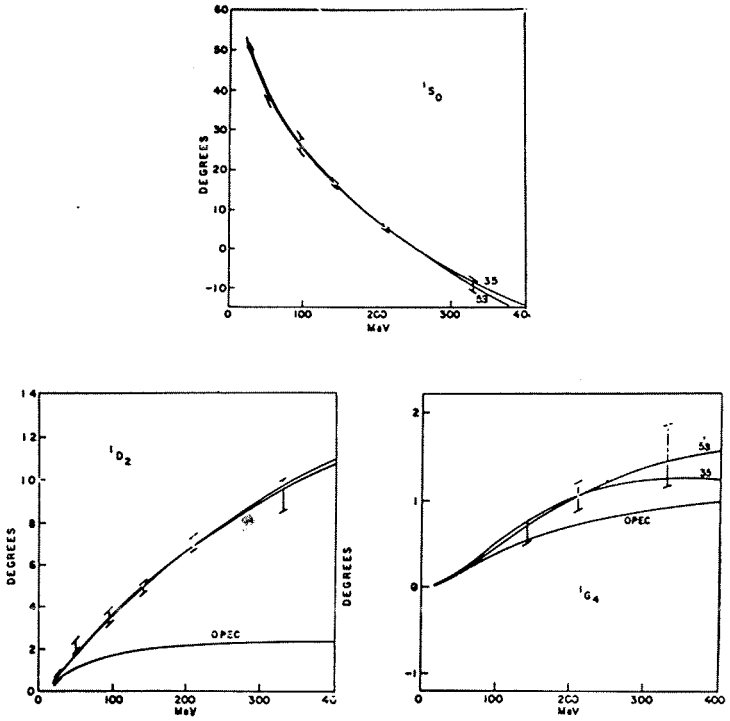

Fig. 7 Singlet p-p phase shifts from R.A. Arndt and M.H. MacGregor, Phys. Rev., 1966, 141, 873.

To get some idea of the spin and parity of this intermediate mass boson, we look first at the central interaction in the triplet-odd state, which is roughly measured by $({}^3P_0 + 3\ {}^3P_1 + 5\ {}^3P_2)/9$. At 25 MeV and above, this is strongly positive, but below 3 MeV it is slightly negative, and an order of magnitude less than the weak negative repulsion predicted by OPE in this state [58]. Taking account of centrifugal shielding, this shows that the intermediate range attraction we found in the singlet-even states (confirmed by the large values of ${}^1D_2$ and ${}^1G_4$ compared to OPE) can be explained as due to a boson of zero spin and positive parity. Turning to the deuteron, we find a quadrupole moment roughly accounted for by OPE, but also the need for an attractive central interaction of intermediate range, showing that this boson also has zero isospin. Whether or not there is a σ-meson with $I = 0$, $J^P = 0^+$, we have reasonable confidence that the π-π state with these quantum numbers is attractive, and the consequent correlation of two-pion exchange in the nuclear force would produce the effect we have just identified.

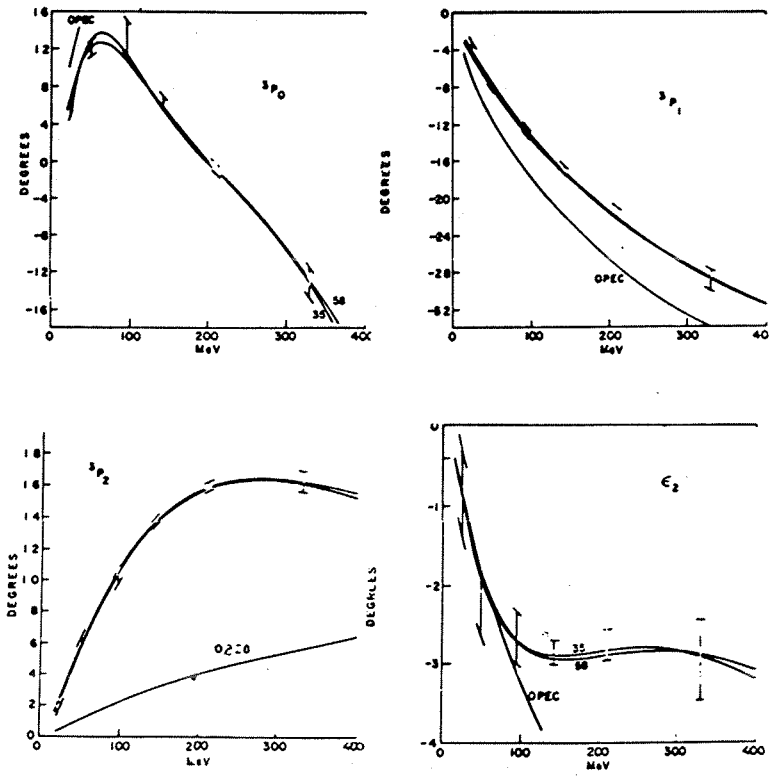

Fig. 8 Triplet $\ell = 1$ p-p phase parameters from R.A. Arndt and M.H. MacGregor, Phys. Rev., 1966, 141, 873.

In order to get more information about the short-range repulsion we found in the ${}^1S_0$ state, we turn to the triplet-odd P-waves as shown in figure 8. We see the +−+ signature of the ${}^3P_{0,1,2}$ phases

at low energy to be expected from the long-range OPE tensor force, but also find that $^3P_0$ changes sign about 210 MeV, giving the --+ signature characteristic of an L.S interaction at higher energies. The short range of this L.S interaction is confirmed by the fact that the $^3F_{2,3,4}$ phases retain the OPE signature up to 300 MeV. Recalling that the exchange of electromagnetic quanta produces repulsion between like charges, and an L.S (Thomas) term, it is no surprise that both features can be explained by the exchange of a heavy quantum with $J^P = 1^-$, that is, a massive vector meson. This identification is further confirmed by the prediction that between unlike (nuclear) charges, this strong repulsion will change to strong attraction, which accounts for the very large $\bar{p}$ p and $\bar{n}$ p annihilation cross-sections in the multi-BeV region. The I = 0, $J^P = 1^-$ ω meson is ready to hand to explain all these features, but the data is not sufficiently precise to show how the effect should be split between the ω and the still heavier Φ with the same quantum numbers, or whether they have tensor as well as vector coupling to the nucleons. On the basis of SU_3, it appears likely that the I=1 ρ makes a much smaller contribution to the nuclear force, but it will require more precise n-p data than those now available before this prediction can be checked in detail. The I = 0, $J^P = 0^-$ η-meson is also expected to give a small contribution, but it is possible to use the forward nucleon-nucleon dispersion relations to give an indication that it is in fact there in the nucleon-nucleon scattering data. We should also note that the failure of the static local assumption to fit the singlet state is in at least qualitative agreement with a velocity-dependent effect to be expected in vector-meson exchange. Finally, if one takes the π, "σ", η , ρ , ω and Φ as given, Ball, Scotti and Wong [60] have shown that one can not only get semi-quantitative fit to nucleon-nucleon scattering with only four adjustable parameters, but also that when one "crosses" this fit to the nucleon-antinucleon system, these, and only these, bosons show up as bound states. Of course, a great deal is left out in this description of the nucleon-antinucleon system, so close agreement with the experimental masses is not obtained or expected, but it does show that we are beginning to understand how the strong interactions hang together and support each other.

This excursion into elementary particle theory was undertaken in order to show how rich and detailed a description of the basic two-nucleon interactions has been made possible by detailed experimental work. Because the theory is confirmed in so much detail, it would seem reasonable that it can be trusted, if the proper techniques can be developed, to allow us to take the two-nucleon T matrix off-shell in a physically consistent way, and hence compute $f_k(p)$ with some confidence. It is to be hoped that, for the low-energy three-nucleon problem, only a rough calculation of $f_k(p)$ will suffice, because of the generally smooth structure of this function adduced in Section III. The same theory will presumably generate genuine three-body forces as well, but I feel we should first push the pairwise interaction calculations far enough to demonstrate the

existence of three-body forces experimentally before tackling the more difficult problem of deriving them from elementary particle theory.

VI CONCLUSION

We have seen that the three-nucleon problem offers more technical difficulties at the phenomenological level, both experimentally and theoretically, than the two-nucleon problem, but that on the experimental side the polarized-target polarized-beam technique, and on the theoretical side the Faddeev equations, give us the opportunity of attacking this problem with a reasonable hope of achieving successes in ten to fifteen years comparable to those achieved in the two-nucleon problem over a corresponding period of time. The immediate theoretical needs for making efficient use of existing experiments and planning new experimental programs are (a) a low-energy theory comparable to effective range theory ; (b) an explicitly unitary parametrization of three-body reactions comparable to two-particle phase shifts and inelasticity parameters ; (c) a complete transcription of the Faddeev two-particle subchannels into the three-particle invariant amplitudes and the unitary three-particle parametrization ; (d) a model-independent high-J analysis for n-d scattering and break-up which exploits the loose structure of the deuteron to provide the analog to the OPE calculation in the two-nucleon system. To some extent, the separable interaction approximation to the Faddeev equations gives a phenomenological framework for answering these questions, but the exact theories still have to be worked out in order to determine where this approximation can be safely applied. At a deeper level, we have also seen that we have to go beyond the phenomenological analysis of nucleon-nucleon scattering into elementary particle theory in order to make physically reasonable three-nucleon calculation, but that the physical picture needed for that extension is reasonably well understood.

VII ACKNOWLEDGEMENT

It would not have been possible for me to prepare this review without extensive assistance from many people. I am indebted on the experimental side to W. Haeberli from Wisconsin,F. Shapiro from Dubna, P.

Catillon and J. Arvieux from Saclay, A.R. Johnston from Belfast and W.R. Gibson from Queen Mary College, J.E. Simmons and J.D. Seagrave from Los Alamos, and R.J. Slobodrian from Berkeley, both for helping me get acquainted with existing published material and for generously providing me with the latest experimental results from their respective groups. On the theoretical side, I have profited from correspondence and discussions with J. Raynal, M.J. Moravcsik, M.D. Scadron, D. Fick, J.K. Perring, and A.C. Phillips. I am particularly indebted to T. Osborn for calculational support, and for continual corrections to my inadequate understanding of scattering theory. This generous assistance is gratefully acknowledged, but any errors of fact, selection, or judgement are my own responsibility.

Appendix

d-p OBSERVABLES WITH POLARIZED BEAM AND TARGET

This discussion of the possible observables in p-d elastic scattering was submitted to the conference by J. Raynal. The algebra has been checked independently by W. Ross (Stanford) and J. Arvieux (Saclay), and is believed correct.

If the 6 x 6 elastic scattering matrix M is expressed in the helicity formalism, incorporating the restrictions due to parity conservation, we find :

$$M^{+}M = \begin{pmatrix} a & b & c & d & e & f \\ b^* & g & h & i & j & e^* \\ c^* & h^* & k & \ell & i^* & -d^* \\ d^* & i^* & \ell & k & -h^* & c^* \\ e^* & -j & i & -h & g & -b^* \\ -f & e & -d & c & -b & a \end{pmatrix}$$

where a, g, k are real

f, j, ℓ are imaginary

b, c, d, e, h, i are complex

making 18 numbers in all.

If there are no doublet-quartet transitions, we have a spin 1/2 scattering (2 expressions) and a spin 3/2 (σ, P, $3T_2$ and $3T_3$: 8 expressions). This hypothesis introduces 8 relations between the polarizations and the correlation of spin parameters. They are :

$$d = (1/\sqrt{2})\ b \quad ; \quad e = \sqrt{2}\ c \qquad \text{(4 relations)}$$

$$j + \ell = (1/\sqrt{2})\ h \ ; \ h \text{ imaginary} \qquad \text{(2 relations)}$$

$$i = \sqrt{2}(g - k) \qquad \text{(2 relations)}$$

For this class of experiments, we can choose the axis of quantization along the beam direction and express the density matrix of the initial state in the usual tensor notation as $T^{(1/2)}_{s_1\mu_1} \otimes T^{(1)}_{s_2\mu_2}$.

The possible observables are then :

$$A_{s_1\mu_1 s_2\mu_2} = \text{Trace}\ (M^+ M\ T^{(1/2)}_{s_1\mu_1} \otimes T^{(1)}_{s_2\mu_2})$$

The complete results, and those for no doublet-quartet transitions, are given in table A-1.

The cross-section is $(1/6)\ A_{0000}$, the polarization of the proton is A_{1100}/A_{0000}. [9,10,11] Experiments done at Saclay with a polarized beam of 22 MeV deuterons gave [26,27,28] A_{0011}, A_{0020} and A_{0022}. Thus we have :

$$2(a + k + g)$$

$$\sqrt{3/2}(b - b^*) + \sqrt{3/2}\ h - \sqrt{3}\ell\ ,\ \sqrt{3/2}(b - b^* + 2h)$$

$$\sqrt{2}(a + k - 2g)$$

$$\sqrt{3}(c + c^*)$$

The last measurement is interesting because one can use it to check the requirement that $A_{1111} = \sqrt{2}\ A_{0022}$ if there are no doublet-quartet transitions. This coefficient is the same as $A_{xx} - A_{yy}$. There are two possible ways of obtaining it :

a. The same as in proton-proton scattering ; one can eliminate the single polarization effects by flipping the polarization of the beam and the target.

b. It is more difficult to obtain it directly because the polarization of the beam is turned and there is a vertical deviation of the beam by the magnet of the target. If we have two transverse polarizations with an angle of $\pi/2$ between them, the correlation is

		complete	simplified
A_{0000}	=	$= 2(a + k + g)$	$= 2(a + k + g)$
A_{1010}	=	$= \sqrt{6}(a - k)$	$= \sqrt{6}(a - k)$
A_{0020}	=	$= \sqrt{2}(a + k - 2g)$	$= \sqrt{2}(a + k - 2g)$
A_{0022}	= A_{002-2}	$= \sqrt{3}(c + c^*)$	$= \sqrt{3}(c + c^*)$
A_{1022}	= $-A_{102-2}$	$= \sqrt{3}(c^* - c)$	$= \sqrt{3}(c^* - c)$
A_{0011}	= A_{001-1}	$= \sqrt{3/2}(b + h - b^* - h^*)$	$= \sqrt{3/2}(b - b^* + 2h)$
A_{0021}	= $-A_{002-1}$	$= \sqrt{3/2}(h + h^* - b - b^*)$	$= -\sqrt{3/2}(b + b^*)$
A_{1011}	= $-A_{101-1}$	$= -\sqrt{3/2}(b + b^* + h + h^*)$	$= -\sqrt{3/2}(b + b^*)$
A_{1021}	= A_{102-1}	$= \sqrt{3/2}(b - b^* + h^* - h)$	$= \sqrt{3/2}(b - b^* - 2h)$
A_{1100}	= A_{1-100}	$= \sqrt{2}(j + d - d^*)$	$= h - \sqrt{2}\ell + b - b^*$
A_{1110}	= A_{1-100}	$= -\sqrt{3}(d + d^*)$	$= -\sqrt{3/2}(b + b^*)$
A_{1120}	= A_{1-120}	$= d - d^* - 2j$	$= -\sqrt{2}\,h + 2\ell + (1/\sqrt{2})(b - b^*)$
A_{111-1}	= A_{1-111}	$= -\sqrt{3}(i + i^*)$	$= -2\sqrt{6}(g - k)$
A_{1111}	= A_{1-11-1}	$= \sqrt{3}(e + e^*)$	$= \sqrt{6}(c + c^*)$
A_{1121}	= $-A_{1-12-1}$	$= \sqrt{3}(e - e^*)$	$= \sqrt{6}(c^* - c)$
A_{112-1}	= $-A_{1-121}$	$= \sqrt{3}(i - i^*)$	$= 0$
A_{1122}	= A_{1-12-2}	$= \sqrt{6}\ f$	$= \sqrt{6}\ f$
A_{112-2}	= A_{1-122}	$= \sqrt{6}\ \ell$	$= \sqrt{6}\ \ell$

Table A-1 Polarized-beam polarized-target observables for elastic p-d scattering in the helicity notation. "Simplified" means that no doublet-quartet transitions are allowed.

A_{1111} sin 2φ and can be measured at $\pi/4$ (see sketch).

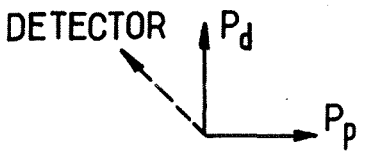

Other experiments might be used to test the absence or presence of doublet-quartet transitions. We note that A_{112-1} is predicted to be zero, but it is very difficult to obtain a component T_{21} in a deuteron beam. It could be obtained by using a polarized deuteron target in which the vector polarization could be flipped independently of the tensor one, and the target could be inclined. A fuller discussion will be published elsewhere.

Notes and References

* Time reversal provides further constraints which are readily translated in term of independent experiments when described in the center of mass system. This number is then further reduced from 648 to 342.

1) A.M. Baldin, Soviet J. Nucl. Phys., 1965, 2, 211.
2) V.P. Alfimenkov, V.I. Luschikov, V.G. Nikolenko, Yu V. Taran and F.L. Shapiro, "Choice of the proper set of neutron-deuteron scattering lengths from experiments on transmission of polarized neutrons through a polarized deuteron target", Dubna preprint E3-3030, 1966 ; I am indebted to Dr Shapiro for sending me this preprint.
3) Derived from $a_2/a_4 = 0.12 \pm 0.04$, D.G. Hurst and N.Z. Alcock, Can. J. Phys., 1951, 29, 36 ; and $\sigma_T = 3.44$ b, E. Fermi and L. Marshall, Phys. Rev., 1949, 75, 578.
4) J.D. Seagrave, Bull. Am. Phys. Soc., 1966, 11, 895 and private discussion.
5) W. Gissler, Z. Krist., 1963, 118, 149.
6) I am indebted to R.E. Donaldson, LRL, Livermore, for permission to quote this unpublished result.
7) A.C. Phillips, Private discussion.
8) R.A. Chalmers, R.S. Cox, K.K. Seth and E.N. Strait, Nucl. Phys., 1965, 62, 497.
9) W. Grüebler, W. Haeberli and P. Extermann, Nucl. Phys., 1966, 77, 394.
10) T.B. Clegg, Bull. Am. Phys. Soc., 1966, 11, 303. I am indebted to Professor Haeberli for sending me plots of these results together with the unpublished results at 12.0 MeV.
11) J.S.C. McKee, D.J. Clark, R.J. Slobodrian and W.F. Tivol, Bull. Am. Phys. Soc., 1966, 11, 896. I am indebted to R.J. Slobodrian for sending me these results prior to publication, and private discussion.
12) H.E. Conzett, G. Igo and W.J. Knox, Phys. Rev. Letters, 1964, 12, 222.
13) H.E. Conzett, H.S. Goldberg, E. Shield, R.J. Slobodrian and S. Yamabe, Phys. Letters, 1964, 11, 68.
14) S.J. Hall, A.R. Johnston and R.J. Griffiths, Phys. Letters, 1965, 14, 212.
15) A.R. Johnston, W.R. Gibson, J.H.P.C. Megaw, R.J. Griffiths and R.M. Eisberg, Phys. Letters, 1965, 19, 289.
16) A.R. Johnston, W.R. Gibson, E.A. McClatchie, J.H.P.C. Megaw and R.J. Griffiths, Phys. Letters, 1966, 21, 309.
17) W.R. Gibson, A.R. Johnston, E.A. McClatchie, J.H.C.P. Megaw and R.J. Griffiths. I am indebted to A.R. Johnston for sending me the latest results of this experiment, which was first reported at the Gatlinburg Conference in 1966, paper 9.2, and to W.R. Gibson for a private discussion.
18) K.L. Kowalski and D. Feldman, Phys. Rev., 1963, 130, 276.
19) J. Hüfner and A. de-Shalit, Phys. Letters, 1965, 15, 52.
20) Proceedings of the 2nd International Conference on Polarization Phenomena of Nucleons, Karlsruhe, 1965 ; P. Huber and H. Schopper, ed., Birkhäuser Verlag, Basel and Stuttgart, 1966, H.H. Barschall, p. 393.

21) J.J. Malanify, J.E. Simmons, R.B. Perkins and R.L. Walter, Phys. Rev., 1966, 146, 632.
22) J.E. Simmons, Private communication.
23) M. Poulet, A. Michalowicz, K. Kuroda, D. Cronenberger and C. Coignet, Phys. Letters, 1966, 22, 636.
24) P.G. Young and M. Ivanovich, Phys. Letters, 1966, 23, 361.
25) P.G. Young, M. Ivanovich and G.C. Olsen, Phys. Rev. Letters, 1965, 14, 831.
26) P. Extermann, University of Wisconsin preprint. I am indebted to Professor Haeberli for sending me this preprint prior to publication.
27) Proceedings of the 2nd International Conference on Polarization Phenomena of Nucleons, Karlsruhe, 1965 ; P. Huber and H. Schopper, ed., Birkhäuser Verlag, Basel and Stuttgart, 1966, J. Arvieux, R. Beurtey, J. Goudergues, M. Lechaczynski, B. Mayer, T. Mikumo, A. Papineau and J. Thirion, p. 370.
28) I am indebted to J. Arvieux and the other authors listed in reference 27 for discussion of these latest results.
29) P.L. Csonka, M.J. Moravcsik and M.D. Scadron, Phys. Rev., 1966, 143, 1324.
30) I am indebted to Dr Fick for sending me these unpublished results prior to the conference.
31) P.L. Csonka, M.J. Moravcsik and M.D. Scadron, Phys. Rev., 1966, 143, 775.
32) M.J. Moravcsik, UCRL-5317-T (1958) ; P. Cziffra, M.H. MacGregor, M.J. Moravcsik and H.P. Stapp, Phys. Rev., 1959, 114, 880.
33) A.F. Grashin, Zh. Eksperim. i Teor. Fiz., 1959, 36, 1717.
34) L.D. Faddeev, Zh. Eksperim. i Teor. Fiz., 1960, 39, 1459 (translation : Soviet Phys. JETP, 1961, 12, 1014.
35) R.L. Omnes, Phys. Rev., 1964, 134, B1358.
36) A. Ahamazadeh and J.A. Tjon, Phys. Rev., 1965, 139, B1085.
37) T. Osborn and H.P. Noyes, Phys. Rev. Letters, 1966, 17, 215.
38) H.P. Noyes, Phys. Rev. Letters, 1965, 15, 538.
39) K.L. Kowalski and D. Feldman, J. Math. Phys., 1961, 2, 499 ; 1963, 4, 507 and Phys. Rev., 1963, 130, 276. K.L. Kowalski, Phys. Rev. Letters, 1965, 15, 798 [Erratum : 908].
40) T. Osborn finds that if a sophisticated quadrature rule is used, a small number of points suffice for the integral even when there is strong short-range repulsion ; this is numerically easier than integrating the radial Schroedinger equation, and gives directly the needed $f_k(p)$ as well as the phase shift.
41) A.G. Sitenko and V.F. Kharchenko, J. Nucl. Phys. (USSR), 1965, 1, 994 [translation : Soviet J. Nucl. Phys., 1965, 1, 708]. See also A.G. Sitenko and V.F. Kharchenko, Nucl. Phys., 1963, 49, 15 and A.G. Sitenko, V.F. Kharchenko and N.M. Petrov, Phys. Letters, 1966, 21, 54.
42) R. Aaron, R.D. Amado and Y.Y. Yam, Phys. Rev., 1965, 140, B1291.
43) R. Aaron, Private discussion.

44) A.N. Mitra, Nucl. Phys., 1962, 32, 529 ; A.N. Mitra and V.S. Bashin, Phys. Rev., 1963, 131, 1264 ; B.S. Bhakar and A.N. Mitra, Phys. Rev. Letters, 1965, 14, 143 ; A.N. Mitra, Phys. Rev., 1965, 139, B1472.
45) A.C. Phillips, Phys. Rev., 1966, 142, 984.
46) R.D. Amado, Phys. Rev., 1966, 141, 902.
47) A.C. Phillips, Phys. Rev., 1966, 145, 733.
48) Proceedings of the 2nd International Conference on Polarization Phénomena of Nucleons, Karlsruhe, 1965 ; P. Huber and H. Schopper, ed., Birkhäuser Verlag, Basel and Stuttgart, 1966, H.P. Noyes, p. 238.
49) H.P. Noyes, Bull. Am. Phys. Soc., 1966, 11, 895 and SLAC-PUB-238.
50) P. Catillon, M. Chapellier and D. Garreta, Paper 6.3 at the Gatlinburg Conference, 1966. I am indebted to P. Catillon for making these and later results available to me by private communication and discussion.
51) J.J. Malanify, P.J. Benalt, T.R. Roberts and J.E. Simmons, (to be published).
52) R.A. Arndt and M.H. MacGregor, UCRL-70075 (submitted to Phys. Rev.). I am indebted to these authors for permission to present their results at this conference.
53) S.I. Bilenkaya, Z. Janout, Yu M. Kazarimov and F. Lehar, Dubna preprint E-2609, "Unambiguous phase shift analysis of the nucleon-nucleon scattering at 23.1 MeV" (1966).
54) J.M. Blatt and L.M. Belves, Phys. Rev. Letters, 1964, 12, 544.
55) D.Y. Wong, Phys. Rev. Letters, 1959, 2, 407.
56) J.K. Perring, Private communication. The main difference is that Perring includes n-p total cross-sections at 24 and 28 MeV given by D.E. Groce, B.D. Sowerby and J.M. Morris, Phys. Letters, 1965, 17, 40 ; n-p differential cross-sections at 27.2 and 28.4 MeV as quoted by W.N. Hess, Rev. Mod. Phys., 1958, 30, 368 , and notes that the n-p polarization measurements are only known to 10 % in absolute normalization, rather than the 1.7 % uncertainty used by Arndt and MacGregor.
57) C.J. Batty, T.C. Griffith, D.C. Imrie, G.J. Lush and L.A. Robbins, Paper 6.2 at the Gatlinburg Conference, 1966.
58) H.P. Noyes, Phys. Rev. Letters, 1964, 12, 171.
59) H.P. Noyes, Nucl. Phys., 1965, 74, 508.
60) J.S. Ball, A. Scotti and D.Y. Wong, Phys. Rev., 1966, 142, 1000.

Work performed under the auspices of the U.S. Atomic Energy Commission.

POLARIZED NUCLEI AND NEUTRONS

F.L. SHAPIRO

Joint Institute for Nuclear Research, Dubna

I INTRODUCTION

In this report I would like to discuss some possibilities of using polarized nuclear targets in neutron physics. But first it is necessary to consider what has been already done in this field. In this respect my task becomes easier because of the report of Dr Schermer [1] who I suppose will speak about the interesting investigations carried out in Brookhaven and possibly also about some of the earlier investigations. Therefore I shall describe only the work performed in Dubna. The Dubna group (V.P. Alfimenkov, V.I. Luschchikov, V.G. Nikolenko, Yu. V. Taran, F.L. Shapiro) used a dynamically polarized proton target to obtain a polarized beam of neutrons [2,3,4]. In experiments with this beam and with a polarized deuteron target the spin dependence of n-d scattering was studied [5], and in experiments with a polarized target of ^{165}Ho the spins of a number of neutron resonance of holmium were determined [6].

II POLARIZATION OF NEUTRONS BY USE OF A POLARIZED PROTON TARGET

The necessity of a new method of neutron polarization was due to the fact that the known methods (based on magnetic scattering of neutrons or on use of nuclear reactions such as Li(p,n) were ineffective in the interesting region of neutron energies 10 eV - 10^5 eV. Filtration of the non-polarized neutron beam through a polarized proton target was chosen as such a new method. The transmitted beam becomes polarized as neutrons with spin oriented anti-parallel

to the proton spin are scattered more intensively than neutrons with parallel spin orientation (fig. 1). Certainly, any polarized nuclear target will give similar effect. The proton target, however, has decisive advantages :

a. It exists.At present in a crystal of lanthanum-magnesium nitrate LMN($La_2Mg_3(NO_3)_{12}.24H_2O$) with the help of the dynamic method it is easy to obtain proton polarization of the order of 70 % [7].

b. The cross-section of n-p scattering is large, has a very strong spin dependence and it does not change within the energy interval from 1 eV up to several dozens of keV. This ensures constancy of the neutron beam polarization in this interval and a large value of polarization (70 %) at a moderate loss in beam intensity (the beam is reduced by the target by 5 times approximately).

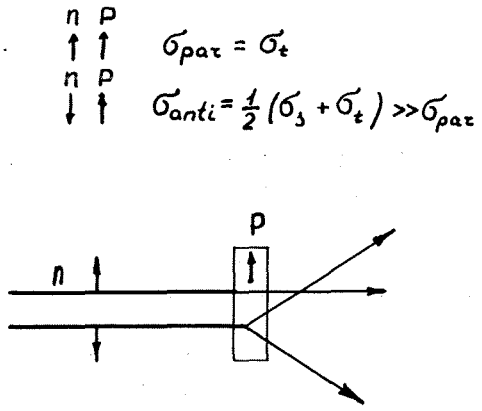

Fig. 1

A calculation of polarization and intensity of the neutron beam transmitted by a proton target is rather simple, since in the energy region considered the interactions is determined only by the s-wave. The total cross-section of interaction of s-neutron with the nucleus can be written in the form * :

$$\sigma = \sigma_o - f_n f_N \sigma_p \qquad (1)$$

where σ_o is the total cross-section for non-polarized particles, $f_n f_N$ are the polarization of neutrons and nuclei, respectively and σ_p is the so-called polarization cross-section :

$$\sigma_p = \frac{I}{2I+1} 4\pi (a_-^2 - a_+^2) + \frac{I}{2I+1} (\sigma_{c-} - \sigma_{c+}) \cdot \qquad (2)$$

Here I is the spin of target nuclei, $a_\pm$, $\sigma_{c\pm}$ are the scattering lengths and the capture cross-sections for neutron-nucleus colli-

sions with total spin I + 1/2 and I - 1/2, respectively.

The transmission of the target for a non-polarized incident neutron beam and the polarization of the transmitted beam are given by the expressions :

$$T = e^{-n\sigma_o t} \; ch.f_N \; n\sigma_p t \tag{3}$$

$$f_n = th.f_N \; n\sigma_p t \tag{4}$$

where n is the density of nuclei in the target, and t is its thickness. At very small neutron energies beam attenuation is caused only by the incoherent component of scattering and by capture. In this case one should substitute into (3) and (4) :

$$\sigma'_o = \sigma_{inc}\left(1 - \frac{I}{I+1} f_N^2\right) + \sigma_{co} \tag{5}$$

$$\sigma'_p = \frac{1}{I+1} \sigma_{inc} + \frac{I}{2I+1} (\sigma_{c-} - \sigma_{c+}) \tag{6}$$

instead of σ_o and σ_p. Here σ_{inc} is the usual incoherent scattering cross-section, and σ_{co} is the capture cross-section for non-polarized particles.

For protons at 1 eV $\lesssim$ E $\lesssim$ 10 keV one has σ_o = 20.4 barns, σ_p = 16.7 barns ; at E $\ll$ 1 eV neglecting capture one has $\sigma'_o = 80(1 - 1/3\, f_N^2)$ barns, σ'_p = 53 barns.

At measurement of effects proportional to the neutron polarization f_n, the optimum target thickness is determined as one giving maximum to the product $f_n^2 T$. In figure 2 calculated values of $f_n^2 T$ for LMN target of optimum thickness at proton polarization f_N = 70 % are shown in function of neutron energy (curve 3). A pure hydrogen f_N = 1 target yields advantage by only a factor of 3.5 as compared to LMN, f = 0.7 (curve 4). In figure 3 the values of optimum neutron polarization are given for LMN, f = 0.7 (curve 3) and for some other neutron polarizers as well. They can by no means be compared with LMN in the energy region of dozens eV - 10^5 eV.

In Dubna at present a target of two single crystals of LMN of total thickness 1.9 cm and of area 3.5 x 5.2 cm^2 is used as a neutron polarizer. Dynamic polarization is conducted under the following conditions ; paramagnetic admixture is 0.5 % ^{142}Nd, temperature is 0.95° K, magnetic field is 17 kOe, frequency is 64 GHz (wave length λ = 4.7 mm), microwave power fed to the cavity is about 150 milliwatts ; the achieved polarization of protons is 70 %.

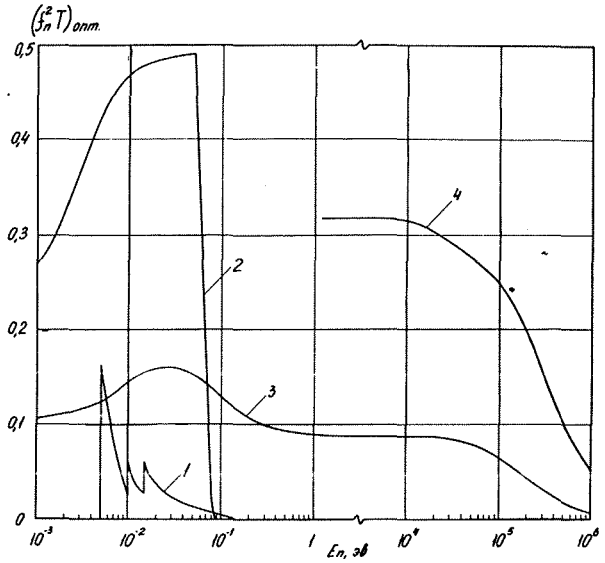
$(\beta_n^2 T)_{опт.}$
0,5
0,4
0,3
0,2
0,1
0
10^{-3}
10^{-2}
10^{-1}
1
10^{4}
10^{5}
10^{6}
E_n, эв
1
2
3
4

Fig. 2

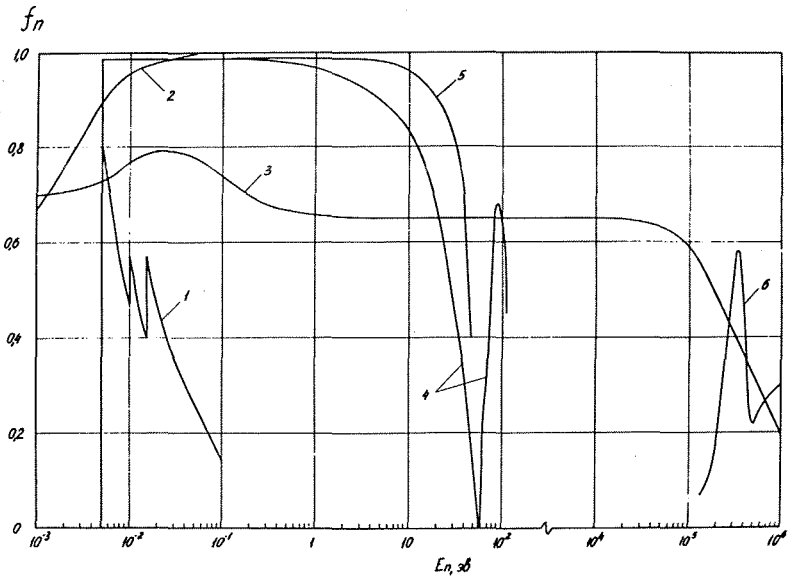
f_n
1,0
0,8
0,6
0,4
0,2
0
10^{-3}
10^{-2}
10^{-1}
1
10
10^{2}
10^{4}
10^{5}
10^{6}
E_n, эв
1
2
3
4
5
6

Fig. 3

This results in 70 % neutron polarization in the resonance energy region, for which the target thickness used is the optimum one. On figure 4 there are shown the results of measurements of the so-called single transmission effect $\varepsilon_1 = T/T_0 - 1$, carried out with the described target at somewhat higher temperature of 1.15° K.

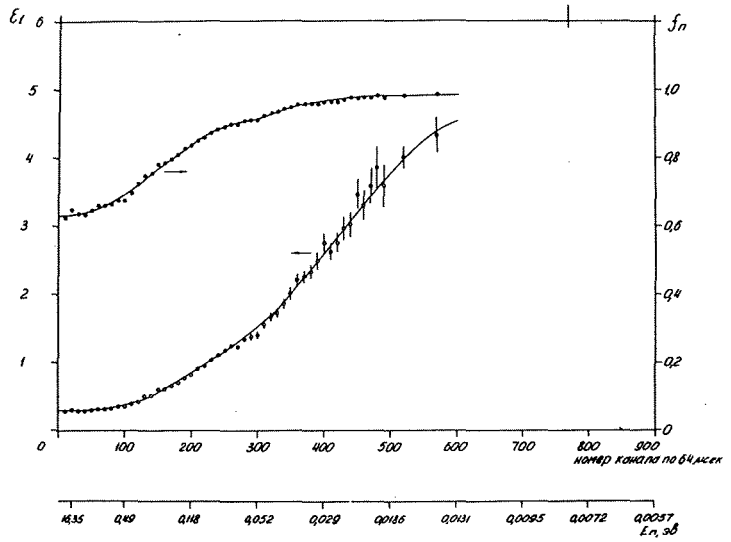

Fig. 4

On the abscissa neutron time of flight of a 60 m distance and corresponding energy in eV are given. At the energy ~ 0.01 eV switching of the proton polarization results over 5 times increase of the neutron beam intensity. At $E \gtrsim 1$ eV one has $\varepsilon_1 = 0.299 \pm 0.005$; using the known value of the polarization cross-section one obtains then for the proton polarization $f_N = 0.60 \pm 0.005$, the error takes into account only the counting statistics of ε_1. This value agrees with the one obtained from measurements by the NMR method with a rather smaller accuracy.

On figure 4 the polarization of the transmitted neutron beam calculated from ε_1 by combining expressions (3) and (4) is presented **.

III SPIN DEPENDENCE OF THE n-d SCATTERING

Experiments on n-d scattering carried out 15 years ago [8] resulted in two alternative sets of n-d scattering lengths :

(i) $a_2 = 0.7 \pm 0.3$ fm , $a_4 = 6.38 \pm 0.06$ fm

(ii) $a_2 = 8.26 \pm 0.12$ fm , $a_4 = 2.4 \pm 0.2$ fm

Results of many theoretical papers (see, for example [9]) point out rather definitely at the correctness of the first set. Nevertheless, taking into consideration the importance of the nuclear three-body problem and the incompleteness of the present conceptions about nuclear forces it seemed necessary to make a choice of the real set with the help of an independent experiment without appealing to the three-body theory. A recent theoretical paper by A.M. Baldin [10] containing arguments in favour of the second set, was very much stimulating in this connection.

In virtue of these considerations, in Dubna an experiment on transmission of polarized neutrons through a polarized deuteron target was undertaken [5]. Using (1) it is easy to obtain the following expression for the so-called effect of double transmission ε_2 :

$$\varepsilon_2 = \frac{J_{par} - J_{anti}}{J_{par} + J_{anti}} = f_n \, t h f_N \, n\sigma_p t \qquad (7)$$

where J_{par}, J_{anti} are neutron beam intensities transmitted through a target with nuclear polarization f_N for parallel and antiparallel orientations of neutron and nuclear spins, respectively ; f_n is the polarization of the incident neutron beam.

According to (2) the polarization cross-section σ_p is proportional to the difference of squares of the doublet ($a_2 = a_-$) and quartet ($a_4 = a_+$) n-d scattering lengths. Consequently, $\sigma_p < 0$ and $\varepsilon_2 < 0$ for the first set for which there is $a_2 < a_4$, while $\sigma_p > 0$ and $\varepsilon_2 > 0$ for the second set ($a_2 > a_4$).

This happens at neutron energy $E \gtrsim 1$ eV. At small energies $\sigma_p = 1/2 \, \sigma_{inc}$, i.e. $\varepsilon_2 > 0$ and is the same for both sets. Thus, if the first set is correct, ε_2 changes its sign at $E \to 0$, i.e. passes through zero at a certain energy $E \ll 1$ eV. For the second set one has $\varepsilon_2 > 0$ at all energies.

The lay-out of the experiment is shown on figure 5. The pulsed reactor IBR (1) served as a source of neutrons, their energy being defined by time of flight. The polarized proton target mentioned above was used as neutron polarizer (3). The polarized deuton tar-

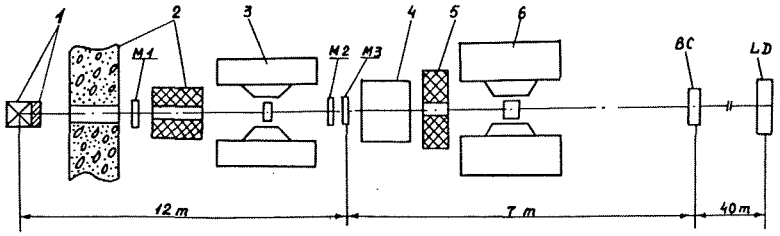

Fig. 5

get (6) was similar to the proton one with the only difference that there was used a deuterated LMN crystal ($La_2Mg_3(NO_3)_{12}\cdot 24D_2O$) of 3.5 cm thickness in the direction of the neutron beam and of cross-section 1.5 x 2.4 cm^2. A hydrogen admixture to the deuterium in the crystal was not more than 0.5 %. Dynamic polarization was carried out under the same conditions as in the proton target, but at temperature of 1.3° K. The polarization was controlled by observing the nuclear magnetic resonance (NMR) signal of deuterons.

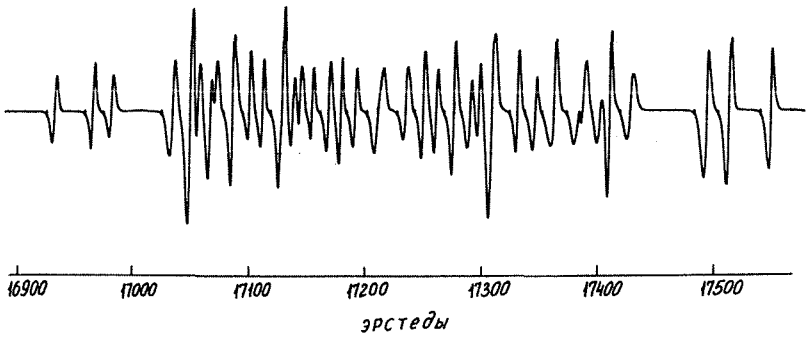

Fig. 6

An example of deuteron signal recording is given on figure 6. The absolute polarization value could not be found in such manner as the NMR detector used did not allow to see the non-enhanced deuteron signal. The sign of deuteron polarization was found by comparing the deuteron NMR signal with that of fluorine in teflon. The latter was recorded at the same frequency of NMR at reduced magnetic field.

A spin rotator (4) for rotation the neutron spin by 180° was placed between the proton and deuteron targets. The neutrons passed through both targets were detected by $^{10}BF_3$ counter bank (BC on fig. 5) mounted at a distance of L = 19 m from the reactor and by a boron liquid detector (LD, L = 60). Boron counters M1 (before the proton target) and M2, M3 (after it) served as monitors. The neutron spin direction was reversed after each 10^5 counts of the M1 monitor (which took about 800 s). Two cycles of measurements were conducted. In the first one (32 of 800 s intervals) the deuteron polarization was positive (i.e. spin parallel to the magnetic field), in the second one (38 intervals) it was negative. Because of this value $\varepsilon = \varepsilon_2$ was measured in the first cycle, whereas $\varepsilon = -\varepsilon_2$ was measured in the second.

Results of measurements are given in figure 7. As it should be expected the effects received in the first (solid points) and in the second (open points) cycles are opposite in signs. Boron counters (circles) and a liquid detector (squares) gave similar results within error limits. All data correspond to negative sign of ε_2. Control experiments with the zero polarization in the deuteron target yielded a zero effect.

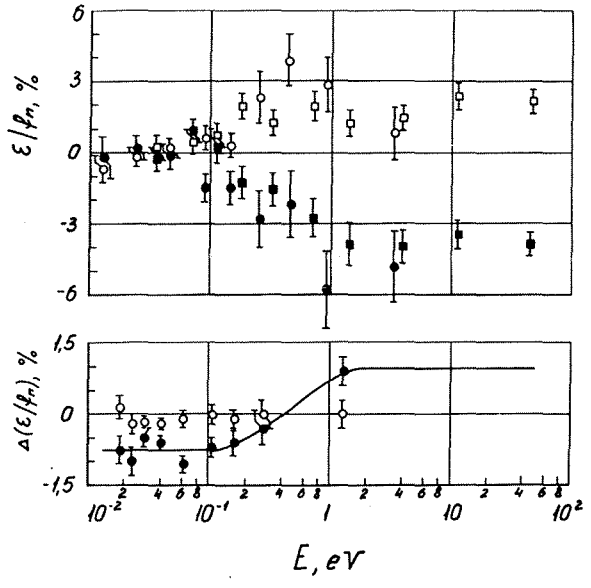

Fig. 7

Before going to conclusions one should take into account the influence of other non-zero spin nuclei present in the deuteron target, since all of them get polarized by the dynamic method. ^{14}N and ^{139}La are most essential. The nitrogen polarization was compa-

red with the deuterium one under conditions the dynamic polarization similar to those in the first cycle of measurements. Signals of ^{14}N and ^{2}D were recorded at the same frequency of NMR, but at different magnetic fields. A recording of the nitrogen signal is illustrated in figure 8. The ratio of nitrogen and deuterium polarizations was found equal to 0.65 ± 0.20. Lanthanum polarization was not measured ; for estimates it was taken with a certain reserve exceeding the deuterium polarization by 2.25 times (frequencies of NMR for lanthanum and deuterium are about the same).

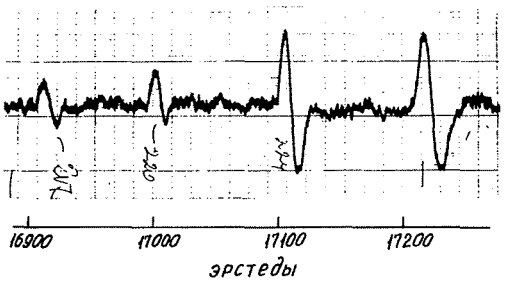

Fig. 8

Polarization cross-sections of lanthanum and nitrogen were calculated from the published data about total and coherent scattering cross-sections. The sign of ^{14}N polarization cross-section is certainly negative due to the fact that slow neutron scattering by nitrogen is largely determined by a negative level with the spin 3/2 (nitrogen spin is I = 1) [11]. The polarization cross-section of lanthanum is not well known. Taking into account the nitrogen and lanthanum contributions the expression for ε_2 takes the form (at $\varepsilon_2/f_n \ll 1$) :

$$\frac{\varepsilon_2}{f_n} = f_N^d \, n_d \sigma_p^d t \left(1 + \sum_{i=N,La} \frac{n_i \sigma_p^i f_N^i}{n_d \sigma_p^d f_N^d}\right) \quad . \qquad (8)$$

From this formula it follows that sign of the double transmission effect ε_2 is governed by deuterium. Therefore, the observed negative sign of the double transmission effect proves that from the two alternative sets of n-d scattering lengths the proper one is the first i.e. that for which $a_2 < a_4$. The energy dependence of ε_2 is difficult to analyse quantitatively because of lack of information on spin dependence of neutron capture cross-sections of nitrogen and lanthanum. In any case it does not contradict to the first set, for which intersets zero level at some energy E ≪ 1 eV.

Using the values of ε_2 obtained for $E \gtrsim 1$ eV and expression (8) one can estimate the achieved deuterium polarization. In the first cycle of measurements it was equal to 0.12 ± 0.05, and in the second one to -0.07 ± 0.03.

IV DETERMINATION OF SPINS OF HOLMIUM NEUTRON RESONANCES

In S-neutron resonances the cross-section is practically determined by only one spin component. For a resonance with spin $J = I - 1/2$ one can neglect the scattering amplitude a_+ and the capture cross-section σ_{c+}; consequently the polarized cross-section (2) for $J = I - 1/2$ resonances will be positive. On the contrary, for a resonance with $J = I + 1/2$ we can take $a_- = \sigma_{c-} = 0$ i.e. the polarized cross-section $\sigma_p < 0$. Accordingly, the double transmission effect is positive ($\varepsilon_2 > 0$) if $= I - 1/2$ and is negative ($\varepsilon_2 < 0$) if $J = I + 1/2$. Measurements of the double transmission effect for holmium were conducted with the installation shown on figure 5 with the following differences. A holmium target was mounted instead of the deuterium one. The BC neutron detector was not used, and the liquid detector LD was placed at a distance of 120 m from the reactor. The polarization of holmium nuclei was achieved statically by cooling of a polycrystalline metal sample down to a temperature of 0.3° K in a magnetic field of 15 kOe. A cryostat with pumping of liquid ^{3}He vapour was used. The internal magnetic field created by atomic f-electrons at the Ho nucleus site is rather great, about 9.10^6 Oe. Under the conditions of the present experiment this results in Ho nuclear polarization of the order of 50 % (it was estimated from the results of neutron measurements). The first experiment with holmium conducted in 1965 is already described [4,6]. At time of flight resolution of about 0.5 μs/m, it was possible to determine the spins of 9 out from the 11 resonances of holmium present in the energy region below 60 eV. Measurements were repeated under conditions of better resolution (about 0.04 μs/m) this year. The improvement of resolution was attained due to the booster mode of operation of the pulsed reactor IBR, in which it is a subcritical amplifier of neutron pulses generated in the active zone of the reactor by a pulsed beam of 30 MeV electrons. The letter are provided by an electron microtron accelerator [12]. In the booster mode the neutron bursts lasted 4 μs instead of 50 μs under of the supercritical reactor conditions. The neutron intensity in the booster regime corresponds to average power of about 1 kW compared to 6 kW under the usual reactor mode. Measurements with holmium were conducted before the final adjustments at the microtron were done, and at that time the power was essentially less

(about 0.15 kW). This did not allow to gather as much statistics as one would prefer to do. An example of experimental results are shown on figure 9. The lower curve is the counting rate for a detector with a holmium sample in the beam ; at the dips the energies of ^{165}Ho resonance levels [13] are marked. The upper curve gives the double transmission effect ε_2. Peaks mark resonances of ^{165}Ho with the spin $J = I - 1/2 = 3$, dips mean that $J = I + 1/2 = 4$. The quantitative analysis described in [6] allows to receive some information about spin of resonances, also in those cases when they are not resolved.

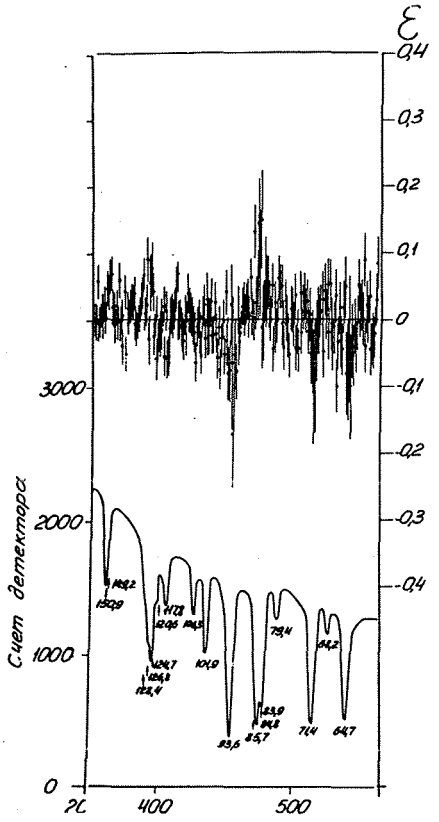

Fig. 9

Spins of 23 levels out of the total number of 29 levels below 160 eV were determined. 10 levels have spin 3, 13 have spin 4. It follows that with 70 % probability the ratio of spin 4 and spin 3 level densities with spins 4 is within the limits 0.9-1.7, whereas the theoretical estimate is 1.19. The strength functions for the two spin states coincide within the limits of the 30 % error.

At present a refrigerator of the Neganov type [14] is under way to obtain temperatures of the order of 0.05° K and some other modifications are being introduced in the installation. After finishing the reconstruction the works on determination of spins of rare earth nuclei will be continued under better conditions both in intensity and in energy resolution.

V SOME ASPECTS OF USING OF POLARIZED TARGETS IN EXPERIMENTS WITH SLOW NEUTRONS

Now I pass on from a description of the experiments done to a discussion of experiments which are worth conducting in future. I shall confine myself to a consideration of the resonant region of neutron energies, and I shall not speak at all either about experiments with thermal neutrons, or those with fast neutrons. I shall not consider as well experiments aimed at receiving solid state physics information (internal magnetic fields, nuclear magnetism and so on). I hope that some of these questions will be touched upon by Dr Schermer.

a. Determination of spins of S-neutron resonances.

Physicists dealing with neutron spectrometry always strived for obtaining complete information concerning resonance parameters one of which is the spin. In recent years there appeared more concrete stimulations for spin determination. They are connected with the development of conceptions of the so-called doorway states [15]. Resonances with spin $I + 1/2$ and $I - 1/2$ arising at the capture of S-neutrons can be excited through various doorway states, various, in particular, in energy and width. In the cases when for one out of two values of spin neutron binding energy coincides with the energy of one of the doorway states (with an accuracy up to its width), and for another one is in the interval between two doorway states, there should be observed a dependence of the neutron strength function $S_0 = \overline{\Gamma_n^0}/D$ on spin. There are indications to the existence of this dependence in some nuclei [16]. The difference in doorway states should result in the difference in spectra of captured γ-rays for resonances with different spins. Thus, one can hope to find some displays of neutron doorway states, if one studies spin dependence of strength functions and spectra of γ-rays of a number of nuclei.

The first stage of this work is sorting of resonances by the spin value. Experiments with polarized neutrons and polarized nuclei of the type of the described above experiment with ^{165}Ho is one of the most direct and effective ways of solving this task. The Brookhaven group succeeded in receiving on appreciable polarization of ^{235}U and in measuring with polarized neutrons the spins of three ^{235}U resonances [17]. The continuation of this work in a wider energy region is rather interesting for the physics of fission, especially due to the fact at the existing theory predicts a strong spin dependence of the fission widths of ^{235}U and of other nuclei.

b. Identification of P-resonances and determination of their spins.

This problem has actually arisen before the neutron spectrometry, since in some cases the existence of P-levels among the observed resonances is clearly seen. Thus, in Nb, Ag, Rh, P-resonances are seen beginning with the energy of the order of hundreds eV. They are distinguished by their small neutron widths, however, one cannot consider every narrow resonance as a p-wave because of the typical very wide spread of neutron widths around the mean value. With an increase of the neutron energy, when the average widths of S and P-resonances approach, their identification by this feature becomes more problematic. At the same time an identification of P-resonances is necessary both for the investigation of their properties and for the increase of accuracy at the determination of the averaged characteristics of S-levels. For this one can use peculiarities of P-resonances concerning angular distributions of scattered neutrons, the form of γ-ray spectra, the depth of interference with the potential scattering [18]. These approaches are not universal and each of them has its difficulties. At the same time the use of polarized (aligned) targets can appear effective in some cases.

The influence of polarization on the cross-section of interaction in P-neutron resonances was considered in Dubna by V.N. Efimov [19] and Yu I. Femin. The total cross-section can be presented in the following form.

$$\sigma = \sigma_o \left\{ 1 + A\vec{f}_n\vec{f}_N + B(\vec{f}_n\vec{n})(\vec{f}_N\vec{e}) + Cf_2P_2(\theta) \right\} .$$

Here σ_o is the cross-section for non-polarized nuclei ; $\vec{f}_n\vec{f}_N$ the neutron polarization and nucleus polarization vectors respectively ; $\vec{n}$ a unite vector in the direction of the neutron beam ; f_2 the alignment of nuclei ; θ the angle between the axis of the alignment of nuclei and $\vec{n}$; P_2 the Legendre polynomial.

For S-neutrons B = C = 0. Therefore detection of the cross-section dependence for non-polarized neutrons on nuclear alignment term (C)

immediately points out that $\ell > 0$. In the same way $\ell > 0$, if in experiments with polarized neutrons and nuclei there is detected cross-section dependence on the mutual orientation of the polarization direction and of the neutron beam (term B). The fact that the effects connected with the terms B and C are large and must clearly be seen in experiments is evident from the following considerations. The resonance spin is formed by vector addition of momenta of the target nucleus (I), of the neutron (S) and of the orbital momentum (ℓ) :

$$\vec{J} = \vec{I} + \vec{S} + \vec{\ell} = \vec{j} + \vec{\ell}$$

where $\vec{j} = \vec{S} + \vec{I}$ is the so-called channel spin ; it takes two values $j_1 = I + 1/2$ and $j_2 = I - 1/2$. For $\ell = 1$ the spin of the resonance can take four values : $J = I \pm 3/2$ and $J = I \pm 1/2$.

Let us take as axis of quantization Z the direction of a neutron flight. Then the $\vec{\ell}$ projection on this axis is equal to $m_\ell = 0$. Let nuclei and neutrons be fully polarized along the axis Z : $m_S = 1/2$, $m_I = I$. Then the sum of momentum projections is equal to $m_I + m_S + m_\ell = I + 1/2$. This means that resonances with the spin $I - 1/2$ and $I - 3/2$ cannot be formed at all. Therefore, for these spin values $\sigma = 0$, i.e. $A + B = -1$. If now neutrons are not polarized, and nuclei are aligned completely along the axis Z, then $|m_I| = I$ and $|m_I + m_S + m_\ell| \geqslant I - 1/2$. Therefore, for levels with spin $I - 3/2$ the cross-section turns to zero, and the coefficient C is equal to -1.***

Levels with spin $I \pm 1/2$ can be formed by two ways : through the spin channel $j_1 = I - 1/2$ and through the spin channel $j_2 = I + 1/2$. Each way is characterized by its neutron width $\Gamma_{nj} = \gamma_j^2$ where γ_j is the amplitude of the neutron width. Are the amplitudes γ_{j_1} and γ_{j_2} of the two spin channels correlated ? This question was not studied experimentally. From theoretical point of view one can think it probable that each amplitude will fluctuate independently. To this we can quote Porter and Thomas' considerations, which explain the law of width fluctuations for S-neutron resonances, and take into account the orthogonality of the wave functions for two spin channels.

Coefficients A, B, C in (8) depend upon the spin of the target nucleus, the spin of the resonance, and for spins $J = I \pm 1/2$ also upon the ratio of the amplitudes γ_{j_1} and γ_{j_2}. An experimental determination of coefficients A, B and C for some resonances would allow to find their spins, to investigate the correlation of spin channels amplitudes γ_{j_1} and γ_{j_2} and to establish separately average values of neutron widths for each of these channels (experiments without polarization give only the sum of these widths).

c. Determination of spins of lower-lying levels.

The compound nuclei formed by capture of neutrons by aligned nuclei preserve in general the some of the alignment. As a result of this capture γ-rays will have an angular anisotropy. Knowing the spin of the resonance measurements of the anisotropy will allow to determine multipolarity of the γ-transitions and spins of levels which are populated by these transitions. The experiment of such kind was recently done by H. Postma and E.R. Reddingius on nuclei ^{143}Nd and ^{145}Nd [22].

d. Measurements of magnetic dipole and electric quadrupole momenta of resonant states of the compound nucleus.

A determination of electromagnetic momenta of resonant states for nuclei excited by neutrons might be very essential for enlarging conceptions about the structure and properties of strongly excited nuclei. The modern development of the neutron spectrometry technique allows already now to think about the conducting of these measurements using the shift in the resonance energy due to the superfine interaction. Let the nucleus whose mass for simplicity is considered infinite be affected by the magnetic field H and let E be the kinetic neutron energy far from the nucleus, then the excitation energy of the compound nucleus E_c measured from the neutron binding energy will be determined by the following expression :

$$E - \mu_o \vec{H} = E_c - \mu_1 \vec{H}$$

where μ_o, μ_1 are the magnetic momenta of the target and compound nucleus. If m, M, I and J are the momentum projections on the direction of H and momenta of the target and compound nucleus respectively, then :

$$E_c = E + \left(\frac{M}{J}\mu_1 - \frac{m}{I}\mu_o\right)H = E + \Delta E \quad .$$

For non-polarized neutrons and nuclei $\langle m \rangle = \langle M \rangle = 0$ and $\langle \Delta E \rangle = 0$. If the nuclei are polarized, then $\langle \Delta E \rangle \neq 0$. As it is easy to show at the capture of non-polarized S-neutrons :

$$\langle \Delta E \rangle = H f_N (\mu_1 - \mu_o) \qquad \text{at} \quad J = I - \frac{1}{2}$$

$$\langle \Delta E \rangle = H f_N \left\{ \mu_1 \left[1 - \frac{1}{(I+1)(2I+1)} \right] - \mu_o \right\} \qquad \text{at} \quad J = I + \frac{1}{2}$$

At $H = 10^7$ Oe (holmium), $|\mu_1 - \mu_o| = 1$ nuclear magneton and at $f_N = 1$ one has $\langle \Delta E \rangle \approx 3.10^{-5}$ eV. In experiments with good energy resolution the shift $\langle \Delta E \rangle$ will result in changing of the

sample transmission at the switching of nuclear polarization, as it is shown in figure 10. The largest effect will be observed at a distance of $X = (E - E_0)/\Gamma/2 = \pm 1$ from the centre of the resonance line ; the optimum thickness of the sample corresponds to $n\sigma_0 t = 4$ where σ_0 is the cross-section at $E = E_0$. Under these conditions the difference in relative changes of transmission to the right and to the left from the centre of the line (at $X = + 1$ and $X = - 1$) is equal :

$$\frac{\delta T}{T} = \frac{8\langle \Delta E \rangle}{\Gamma} = 8.3 \cdot 10^{-5}/7.5 \cdot 10^{-2} \approx 0.3\ \%$$

where $\Gamma = 7.5 \cdot 10^{-2}$ eV is the level width. Such an effect can be measured with the help of the best modern neutron spectrometers, it is difficult to do it, but it is not hopeless. In a similar way one can come to measurements of electric quadrupole momenta of resonances. However, here even in the most favourable cases one can expect smaller effects by an order of magnitude.

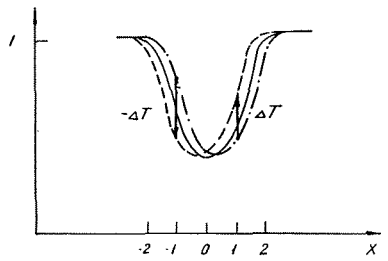

Fig. 10

For the sake of completeness it is worth noticing that measurements of magnetic momenta of resonances can be carried out also with non-polarized nuclei, but with polarized neutrons and even without any polarization at all, under the use of Bragg reflection from antiferromagnetic crystals [20]. However, each method offers its difficulties, and it is possible that the method of polarized nuclear targets does not imply the greatest ones.

e. Polarized targets at measurements of averaged cross-sections.

Recently, Marshak et al [21] reported about investigations of the 350 keV neutron interaction with the nuclei of ^{165}Ho in which were used polarized and aligned holmium targets. The total neutron cross-section of holmium at this energy is equal to 7.94 barns. It changed by 1.3 + 0.4 % at the alignment of holmium nu-

clei perpendicularly to the beam direction, an effect due to the non-sphericity of the holmium nucleus. It is well accounted for by the optical model with usual parameters of potential and with the deformation known from other experiments. In experiments with polarized neutrons and the polarized target within the accuracy $\pm$ 0.3 % there was observed no dependence of the total cross-section from the mutual orientation of the nucleus and neutron spins. From here for the value of the spin-spin interaction term in the optical potential there was obtained an estimate $V_{ss} = -0.13 \pm 0.14$ MeV, i.e. this term is very small.

As it was pointed out above, if the conception of discrete doorway states is correct, one should expect a substantial spin dependence at interaction for some nuclei at certain energies. From this point of view it is of interest to conduct measurements with polarized neutrons and polarized targets for several nuclei in function of energy with resolution of the order of 10 keV or even better. And in the energy region below 100 keV a neutron polarizer with a LMN crystal can be employed for such measurements.

Notes and References

* The minus sign in (I) is chosen in order to have $\sigma_p > 0$ for protons.
** At $E \ll 1$ eV it is necessary to use (5) and (6), however, at $f_n \simeq 1$ the difference is small.
*** Note that the sample transmission for non-polarized neutrons depends upon the target polarization-expression (3). If together with alignment nuclei are polarized, this effect (i.e. the single transmission effect) operating at all l must be distinguished from the alignment influence.

1) R. Schermer, Report at this Conference.
2) Yu. Taran and F. Shapiro, Zh. Eksperim. i Teor. Fiz., 1963, 44, 2185.
3) P. Draghicescu et al, Phys. Letters, 1964, 12, 334.
4) F.L. Shapiro, "Nuclear structure study with neutrons", North Holland, 1966, p. 223.
5) V.P. Alfimenkov et al, JINR preprint E3-3030, 1966.
6) V.P. Alfimenkov et al, Yadern. Fiz., 1966, 3, 55.
7) C.D. Jeffries, "Dynamic orientation of nuclei", Moscow, 1966.
8) D. Hurst and N. Alcock, Can. J. Phys., 1951, 29, 36.
E.O. Wollan et al, Phys. Rev., 1951, 83, 700.
9) V.N. Efimov, Zh. Eksperim. i Teor. Fiz., 1957, 35, 137.
R. Aaron et al, Phys. Rev., 1965, 140, B1291.
10) A.M. Baldin, Yadern. Fiz., 1965, 2, 211.
11) A.A. Bergman, "Trudy P.I.A.N.", 1964, 24, 169.
12) V.D. Ananjev et al, JINR preprint P-2372, 1965.

13) E.N. Karjarina et al, JINR preprint P-2593, 1965.
14) B.S. Neganov, JINR preprint, 1966.
15) H. Feshbach, "Nuclear structure study with neutrons", North Holland, 1966, p. 257.
16) J. Julien, "Nuclear structure study with neutrons", North Holland, 1966, p. 156.
17) V. Sailor et al, Bull. Am. Phys. Soc., 1966, 11, n° 1, 29.
18) G.V. Muradyan, Phys. Letters, 1965, 14, 123.
19) V.N. Efimov, JINR preprint P-1369, 1963.
20) F.L. Shapiro, JINR preprint E-2834, 1966.
21) R. Wagner et al, Phys. Rev., 1965, 139, B29.
22) H. Postma and E.R. Reddingius, Preprint Kamerling Onnes Lab., 1966.

POLARIZED TARGETS AND NEUTRONS

R.I. SCHERMER

Brookhaven National Laboratory, Brookhaven

I CONSIDERATIONS FOR TARGET DESIGN

Of all the possible experiments involving nuclear reactions with polarized targets, those with slow neutrons are probably the simplest to perform. The primary reason for this is that the heat produced in these reactions may be easily handled at temperatures obtained by adiabatic demagnetization, that is $\lesssim$ 200 ergs/mn. As a corollary, since the only energy which is deposited in the sample is due to the reaction under study, rather than to Coulomb excitation or nuclear recoil, we are free to adjust the target thickness as required to optimize the effects of this reaction.

For instance, consider the reaction $^3He(n,p)^3H$, Q = 764 keV. At the Brookhaven Graphite Research Reactor (BGRR), we can get a monochromatic, polarized neutron beam of $\sim 2 \times 10^4$ n/s. This produces 1.5 ergs/mn in the sample, a negligible amount of heat. Even at the HFBR, with 80 times this neutron intensity, the power input is still reasonable. Only for the special case of fission in which Q $\sim$ 200 MeV do we find that there is enough power input at the BGRR to produce a noticeable temperature gradient between the sample and the refrigerating salt. At the HFBR we can only use a small fraction of the available flux, but in fact we know that 2×10^4 n/s is already a very adequate beam intensity so we do not mind this limitation. For (n,σ) or (n,β) reactions the main heat input into the sample is from the surroundings or from natural radioactivity in the sample itself.

Another attractive feature of slow neutron experiments is that the occurrence, in a typical polarized target, of many different nuclear species usually presents no problem. One may selectively study a particular isotope by using a neutron energy corresponding

to a resonance in the cross-section. The only common nucleus to avoid in this regard is the proton. Crystalline samples must be grown from deuterated solutions and many samples must be protected to prevent their adsorbing water vapour.

Since we are interested in doing experiments on a great variety of nuclei, we need an orientation technique which is generally applicable without major modifications in equipment. The various equilibrium methods have worked extremely well in this regard, and to date only the study of (n,d) scattering by the Dubna group has required a dynamically oriented target. A possible restriction on equilibrium methods is that the large area neutron beam from a LINAC or pulsed reactor requires a correspondingly large target area, e.g. 100 cm^2 at Dubna. The heat leak into the sample increases with the area, so that some difficulty might be experienced using adiabatic demagnetization. However, the dilution refrigerator described at this meeting by Prof. Neganov should overcome this problem.

Any restrictions on the target are generally set by the requirements of low temperature physics. The sample should have a large ratio of thermal conductivity to heat capacity, so that it may be cooled to low temperatures in a short time. A short nuclear spin-lattice relaxation time is also required. Several different targets must often be prepared in which the same isotope is placed in different physical or chemical environments. We have found that the choice of one particular target material over another is principally dictated by what is known a priori about the nuclear and/or magnetic properties of the system.

II EXPERIMENTAL TECHNIQUES

In the pioneer experiments of Bernstein et al [1], polarized ^{55}Mn nuclei were activated by polychromatic, polarized, thermal neutrons and the relative activation due to neutrons in the two spin states was determined. In later experiments of Roberts et al [2] and Dabbs [3], the polarized neutrons were transmitted through the sample and counted. Stolovy [4] was the first to report on measurements using monochromatic polarized neutrons at resonance energies, obtained by crystal diffraction of a reactor beam. This was closely followed by the first results from the Brookhaven group, led by V.L. Sailor [5]. These latter two groups have engaged in a continuing program of measurements since 1960. In 1965 Shapiro [6] reported on the first measurements from Dubna. These differ from the previous work in that they involve a pulsed

reactor, time of flight measurements, and the neutrons are polarized by transmission through a microwave pumped, polarized proton target.

I shall deal exclusively with transmission measurements. Since we are dealing with S-wave neutrons, there is no additional information to be gained in principle by scattering experiments. However, Bragg diffraction from an array of polarized nuclei shows some interesting effects and is possibly the best way to study the spin dependence of the nuclear scattering in many cases. Such experiments do not appear to have been done yet.

In passing, I will mention that, besides transmission measurements, experiments have been done by Dabbs et al [7] on the angular distribution of fission fragments, and by Postma [8] on angular distribution of capture γ rays. Both experiments use aligned targets and unpolarized beams.

We have been working under what must be considered very modest experimental conditions by present standards. As already mentioned, the neutron flux at the BGRR is considerably lower than that obtainable on many other reactors. The magnetic field at the nuclear sample is only 15 kOe, which is certainly much smaller than can be obtained using superconducting magnets. The lowest temperature which we have held for a useful length of time has been .045° K. Temperatures a factor of two lower are, however, very reasonable to consider, either obtained by adiabatic demagnetization or with a dilution refrigerator. It seems probable that, unless some unforeseen problem arises, the dilution refrigerator will replace demagnetization for temperatures above $\sim$ .02° K. Temperatures much lower than this still require very exacting technique. Further, the heat load which may be tolerated decreases as T^3, since heat transport at these temperatures is determined by the thermal resistance at a boundary between materials. Thus, while the allowable heat load in our apparatus at .045° K is $\sim$ 200 ergs/mn, and possibly an order of magnitude greater with a dilution refrigerator, the allowable heat load at 10^{-3}° K still remains of the order of 1 erg/mn.

The most important experimental parameters under our control are the neutron energy and the temperature and magnetic field at the sample. Varying the neutron energy enables one to distinguish different nuclei in the sample, or to distinguish scattering from reaction. It is usually insufficient to make measurements at just one temperature. One must often separate the effect of scattering by unpaired electrons in a target, which is temperature independent under proper conditions, from the nuclear effects which do have a temperature dependence. Varying the temperature also alerts one to the possibility that the sample temperature is different from that of the refrigerating salt either because of power deposited in the sample, or because of long relaxation times. The variation of nuclear polarization with temperature may also be used to derive information

about the environment of the nucleus. Varying the magnetic field enables us to check on the magnetic properties of the sample, which are important, since a lack of magnetic saturation affects the observed polarization.

In addition, we have found it vital to be able to translate the sample vertically several inches to allow us to make open beam measurements. We also must occasionally replace the detector with a second crystal to analyse the beam polarization.

Figure 1 shows a plan view of the apparatus, which is basically a demagnetization cryostat mounted on a crystal spectrometer. (I believe it is the world's second largest demagnetization cryostat ; we are now testing a larger one to install at the HFBR). The large size is simply to give a longer running time per liquid helium fill.

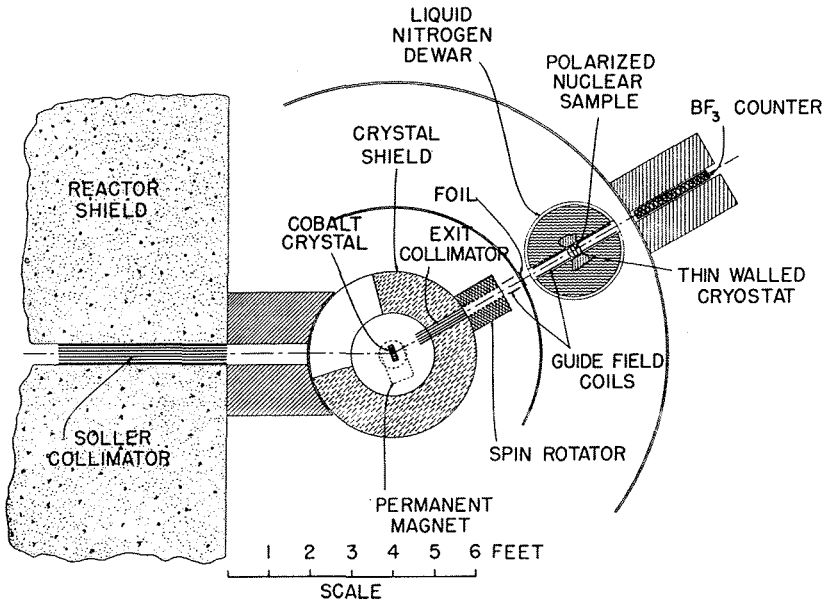

Fig. 1

Almost one half the ^4He bath is lost in pumping down to 1° K. The large nitrogen jacket is a result of placing all the magnets in the liquid nitrogen for cooling. Present technique would be to place a much smaller 1° K ^4He bath inside the main 4.2° K bath with a consequent large reduction in size. The inclusion of a superconducting magnet brings the size back up again, however.

The beam from the graphite reactor is polarized and monochromated by diffraction from a $Co_{.94} - Fe_{.06}$ single crystal. An arrangement of guide fields prevents the beam from depolarizing, and there is a helix of permanent magnets which may be set so as to reverse the direction of neutron polarization when desired.

Figure 2 shows a view of the cryostat interior. Re-entrant evacuated windows bring the neutron beam through the liquid nitrogen and the coils of the sample polarizing magnet. The sample, two paramagnetic salts and their associated lead superconducting heat switches are mounted inside a separate vacuum space, which in turn is suspended within the 1° K ^{4}He bath. The salt we have used almost exclusively is iron ammonium alum in the form of crystals grown onto a bundle of 10,000 fine copper wires. The upper salt is 350 gms, and the lower 250 gms. The former serves as a thermal guard for the latter and, if demagnetized first, scavenges any residual gas remaining in the high vacuum space. The magnetic susceptibility of the lower salt serves as our thermometric parameter. We have recently inserted an ordinary ^{3}He refrigerator at 0.35° K between the pumped ^{4}He bath and the upper refrigerating salt.

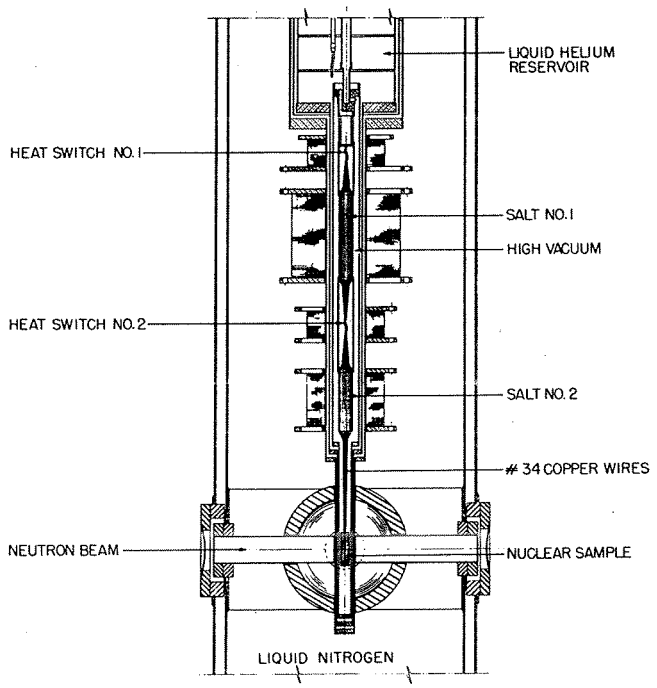

Fig. 2

For a typical sample, we can obtain many hours of data at low temperature. With the ^3He refrigerator in place we have observed warm up rates of 2×10^{-3}° K/hour from .045° K to 0.35° K, which gives us more than one day below 0.1° K. Temperatures between 0.35 and 1° K may be held indefinitely. For qualitative work, or for assigning spins to slow neutron resonances, one such demagnetization may easily suffice. Accurate quantitative work usually takes a number of such cycles.

III EXAMPLES OF EXPERIMENTS WHICH HAVE BEEN PERFORMED

Having chosen a set of experimental conditions, we then count transmitted neutrons, reversing the neutron polarization after some standard time of the order of ten minutes. We form the quantity which we call the transmission effect :

$$\varepsilon = \frac{T_p - T_a}{T_p + T_a}$$

where T_p and T_a stand for neutron transmission with the spin respectively parallel and antiparallel to the direction of the external field which is applied to the nuclear sample. This is not necessarily the direction of nuclear polarization.

For the simplest cases, the transmission effect is given by :

$$\varepsilon = - f_n \frac{1 + \varphi}{2} \tanh \left(N t \sigma_o f_N \frac{\sigma_p}{\sigma_o}\right)$$

where f_n is the neutron polarization and φ the efficiency with which it can be reversed, N the number of nuclei per cm^3, t the sample thickness, and f_N the nuclear polarization along the external field direction. σ_o is the cross-section for unpolarized neutrons and σ_p a "polarization cross-section" related to the quantity C_{nn} used by previous speakers. The cross-section with polarization is given by :

$$\sigma = \sigma_o + \sigma_p f_N \cdot f_n$$

$$\sigma_o = \frac{I + 1}{2I + 1} \sigma_+ + \frac{I}{2I + 1} \sigma_- = \sigma(I + \tfrac{1}{2}) + \sigma(I - \tfrac{1}{2})$$

$$\sigma_p = \frac{I}{2I + 1} (\sigma_+ - \sigma_-) = \frac{I}{I + 1} \sigma(I + \tfrac{1}{2}) - \sigma(I - \tfrac{1}{2})$$

Note that this definition of σ_p has the opposite sign from that used by Shapiro [6]. The quantity $f_n(1+\varphi)/2$ may be determined by analysing the beam polarization and varies between 0.84 and 0.9, depending on the beam energy. $Nt\sigma_o$ is the target thickness measured in mean free paths when either the target or the beam is unpolarized, and is determined from a transmission measurement made with zero field applied to the sample. It is easily shown [6] that the minimum fractional error in ε for a given counting time occurs when $Nt\sigma_o \approx 2$.

The detailed expression for ε when one considers the effects of energy resolution, beam depolarization in the sample and contributions from more than one isotope has been given elsewhere [5,9]. The simple expression will suffice to illustrate the kinds of experiments we have done with the system.

a. Determining the angular momentum of a slow neutron resonance, J. For S wave neutrons $J = I \pm 1/2$. At a resonance one of the two terms $\sigma(I \pm 1/2)$ is much larger than the other, and we have either $\sigma_p/\sigma_o = I/I+1$ when $J = I + 1/2$ or $\sigma_p/\sigma_o = -1$ when $J = I - 1/2$. If we know the algebraic sign of f_N, the J value follows from the algebraic sign of ε. The magnitude of ε is unimportant which is extremely helpful since the magnitude of f_N may be completely unknown.

In an elegant variation of this technique [10], it is not necessary to show the sign of f_N, a priori, if one has two resonances which give transmission effects of opposite sign. Using the ratio of these effects one can determine the J values of the two resonances individually and then deduce the sign of f_N from the measurements. Further, the method is insensitive to gross uncertainties in the resonance parameters.

Using the above techniques, the two groups in the United States have assigned J values to about 50 resonances lying below 15 eV in 20 isotopes, of elements chiefly within the 4f and 5d groups in the periodic table. The Dubna group has added a number of assignments [6] for higher energy levels in ^{165}Ho.

b. Many nuclei do not possess levels of low enough energy to be studied using reactor neutrons, or at least those obtainable from a crystal spectrometer. It is often of interest, however, to determine the fraction of the low energy cross-section in each spin state. For many nuclei of medium mass, this may be of interest in analysing the results of capture γ-ray experiments. Such a determination has been made [11,12] for ^{59}Co and ^{165}Ho and there are many more suitable nuclei. For the very light nuclei it may be possible to correlate these results with those obtained from charge particle work or with theoretical predictions. Such experiments have been performed on ^{1}H, ^{2}H, ^{3}He, ^{6}Li, ^{9}Be and ^{10}B. [13]

Prof. Shapiro has already spoken at this meeting about the (n,d) experiment performed at Dubna. I will briefly show our results on ^{3}He ; these have already been published [14]. We used a target of ^{3}He adsorbed on zeolite. This was mixed with lead powder to improve the heat conductivity, pressed into a slab and soldered to a copper foil leading to the refrigerating salt. Polarization was by "brute force" -- the interaction of the ^{3}He moment with the applied field. From the observed transmission effects, we can calculate the product $f_N(\sigma_p/\sigma_o)$ and then express this in terms of the susceptibility per ^{3}He nucleus since $\chi = \mu f_N/H$. Finally we put the result in the standard form used in low temperature work in which we plot $\chi T/C$, where C is the Curie Constant $\mu^2(I + 1)/3Ik$. Figure 3 is a plot of $\chi T/C\ (\sigma_p/\sigma_o)$ vs T for one run, representing about 1/4 of the data. If the ^{3}He susceptibility obeyed Curie Law, we would get a horizontal line on this plot.

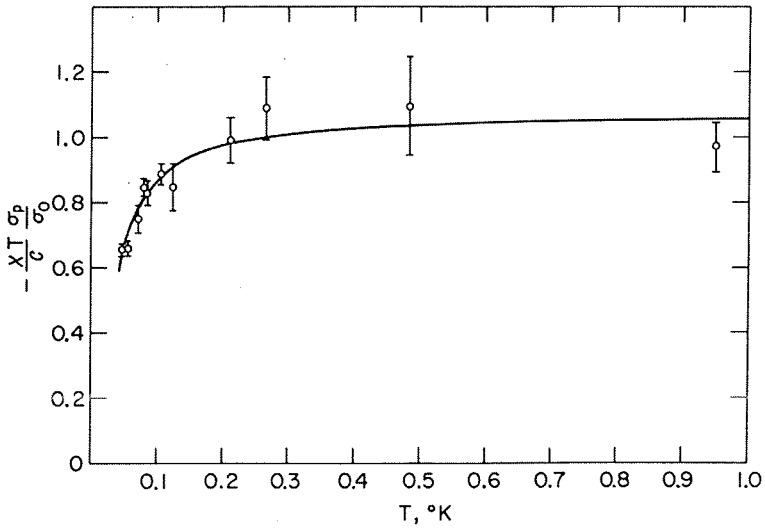

Fig. 3

In fact, the system orders at low temperature in such a way as to reduce the susceptibility. To obtain (σ_p/σ_o), we are interested in the ordinate at high temperature. Putting all the data together, we get $\sigma_p/\sigma_o = -1.013 \pm 0.042$, which we can rewrite as $\sigma(I - 1/2)/\sigma_o = 1.010 \pm 0.032$. That is, all the cross-section is in the $I - 1/2 = 0$ channel within the experimental accuracy of 3 %. This result is exactly what one expects from all current theoretical and experimental results on the four nucleon system.

I would like to emphasize that this experiment was performed by brute force polarization, the largest transmission effect being

2.2 %, corresponding to f_N = 1.65 % at .045° K. Even though the polarization may seem very small it is still possible to do very precise experiments at thermal neutron energies, where the counting rate is high.

Once we know σ_p/σ_o for this system, we can now turn around and investigate the susceptibility of ^{3}He in its various physical states, which is a program that we are now actively pursuing. This trick of using a nucleus with properties determined in one part of an experiment as a probe to look at the interactions of the nucleus with its environment is one on which much time has been spent. In particular, if one works at a neutron resonance where (σ_p/σ_o) has a simple form, then one can measure hyperfine fields after determining the resonance J value, say by brute force polarization. For example, Stolovy [15] has recently completed a study of hyperfine fields in compounds of Fe with Ta, Re, Ir and Pt, which shows how the induced field at the nucleus of these transition elements varies with atomic number. We have some preliminary results on Hf to extend this work.

The most spectacular example of such a study occurs in holmium metal, in which the HFS is so large that one may trace out the complete Brillouin function [16] (fig. 4). The coupling constant determined in this way agrees very well with that determined by specific heat measurements.

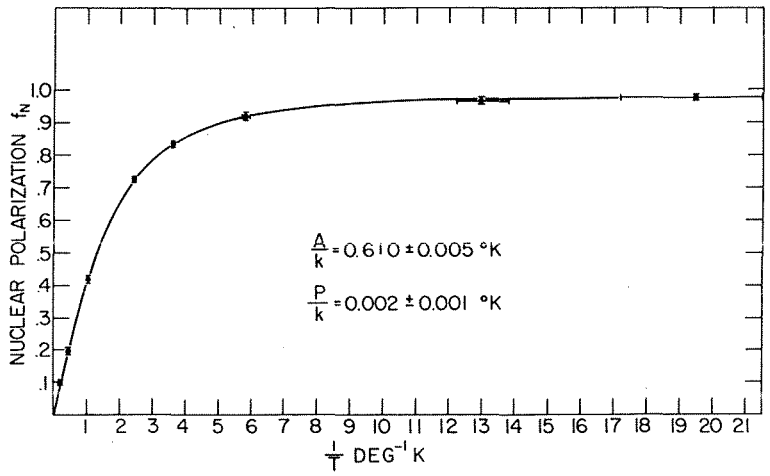

Fig. 4

Finally, we have on occasion turned the experiment completely around and used the transmission effect to measure the sample temperature. For instance, in the ^{3}He work described before, we were

able to show that the lead zeolite matrix came to the same temperature as the paramagnetic salt by studying the nuclear polarization of ^{185}Re, included in the sample as filings of $Fe_{.91}\ Re_{.09}$ alloy.

I have tried to give an idea of the range of problems which may be attacked by studying the transmission of polarized neutrons through polarized targets, while avoiding detailed discussion of particular problems. The references cited are not a complete list of all publications in this field, but any paper missing is cited somewhere in the papers listed here.

References

1) S. Bernstein, L.D. Roberts, C.P. Stanford, J.W.T. Dabbs and T.E. Stephenson, Phys. Rev., 1954, 94, 1243.
2) L.D. Roberts, S. Bernstein, J.W.T. Dabbs and C.P. Stanford, Phys. Rev., 1954, 95, 105.
3) J.W.T. Dabbs, L.D. Roberts and S. Bernstein, Phys. Rev., 1955, 98, 1513.
4) A. Stolovy, Phys. Rev., 1960, 118, 211.
5) H. Postma, H. Marshak, V.L. Sailor, F.J. Shore and C.A. Reynolds, Phys. Rev., 1962, 126, 979.
6) F.L. Shapiro, Proceedings of the International Conference on the Study of Nuclear Structure with Neutrons, Antwerp 1965, (M. Neve de Mevergnies, P. Van Assche and J. Vervier, eds.), p. 223.
7) J.W.T. Dabbs, F.J. Walters and G.W. Parker, Bull. Am. Phys. Soc., 1963, 8, 69.
8) H. Postma, (unpublished).
9) F.J. Shore, C.A. Reynolds, V.L. Sailor and G. Brunhart, Phys. Rev., 1965, 138, B1361.
10) H. Postma, F.J. Shore and C.A. Reynolds, Physica, 1964, 30, 713.
11) R.I. Schermer, Phys. Rev., 1963, 130, 1907.
12) R.I. Schermer, Phys. Rev., 1964, 136, B1285.
13) Except for ^{3}He this work remains unpublished. Preliminary results may be found in the Brookhaven National Laboratory Annual Reports for the years 1961-1963.
14) L. Passell and R.I. Schermer, Phys. Rev., 1966, 150, 146.
15) A. Stolovy, Phys. Rev., (to be published).
16) G. Brunhart, H. Postma and V.L. Sailor, Phys. Rev., 1965, 137, B1484.

Work performed under the auspices of the U.S. Atomic Energy Commission.

EFFECTS OF RADIATION DAMAGE ON PROTON RELAXATION TIME IN LANTHANUM MAGNESIUM DOUBLE NITRATE

W.N. HARDY and G. SHAPIRO

Département de Physique Nucléaire, Saclay

INTRODUCTION

During the past few years, several laboratories have built and used targets containing polarized protons in particle scattering experiments. The material most commonly used for this purpose is lanthanum magnesium double nitrate (LMN) : $La_2Mg_3(NO_3)_{12}\cdot 24H_2O$ with about 1 % doping of neodymium.

Proton polarizations in excess of 70 % have been achieved in this crystal. In cases where these targets have been exposed to intense beams, it has been found that the cumulative effects of radiation damage due to such beams has been such as to reduce the polarization attainable in such crystals. Experience with protons of 150 MeV (B. Rose, paper at Williamsburg Conference) and 26 MeV (D. Garreta, private communication) indicate that the flux necessary to produce such effects is of the order of 10^{12} particles per square centimeter. These workers further note that : i) the polarizability recovers partially when the crystal is annealed at room temperature ; and ii) there is a correlation, though not a linear one, between the polarizability of the target and the proton relaxation time T_1.

The present investigation was undertaken in an effort to place more exact figures on the radiation flux required to change the nuclear magnetic resonance characteristics of this crystal, and also to determine whether the damage done by electrons, which have low specific ionization and small nuclear cross-sections, might be less than that of slow protons.

The procedure consisted of immersing a LMN crystal in liquid helium at 1.2° K in close proximity to a source of strontium-90, and in an external magnetic field of 7000 gauss. The proton relaxation time was measured by nuclear magnetic resonance techniques as the irradiation proceeded.

RADIOACTIVE SOURCE ; INTENSITY AND SPECTRUM

The source consisted of approximately 20 millicuries of strontium-90, in equilibrium with its daughter nuclide yttrium-90, deposited in a standard (type SC2) sealed stainless steel cylindrical container. The radiation was emitted principally through a window of 0.15 mm thickness and 4.8 mm diameter.

The source intensity was measured by determining the electric current carried out off by the beta particles. The source was shielded on all sides except that of the thin window by sufficient aluminium to stop all betas emitted in other directions. The assembly was suspended in an evacuated (10^{-4} mm Hg) container whose walls were kept at - 300 volts potential (increasing this potential difference to - 1000 volts made no significant change). The current to ground under this conditions was 7.06×10^{-12} amperes. Assuming the source to be distributed over the 4.8 mm diameter window, this yields an average surface intensity of 0.88×10^{12} electrons per square centimeter per hour.

Strontium-90 and yttrium-90 are both single beta-emitters with end-points of respectively 0.54 MeV and 2.26 MeV. Since the spectrum can often be distorted by passage through matter, an attempt was made to measure the spectrum crudely by covering the thin window with various thicknesses of aluminium and determining the current of electrons which then emerged. It was found that this current was a decreasing exponential function of the thickness of aluminium with mean free path of 0.17 gram per square centimeter.

Since the crystal under irradiation was 0.5 mm thick, with density 2 g/cm^3, this means that the electron intensity falls by a factor 1.8 in passing through the crystal, and that the average intensity throughout the sample is 0.75 of its value at the entering surface.

It is a fairly good approximation to the <u>average</u> range-energy behaviour of electrons (see Segré, Experimental Nuclear Physics, Vol. I, p. 294) to say that the electrons lose energy at a constant minimum rate ($\sim$ 2 MeV per gram per cm^2) down to nearly the

end of their range, at which point they deposit the remainder of their energy ($\sim$ 0.18 MeV). One can then calculate the amount of energy deposited in a given volume as the sum of the minimum-ionizing energy loss of the electrons passing through the volume plus 0.18 MeV for each electron that stops in the volume. Using the observed exponential attenuation this shows that the energy deposited is 3 MeV per g/cm^2 for each electron incident on an element of volume, or the equivalent of 1.5 times minimum ionization.

That this estimate is insensitive to the details of the electron spectrum can be recognized by noting that we would get the same calculated dose from the extreme assumption that all the electrons had 0.51 MeV kinetic energy which was deposited in an average thickness of 0.17 g/cm^2.

In the actual irradiation, the source was separated from the crystal by a flat ring of teflon of thickness 1.45 mm and inside diameter of 4.1 mm. On the assumption that the strontium-90 is distributed evenly across the face of the source, one calculates that the intensity at the center of the front crystal surface is reduced by a factor of 0.42 from that at the surface of the source.

The combination of these factors yields an average dose within the irradiated crystal of, within a factor two, the equivalent of 0.42×10^{12} minimum ionizing electrons per cm^2 per hour.

MEASUREMENT OF T_1

The magnitude of the proton magnetization was measured by applying a 90° pulse at the proton magnetic resonance frequency of 30 MHz and observing the free induction signal, which is proportional to the proton polarization immediately before the pulse.

The 90° pulse reduces the proton polarization to zero. The polarization will then grow back to its equilibrium value, A_∞, with a time constant T_1. A second 90° pulse occuring at an interval τ after the previous pulse will measure an induction signal $A(\tau)$, which is smaller than A_∞. (A_∞ is measured by waiting a time much longer than T_1). If the recovery is purely exponential, T_1 can be determined from the formula :

$$T_1 = \tau \left[\ell_n \frac{A_\infty - A(\tau)}{A_\infty} \right]^{-1} . \qquad (1)$$

In fact the decay is not pure exponential both because T_1 is changing during the measurement due to the continued irradiation and because the irradiation is not uniform throughout the crystal resulting in T_1 being different for different protons.

Nevertheless formula (1) was used to obtain an apparent T_1. While this value is not to be taken as an absolute measurement of T_1, it is sufficiently reproducible to be used as an indication of changes in the proton relaxation time. Typical values of T_1 used were 10 minutes.

The temperature was determined from the vapour pressure of the helium, which was 0.7 mm Hg, corresponding to 1.2° K.

RESULTS

1) The apparent proton relaxation time, measured as 22 minutes within 3/4 hour of the start of irradiation, fell to 12 minutes after two more hours of continued irradiation at 1.2° K.

2) After eleven additional hours of irradiation, mostly at 4.2° K, the proton relaxation time had dropped to 4 minutes, measured at 1.2° K.

3) An attempt to anneal the crystal at $\sim$ 77° K for 5 minutes produced no change in the proton relaxation time when recooled to 1.2° K.

4) The crystal was brought to room temperature and the source removed. After 1 1/2 hours the crystal was recooled to 1.2° K, and the proton relaxation time was found to have increased to 16 minutes.

5) The proton relaxation time at 4.2° K was measured several times before, during and after the irradiation. In contrast to the behaviour at 1.2° K, the 4.2° K T_1 remained constant at 6.5 $\pm$ 2 seconds.

CONCLUSION

This experiment indicates that a radiation dose of the order of 10^{12} particles per square centimeter is sufficient to alter considerably the characteristics of the proton resonance, in particular its relaxation time T_1, and, one infers, its polarizability.

The order of magnitude of the tolerable radiation dose is in agreement with that observed at Harwell and at Saclay with protons of much lower velocity. It is perhaps surprising that the critical flux of damaging particles is insensitive to the specific ionization or the nuclear interaction properties of these particles.

We wish to thank M.C. Hayoun of the Department of Radioelements for supplying the source, and M.J. Vagner for making the intensity measurements.

THE LIVERPOOL POLARIZED PROTON TARGET

P. J. HAYMAN
Liverpool Target Group, England

The advantage of superconducting coils when used to generate the magnetic field for a polarized proton target were recognized some years ago. As yet, only a few targets using this method of field production have been produced, and used in experiments to the present date. The Liverpool target (fig. 1) represents a compromise between accessibility whilst used as a development target and suitability for later use in experiments at the new 4 GeV electron accelerator NINA, which is sited near Liverpool. The compactness of the coils necessary to generate fields in the region 18-25 kG itself represents an improvement when access of particle beams to the target material is being considered, and for the detection of the scattered particles.

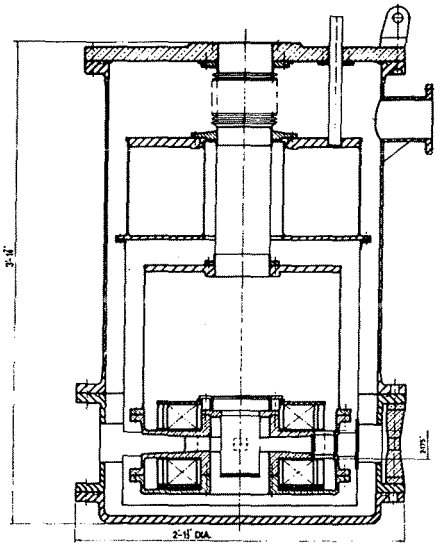

Fig. 1 General assembly of the Liverpool polarized proton target.

In order that we should not have to learn a new art besides polarized target making, one of the boundary conditions in the design of the target was the decision to use commercially available coils and to mount them in a near Helmholtz arrangement (fig. 2) where :

$$\cos^2 \theta = \frac{1}{5} \cdot \qquad (1)$$

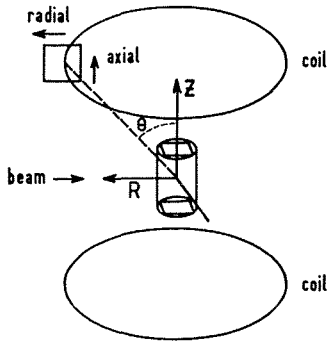

Fig. 2 Optimum dimensions for coils of finite size.

The coils are AVCO SC600, with extra windings to increase the field from 19 kG designed limit to 20 kG. Although normally operated at 4.2° K we have made provision that we can operate them at 1.2° K so that we need only a single helium bath for the coils and the target material. By buying commercial coils, we have lost the freedom to choose the winding dimensions so as to neutralize the effects of their finite size on field uniformity in the region where the target material is to be placed (see for example Franzen [1]) (fig. 2) where :

$$\frac{\text{axial dimension}}{\text{radial dimension}} = 0.928 \cdot \qquad (2)$$

When both of the conditions (1) and (2) are satisfied, the contribution of second order terms in the field expansion about the origin is eliminated ; our ratio is 0.86.

Instead, we have calculated field values by two methods over the region of the target volume using a Legendre polynomial expansion of the field about the target centre, and a simple application of the Biot-Savart Law and used our single free parameter, the coil separation, to find the target coil volume which satisfies the minimum field uniformity deviation condition. $\dot{H}$ = 1 gauss, as suggested by Shapiro [2]. These notes will, perhaps, help others interested in commercially available coils which do not satisfy (2)

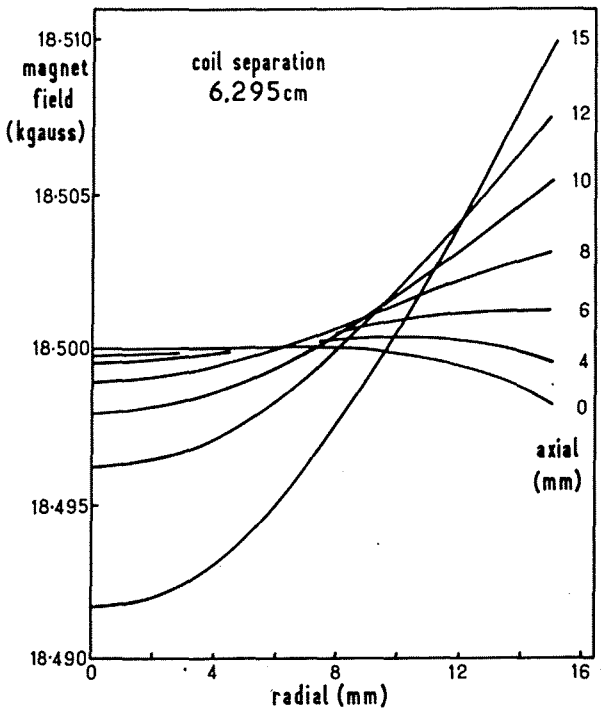

Fig. 3 Variation of magnetic field as a function of radius for different axial positions.

as yet. The variation of field, as a function of radial positions for different axial positions from the plane of symmetry is shown in figure 3. The more useful plot using the uniformity condition as the free parameter is shown in figure 4. Taking a deviation, $\Delta H = \pm 1/2$ gauss and defining the useful volume of uniform field (fig. 2) $V = \pi R^2(2z)$, we see the limits on V set by R_{max} and z_{max}.

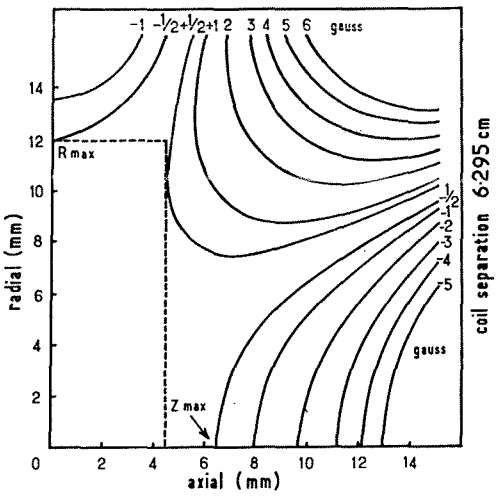

Fig. 4 Contours of field uniformity ΔH.

These volumes are plotted as a function of the separation of the coils in figure 5 and indicate the largest theoretical volume, corresponding to a physical target of volume :

$$V_p = \left(\frac{2R}{\sqrt{2}}\right)^2 (2z) = \frac{2}{\pi} V_{max} \quad .$$

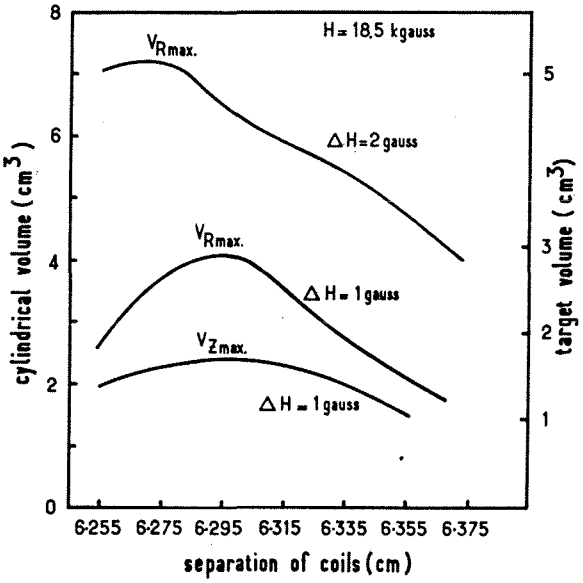

Fig. 5 Optimum target volumes for different coil spacings for ΔH = 1 gauss and ΔH = 2 gauss.

The target then has dimensions :

. Thickness in beam direction x area = 1.7 cm x (1.7 cm x 1 cm) = 2.9 cm

Relaxing ΔH to $\Delta H = \pm 1$ gauss gives corresponding figures :

. Thickness in beam direction x area = 2.1 cm x (2.1 cm x 1.2 cm)

$$= 5.1 \text{ cm}^3 = 0.31 \text{ cu. in.} \qquad (3)$$

which is an increase in volume of 75 %. This limitation of target volume represents a severe constraint in an experimental arrangement.

References

1) W. Franzen, Rev. Sci. Instr., 1962, 33, 933.
2) G. Shapiro, Progress in Nuclear Techniques and Instrumentation, Vol. 1, p. 198.

AN ATTEMPT TO IDENTIFY THE PHYSICAL MECHANISM OF RADIATION DAMAGE

P. J. HAYMAN

Liverpool Target Group, England

Radiation damage effects have been given as the cause for reduction in polarization in polarized targets using LMN in experiments on p-p scattering at 150 MeV [1] and 20 MeV [2]. Since similar effects will be observed in experiments on e-p scattering and in addition because of the much lower cross-sections, a greater flux of incident particles will have to be tolerated in order to obtain results of commensurate statistical significance, it is important to try to identify the mechanism of radiation damage so that target materials can be chosen for electron scattering experiments which are more resistant to the cause.

The basic data are given in table I where energy dissipated in the target by ionization loss only is considered. Taking a combination of the two results and assuming a linear reduction in polarization with incident particle flux, then for 100 % full in polarization the energy release via ionization loss E_i is :

$$E_i = (11 \pm 7) \times 10^{13} \text{ MeV/cm}^3 \qquad (1)$$

for a flux I of :

$$I = (2.6 \pm .4) \times 10^{12} \text{ protons/cm}^2 \ . \qquad (2)$$

If the crystal lattice is damaged by the energy released via ionization loss then it is possible that any impurity in the crystal might be preferentially disturbed. In the case of LMN with paramagnetic ions of Nd X-ray analysis [3] has shown a 1/5 % concentration of Nd corresponding to density J_{Nd} :

$$J_{Nd} = 3 \times 10^{18} \text{ Nd ions/cm}^3 \ . \qquad (3)$$

Harwell target : P. Brogden [1], 150 MeV protons.	
Size (6 x 6 x 1) mm^3	
30 % fall in polarization for 4 x 10" protons	
1 MeV ionization loss in 1 mm, i.e.	1.1×10^{13} MeV cm^{-3}
Saclay target : D. Garreta [2], 20 MeV protons.	
Size (2 x 2 x 0.1) mm^3	
50 % fall in polarization for 1.5×10^{12} protons cm^{-2}	
0.6 MeV ionization loss in 0.1 mm, i.e.	9×10^{13} MeV cm^{-3}

Table I

The energy absorbed per Nd ion which is often referred to as the displacement energy E_d, can be obtained from (1) and (3) giving :

$$E_d = (37 \pm 23) \text{ eV} \quad . \qquad (4)$$

Atoms adjacent to the Nd ions bound in a lattice will oppose any removal of the Nd ions. If E_c is the energy of sublimation of an atom then for crystal interiors :

$$E_d \sim 6E_c$$

so that from (4) :

$$E_c \sim (6 \pm 4) \text{ eV}$$

which is the typical value for an atom or ion in a solid, when a Frenkel pair is produced. It is thus possible to account for the absorption of the energy liberated by ionization loss but only by a mechanism which allows preferential absorption of energy by the impurity.

Another more direct method of energy release inside the crystal could take place by a displaced ion moving through the crystal. Thus for a density of La atoms, J_{La} ($J_{La} = 1.6 \times 10^{21}/cm^3$) where the cross-section for protons on La is $\sigma_{La} \sim 10^{-24}$ cm^2 the number of displaced La ions (using 2) would be :

$$N_{La} = I \, \sigma_{La} \, J_{La}$$

$$= (4.2 \pm .8) \times 10^9/cm^3 \quad .$$

Each displaced La ion could be given a kinetic energy, T, by a 150 MeV proton of maximum value :

$$T_m \simeq 5 \text{ MeV}$$

and having a range of about 10 000 Å. This ion would cause a disturbance over a transverse region of up to 100 Å, in a manner si-

milar to that described by Brinkman and called a "displacement spike". The displacement of other ions by the original displaced ion will cause the track of the original ion to be heated and any resultant annealing would cause dislocation loops and disorder. The total number of Nd ions in these disordered regions will be N :

$$N \sim 10^{12}/cm^3$$

or only 10^{-6} of the total number per cm^3. It does not seem likely that this mechanism can explain the observations of the fall in polarization although the observation of recovery of the polarization on annealing of LMN crystals to room temperature is contained in the mechanism.

The hope for hydrocarbon materials used in electron scattering experiments is that either paramagnetic centres can be produced with the right g-values and electron line widths by radiation damage as the experiment is being done and using the large ($\sim 10^{15}$ electrons) fluxes necessary because of the low cross-sections or that more resistant materials are used such as the aromatic hydrocarbons whose radiation protection has been ascribed to the resonant structure of the benzene ring [5].

References

1) P. Brogden, Harwell, Private communication.
2) D. Garreta, Saclay, Private communication.
3) H. Atkinson, Private communication.
4) J.A. Brinkman, see e.g. Radiation Damage in Crystals by L.T. Chadderton, (Methuen), 1965.
5) A. Charlesby, Atomic Radiation and Polymers, (Pergamon), 1960.

RECENT RESULTS ON PROTON POLARIZATION IN SEVERAL HYDROCARBONS

R. P. HADDOCK and R. J. WAGNER
University of California, Los Angeles

I INTRODUCTION

A series of experiments have been done at U.C.L.A. in which the protons in solid toluene, and several other similar hydrocarbons, have been significantly polarized by the method known as the "solid state effect". The hydrocarbons are doped with a small amount of the stable free radical Diphenyl Picrylhydrazil (DPPH) and the polarization enhancements are observed as a function of concentration and temperature. All observations were made using magnetic fields of 20.4 kG and microwave frequencies near 57 GHz in a temperature range of 4.2° K to near 1° K.

II MICROWAVE AND MAGNET SYSTEM

A reflex klystron generating microwave power in the range 57 to 62 GHz is used. This tube produces about 200 mW. Maximum power output near 57 GHz, the frequency used in most of these experiments. An untuned microwave cavity, 7/8 in. square by 2 in. high contains the small samples in a teflon holder. A 5 in. tapered transition joins the cavity with a length of thin-walled, silver plated stainless steel RG-96/U waveguide, which connects the microwave circuitry external to the cryostat.

An electromagnet with 12 in. flat pole pieces and a 2 1/4 in. gap produces the static magnetic field. In the majority of the results reported here, this field was limited by the power supply to about 20,400 gauss. This condition was later improved by going to shimmed tapered pole pieces and a larger power supply. The region of field homogeneity has also been considerably improved.

III MEASUREMENT OF THE PROTON POLARIZATION

A Q-meter type NMR along with field modulation is employed to monitor the polarization of the protons in the sample. The system is driven by a variable frequency VHF oscillator with an internally matched variable attenuator. Approximately 3 turns of number 32 copper wire wound on the teflon sample holder form the NMR coil. The radio frequency signal (85 MHz) is amplified, detected, and audio amplified before phase sensitive detection occurs.

The NMR derivative is displayed as recorder output and the enhancement is determined from a comparison of the polarized and the thermal equilibrium signals. Readings are made from a variable attenuator, made up of 1 % resistors, and calibrated against an oscilloscope. No corrections were made for changes in the line shape of the signal. Several of the results have been integrated by hand and the polarizations thus calculated were compared. The resulting difference was not found to be significant.

Nuclear relaxation times, T_{1n}, are observed by polarizing the protons, removing the microwave power, and monitoring the decay of the resonance signal. In all of these measurements the oscillator power was maintained at a level about 10 % of that at which saturation effects could be seen.

IV THE CRYOSTAT SYSTEM

A pyrex helium research dewar which contains a maximum of 2 liters was used. The unit is of conventional design for use with electromagnets and was cooled by liquid nitrogen in an outer jacket. A 140 c.f.m. pump on a 4 in. line is used to achieve temperatures near 1° K. A dial manometer on the pumping line was used to measure

the pressure over the helium and to provide the temperature indication. The calibration of this manometer is uncertain at the lowest pressures.

V PREPARATION OF SAMPLES

The materials used in these experiments have been obtained from the Eastman Organic Chemical Company and are used as supplied. The table lists the materials used and the Eastman catalogue number.

Material	Eastman number	Formula
Toluene # 1	X325 (from sulfonic acid)	$C_6H_5CH_3$
Toluene # 2	325 (sulfur free)	$C_6H_5CH_3$
Ethylbenzene	719	$C_6H_5CH(CH)_3$
Cumene	1481	$C_6H_5CH(CH)_3$
2,2-diphenyl-1-picrylhydrazyl	7703	$(NO_2)_3C_6H_2NN(C_6H_5)_2$

The proper amounts of each material for the desired concentration is weighed and mixed in a small beaker. Amounts of about 10 grams are usually made at one time. The solution is allowed to stand for about 15 minutes with occasional slight agitation. After this no undissolved DPPH appears to remain.

A small amount of the solution is then drawn from the beaker and injected into the sample holder. The microwave probe is then placed in the cryostat and the sample is allowed to solidify.

Some samples were allowed to freeze slowly, and others were dunked into liquid nitrogen to freeze suddenly in order to determine whether freezing rate played any effect. The resulting data did not reflect any consistent trend from which a definite conclusion could be drawn.

No accurate analysis of the concentration of DPPH was performed on the solutions. The concentrations were assumed to be those initially prepared.

VI EXPERIMENTAL RESULTS

The bulk of the measurements in this program were made using toluene, doped with 0.5 to 3 % DPPH. Recently, polarization has been observed in ethylbenzene and in cumene. The early measurements on toluene were on samples of approximately 200 milligrams. This size was determined largely by the poor homogeneity of the magnet.

Once the tapered pole pieces and the larger power supply were obtained, samples up to 7 grams were tried. The enhancements for the larger sample volumes were lower than those obtained with the smaller samples. It is felt that this is due to internal heating of the material by the microwave power. Methods of breaking the samples in smaller sized segments have been attempted, however, a satisfactory improvement has not yet been achieved. This approach has not yet been fully explored, however.

A table follows which lists the experimental results observed in this program.

Material	Concentration (%)	T(°K)	Approximate Volume (cm^3)	Enhancement	T_{1n} (s)
Toluene # 1	0.5	4.2	0.2	5	8
"	0.5	2	0.2	25	30
"	0.5	~1	0.2	40	120
"	1	4.2	0.2	30	5
"	1	2	0.2	50-70	20
"	1	~1	0.2	90-110	60
"	2	4.2	0.2	40-45	2
"	2	2	0.2	80-100	10-15
"	2	~1	0.2	125-150	35-45
Toluene # 2	2	~1	1 *	100	40
"	2	~1	7 *	70-75	40-45
Ethylbenzene	2	~1	1 *	105	70
Cumene	2	~1	7 *	60	40

* Magnetic field of 21,800 gauss. In all others the field was 20,400 gauss.

Wherever two numbers are given, a series of experiments have yielded a range of values between these two numbers.

Comparison of our data on toluene with other laboratories has shown some disagreement, especially in the values of T_{1n}. Lack of standardization in the materials used, sample size, and measure-

ment of temperatures near 1° K, are probable culprits. The data presented here attempts to show the behaviours of the pertinent parameters as measured by us. Work will continue in our laboratory to help better understand proton polarization in these materials and to help resolve the discrepancies.

Work supported in part by the U.S. Atomic Energy Commission under Contract AEC AT(11-1)-34 Project 106. Technical report MPG 66-11.

SIZEABLE PROTON POLARIZATIONS IN FROZEN ALCOHOL MIXTURES

M. BORGHINI, S. MANGO, O. RUNOLFSSON
and J. VERMEULEN

CERN, Geneva

We present here preliminary results of a work which is part of a research programme for high proton polarizations in highly hydrogenated substances. The method of polarization was the "solid effect". The samples were ethanol-water, ethanol-methanol, and ethanol-propanol mixtures doped with porphyrexide, a free radical with a formula $(CH_3)_2CN(:O)C(:NH)NHC:NH$ [1]. The mixtures were saturated at room temperature with about 3 % by weight of porphyrexide. The experiments were carried out in a field of 25 kG, at temperatures around 1.05° K, obtained in a continuous flow cryostat [2] ; the cooling time from room temperature to liquid helium temperature was 55 minutes. The samples were contained in a rectangular holder made of copper, 3.5 x 7 x 14 mm, closed on one side by a teflon window 3 x 6 mm. This holder was located inside a 18 cm^3 copper cavity filled with helium, and connected to a 20 W carcinotron oscillating at 70 Gc/s. The polarization was measured by NMR as in the Saclay-CERN polarized targets [3], the coil being immersed in the samples and care being taken not to saturate the NMR signals.

Maximum polarizations of 35 ± 2 % were obtained for the lowest attainable temperature, with a reduced microwave power of about 500 mW. The polarization depends markedly on the concentration of the various mixtures, as shown is figures 1, 2 and 3. Figure 4 shows the melting point of ethanol-water mixtures : a correlation seems to exist between the melting point and the obtained polarizations, although we are not able now to understand why. No attempt has yet been made to observe the electronic resonance line of the frozen free radical : from the known over-all hyperfine splitting (30 gauss) and the anisotropy of the g-factor, we estimate its width to be between 60 and 90 gauss. No attempt has been

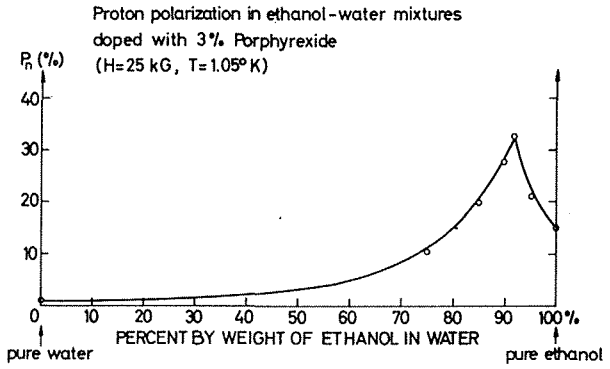

Fig. 1

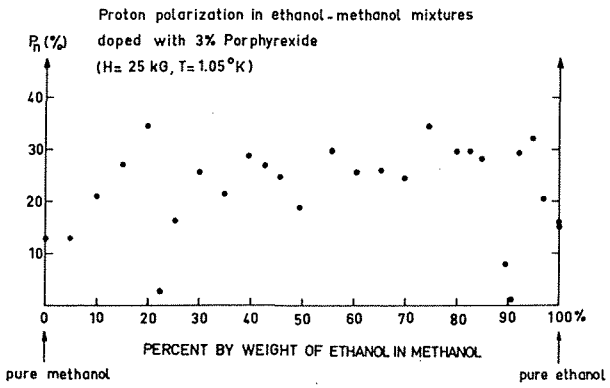

Fig. 2

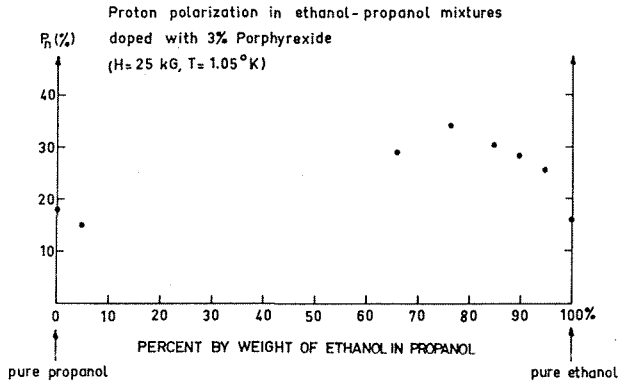

Fig. 3

made either to take off oxygen gas possibly dissolved into the samples. The nuclear relaxation times were of 3 to 7 mn in samples without free radical, were a little longer with a small amount of it, and of about 2 mn at 1.05° K with its maximum concentration. The polarization times ranged between 5 and 10 s for the optimum polarizations.

Results obtained in other samples with various free radicals are given in table I. Polarization and nuclear relaxation time measu-

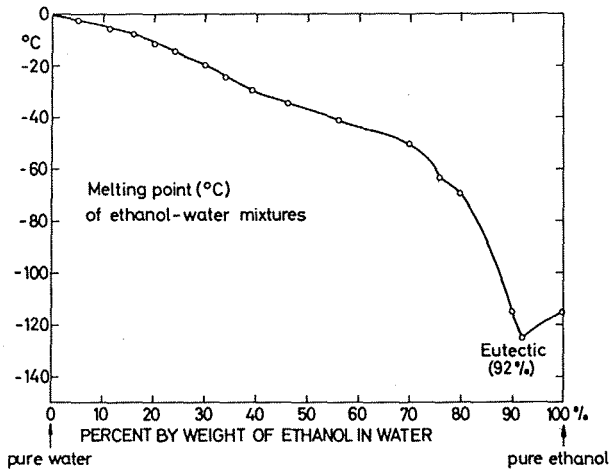

Fig. 4

Table 1

Some preliminary results on proton dynamic polarizations in organic compounds containing free radicals*)

Compound		Free radical**)														
		DPPH			PR			BPA			PB			PAC		
	***)	1	2	3	1	2	3	1	2	3	1	2	3	1	2	3
Benzene	C_6H_6	5	2%	1					×)							
Toluene	C_7H_8	2	23%	12				4	15%	4						
m-Xylol	C_8H_{10}							4	10%	2						
Isodurol	C_9H_{12}	4	5%	1												
Tetrahydrofuran	C_4H_8O	2	4%	1												
2,5 Dimethyl-tetrahydrofuran	$C_6H_{12}O$							2	17%	1						
Diethylether	$C_4H_{10}O$	4	9%	3												
Methanol†)	CH_4O				3	13%	3									
Ethanol†)	C_2H_6O				4	16%	5									
Propanol†)	C_3H_8O				3	18%	2									
Plexiglas (solvent)	$[C_5H_8O_2]_n$	3	14%	7							10	10%	6	4	22%	8
		Chloroform									Chloroform			Benzene		
Polystyrene (solvent)	$[C_8H_8]_n$							4	20%	1				5	23%	1
								Toluene						Benzene		
Polyisobutylene (solvent)	$[C_4H_8]_n$				6	7%	1									
					Tetrahydrofuran											
Polymerized BPA									30%							

*) Magnetic field 25 kG, temperature 1.05°K.

**) DPPH = 1,1-diphenyl 2-picryl-hydrazyl; PR = Porphyrexide; BPA = 1,3-Bisdiphenylene 2-phenyl-allyl, PB = Porphyrindene; PAC = Picryl-N-amino-carbazyl.

***) Col. 1: radical concentrat. in % by weight; col. 2: max. polarizations; col. 3: No. of samples with varied concentrat.

×) With 4% BPA + 0.3% DPPH in toluene, a polarization of 20% was obtained.

†) See Figs. 1, 2 and 3 for mixtures of alcohols.

rements in frozen toluene containing DPPH are shown on figures 5 and 6, together with the results of Wagner and Haddock [4]. Figure 7 shows the peculiar behaviour of the polarization of M-Xylol versus the microwave frequency.

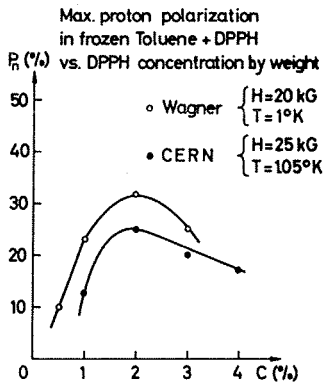

Fig. 5

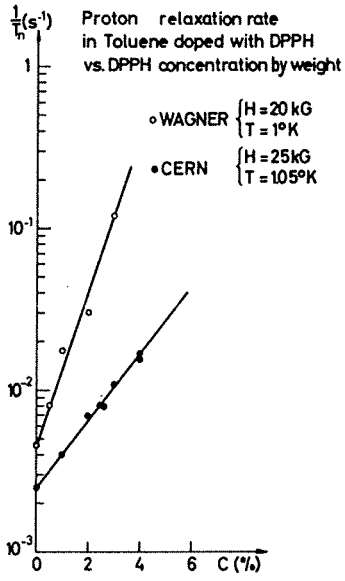

Fig. 6

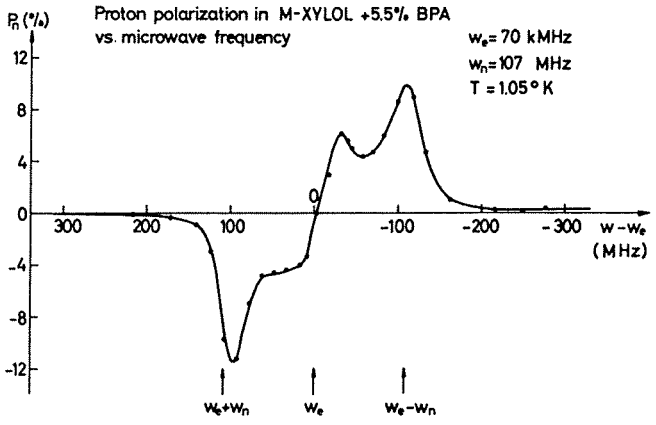

Fig. 7

We wish to thank Dr P. Roubeau for having provided us with some of his cryostats, and Dr Ch. Ryter for the design of our electronics ; Mrs J. Conciencia and M. Uldry for their great assistance during the installation and the operation of the apparatus ; and Prs W. Paul and P. Preiswerk for their continuous interest and support.

References

1) Fluka, Chemische Fabrik, CH-9470 Buchs, Switzerland.
2) P. Roubeau, Thesis, Grenoble 1966.
3) M. Borghini, P. Roubeau and Ch. Ryter, Nucl. Instr. Methods, (to be published).
4) R.J. Wagner and R.P. Haddock, Phys. Rev. Letters, 1966, 16, 1116.
R.J. Wagner, Thesis, Los Angeles, 1966.

MEASUREMENTS OF THE POLARIZATION AND ITS REVERSAL BY FAST PASSAGE

M. CHAPELLIER

Centre d'Etudes Nucléaires de Saclay

The usual method of measuring the polarization is to compare the NMR enhanced signal with a signal obtained at thermal equilibrium, at a known temperature. We present here three other methods. The two first were used with polarized targets, the third was used with NMR experiments.

1. Measurement of the polarization of very small samples : method of the Lorentz field.

A. Abragam, M. Borghini and M. Chapellier, Compt. Rend., 1962, 255, 1343.

2. Absolute measurement of the polarization of big targets by the external field produced by the protons of the sample.

A. Abragam, Compt. Rend , 1964, 258, 1773.
M. Chapellier, Compt. Rend., 1964, 258, 112.

3. Absolute measurement of the spin temperature of nuclei with $S > 1/2$ and of their polarization.

A. Abragam and M. Chapellier, Phys. Letters, 1964, 11, n° 3 , 207.

POLARIZATION REVERSAL BY ADIABATIC FAST PASSAGE

It can be very interesting to reverse the polarization of a target, either to do it quickly or to obtain negative polarization in Jef-

fries' method of spin refrigerator.

The usual conditions (see for instance A. Abragam, "The principles of nuclear magnetism") for an adiabatic fast passage in solids are the following :

$$\frac{1}{T_1} \ll \frac{1}{H_1} \frac{dH_o}{dt} \ll \gamma H_1 \quad .$$

These conditions give values of H_1 and dH_o/dt not very realistic in the case of LMN. In fact, one has to replace H_1 by $(T_1)_R$, the relaxation time in the rotating frame. By assuming $(T_1)_R$ not shorter than T_{1e} (but very much shorter than T_1 in the laboratory) let us say $(T_1)_R \sim 0.1$ s (instead of $T_1 \simeq 10^4$ s for LMN) one needs :

$$2.7\ 10^4\ H_1^2 \gg \frac{dH_o}{dt} \gg 10\ H_1 \qquad \left.\begin{matrix} H_o \\ H_1 \end{matrix}\right\} \text{ in gauss}$$

The higher H_1, the easier can this relation be satisfied but then the passage through the resonance must be fast.

No systematic experiments have been done on this subject, but we have already adiabatically reversed the polarization in a sample of LMN, in a coil of 1 cm^3 with about 100 V across the coil ($H_1 \sim 2$ gauss), by sweeping the frequency instead of H_o at a speed which corresponds to $dH_o/dt = 1000$ gauss/s. The efficiency was about 70 % and can probably be better.

IMPRIMERIE LOUIS-JEAN
Ouvrages scientifiques
TYPO-OFFSET
GAP (Hautes-Alpes)

Dépôt légal n° 164
1967